The effects of digestion resistant carbohydrates on the colon microbiota and colon tissue transcriptome of weanling rats

Wayne Young

A thesis submitted in partial fulfilment of the requirements for

the degree of Doctor of Philosophy in Microbiology,

University of Otago, 2011.

Abstract

Digestion-resistant carbohydrates (DRC) in the diet pass to the terminal ileum and large bowel where they may be fermented by resident bacteria. The bacterial communities in the bowel of young animals undergo dramatic shifts in composition following weaning. These compositional and associated biochemical changes may have long-lasting impacts on the host. However, the mechanisms by which diet induced changes in the microbiota influence host physiology requires further investigation. This study examined whether bacterial community compositions could be engineered by supplementing the diet of newly-weaned rats with different forms of DRC and the subsequent effects these altered microbial communities had on host physiology.

Newly weaned conventionally raised or germ-free male 21-28 day old Sprague-Dawley rats were fed a basal diet or basal diets supplemented with DRC at concentrations up to 5% for 14 or 28 days. Colonic digesta was collected from each rat for analyses to determine short chain fatty acid (SCFA) concentrations and to compare bacterial community structure by temperature gradient gel electrophoresis (TTGE) and 454 pyrosequencing analysis of the V3 hypervariable region of the 16S rRNA gene. DRC induced alterations in the host transcriptome were assessed by microarray analysis of RNA extracted from colon tissue.

Feeding DRC significantly increased concentrations of SCFA in the colon digesta of young rats. The DRC induced changes in SCFA concentrations were also accompanied by alterations in the colonic microbiota structure. Each type of DRC altered the microbiota in a distinctive manner, which could be clearly differentiated from those of rats fed the basal diet. Feeding DRC also resulted in more uniform microbiota compositions compared to the basal diet. The alterations in microbiota composition were associated with changes in host colon gene expression profiles. Each form of DRC altered colonic gene expression in a distinct manner with profiles from rats fed the same diet showing greater similarity than those fed different diets. Differentially expressed genes in the colon

were involved in a number of biological functions including energy metabolism, immune function, and cellular growth and differentiation. Comparisons of the effects of DRC on host gene expression between conventionally raised and germ-free rats showed that the resident microbiota was a determining factor of the host response to DRC. Feeding DRC to conventionally raised rats resulted in the differential expression of different sets of genes compared with feeding DRC to germ-free rats.

The results of this study show that the bacterial communities in the colon of newly-weaned rats can be engineered by supplementing the diet with DRC. Using this approach, unique bacterial communities with enhanced fermentative capacity, increased uniformity, and distinct effects on host gene expression were selected. The findings from this study provide support and future scope for the development of different dietary supplements that target different parameters of large bowel function.

Acknowledgments

I offer my deepest appreciation to my supervisors and mentors Dr Nicole Roy, Dr Julian Lee and Professor Gerald Tannock for their support, guidance, wisdom and knowledge during the course of this work. It has been a deeply enriching, educational and rewarding process, and for that I will always be very grateful. Thank you Nicole, it has been a great pleasure to work with you and benefit from all your help, enthusiasm, knowledge and kindness. Julian, thank you so much for all your encouragement, support and wisdom. It was excellent knowing I could always drop by your office for a chat. Gerald, it has been a great privilege to have you as a mentor. I consider myself to be extremely fortunate to have been given the opportunity to learn from your knowledge and experience. Thank you for imparting on me the importance of always thinking clearly and critically. I could not have had a better supervisor.

I would like to thank Zaneta Park for all the invaluable help and knowledge with Bioconductor and microarray analyses. Thank you for teaching me the dark arts of R. I would also like to offer my sincere thanks to Dr Blair Lawley, Dr Mark McCann, Karen Munro, Kelly Armstrong, Anna Russ and Grant Taylor for their advice and expertise, without which this work would be far poorer. I am indebted to Janice Rhodes, Hannah Smith, and Sheridan Martell for all their help with the rat studies. In particular, I would also like to thank Dr Gemma Henderson, Leigh Ryan and Hailey Hillson for their important contribution to the germ-free rat study. Furthermore, I would like to thank Dr Christine Butts, Dr John Monro and Dr Juliet Sutherland for their support and advice. Thanks also to Andrew McLachlan for statistical support and advice. Of course, I need to thank Dr Douglas Rosendale and Jane Mullaney for many stimulating conversations in the tea-room and for providing much needed opportunities for sharing a few laughs over a cup of coffee.

I would like express my thanks to Plant and Food Research, AgResearch, the University of Otago and the Tertiary Education Commission for funding this work.

I would like to say a special thanks to the late Mervyn Birtles. Thank you for all your histology advice and expertise. I will always remember your warmth and enthusiasm.

Finally, I would like to thank my wife, Dr Christina Moon. Thank you for keeping me grounded. Thank you for your encouragement, support and love. Thank you for being you.

Table of Contents

Abstract i

Acknowledgments iii

List of Figures ix

List of Tables x

List of Abbreviations xii

Chapter 1. Introduction 1

1.1 Large bowel ecosystem 2

1.2 Bacterial carbohydrate metabolism 6

1.2.1 Defining digestion resistant carbohydrates 6

1.2.2 Carbohydrate breakdown and energy harvest 7

1.2.3 Plant cell wall associated carbohydrates 14

1.2.4 Resistant starch 15

1.2.5 Inulin 17

1.2.6 Konjac glucomannan 19

1.2.7 β-glucans 19

1.2.8 Seaweed 20

1.2.9 Fermentation products in the large bowel 21

1.3 Diversity and composition of the large bowel microbiota 23

1.3.1 Establishment of the microbiota 23

1.3.2 Microbial community structure 24

1.3.3 Butyrate producing bacteria 28

1.3.4 Lactobacilli and bifidobacteria 29

1.3.5 Bacteroidetes 32

1.4 Bacteria and host interactions 33

1.4.1 Influence of microbiota on early large bowel development 33

1.4.2 Development and regulation of the immune response 34

1.4.3 Modulation of the immune system by bacterial structural components 36

1.4.4 Regulation of mucosal barrier function by bacterial components 40

1.4.5 Systemic effects of microbiota metabolism 42

1.4.6 Microbiota and obesity 45

1.5 Hypothesis and aims 48

Chapter 2. Methods and Materials....52

2.1 Animals....52
2.2 Diets....53
2.3 Study design....54
2.4 Procedure for set up and use of germ-free isolators....58
2.4.1 Checking germ-free isolators and rats for contamination....59
2.5 Sample collection....59
2.6 Histology....60
2.7 SCFA and carboxylic acid analysis....61
2.8 Isolation of DNA from colonic digesta....62
2.9 Isolation of RNA from colonic digesta....63
2.10 RT-PCR of colonic digesta RNA....65
2.11 TTGE profile analysis....66
2.12 Cloning and identification of TTGE fragments....70
2.12.1 Extraction of DNA from cut bands....70
2.12.2 S1 nuclease treatment of cut band DNA....70
2.12.3 Amplification of TTGE cut band DNA....71
2.12.4 Cloning of TTGE cut band DNA....72
2.12.5 Sequence analysis of plasmids containing TTGE cut band DNA....74
2.13 Quantitative PCR of TTGE fragment sequences in colon digesta DNA....74
2.14 Identification of colonic microbiota using next generation sequencing....77
2.14.1 Analysis of 454 sequence data....81
2.15 Isolation of RNA from colon tissue....84
2.16 Microarray Analysis....85
2.16.1 Microarray hybridisation....86
2.16.2 Microarray data acquisition....88
2.16.3 Microarray quality checking and normalisation....88
2.16.4 Determination of differentially expressed genes....89
2.16.5 Biological processes associated with differentially expressed genes....90
2.16.6 Biological network analysis using IPA....90
2.16.7 KEGG pathways analysis using GSEA....91
2.17 RT-qPCR analysis of rat gene expression....94

Chapter 3. Results....95

3.1 Diet intake....95
3.2 Rat weights....95
3.3 DRC induced changes in colon mucosal morphology....97
3.4 DRC induced alterations in colonic SCFA concentrations....99
3.5 DRC induced changes in bacterial TTGE profiles....104
3.6 Microbiota composition in DRC fed rats....104

3.6.1 Phylogenetic analysis of bacterial 16S rRNA sequences 106
3.6.2 Species diversity estimate 106
3.7 Alterations in 16S rRNA TTGE profiles in response to DRC dose 112
3.8 DRC and microbiota induced alterations in colon gene expression 119
3.8.1 Differentially expressed genes vary with type of DRC 121
3.8.2 RT-qPCR confirmation of microarray gene expression results 136
3.8.3 Biological processes associated with differentially expressed genes 140
3.8.4 Biological interaction networks associated with differentially expressed genes 148
3.8.4.1 Network of differentially expressed genes between CR-BD and CR-IN 148
3.8.4.2 Network of differentially expressed genes between CR-BD and CR-KJ 149
3.8.4.3 Network of differentially expressed genes between CR-BD and CR-RS 149
3.8.4.4 Network of differentially expressed genes between GF-BD and GF-KJ 149
3.9 Expression of KEGG pathway gene sets altered by DRC 154

Chapter 4. Discussion 163

4.1 Rat body weight and food intake 164
4.2 DRC induced changes in colon mucosal morphology 165
4.3 DRC induced changes in colonic fermentation 166
4.4 Effects of DRC on colonic microbiota profiles 171
4.4.1 TTGE profiling 171
4.4.2 Identification and qPCR analysis of TTGE bands 173
4.5 Identification of microbiota using next generation sequencing 173
4.5.1 DRC induced changes in Bacteroidetes to Firmicutes ratios 174
4.5.2 DRC induced alterations in *Lactobacillus* and *Bifidobacterium* proportions 175
4.5.3 DRC induced alteration in proportions of clostridial cluster IV and XIVa 176
4.5.4 Microbial diversity 177
4.5.5 Comparisons with human microbiota 178
4.6 DRC induced changes in colonic gene expression 179
4.6.1 Biological interaction networks 181
4.6.1.1 Biological interaction network: CR-BD vs. CR-IN 181
4.6.1.2 Biological interaction network: CR-BD vs. CR-KJ 182
4.6.1.3 Biological interaction network: CR-BD vs. CR-RS 182
4.6.1.4 Biological interaction network: GF-BD vs. GF-KJ 183
4.6.1.5 Summary of biological interaction networks 184
4.7 DRC induced changes in expression of KEGG pathways 184
4.8 Perspective on variation observed between rats 186
4.9 Conclusion 188
4.10 Future directions 189

Appendices 192

Appendix A. SCFA sample spiking 192

Appendix B. SCFA standard curves **193**
Appendix C. Standard curves for qPCR analysis of TTGE cut bands **194**
Appendix D. Melting curves for qPCR analysis of TTGE cut bands **195**
Appendix E. TTGE cut band sequences **196**
Appendix F. Boxplots of microarray red and green signal intensities **197**
Appendix G. Boxplots of raw microarray red/green ratios **198**
Appendix H. Boxplots of loess normalised microarray red/green ratios **199**
Appendix I. MA plots of raw microarray red/green ratios **200**
Appendix J. MA plots of loess normalised microarray red/green ratios **201**
Appendix K. Within-array normalised red and green signal densities **202**
Appendix L. Between-array normalised red and green signal densities **203**

References **204**

List of Figures

Figure 1. Diagram of the large bowel ecosystem. 5
Figure 2. Diagram of polysaccharide breakdown pathways. 10
Figure 3. Overview of analytical approaches. 51
Figure 4. Principal of temperature gradient gel electrophoretic (TTGE) analysis. 69
Figure 5. Roche 454 Sequencing workflow. 80
Figure 6. Microarray hybridisation workflow. 92
Figure 7. Analysis of microarray data. 93
Figure 8. Principal component analysis of SCFA profiles. 102
Figure 9. Effect of DRC dose on colonic SCFA concentrations. 103
Figure 10. Bacterial 16S rRNA TTGE Profiles. 107
Figure 11. Phylogenetic analysis of bacterial 16S rRNA sequences. 110
Figure 12. Microbiota diversity estimate. 111
Figure 13. Multidimensional scaling analysis of TTGE profile in response to DRC dose. 114
Figure 14. DRC dose response of bacterial 16S rRNA TTGE profiles from pooled DNA. 117
Figure 15. Response of bacterial 16S rRNA gene copy numbers to DRC dose. 118
Figure 16. Numbers of unique and shared differentially expressed genes. 125
Figure 17. Heatmap of colonic gene expression profiles. 126
Figure 18. PCA plot of colonic gene expression profiles. 127
Figure 19. Network of differentially expressed genes in colon tissue between CR-BD and CR-IN rats. 150
Figure 20. Network of differentially expressed genes in colon tissue between CR-BD and CR-KJ rats. 151
Figure 21. Network of differentially expressed genes in colon tissue between CR-BD and CR-RS rats. 152
Figure 22. Network of differentially expressed genes in colon tissue between GF-BD and GF-KJ rats. 153
Figure 23. KEGG Fatty acid metabolism pathway. 159
Figure 24. KEGG O-glycan biosynthesis pathway. 160
Figure 25. KEGG Tight junction pathway. 161
Figure 26. Differentially expressed KEGG pathways. 162

List of Tables

Table 1. Diet composition for study 1 (g/kg) 55
Table 2. Diet composition for study 2 (g/kg) 56
Table 3. Diet composition for study 3 (g/kg) 57
Table 4. Primers and amplification conditions for quantitative analysis of TTGE fragment DNA 76
Table 5. RDP sequences used for comparative phylogenetic analysis 83
Table 6. Study 1 – Body weights of conventionally raised rats after 28 days of feeding 96
Table 7. Study 3 – Body weights of germ free rats after 28 days of feeding 96
Table 8. Colon crypt length in rats from studies 1 and 3 98
Table 9. Colon crypt goblet cell frequency in rats from studies 1 and 3 98
Table 10. SCFA concentrations in colonic digesta of rats from study 1 101
Table 11. Colonic SCFA concentration response to increasing doses of RS or KJ 101
Table 12. Group prediction of bacterial 16S rRNA TTGE profiles 108
Table 13. Percentage of total bacterial 16S rRNA sequences 109
Table 14. Identification of excised TTGE bands 115
Table 15. TTGE band bacterial 16S rRNA gene copy numbers in response to RS dose 116
Table 16. Numbers of differentially expressed genes in colon tissue 120
Table 17. Distribution of predicted and actual group membership of colonic gene expression profiles 128
Table 18. Differentially expressed genes in colon tissue between CR rats fed BD and IN 129
Table 19. Differentially expressed genes in colon tissue between CR rats fed BD and RS 130
Table 20. Differentially expressed genes in colon tissue between CR rats fed BD and KJ 131
Table 21. Differentially expressed genes in colon tissue between GF rats fed BD and KJ 132
Table 22. Differentially expressed genes in colon tissue between CR and GF fed BD 133
Table 23. Differentially expressed genes in colon tissue between CR and GF fed KJ 134
Table 24. Differentially expressed genes in colon tissue between CR and GF fed RS 135
Table 25. Validation of *Galntl4* microarray gene expression results by RT-qPCR 137
Table 26. Validation of *Galnt2* microarray gene expression results by RT-qPCR 137
Table 27. Validation of *Hspca* microarray gene expression results by RT-qPCR 138
Table 28. Validation of *Mcpt1* microarray gene expression results by RT-qPCR 138
Table 29. Validation of *Mrps31* microarray gene expression results by RT-qPCR 139
Table 30. Significantly over-represented biological processes between CR rats fed BD and IN 141
Table 31. Significantly over-represented biological processes between CR rats fed BD and RS 142
Table 32. Significantly over-represented biological processes between CR rats fed BD and KJ 143
Table 33. Significantly over-represented biological processes between GF rats fed BD and KJ 144
Table 34. Significantly over-represented biological processes between CR and GF rats fed BD 145
Table 35. Significantly over-represented biological processes between CR and GF rats fed KJ 146

Table 36. Significantly over-represented biological processes between CR and GF rats fed RS 147
Table 37. Differentially expressed KEGG pathways in colon tissue of CR rats fed DRC 156
Table 38. Differentially expressed KEGG pathways in colon tissue of GF rats fed DRC 157
Table 39. Differentially expressed KEGG pathways in colon tissue between CR and GF rats 158

List of Abbreviations

acetyl-coA	Acetyl coenzyme A
ANOVA	Analysis of variation
APCs	Antigen presenting cells
ATP	Adenosine-5'-triphosphate
BD	Basal diet
BHI	Brain Heart Infusion
Caco-2	Epithelial colorectal adenocarcinoma cells
CBA	Conjugated bile acids
cDNA	Complementary DNA
coA	Coenzyme A
CR	Conventionally raised
cRNA	Complementary RNA
Ct	Crossing threshold
Cy3	Cyanine 3
Cy5	Cyanine 5
DCs	Dendritic cells
DGGE	Denaturing gradient gel electrophoresis
DNA	Deoxyribonucleic acid
DRC	Digestion resistant carbohydrate
DSS	Dextran sulphate sodium
FC	Fold change
FDR	False discovery rate
FID	Flame ionisation detector
FOS	Fructo-oligosaccharides
Galnt2	Polypeptide N-acetylgalactosaminyltransferase 2
Galntl4	Polypeptide N-acetylgalactosaminyltransferase like protein 4
GALT	Gut associated lymphoid tissue
GC	Gas chromatography
GF	Germ-free
GL	Glucagel™
GSEA	Gene set enrichment analysis
H&E	Haematoxylin and eosin
HBM	Human baby microbiota
IBD	Inflammatory bowel disease
IgA	Immunoglobulin A
IL-10	Interleukin 10
IN	Inulin
IPA	Ingenuity Pathway Analysis
KEGG	Kyoto Encyclopedia of Genes and Genomes
KJ	*Amorphophallus konjac* C. Koch
LGT	Lateral gene transfer
LPS	Lipopolysaccharide
MDS	Multidimensional scaling
MLN	Mesenteric lymph nodes

MTBSTFA	N-methyl-N-E-butyldimethylsilytrifluoracetamide
NAD^+	Nicotinamide adenine dinucleotide (oxidised)
NADH	Nicotinamide adenine dinucleotide (reduced)
$NADP^+$	nicotinamide adenine dinucleotide phosphate
NF-κB	Nuclear factor kappa-light-chain-enhancer of activated B cells
NGS	Next generation sequencing
NOD	Nucleotide binding oligomerisation domain
OTU	Operational taxonomic unit
PBMCs	Peripheral blood mononuclear cells
PBS	Phosphate buffered saline
PCA	Principal component analysis
PCR	Polymerase chain reaction
PP	Peyer's patches
Pparα	Peroxisome proliferator-activated receptor alpha
PRR	Pattern recognition receptor
PUL	Polysaccharide utilisation loci
qPCR	Quantitative polymerase chain reaction
RDP	Ribosomal Database Project
RNA	Ribonucleic acid
rRNA	Ribosomal RNA
RS	Resistant starch
RS1	Type 1 resistant starch
RS2	Type 2 resistant starch
RS3	Type 3 resistant starch
RS4	Type 4 resistant starch
RT-PCR	Reverse transcription polymerase chain reaction
RT-qPCR	Reverse transcription quantitative polymerase chain reaction
SCFA	Short chain fatty acid
spp.	Species
SusC	Starch utilisation system C
SusD	Starch utilisation system D
TER	Transepithelial electrical resistance
TLR	Toll-like receptor
TNBS	2,4,6-trinitrobenzenesulphonic acid
TTGE	temperature gradient gel electrophoresis
UN	*Undaria pinnatifida*
UPGMA	Unweighted pair group method with arithmetic mean

Chapter 1. Introduction

The human gastrointestinal tract is home to an estimated 100 trillion microorganisms. Collectively referred to as the microbiota, they are thought to outnumber the cells of their host by 10 fold and represent by far the largest microbial community associated with the human body (Savage, 1977). This complex ecosystem represents a huge reservoir of metabolic capability and plays a crucial role in a number of developmental and nutritional processes in the intestine. The adaptive co-evolution of the microbial community and their hosts has enabled humans to harvest nutrients from sources that they would otherwise lack the ability to utilise (Backhed et al., 2005) (Figure 1). The intestinal microbiota also stimulates the development of the immune system and assists the host by excluding pathogens. Studies have revealed how members of the intestinal microbiota are able to manipulate host physiology to the benefit of both microbe and host (Kelly et al., 2004). Community composition and metabolic activity of the microbiota are influenced by a variety of factors including the diet and health status of the host (De Filippo et al., 2010; Lindsay et al., 2006). Likewise, the resident microbiota may also be an important factor in a number of diseases or conditions, including colon cancer, inflammatory bowel diseases, and obesity (O'Keefe et al., 2009; Sokol et al., 2008; Turnbaugh et al., 2009a). Furthermore, this large and dynamic community undergoes dramatic changes after initial colonisation of the host at birth, and develops through weaning and maturity (Hooper, 2004).

Due to the potential for beneficially influencing function and health by manipulating the intestinal microbiota, there is much interest in the use of dietary supplements. In particular, engineering the microbiota through dietary intervention in the young when the large bowel community is in transition and still undergoing major changes may be a useful strategy for promoting health benefits later in life. Commonly used dietary supplements include prebiotics and probiotics. Prebiotics are a term used to describe food ingredients that resist degradation and absorption in the upper digestive tract and selectively enrich the population or metabolic activity of one or a limited number of resident bacteria that are beneficial to the host (Gibson and Roberfroid, 1995), while probiotics are

live microorganisms that are thought to confer a health benefit when administered in adequate amounts (Fuller, 1989). The most commonly used probiotics are strains of lactobacilli and bifidobacteria, but others may also include some bacilli and yeasts. However, the mechanisms of action for the effects of dietary supplements such as prebiotics or probiotics on host physiology are poorly understood, and many health claims for supplement use are not adequately supported by scientific evidence. Therefore, this study examined the interactions between diet, microbiota and the large bowel during the post-weaning phase using a rat model. Diets supplemented with carbohydrates that resist mammalian digestive enzymes were fed to newly-weaned male Sprague-Dawley rats. Following dietary intervention, changes in microbial community composition and biomarkers of large bowel function were examined.

1.1 Large bowel ecosystem

The large bowel comprises the caecum and colon. In humans, the caecum is a small rudimentary structure that terminates in the vermiform appendix. However, in many other animals, such as rodents and pigs, the caecum is much more prominent. The large bowel is a nutrient dense environment encompassing a complex ecosystem that houses vast numbers of microorganisms. Despite the suitability of this habitat for microbial life, selection pressures within the adult human intestine result in a microbiota predominantly comprised of members from just two bacterial phyla – the Gram-negative Bacteroidetes and low G+C content, Gram-positive Firmicutes (Backhed et al., 2005; Qin et al., 2010). Of the 55 known bacterial phyla, only a further 6 have been identified in the adult human gastrointestinal tract (Backhed et al., 2005; Costello et al., 2009). In contrast, ecosystems such as soil are known to harbour 20 or more bacterial phyla (Backhed et al., 2005). Although microbial diversity at the phyla level is limited in the large bowel, there is broad phylogenetic diversity within the phyla present. The human intestine is thought to be inhabited by over 800 bacterial species, most of which belong to the clostridial cluster XIVa group, clostridial cluster IV group, and *Bacteroides-Prevotella* group (Turnbaugh et al., 2010). Also resident, but in

smaller numbers, are members of the Actinobacteria and Proteobacteria phyla. Fungi and Archaea can also be found, but collectively they account for only 1% of the microbiota in the large bowel (Eckburg et al., 2005; Palmer et al., 2007). Furthermore, diversity of the Archaea in the human large bowel is limited to only two described species, *Methanobrevibacter smithii* and *Methanosphaera stadtmanae* (Duncan et al., 2007b; Eckburg et al., 2005).

The large bowel is the primary site of microbial colonisation with bacterial concentrations reaching $10^{11} – 10^{12}$ per gram of content (Leser and Molbak, 2009). In contrast, the stomach and proximal ileum contain far fewer numbers of bacterial due to low pH and rapid flow rate. Bacterial concentrations in this region are typically $10^3 – 10^5$ per gram of content, which are mainly composed of acid-tolerant lactobacilli and streptococci (Hayashi et al., 2005; Leser and Molbak, 2009). Bacterial diversity and densities increase dramatically further down the intestinal tract. The distal ileum contains up to 10^8 microbes per gram of content and is considered a transitional zone between the small intestine and large bowel. Within the large bowel itself, three distinctive habitats have been described. Firstly, there is the firmly attached layer of the mucus that covers the epithelium which forms a protective barrier and is only sparsely populated with bacteria (Johansson et al., 2008). Above the firmly attached mucus is a loosely adherent layer of mucus that is densely populated with mucus-associated bacteria (Johansson et al., 2008). Finally, the large bowel lumen and digestive residues contain vast numbers of microbes that collectively function as an anaerobic bio-reactor capable of harvesting carbon and energy from indigestible plant-derived polysaccharides (Louis et al., 2007).

The understanding of the bacterial community composition has been gained initially through culture-based methods. However, culture-independent nucleic acid based methods indicate that the majority of resident bacterial species have yet to be cultured in the laboratory (Eckburg et al., 2005; Rajilic-Stojanovic et al., 2007; Turnbaugh et al., 2010). Therefore, the best estimates of bacterial

species diversity stem from molecular phylogenetic methods of identification. Analysis of the variable regions of the 16S rRNA gene and fingerprinting methods, such as denaturing gradient gel electrophoresis (DGGE), have proved to be invaluable tools for elucidating community composition and diversity (Clarridge, 2004). The advent of next generation, high throughput sequencing technologies has further expanded the understanding of the intestinal microbiota structure and function. These will undoubtedly continue to provide additional insights as their use becomes more widespread. Diversity estimates continue to rise with the identification of previously unknown bacteria using next generation sequencing technologies. However, when considering diversity estimates gained from these methods, it is becoming apparent that some of these numbers may be somewhat inflated due to sequencing errors (Reeder and Knight, 2009). In a recent study where known mixtures of microbes were characterised by 454 pyrosequencing of 16S rRNA genes, it was found that the estimate of diversity was up to an order of magnitude higher than the true value, depending on the methods used for data analysis (Quince et al., 2009). Nevertheless, it is clear the large bowel houses a highly diverse microbiota at the species level. It is also important to recognise that the ecosystem of the large bowel is extremely dynamic. At any given time, the microbiota present is composed of established resident bacteria that form long term associations with the host (autochthonous components) and transient bacteria introduced from ingested food, water and the environment (allochthonous components) that do not colonise the gastrointestinal tract.

Often referred to as commensal bacteria, members of the microbiota are perhaps more accurately described as mutualists. In exchange for providing nutrients and a suitable habitat, they endow humans with a number of attributes that would otherwise be absent. Far from being mere bystanders, the enormous contingent of microbes residing in the large bowel has been recognised to play an active role in maintaining health and development. In broad terms, the microbiota is involved in three interrelated processes that directly affect their host: (1) energy harvest, (2) stimulation of cellular proliferation, and (3) stimulation and of the immune system.

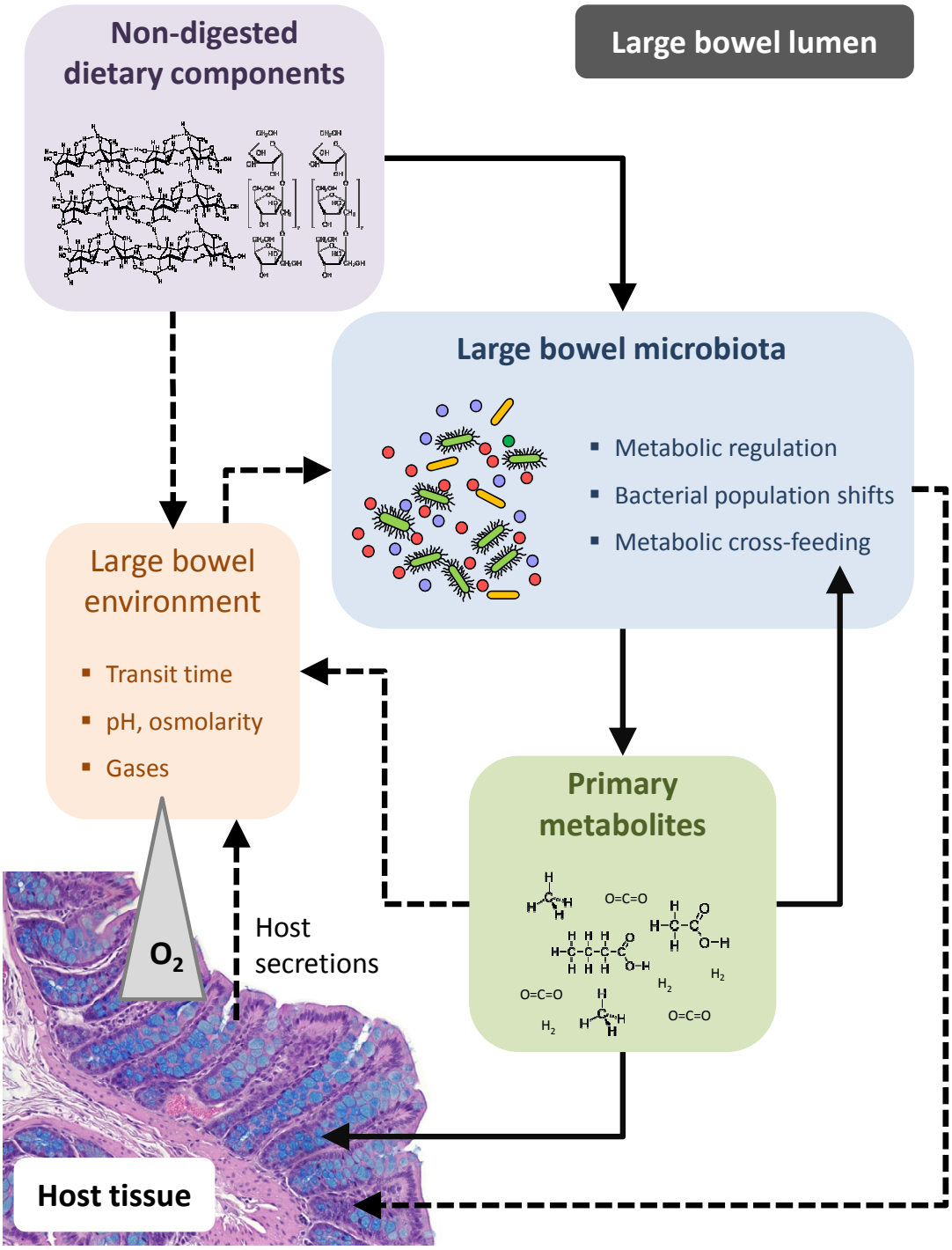

Figure 1. Diagram of the large bowel ecosystem. Solid arrows indicate direction of metabolic flows and dashed arrows indicate other influences. Non-digested dietary components may be metabolised by members of the resident microbiota resulting in primary metabolites that are absorbed by the host and/or metabolised by other members of the microbiota. Shifts in bacterial populations may have further downstream effects on interactions with immune components of host tissue and metabolic flows. Figure adapted from Louis et al., 2007.

1.2 Bacterial carbohydrate metabolism

Bacteria in the large bowel are only able to access host produced substrates, such as mucins, or dietary residues that escape digestion in the upper intestinal tract. Dietary materials that are not broken down or absorbed in the small intestine pass into the large bowel where they provide a source of nutrients and energy to the resident microbial community. The association of diets rich in dietary fibre with a reduced incidence of gastrointestinal diseases was observed in an early study by Burkitt when he compared western populations with those in developing countries such as Africa, Pakistan and India (Burkitt, 1973). Another early study found that patients with diverticular disease that were given diets supplemented with wheat bran showed a marked relief of symptoms (Painter et al., 1972). Since these early studies, there has been great interest in the bacterial metabolism of carbohydrates that are resistant to mammalian digestive enzymes.

1.2.1 Defining digestion resistant carbohydrates

Traditionally, non-digestible plant materials have been referred to as 'dietary fibre'. However, beyond this broad description, defining dietary fibre is surprisingly difficult. The major component of dietary fibre is the carbohydrate cellulose, the most abundant biomaterial on Earth (Goodlad and Englyst, 2001). Although composed entirely of glucose units, cellulose cannot be degraded by mammalian digestive enzymes due to the arrangement of the linkages between units. Lignin, perhaps the second most abundant organic polymer, is another major non-digestible plant material (Goodlad and Englyst, 2001). Unlike cellulose, lignin is not a carbohydrate, but is instead a complex polyphenol biopolymer. Dietary fibre also encompasses compounds such as waxes, cutins and phytosterols (Gray, 2006).

In the interests of clarification, this study will use the term 'digestion resistant carbohydrates' (DRC), rather than 'dietary fibre'. The definition of DRC is restricted to carbohydrates composed of three or

more monosaccharide units that are resistant to digestion in the small intestine.

1.2.2 Carbohydrate breakdown and energy harvest

The microbiota in the large bowel ferment DRC to form CO_2, H_2, lactic acid, succinic acid, and short chain fatty acids (SCFA) such as acetic, propionic and butyric acid (Figure 2) (Miller and Wolin, 1979). These SCFA are an important source of energy and carbon for both microbes and host. It has been estimated that 5-10% of total energy requirements for humans are acquired from SCFA (McNeil, 1984). In animals with a relatively large bowel and well developed caecum, microbial derived SCFA may account for up to 40% of their energy intake (McNeil, 1984). Furthermore, it has been shown that butyric acid is a major source of energy for colonocytes in rats and humans, with up to 80% of oxygen consumption in those cells due to butyrate oxidation (Ardawi and Newsholme, 1985; Roediger, 1980, 1982). Indeed, butyrate is thought to be the preferred energy source for colonocytes, and is rapidly absorbed by the epithelium (Roediger, 1982). The importance of bacteria-derived nutrients is highlighted by studies using germ-free mice. These studies show germ-free mice require 30% more calories than conventionally raised mice in order to maintain the same body weight (Coates, 1975). Feeding DRC in the form of guar gum has been shown to increase crypt cell proliferation in the caecum and colon of mice colonised with a resident microbiota, but these proliferative effects did not occur in germ-free mice (Pell et al., 1995). Germ-free rodents are also characterised by reduced fat deposition and enlarged caecums resulting from a substantial build-up of luminal fluid and mucins (Backhed et al., 2007; Coates, 1975; Crawford et al., 2009; Fontaine et al., 1996). However, amounts of mucosa-associated mucin are lower than that found in colonised rodents (Kleessen et al., 2003). Colonisation of germ-free rats also resulted in an increase of the proportion of acidic mucins in the luminal content (Fontaine et al., 1996). This increase in luminal mucin accumulation in germ-free rodents is not yet fully understood, but may be influenced by the lack of bacterial mucinases in the large bowel (Coates, 1975).

The amount and type of DRC that reaches the large bowel can have a major impact on the microbial community composition and metabolism. A wide range of DRC can be found in dietary material, but the primary component is usually insoluble plant complex carbohydrates (Gray, 2006). This is typically composed of plant cell wall polysaccharides and various storage oligosaccharides and polysaccharides such as inulin, a fructose polymer with a terminal glucose unit (Niness, 1999). Other forms of DRC include β-glucans, glucomannans, and starches that escape digestion in the small intestine (Englyst et al., 2007). These polysaccharides have a diverse range of physical and chemical properties, and may exhibit various states of solubility, chain length, secondary structures, and associations with other molecules. Starches that would otherwise be readily digested may be physically protected from enzymes in the small intestine by plant cell wall polysaccharides, or they may occur as insoluble particles suspended in a colloidal solution (Englyst et al., 2007). Components of digestion resistant plant cell wall polysaccharides such as arabinose and xylan may become available following their release from plant structures. A consequence of this diversity of substrates is the creation of a huge number of ecological niches that become available for occupation.

The 2.85 Gb human genome contains only 98 known or predicted glycoside hydrolases, which are enzymes that hydrolyse the glycosidic link in complex carbohydrates to produce two smaller sugars (Backhed et al., 2005). Furthermore, the human genome is deficient in enzymes that target common components of dietary fibre, such as pectin-, xylan-, and arabinose-containing carbohydrates (Backhed et al., 2005). However, it has been estimated that the metagenome of the large bowel microbial community may contain over 100 times the number of genes than that of the human genome (Ley et al., 2006a; Qin et al., 2010). This represents a rich source of metabolic potential and provides humans with carbohydrate degrading capabilities that they would otherwise lack. The microbiota allows the host to readily utilise glycans such as pectins and hemicelluloses. Although cellulolytic bacteria can be found in the large bowel of humans and rodents, cellulose, the most abundant plant cell wall glycan, remains highly resistant to fermentation (Smith et al., 1998).

However, the fermentability of cellulose appears to be related to its structure: purified crystalline cellulose is highly resistant to degradation, while up to 70% of cellulose from dietary fibre may be fermented in the large bowel (Slavin et al., 1981; Smith et al., 1998).

In contrast to humans, the 6.3 Mb genome of a prominent carbohydrate degrading member of the large bowel microbiota, *Bacteroides thetaiotaomicron*, contains a huge assortment of genes involved in binding and metabolising carbohydrates (Backhed et al., 2005). These include 226 predicted glycoside hydrolases, 15 polysaccharide lysases, and 163 paralogs of 2 extracellular proteins (SusC and SusD) involved in glycan binding and transport (Sonnenburg et al., 2006; Sonnenburg et al., 2005). This broad array of genes allows *B. thetaiotaomicron* to metabolise both host derived mucin O-linked glycans and dietary glycans such as starches, fructans, pectins, and hemicelluloses (Sonnenburg et al., 2005). Feeding polysaccharide enriched diets to gnotobiotic mice colonised with *B. thetaiotaomicron* resulted in increased expression levels of a subset of starch utilisation system paralogs (SusC and SusD), xylanases, arabinosidases, and pectate lyase in the transcriptome of this bacteria (Martens et al., 2009b; Sonnenburg et al., 2005). In contrast, *B. thetaiotaomicron* colonised mice fed simple sugar diets lacking polysaccharides resulted in elevated transcription of an alternate set of SusC and SusD paralogs, and glycoside hydrolases involved in catalysing mucin derived carbohydrates (Sonnenburg et al., 2005). *Bacteroides thetaiotaomicron* has also been shown to expand the diversity of glycans targeted for degradation when colonised with *Bifidobacterium longum* in gnotobiotic mice. Mechanisms for utilising mannose- and xylose-containing carbohydrates are up-regulated and occur independently of host genotype (Sonnenburg et al., 2006).

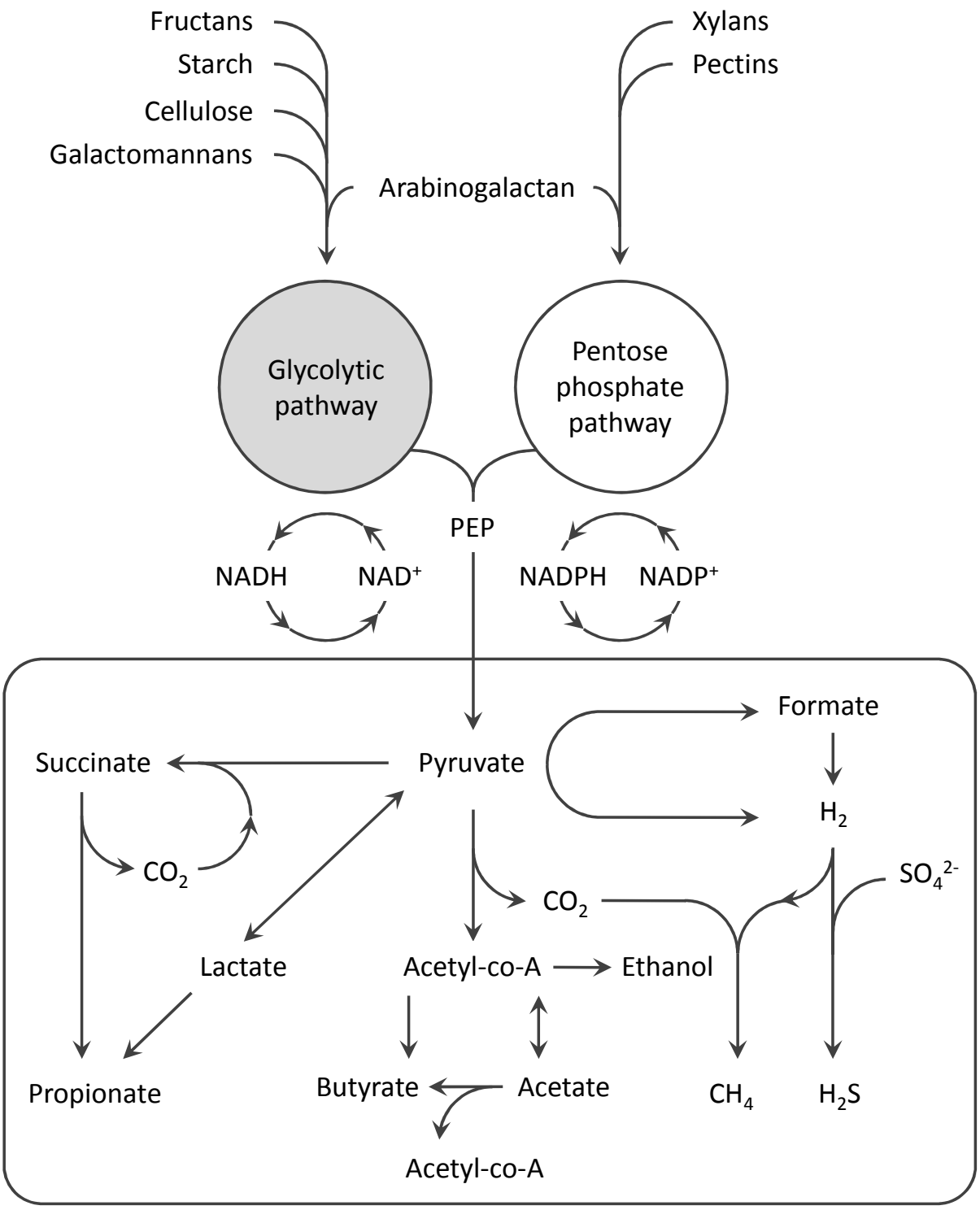

Figure 2. Diagram of polysaccharide breakdown pathways. Polysaccharide fermentation pathways in the large bowel leading to formation of major fermentation products. PEP, phosphoenolpyruvate. Adapted from Macfarlane and Macfarlane (2003).

Despite the ability of phylogenetically diverse microbes to attain new metabolic capabilities by lateral gene transfer (LGT), the ability to function as anaerobic fermenters in the large bowel is largely limited to members of the Bacteroidetes and Firmicutes (Ley et al., 2006a). Genetic rearrangement events such as LGT have been shown to play an important role in directing the adaptation of Bacteroidetes to function in the large bowel environment (Xu et al., 2007). Moreover, a recent study has shown that the resident microbiota is able to acquire genes from environmental microbes by LGT. The transfer of seaweed carbohydrate degrading enzymes from *Zobellia galactanivorans*, a marine Bacteroidetes, to the intestinal bacteria *Bacteroides plebeius* isolated from Japanese individuals was demonstrated through genomic and functional analyses (Hehemann et al., 2010). However, the known differences in G+C content between the Bacteroidetes and Firmicutes would seem to indicate that continual exchange of genes between the two groups has not occurred throughout their evolution, as their genomes remain distinct (Ley et al., 2006a). Therefore, it seems likely their co-dominance in the large bowel community is a result of their distinct and complementary metabolic activities.

Direct competition for limited resources is a precarious proposition for participants. Each competitor faces the risk of being eliminated if it is unable to overcome their opposition. However, competition can be avoided if community members are able to partition resources or co-operate, possibly creating new ecological niches in the process. Resource partitioning occurs when a new niche and previously unused resources become available. For example, *Escherichia coli* has been shown to populate diverse niches when mono-associated with germ-free mice (Ley et al., 2006a).

The process of diversification can lead to further diversity as new niches are created. Bacteria which adhere to particulate material in the large bowel are similar in composition to unattached colonies when analysed using culture based methods (Macfarlane and Macfarlane, 2006). However, it is likely that these different groups of bacteria occupy different roles in the intestinal ecosystem. Adherent

populations have been shown to be more efficient at degrading polysaccharides, while nonadherent bacteria fermented oligosaccharides more rapidly (Macfarlane and Macfarlane, 2006). Furthermore, the two groups appeared to have distinct metabolic activities, with acetate being the predominant SCFA produced by adherent colonies, while nonadhering populations produced higher levels of butyrate (Macfarlane and Macfarlane, 2006). This suggests that bacteria which are otherwise similar may exert quite distinct effects on the host through alterations in the large bowel ecosystem.

Microbial communities are able to form complex chemical food networks, whereby metabolites from one organism can act as a substrate for another, which in turn may enhance the activity of the first by producing new substrates or removing waste material. For example, cellulolytic bacteria in the large bowel may require the ability to breakdown matrix polysaccharides such as xylan-, pectin-, and mannan-containing carbohydrates in order to access cellulose fibrils. However, the solubilised products from the matrix polysaccharides are not necessarily utilised by the degrading bacteria themselves, which therefore become available for other microbes in the community (Duncan et al., 2004a).

Microbial interactions and substrate utilisation kinetics have also been demonstrated with cross-feeding experiments using co-cultures of *Bifidobacterium longum* BB536, and two acetate-converting, butyrate producing large bowel bacteria, *Anaerostipes caccae* DSM 14662 and *Roseburia intestinalis* DSM 14610, with oligofructose as the sole energy source (Falony et al., 2006). *Anaerostipes caccae* DSM 14662 is unable to degrade oligofructose, and therefore cannot survive on this substrate. However, in co-culture, *A. caccae* DSM 14662 was able to grow on fructose and acetate released from the degradation of oligofructose by *B. longum* BB536. In contrast, *R. intestinalis* DSM 14610 is able to degrade oligofructose, but it was only able to grow after the addition of acetate provided by the degradation of oligofructose by *B. longum* BB536. Lactate is another fermentation waste product released by many *Bifidobacterium* species. Their fermentation

efficiency is increased by the presence of lactate fermenters such as *Eubacterium hallii*, which in turn produce butyrate as a waste (Belenguer et al., 2006; Duncan et al., 2004b). Subsequently, butyrate becomes available for use by the host. It is conceivable that a butyrate producing consortium as a whole would be more favourably selected for by the host over communities that produced less favourable by-products.

Further examples of diet, microbe and host interactions in the large bowel are illustrated in studies using gnotobiotic mice mono-associated with *B. thetaiotaomicron* or butyrate producing *Eubacterium rectale*, or co-colonised with both. In the presence of *E. rectale*, *B. thetaiotaomicron* stimulates the production of host derived mucosal glycans that it can exploit, but *E. rectale* is unable to use (Mahowald et al., 2009). In addition, *B. thetaiotaomicron* increases expression levels of a wide variety of polysaccharide utilisation loci (PUL) to expand the variety of carbohydrates targeted (Mahowald et al., 2009). In response to *B. thetaiotaomicron* co-colonisation, *E. rectale* decreases transcription of its own glycan degrading enzymes, and instead increases expression levels of a number of carbohydrate transporters (Mahowald et al., 2009). Co-colonisation with *B. thetaiotaomicron* also appears to stimulate increased conversion of acetate to butyrate by *E. rectale*. Although net butyrate concentrations in the caecum were unchanged between mice colonised with *E. rectale*, or co-colonised with *E. rectale* and *B. thetaiotaomicron*, host expression of a butyrate transporter, MCT-1, were significantly up-regulated in the mucosa (Mahowald et al., 2009). Manipulation of the diet in these experiments has been also shown to alter bacterial colonisation levels and butyrate production in co-colonised mice. Colonisation levels of *E. rectale* and caecal butyrate concentrations were lower in mice that had been fed high sugar diets rich in sucrose, maltodextrose and cornstarch, whereas *B. thetaiotaomicron* colonisation levels remained unchanged (Mahowald et al., 2009). Transcriptome analysis of both species showed that *B. thetaiotaomicron* was able to shift expression of PUL targeting plant polysaccharides to those involved in utilising host produced glycans in response to a high sugar diet. In contrast, *E. rectale* lacks the machinery to

utilise host mucosal polysaccharides, and in response to a high sugar diet, reduced the expression levels of several genes encoding glycoside hydrolases and sugar transporters. These observations, in conjunction with the ability of the host to utilise the simple sugars present in the high sugar diet, may explain the lowered colonisation levels of *E. rectale*.

In addition to fermentation, other metabolic pathways are also employed by the microbiota. However, their utilisation is often limited to certain phylogenetic lineages. Sulphate reduction is carried out by Deltaproteobacteria and *Desulfotomata* species within the Firmicutes, and methane production is limited to the Archaea (Conway de Macario and Macario, 2009; Ley et al., 2006a). In contrast, fermentation is a widespread capability in the large bowel community and is a principal energy pathway for the Bacteroidetes and Firmicutes, which constitute the majority of the microbiota (Ley et al., 2006a).

The network of food, microbe and host interactions have the potential to be incredibly complex and are subject to large changes as the community adjusts to variations in substrate and energy availability. The collective activities of the community members become a characteristic property of the community and may have wide ranging effects on the host. Therefore, it is likely the composition and metabolic profile of the microbiota is shaped by early colonisation events and complex interactions between diet, microbial community members and the host.

1.2.3 Plant cell wall associated carbohydrates

Plant cell walls are a major source of digestion resistant materials that reach the large bowel. The primary polysaccharides that make up plant cell walls are cellulose, hemicellulose and pectin. The cellulose microfibrils form a complex network linked by hemicelluloses polymers, which is embedded in a pectin matrix. Cellulose is a linear polymer composed of up to ten thousand $\beta(1\rightarrow4)$ linked D-glucose units. In contrast, hemicellulose is a branched polysaccharide made up of xylose in

conjunction with other monomers, which may include arabinose, mannose, galactose and rhamnose. Pectins are complex structural polysaccharides containing 1,4 linked α-D-galactosyluronic acid residues. Hemicellulose and pectin are readily degraded by bacteria resident in the large bowel of humans and rodents (Hove and King, 1979; Macfarlane et al., 1998; Nyman and Asp, 1982). However, microbial breakdown of cellulose in the large bowel of non-ruminants is incomplete (Slavin et al., 1981). While many, if not most, bacteria in the large bowel produce enzymes that target isolated polysaccharides, it appears very few possess the complex machinery required to breakdown cellulose rich plant cell wall material.

1.2.4 Resistant starch

Much like cellulose, starch is a carbohydrate comprised of glucose units. Whereas cellulose is quite simple in structure, starch is more complex. It is composed of amylose, a helical polymer of primarily α(1→4) linked glucose units, and amylopectin, a highly branched polymer of glucose. Starch is ubiquitous in all green plants and is used as a storage carbohydrate. As such, it is a major source of carbohydrate in the human diet and is present in staple foods such as potatoes, wheat, maize, and rice. Starches that are high in amylopectin tend to be more easily digested by mammalian digestive enzymes (Englyst et al., 2007). The fraction of starch which escapes digestion by host amylases, known as resistant starch (RS), are an important source of fermentable substrates that reach the large bowel.

RS is found in a number of forms with differing physical and chemical properties, which affect their digestibility and fermentability. Different forms of RS are usually classified into four main types based on these properties (Englyst et al., 2007). RS1 type starches are those that are physically trapped within plant cells and food matrices, such as partially milled and whole grains. RS2 are α-amylase resistant native starch granules, such as that found in raw potatoes and green bananas. RS3 consists of retrograded starches, which are formed by cooking and cooling starch containing foods.

RS4 are starches that have been chemically modified to prevent digestion by amylolytic enzymes. Other properties that may also influence digestibility and fermentation patterns of different sources of RS include granule size and variations in proportion of RS. Due to the diversity in forms of RS, they are likely to have different effects on microbial community activity and host physiology, although feeding RS has consistently been shown to increase large bowel SCFA concentrations in human and animal studies (Jenkins et al., 1998; Le Leu et al., 2009).

The starch degrading machinery of *B. thetaiotaomicron* has been extensively studied. The genome contains multiple genes organised into numerous PUL that are involved in glycan binding, breakdown, and transport (Martens et al., 2009b). Outer membrane binding proteins SusC and SusD attach to starch molecules where they are hydrolysed by SusG, a cell surface α-amylase. Released breakdown products are transported into the periplasmic compartment by SusC (Martens et al., 2009a). Here, the internalised oligosaccharides are further degraded into their component sugars by hydrolases SusA and SusB. Other amylolytic bacteria found in the large bowel include some high G+C content Gram positive *Bifidobacterium* species, and low G+C content Gram positive anaerobes such as *Butyrivibrio fibrisolvens* 16 ⁄ 4 and *Roseburia inulinivorans* A2-194 (Macfarlane and Englyst, 1986; Ramsay et al., 2006).

A number of studies have shown that feeding RS increases large bowel SCFA concentrations and modifies microbial community structure (Bauer-Marinovic et al., 2006; Jenkins et al., 1998; Le Blay et al., 2003). Animal studies have also shown that dietary RS may be able to modulate host physiology in a beneficial manner through epithelial repair as RS has been shown to reduce dextran sulphate sodium (DSS) induced colonic injury in rats (Moreau et al., 2003). Dietary administration of RS3 has also been shown to lower the incidence of tumour formation in a 1,2-dimethylhydrazine-induced rat model of colon cancer (Bauer-Marinovic et al., 2006). Furthermore, recent findings show that RS

increases apoptotic responses to azoxymethane induced DNA damage in the colon of rats (Le Leu et al., 2009).

1.2.5 Inulin

Inulin and fructo-oligosaccharides (FOS) are linear polymers of β(2→1) linked fructose units with a terminal glucose residue. Polymers of 3-9 sugar units are generally classified as FOS, while longer chain polymers of up to 60 units are known as inulin, which is less soluble than FOS due to its longer chain length. Most commercially available inulin and FOS are extracted from chicory root or synthesised from sucrose. The presence of β(2→1) links protect inulin and FOS from digestion by mammalian digestive enzymes (Roberfroid, 2007).

Inulin and FOS have been shown to be almost completely fermented by the large bowel microbiota (Macfarlane et al., 1998). Both inulin and FOS have been demonstrated to expand populations of bifidobacteria and lactobacilli in the large bowel, and have therefore been classified as prebiotics (Gibson and Roberfroid, 1995). Although early studies examining the effects of inulin and FOS have focussed on the responses of these two groups of bacteria, it is clear that other members of the community are also stimulated. While many strains of *Bifidobacterium* species have been shown to grow on FOS as a substrate, few are able to grow in monoculture with inulin as a substrate (Rossi et al., 2005). However, bifidobacteria have been shown to utilise mono- and oligosaccharides produced by primary inulin degraders in batch cultures inoculated with human faecal slurries (Rossi et al., 2005). Similar to bifidobacteria, the ability to ferment inulin is not a common trait among lactobacilli. Although several *Lactobacillus* species are able to degrade FOS (Kaplan and Hutkins, 2000), only *Lactobacillus paracasei* has been shown to ferment inulin (Goh et al., 2007; Makras et al., 2005). Changes in bacterial metabolism, represented by alterations in RNA DGGE profiles, but not community structure, identified by DNA DGGE profiles, have also been observed in human faecal *Bifidobacterium adolescentis* following dietary supplementation with FOS (Tannock et al., 2004). The

variation observed in bacterial responses to inulin and FOS is most likely due to a combination of differences in polysaccharide chain length and microbial community composition.

A common effect of dietary supplementation with inulin or FOS is a net increase of butyric acid in the large bowel. However, inulin and FOS are primarily fermented by acetate and lactate producing bacteria. Stable isotope labelling experiments using ^{13}C showed that newly synthesised butyrate produced in faecal batch cultures following the addition of FOS was primarily derived from acetate and lactate conversion (Morrison et al., 2006). It is likely that inulin and FOS-induced production of butyrate in the large bowel is, at least in part, the result of stimulation of bacteria from the clostridial cluster XIVa group. Many members of this group form a major component of the microbiota and include many known butyrate producers (Falony et al., 2009). Feeding inulin and FOS to germ-free rats colonised by a human faecal microbiota has been shown to increase numbers of bacteria belonging to the clostridial cluster XIVa group in the colon, caecum and faeces (Kleessen et al., 2001).

Inulin and FOS are the subject of substantial interest due to a number of potentially health promoting properties. Dietary supplementation with inulin has been shown to increase Mg^{2+} and Ca^{2+} uptake in the caecum of rats (Coudray et al., 2005). Fermentation products of inulin-type fructans from faecal cultures have also been shown to decrease proliferation and promote apoptosis in two human cancer cell lines (Munjal et al., 2009). There is also evidence that FOS may exert anti-inflammatory effects *in vivo*. Administration of inulin and FOS, either alone or in combination with *B. infantis*, has been shown to ameliorate the severity of DSS-induced colitis in rats (Osman et al., 2006). In another study, the severity of inflammation in transgenic rats (HLA-B27) that spontaneously develop bacteria-dependent colitis was reduced by feeding inulin (Hoentjen et al., 2005). This reduction in colonic inflammation was also associated with a shift in microbial community profiles, with an increase in caecal *Lactobacillus* and *Bifidobacterium* populations.

1.2.6 Konjac glucomannan

Konjac glucomannans are soluble polysaccharides derived from the tuber of *Amorphophallus konjac* C. Koch, where they function as energy reserves. Glucomannan is primarily a straight chain polymer of β(1→4) linked D-mannose and D-glucose units, with a small degree of branching through β(1→4) glucosyl linkages (Katsuraya et al., 2003). The constituent mannose and glucose sugar units are present in a ratio of 1.6:1 (Katsuraya et al., 2003). Flour produced from konjac corms is commonly used as a gelling and thickening agent in Asian countries. *Amorphophallus konjac* corms are comprised of up to 75% glucomannan by dry weight (Li et al., 2005).

Konjac glucomannan is resistant to hydrolysis by digestive enzymes in the small intestine, and reaches the large bowel where it becomes a substrate for microbial fermentation (Farage Hashmi et al., 2007; Inoue, 1942). Human and animal studies show dietary konjac glucomannan elevates large bowel SCFA concentrations and modifies the microbial community composition (Chen et al., 2006; Chen et al., 2005). Human subjects consuming konjac glucomannan supplemented diets exhibited higher faecal bifidobacteria and lactobacilli counts (Chen et al., 2006; Chen et al., 2008). In addition to effects on microbiota metabolism and composition, feeding konjac glucomannan has also been shown to influence aspects of host physiology. Rats fed high viscosity konjac glucomannan showed an increase in luminal accumulation of mucin and higher numbers of mucus producing goblet cells in the small bowel (Ito et al., 2009). Furthermore, konjac flour has been shown to exhibit anti-obesity properties by reducing weight gain and fat deposition in rats fed high fat diets (Li et al., 2005).

1.2.7 β-glucans

Non-cellulosic β-glucans are a diverse group of polymers composed of β(1→3) and (1→4) or (1→6) linked glucose units (Muralikrishna and Rao, 2007). Commercially available sources of β-glucans are commonly derived from the cell wall of *Saccharomyces cerevisiae*, and grains such as oats and barley.

Like cellulose, non-cellulosic β-glucans are unaffected by digestive enzymes in the small intestine. However, unlike cellulose, β-glucans are readily fermented by the intestinal microbiota in the large bowel of humans and rodents, resulting in altered microbial community composition and net increases in luminal and faecal SCFA concentrations (Drzikova et al., 2005; Snart et al., 2006).

1.2.8 Seaweed

Other sources of DRC include red and brown seaweeds. Both types of algae have a DRC content that can account for up to 35% of dry weight (Goni et al., 2001). Seaweeds are commonly used food ingredients in the Asian countries. The most frequently consumed seaweeds include the brown algae *Undaria pinnatifida*, and the red algae *Porphyra tenera*, more commonly known as wakame and nori, respectively.

The digestion-resistant fraction of polysaccharide found in brown algae is predominantly composed of laminarans, alginates, fucans and cellulose (Jiménez-Escrig and Sánchez-Muniz, 2000). The major matrix polysaccharide in brown algae is alginate, a polymer consisting of homopolymeric blocks of β(1→4) linked D-mannuronate and α-L-guluronate. The primary polysaccharides in red algae are sulphated galactans (agar and carrageenans), xylans, mannans and cellulose (Jiménez-Escrig and Sánchez-Muniz, 2000).

Alterations in the large bowel microbial activity by wakame and nori have been examined in rat experiments. Rats fed edible seaweed had lower caecal concentrations of SCFA than those in the cellulose control group (Goni et al., 2001). Furthermore, caecal inoculum from rats fed seaweed exhibited reduced *in vitro* fermentative ability using a variety of carbohydrate substrates compared to that from rats fed cellulose control diets (Goni et al., 2001). Because seaweed is not a food ingredient that laboratory rats are commonly exposed to, these findings probably reflect a lack of evolutionary adaptation on the part of the microbiota for the breakdown of these carbohydrate

substrates. In contrast, seaweed polysaccharides are readily fermented *in vitro* by human faecal bacteria (Michel et al., 1996).

1.2.9 Fermentation products in the large bowel

Fermentation by anaerobic bacteria in the large bowel is an important process for obtaining energy from the oxidation of organic compounds. The principal substrates are carbohydrates, for which the diverse microbial population produce a rich arsenal of enzymes required to catabolise them. However, not all carbohydrates are degraded at the same rate. Starch and pectin are fermented more rapidly by human faecal bacteria than xylan or arabinogalactan (Macfarlane and Macfarlane, 2003; Macfarlane et al., 1998). Different carbohydrates are preferentially degraded by intestinal bacterial, which give rise to distinct patterns of SCFA formation (Macfarlane and Macfarlane, 2003; Macfarlane et al., 1998). Acetate has been shown to be the primary fermentation product of pectin and xylan, while arabinogalactan breakdown gives rise to acetate and propionate (Macfarlane and Macfarlane, 2003).

The major fermentation products include SCFA (acetic, propionic and butyric acid), lactate, succinate, CO_2, and H_2. Most intestinal bacteria use the Embden-Meyerhof-Parnas pathway of glycolysis to produce pyruvate, the primary precursor of fermentation products, from glucose-6-phosphate (Miller and Wolin, 1979). Lactate is produced from pyruvate by the action of NADH dependent lactate dehydrogenase (Miller and Wolin, 1979). The addition of a carboxyl group to pyruvate forms oxalacetate, which is eventually converted to succinate, a precursor for propionate (Miller and Wolin, 1996). Acetate is converted from acetyl coenzyme A (acetyl-CoA), which in turn is produced by the oxidation of pyruvate (Miller and Wolin, 1996). Acetyl-CoA can also be converted into butyrate through a number of intermediate steps via the butyrate kinase, or butyryl-CoA CoA transferase pathways (Charrier et al., 2006). Human intestinal bacteria are also capable of producing butyrate

using lactate as a precursor (Bourriaud et al., 2005). Ethanol, H_2 and CO_2 are also produced from pyruvate (Miller and Wolin, 1979, 1996).

Although the conversion of pyruvate into fermentation products is a widely used route for most members of the microbiota, a noticeable exception occurs in bifidobacteria, which utilise an alternate pathway to produce primarily acetate and lactate as fermentation products (Miller and Wolin, 1979). Aldolase, an enzyme required for glycolysis, and glucose-6-phosphate dehydrogenase, a component of the hexosemonophosphate pathway, are absent in bifidobacteria (de Vries and Stouthamer, 1967). In the absence of a detectable glycolytic system or hexosemonophosphate shunt pathway, bifidobacteria have been shown to produce acetate from glucose via the phosphoketolase pathway (de Vries and Stouthamer, 1967; Wolin et al., 1998).

The major SCFA found in the faeces and large bowel contents are acetate, propionate and butyrate. The precise proportion of these acids may depend on a number of factors including diet, community composition and host genotype. Acetate forms the largest component, typically comprising 60-75% of the total SCFA pool (Miller and Wolin, 1996). Substantial quantities of acetate are also used during butyrate synthesis (Duncan et al., 2004a; Miller and Wolin, 1996). Numerous bacterial groups produce acetate, but groups that form propionate and butyrate are more restricted in the large bowel. These groups have been the focus of many studies due to the potential influence of propionate and butyrate on host physiology and health. Propionate is thought to play a role in regulating energy metabolism and lipogenesis by stimulating expression of leptin, an appetite suppressing hormone, in adipose tissue (Xiong et al., 2004). Propionate may also be involved in the regulation of inflammation by down-regulating resistin, a pro-inflammatory cytokine (Al-Lahham et al., 2010). In contrast, butyrate is the primary energy source for colonocytes and has been shown to stimulate intestinal mucosal growth in healthy rats (Kripke et al., 1989; Roediger, 1980). There is also evidence that butyrate may reduce inflammation in the colon and modify physiological processes

associated with colorectal cancer (Le Leu et al., 2009; O'Keefe et al., 2009; Saemann et al., 2000; Segain et al., 2000).

1.3 Diversity and composition of the large bowel microbiota

1.3.1 Establishment of the microbiota

Colonisation of the newborn gastrointestinal tract begins immediately during the birth process. Enterobacteria and streptococci are among the first bacteria to be detected in the faeces, and colonisation by *E. coli* occurs within 48 hours (Mackie et al., 1999; Mah et al., 2007; Palmer et al., 2007). Within the first week bifidobacteria, clostridia and *Bacteroides* species become established (Stark and Lee, 1982). Succession of the microbiota community and the temporal pattern with which it evolves during the first year of life is highly variable between infants (Palmer et al., 2007). The plastic nature of the microbiota during early stages of life is also demonstrated by the greater fluctuation in day to day and diet-induced changes in faecal bacteria profiles compared to adults (Palmer et al., 2007).

Similarities between the infant microbiota and bacterial composition in breast milk and vaginal swabs suggests the development of the community in infants may be influenced by exposure to specific bacteria in the environment (Palmer et al., 2007). The vertical transmission of bacteria from mother to offspring has been demonstrated by studies showing babies delivered by caesarean section have different intestinal microbial community patterns compared to those born vaginally (Biasucci et al., 2008). Furthermore, it has been shown that related mice and humans have more similar microbiota profiles compared to unrelated individuals (Zoetendal et al., 2001). These findings show the microbiota may be inherited from the mother and that the resulting communities demonstrate a certain degree of stability over time.

During the early period of life, the composition of the microbial community is also greatly influenced by diet. In breast-fed infants, bifidobacteria and *Bacteroides* species rapidly dominate the community by day 5-6 (Mackie et al., 1999). By 4 weeks of age, the community in breast-fed babies shifts to one dominated by bifidobacteria, with relatively few enterobacteria and enterococci (Stark and Lee, 1982). In contrast, formula-fed infants exhibit a more diverse community with a relatively lower abundance of bifidobacteria (Favier et al., 2002). While the mechanism for this difference in bifidobacteria colonisation is not fully understood, it is possible that their numbers may be enriched by oligosaccharides found in human breast milk, which collectively form the third largest solid component of milk (Newburg, 2000). Bifidobacteria readily achieve high growth rates using human milk oligosaccharides as a substrate, and comparative genomic analysis has shown the *B. longum* genome features distinct gene clusters with predicted human milk oligosaccharide binding and transport functions (Locascio et al., 2010). Bifidobacteria have also been found in breast-milk, which may further explain their higher abundance in breast fed infants (Martin et al., 2009).

The introduction of solids to the diet of breast-fed infants result in a major shift in community composition towards resembling that of formula fed babies, characterised by a rapid increase in enterobacteria and enterococci, followed by colonisation of clostridia and *Bacteroides* species (Stark and Lee, 1982). However, by 12 months of age, the communities of formula- and breast-fed infants are no longer distinguishable and resemble those of adults (Mackie et al., 1999; Palmer et al., 2007; Stark and Lee, 1982).

1.3.2 Microbial community structure

Application of molecular techniques to examine the 16s rRNA gene has greatly accelerated the phylogenetic analysis of resident bacterial species in the large bowel, including many of those that are presently unculturable. Indeed, most studies indicate that the majority of bacterial species identified in the large bowel have yet to be cultured (Hayashi et al., 2006; Rajilic-Stojanovic et al.,

2007; Turnbaugh et al., 2010). Molecular and cultivation-based studies show the greatest species diversity is found among the Firmicutes phylum in humans, although the diversity of this group is greatly underestimated using culture-dependent methods (Rajilic-Stojanovic et al., 2007). Molecular analyses also reveal a wide diversity in the Bacteroidetes compared to estimates gained from culture-based methods (Rajilic-Stojanovic et al., 2007). However, a much larger overlap is present in Bacteroidetes species detected by the two methods, indicating more members of this abundant group have already been isolated (Rajilic-Stojanovic et al., 2007).

The Bacteroidetes and Firmicutes phyla dominate the large bowel community in the adult, accounting for up to 90% of the bacterial species present, with the remaining proportion primarily composed of bacteria from the Actinobacteria and Proteobacteria phyla (Costello et al., 2009; Qin et al., 2010). Within this loosely defined community outline, there is considerable variation in the relative abundance of species present between individuals. Even within the large bowel, variation in species diversity and abundance has been identified in different compartments, such as the ascending colon, descending colon, rectum and faeces (Eckburg et al., 2005). The source of this variation is not yet fully understood and is the subject of extensive study. However, a number of factors have been shown to influence the microbial community structure including diet, host phenotype, and kinship (De Filippo et al., 2010; Ley et al., 2005; Ley et al., 2006b; Manichanh et al., 2006). Community composition of the caecum in mice has been shown to be more similar between mothers and their offspring compared to unrelated mice (Ley et al., 2005). Furthermore, this similarity is shared between offspring from different litters (Ley et al., 2005). Similarly, faecal community profiles in humans have a more similar structure between related individuals, regardless of whether they live together or in separate residences (Turnbaugh et al., 2009a). However, it is apparent that factors other than host genotype play a major role in shaping the microbial community. Surprisingly, studies examining faecal microbial communities show profiles between monozygotic twins are no more similar to each other than those from dizygotic twins (Turnbaugh et

al., 2009a), suggesting environmental factors may play a larger role than genotype in dictating microbiota composition.

The health status of the host has been shown to influence the large bowel microbiota profile in a number of studies. A decrease in the abundance and diversity of the Firmicutes has been demonstrated in faecal samples from patients with Crohn's disease (Manichanh et al., 2006). Furthermore, postoperative recurrence of ileal Crohn's disease is higher in patients with lower proportions of mucosa associated *Faecalibacterium prausnitzii* (Sokol et al., 2008). Cluster analysis of the community profiles obtained by deep sequencing from normal individuals or patients with Crohn's disease or ulcerative colitis also show a clear delineation based on disease status (Qin et al., 2010). Age-related changes in the Bacteroidetes to Firmicutes ratio have also been reported in a study examining faecal microbial diversities in infants, adults and elderly individuals (Mariat et al., 2009). Furthermore, a reduction in the diversity of phylotypes belonging to the clostridial cluster XIVa group have also been identified in the elderly compared to adults (Hayashi et al., 2006). There is also evidence from human and rodent studies that the microbiota may play a role in obesity. Phylum wide decreases in the abundance of Bacteroidetes and a concomitant phylum wide increase in Firmicutes numbers have been observed in obese people and rodents (Ley et al., 2005; Ley et al., 2006b).

Current diversity estimates of the microbiota vary between surveys, but a recent study of the microbial community in twins using deep pyrosequencing of the V2 region of the 16S rRNA gene indicates approximately 800 phylotypes are present in the large bowel (Turnbaugh et al., 2010). A remarkable aspect of our bacterial community is the distinctiveness of profiles between individuals. Analysis of over 10^6 sequences from a pair of identical twins indicated that only 39% and 53% of species detected in the faeces, respectively, were shared between the two communities (Turnbaugh et al., 2010). A wider survey examining 31 monozygotic and 23 dizygotic twin pairs and their

mothers was unable to characterise a core set of bacterial species shared between all individuals (Turnbaugh et al., 2010). Of the most abundant species level phylotypes across all community sets, only 37 were present in >50% of the samples, and only one species, a member of the Lachnospiraceae family, was found in 99% of the individuals (Turnbaugh et al., 2010). In a recent study of 124 European individuals, metagenomic sequencing of large bowel communities produced a catalogue of 3.3 million microbial genes assembled from 576.7 Gigabases of sequence (Qin et al., 2010). Despite such broad sequence coverage, phylogenetic analysis showed only 18 species that were present in all individuals (Qin et al., 2010). However, this study was able to identify 75 bacterial species that were common to >50% of the sample group, and 57 species that were shared by >90% (Qin et al., 2010). Although the large bowel microbial community structure is highly variable between individuals, it is remarkably stable over time in adults (Costello et al., 2009; Ley et al., 2006b). Bacterial communities found in the skin, hair, nostril, and ear have all been shown to exhibit greater day to day variation than that found in the large bowel microbiota (Crawford et al., 2009). The stability of the microbial community suggests its structure is shaped by strong selective and homeostatic mechanisms present in the large bowel.

In order to understand the relationship between the substantial diversity present in the large bowel community and their function, a number of metagenomic studies have carried out relating community phylotype composition to the collective genomes of the microbiota (the microbiome) (Qin et al., 2010; Turnbaugh et al., 2009a). These studies have shown that despite the absence of an obvious core microbial community, individuals shared an extensive collection of microbial genes that form a core microbiome at the gene level (Turnbaugh et al., 2009a). Analysis of the microbiome revealed a common pool of housekeeping genes required for bacterial function and a set of genes that appear to facilitate bacterial adaptation to the large bowel environment (Qin et al., 2010; Turnbaugh et al., 2009a). This second category included genes that encode for an extensive collection of carbohydrate-active enzymes, factors for binding to host proteins, synthesis of SCFA,

and the production of essential amino acids and vitamins (Qin et al., 2010; Turnbaugh et al., 2009a; Turnbaugh et al., 2006). From these studies, it appears the diversity in the microbiota is underpinned by a set of core functional processes that is shared across communities of varying composition. These results also suggest a functional plasticity among members of the microbiota; different members of the community are able to undertake similar roles under different conditions.

1.3.3 Butyrate producing bacteria

Butyrate producing bacteria in the large bowel are predominantly Firmicutes belonging to clostridial clusters IV and XIVa (Barcenilla et al., 2000). These two clusters constitute a major component of the faecal microbiota in healthy humans, with up to 23% of bacteria belonging to the clostridial cluster XIVa group and up to 22% representing members of clostridial cluster IV (Lay et al., 2005).

The clostridial cluster XIVa group is highly diverse and includes genera such as *Butyrivibrio*, *Clostridium*, *Coprococcus*, *Dorea*, *Eubacterium*, *Lachnospira*, *Roseburia*, and *Ruminococcus*, which are oxygen-sensitive anaerobes (Hayashi et al., 2006; Suau et al., 1999). Major butyrate producing species in this group include *E. rectale* and *Roseburia* spp. (Aminov et al., 2006; Barcenilla et al., 2000). A prominent butyrate producer from the clostridial cluster IV group found in the human colon is *F. prausnitzii* (Suau et al., 1999). Butyrate forming bacteria among the Firmicutes are distributed across the division, with the clostridial cluster IV and clostridial cluster XIVa groups containing butyrate producers and non-producers. Phylogenetic trees based on 16S rRNA sequences show that butyrate producing species such as *Eubacterium*, *Roseburia* and *Clostridium* are interspersed with genera that do not produce butyrate, such as *Ruminococcus* (Hold et al., 2003; Pryde et al., 2002).

Fermentative bacteria are able to utilise alternate pathways to generate different fermentation end products. Under different environmental conditions, many butyrate forming bacteria are also capable of producing lactate, formate, H_2 and CO_2 (Belenguer et al., 2006; Falony et al., 2009; Falony

et al., 2006). They are therefore able to maintain redox balance and regulate ATP production by employing alternate pathways in response to the availability of different carbon sources (Macfarlane et al., 1998; Miller and Wolin, 1996). Butyrate producing bacteria are capable of utilising a wide variety of carbohydrate substrates, including starch, xylan, and inulin (Duncan et al., 2004a). Synthesis of butyrate in human intestinal bacteria occurs through the condensation of two molecules of acetyl-CoA in a system where acetate is incorporated in butyrate through the action of a CoA-transferase (Charrier et al., 2006; Miller and Wolin, 1996).

Certain butyrate producing bacteria may have a role in modulating inflammatory bowel disease (IBD). Metagenomic studies have shown that the diversity and prevalence of the Firmicutes, and the clostridial cluster IV group in particular, is reduced in patients with Crohn's disease (Manichanh et al., 2006). *Faecalibacterium Prausnitzii* has also been shown to reduce production of inflammatory cytokines in peripheral blood mononuclear cells (PBMCs) (Sokol et al., 2008). Furthermore, a reduction in severity of 2,4,6-trinitrobenzenesulphonic acid (TNBS) induced colitis has been observed in mice given intragastric administration of *F. Prausnitzii* (Sokol et al., 2008). The possible reduction in butyrate available for intestinal epithelial cells may be a factor that influences IBD, as butyrate exhibits anti-inflammatory properties and is an important energy source for colonocytes (Roediger, 1982; Saemann et al., 2000). However, the explanation for the reduced diversity and numbers of Firmicutes in IBD remains unknown. It seems likely that mucosal immune regulation and changes in the intestinal environment play a role in determining the microbial community composition.

1.3.4 Lactobacilli and bifidobacteria

Bifidobacterium and *Lactobacillus* genera are Gram-positive bacteria that ferment carbohydrates to form organic acids. Lactobacilli are capable of producing a number of fermentation products, including lactic acid, while bifidobacteria predominantly form lactic and acetic acid (Kleerebezem and Vaughan, 2009). Bifidobacteria are members of the Actinobacteria phylum and may comprise up to

4% of the total faecal community in adult humans (Mueller et al., 2006). In the infant, bifidobacteria are more prevalent, and may form up to 25% of the total faecal community at 3 days of age, and up to 53% by 3 months (Adlerberth and Wold, 2009; Costalos et al., 2007; Mah et al., 2007). Lactobacilli are Gram-positive acidophilic, anaerobic or aerotolerant Firmicutes that produce lactic acid as their major end product of carbohydrate fermentation (Tannock, 2004). The low numbers of bacteria found in the small intestine are primarily lactobacilli, which can also be found in the stomach (Hayashi et al., 2005; Reuter, 2001). In adult humans, lactobacilli make up only a small proportion of the large bowel community, typically around 1% (Mueller et al., 2006). However, numbers of lactobacilli detected in the faeces may be variable as they are a common component in many foods, particularly in fermented products (Tannock, 2004).

Analysis of *Lactobacillus* genomes reveal numerous deficiencies in the ability to produce a number of amino acids and other cellular compounds required for growth (Tannock, 2004). To compensate, lactobacilli have complex nutrient requirements and utilise a diverse array of transport systems. Lactobacilli also possess a large number of genes devoted to carbohydrate internalisation and utilisation (Kleerebezem and Vaughan, 2009). Specific adaptations for adhering to host produced mucus and bile salt hydrolases have also been found in several *Lactobacillus* species, which would further enable lactobacilli to survive in the intestinal environment (Boekhorst et al., 2006; Martin et al., 2008; Tannock et al., 1994). The genomes of bifidobacteria are highly conserved and many of their genes share the same physical localisation on their chromosome (Kleerebezem and Vaughan, 2009). Approximately 10% of their genome is dedicated to carbohydrate metabolism, binding and transport (Jones et al., 2008; Schell et al., 2002).

The activity and numbers of bifidobacteria and lactobacilli in the large bowel of humans are influenced by a number of factors that may include diet, age and geographical location (Chen et al., 2008; Humblot et al., 2005; Mueller et al., 2006; Snart et al., 2006). In rat studies, β-glucan

supplemented diets resulted in higher numbers of *Lactobacillus acidophilus* in the caecum, while dietary FOS elevated caecal levels of *Bifidobacterium animalis* and *Bifidobacterium lactis* (Montesi et al., 2005; Snart et al., 2006). A cross-sectional study examining the faecal microbiota in four European countries showed that bifidobacteria abundance was 2-3 times higher in the Italian study population compared to the French, German, and Swedish study groups (Mueller et al., 2006).

Despite the relatively low numbers of lactobacilli and bifidobacteria in the adult large bowel, they are the subject of much interest as they are thought to be associated with numerous health promoting effects. Lactobacilli and bifidobacteria are the most commonly used microbes in probiotic products, and have been actively promoted by the food industry (Kleerebezem and Vaughan, 2009; Reuter, 2001). However, claims advocating the health benefits of lactobacilli containing food supplements have not been adequately supported by scientific evidence to date. Clinical studies investigating the efficacy of probiotic treatments for various conditions have shown mixed results. Administration of *Lactobacillus rhamnosus* GG has been shown to reduce the risk of hospital-acquired gastrointestinal and respiratory infections (Hojsak et al., 2010), while treatment with probiotics was shown to be effective at reducing cold and influenza-like symptoms in 3 to 5 year old children (Leyer et al., 2009). However, a review from the Cochrane Library examining the use of probiotic bacteria for maintaining remission in individuals with Crohn's disease found no evidence for beneficial effects from probiotic treatment (Rolfe et al., 2006). Similarly, despite the increasing use of probiotics as an alternative treatment for antibiotic associated *Clostridium difficile* infection, clinical studies have not shown convincing evidence that probiotic products are able to prevent or ameliorate *Clostridium difficile* infection (Miller, 2009; Pillai and Nelson, 2008). Nonetheless, there is considerable evidence that lactobacilli and bifidobacteria are able to influence host biological processes in a number of ways that may be beneficial, which include suppression of inflammatory cytokine production, competitive exclusion of pathogens, and anti-proliferative effects in cancer cell lines (Coakley et al., 2006; Kleerebezem and Vaughan, 2009; Martin et al., 2008; Niers et al., 2005; Rousseaux et al., 2007; Servin, 2004).

1.3.5 Bacteroidetes

The Bacteroidetes are a major component of the microbiota. Species from the *Bacteroides* and *Prevotella* genera are the most commonly represented members of the Bacteroidetes found in the large bowel (Hopkins and Macfarlane, 2002). *Bacteroides* species are anaerobic, Gram-negative rod shaped bacteria that comprise approximately 25-50% of the microbiota (Eckburg et al., 2005; Mah et al., 2007; Turnbaugh et al., 2009a). Investigations of community diversity reveal large variations in Bacteroidetes composition in the large bowel (Eckburg et al., 2005; Turnbaugh et al., 2010). Indeed, metagenomic analysis of the microbiota in twins indicated a greater variation in the distribution of Bacteroidetes across the study group than that found in the Firmicutes (Turnbaugh et al., 2010). Species diversity of the Bacteroidetes has also been found to vary with age (Hopkins and Macfarlane, 2002).

Bacteroides thetaiotaomicron, a prominent member of the Bacteroidetes, has been extensively studied as a model organism for the identification and elucidation of mechanisms employed by this phylum for utilising host and dietary carbohydrates. Analyses of the completed genome sequences of *B. thetaiotaomicron* and *Bacteroides fragilis* have greatly improved our understanding of the adaptations these organisms possess that allow them to thrive in the large bowel environment. Perhaps the most noticeable adaptation is the considerable proportion of the genome dedicated to degradation and utilisation of carbohydrates in *B. thetaiotaomicron* (Martens et al., 2009a). Other adaptations include mechanisms for sensing diverse nutrients, multiple transporter systems to dispose of toxic wastes, and the ability to interact with the host to tailor favourable environmental conditions (Kelly et al., 2004; Koropatkin et al., 2009; Wexler, 2007). Additional adaptations include the ability to modulate cell surface polysaccharides, thereby evading host immune defences. *Bacteroides fragilis* has been shown to alter surface antigenicity by producing at least eight different capsular polysaccharides regulated through reversible inversions of promoter containing DNA segments (Krinos et al., 2001).

1.4 Bacteria and host interactions

In addition to releasing carbon and energy from what would otherwise be inaccessible sources of nutrients, the resident microbial community play a crucial role in modulating a wide range of host physiological processes. The microbiota has been shown to have a vital role in the development and growth of the large bowel mucosa and education of the immune system (Goodlad et al., 1989; Macpherson and Uhr, 2004b; Pabst and Rothkotter, 1999). Bacterial interactions with host immune processes continue throughout life and have been implicated in the promotion and suppression of inflammatory diseases (Manichanh et al., 2006; Sokol et al., 2008). Products of bacterial metabolism have also been shown to affect processes implicated in the development of cancer (O'Keefe et al., 2009). Furthermore, recent studies have shown that the development of obesity is influenced, at least in part, by the resident microbiota (Turnbaugh et al., 2006; Vijay-Kumar et al., 2010).

1.4.1 Influence of microbiota on early large bowel development

Development of the microbial community leading up to weaning coincides with dramatic changes in morphology and function of the large bowel. Changes in absorptive capability of the small intestine enable the gradual transition from a high-fat milk diet to a carbohydrate rich solid diet. During this period, withdrawal of maternal immunoglobulins present in the milk accompany important changes in the mucosal immune system, such as an increase in intraepithelial and lamina propria lymphocytes in the villi of the small intestine (Hooper, 2004).

The question of whether these changes are inherent processes programmed by the host DNA, or if they are driven by exposure to the resident microbiota, has been examined by studies using germ-free animals. Findings from these studies have highlighted the profound effects of the microbiota on the intestinal morphology and physiology. Bacterial colonisation of germ-free rodents and rabbits result in thickening of the mucosa, increases in colon crypt depth, stimulation of crypt cell proliferation, and shorter and broader ileal villi (Boot et al., 1985; Sharma et al., 1995). Other effects

of bacterial exposure include an increased epithelial cell turnover, thicker colonic epithelial mucus layer, and increased numbers of mucus containing goblet cells (Goodlad et al., 1989; Kleessen et al., 2003; Meslin et al., 1993). Furthermore, presence of the microbiota has also been shown to modify the structure of mucin secreted by the host. The mucus layer produced from goblet cells are an integral component of the mucosal barrier. Epithelial glycans expressed by the host prior to weaning are primarily terminated by sialic acid (Hooper, 2004). However, during weaning there is a shift towards expression of fucose terminated glycans, facilitated by a corresponding change in expression of fucosyltransferases that modify the terminal residues (Bry et al., 1996; Hooper, 2004). This shift in glycan structure is not observed in germ-free mice, but can be initiated by subsequent colonisation with *B. thetaiotaomicron* (Bry et al., 1996).

1.4.2 Development and regulation of the immune response

The intestinal epithelium layer serves as a vital barrier between the extensive microbial communities in the lumen and the diverse array of cells within the host that can only function when protected from disruption by external elements. In addition to providing a physical barrier, the intestinal epithelium also actively secretes antimicrobial compounds which localise to the mucus layer (Meyer-Hoffert et al., 2008). In the small bowel, these are produced by Paneth cells which are specialised epithelial cells that harbour secretory granules containing numerous antimicrobial peptides (Meyer-Hoffert et al., 2008). Angiogenin-4 (Ang4), a Paneth cell granule protein that exhibits potent bactericidal activity, is expressed during weaning in conventional mice and rapidly increases to adult concentrations, but is expressed at much lower levels in germ-free mice (Hooper et al., 2003). The role of the microbial community in regulating Ang4 expression was demonstrated by the colonisation of germ-free mice with a conventional intestinal microbiota, which resulted in increased expression levels that reached those found in adult conventional mice (Hooper et al., 2003). The restoration of Ang4 also occurred when germ-free mice were colonised with only *B. thetaiotaomicron* (Hooper et al., 2003). Therefore it seems likely that bacterial interactions with the host play an important role in

shaping the composition of antimicrobial factors in the intestine during the weaning process. Furthermore, it is possible that species such as *B. thetaiotaomicron* are capable of shaping the luminal environment to better suit its requirements with these interactions. For example, *B. thetaiotaomicron* is able to regulate host inflammatory activity by enhancing nuclear transport of the RelA subunit of NF-κB, a transcription factor involved in the regulation of numerous inflammatory genes (Kelly et al., 2004). The dependence on microbial input for the expression of Ang4 and fucosyltransferases also suggest the mammalian bowel is genetically programmed to interact with the resident microbiota, which is essential for normal development.

Lymphocytes in the intestine undergo important developmental changes after encountering antigens in gut associated lymphoid tissues (GALT) such as Peyer's patches (PP) and lymphoid aggregates in the colon, and mesenteric lymph nodes (MLN) (Mowat, 2003). Professional antigen presenting cells (APCs) such as dendritic cells (DCs) and macrophages, and non-professional APCs such as epithelial cells play a crucial surveillance role during development of the GALT (Mowat, 2003). Collectively, these cells monitor the microbial community and regulate immune responses against potentially harmful invaders (Kelsall and Rescigno, 2004). APCs and intestinal epithelial cells survey the microbial environment using a family receptors known as Toll-like receptors (TLRs), which recognise common structural elements of bacteria such as lipopolysaccharide (LPS), peptidoglycans, CpG motifs in bacterial DNA, or double stranded viral RNA (Stagg et al., 2003). DCs are also able to detect a number of bacterial cell wall components via several C-type lectin receptors, the most well known of which is DC-SIGN (Stagg et al., 2003). Interaction of DC-SIGN with *Lactobacillus reuteri* and *Lactobacillus casei* have been shown to prime DCs to direct the development of regulatory T cells, which are characterised by increased IL-10 secretion and inhibitory effects on other immune cells (Smits et al., 2005).

Considering the complex processes involved in regulation of the immune response, it seems likely that the resident microbiota has a major impact on the development of the intestinal adaptive immune system. The production of IgA has been shown to be dependent on the presence of bacteria (Macpherson and Uhr, 2004a). High affinity neutralising IgA is an important immunoglobulin in the maturing bowel, which is produced in large quantities and is secreted primarily as a dimer across the epithelial cell layer (Macpherson and Uhr, 2004a). Secreted IgA is able to neutralise viruses and toxins, limit bacterial association with the intestinal epithelium cell surface, and restrict the penetration of commensal bacteria into the mucosa (Hooper and Macpherson, 2010). DCs are able to monitor bacteria that associate with the mucosal surface by sampling bacterial antigens transported across the epithelium in Peyer's patches, or actively sampling luminal bacteria at the apical surfaces of epithelial cells (Uhlig and Powrie, 2003). The bacteria-loaded DCs are then able to direct B cells to become IgA secreting plasma cells (Macpherson and Uhr, 2004b). Furthermore, DCs have been shown to retain small numbers of commensal bacteria for several days, allowing the continued selective induction of IgA (Macpherson and Uhr, 2004b). The IgA producing plasma cells migrate from the lymphoid tissue into the lamina propria where IgA is secreted and transported across the epithelial cell layer. However, the bacteria containing DCs remain in the lymphoid tissues which ensure responses to commensal bacteria are localised, thereby preventing the induction of potentially harmful systemic immune responses (Macpherson and Uhr, 2004b).

1.4.3 Modulation of the immune system by bacterial structural components

The mucosal immune system is a complex assembly of components that must function to protect the host from invading pathogens, but at the same time promote tolerance to the huge consortium of commensal microbes and food antigens present in the large bowel. However, the presence of the microbial community is also essential for the development of both the innate and adaptive immune systems.

The innate arm of the immune response is mediated by innate or natural immune cells that can respond to signalling from pattern recognition receptors (PRRs) which bind to a variety of bacterial molecular components. PRRs are expressed on a wide range of cells throughout the gastrointestinal tract including epithelial cells, macrophages, DCs, and adipocytes (Cario, 2005). Surface bound TLRs and the nucleotide binding oligomerisation domain (NOD) family of intracellular receptors are the most well known of the PRRs. Stimulation of these receptors can result in production of inflammatory cytokines and chemokines through the activation of NF-κB, a rapid acting transcription factor present in all cells in an inactive state (Cario, 2005). TLRs are expressed extremely early in development. TLR2 and TLR4 have been found in foetal human intestine, indicating the capacity for the immature enterocyte to mount an immediate response to bacterial molecular motifs (Fusunyan et al., 2001). These receptors are key mediators of innate host defence in the mucosa and have an important role in maintaining mucosal and commensal homeostasis. However, the maintenance of homeostasis is a challenging process as many pathogenic and commensal bacteria express the same molecular motifs that activate TLRs. Therefore, careful regulation of TLR expression and TLR-induced processes are required to ensure tolerance to commensal bacteria while promoting proinflammatory signals and active immunity towards pathogens. Otherwise, dysregulation of TLR-mediated surveillance and responses may result in unwanted autoimmune and inflammatory diseases. Regulation of TLR activation in epithelial cells lining the intestinal tract is especially important given their close proximity to the resident microbiota.

The paradox of differential TLR recognition of pathogenic and commensal bacteria that display similar molecular motifs may in part be explained by their subcellular localisation on epithelial cells and their localisation in different morphological compartments of the large bowel epithelium. For example, TLR3, which recognises double stranded viral RNA, is expressed in the intestinal epithelium at relatively high levels (Furrie et al., 2005). In contrast TLR2, which recognise molecular motifs from Gram-positive bacteria, and TLR4, which is activated by LPS, are expressed only in crypt epithelial

cells (Furrie et al., 2005). Furthermore, expression is lost as the cells mature and move away from the base of the crypt towards the lumen (Furrie et al., 2005). It is possible that this pattern of expression allows tolerance to be maintained by restricting bacteria-induced responses to the crypt epithelium. However, responses to viral pathogens by TLR3 signalling are enabled for all mature epithelial cells to reduce the likelihood of intracellular infection.

Induction of proinflammatory signals by flagellin occurs when basolaterally expressed TLR5 is stimulated in epithelial cells, whereas flagellin contact with apical TLR5 has no effect (Gewirtz et al., 2001). Immunlocalisation experiments have shown that expression of TLR5 in intestinal epithelial cells is restricted to the basolateral surface (Gewirtz et al., 2001). Flagellin is found in pathogenic bacteria, such as *Salmonella typhimurium*, and commensal bacteria, such as some *E. coli* strains. Therefore, both have the potential to induce epithelial inflammatory signals. However, the subcellular localisation pattern of TLR5 expression ensures that only bacterial that have translocated from the luminal compartment to the basolateral membrane domain elicit an immune response. Such invasive translocation of flagellin can be mediated by pathogenic bacteria such as *S. typhimurium*, but do not occur with commensal bacteria (Gewirtz et al., 2001). The ability to distinguish between pathogenic and commensal bacteria is vital if the host is to avoid a perpetual state of immune activation.

Dynamic redistribution of TLRs may also be determined by cell differentiation status and ligand exposure. Induction of colitis in mice with DSS has been shown to decrease expression levels of TLR5, but increase transcription of TLR2 and TLR4 (Ortega-Cava et al., 2006). Infants that have been colonised with high amounts of *B. fragilis* exhibit decreased abundance of TLR4 in PBMCs (Sjogren et al., 2009). Furthermore PBMCs from these infants produced lower levels of inflammatory cytokines and chemokines, such as IL-6 and CCL4, upon stimulation with LPS compared to infants with lower numbers of faecal *B. fragilis* (Sjogren et al., 2009). It is possible that exposure to *B. fragilis* early in

life induces tolerance to LPS. Although signalling of TLR4 is generally thought to occur following binding of LPS at the cell surface, TLR4 has also been found in the Golgi apparatus. Intracellular TLR4 has been shown to bind to internalised LPS and initiate downstream signalling by MyD88, an adaptor molecule required for TLR-mediated induction of inflammatory cytokines (Hornef et al., 2003). Prevention of LPS internalisation also impairs bacterial recognition by intestinal epithelial cells, but is not impaired in macrophages (Hornef et al., 2003). The requirement for internalisation of LPS for signalling in intestinal epithelial cells may be a mechanism to prevent the induction of inflammatory signals from commensal bacteria interactions with apical TLR4. This may also explain some of the observed differences in TLR-induced responses between intestinal epithelial cells and immune cells.

NOD1 and NOD2 are intracellular receptors for bacterial components that have an important role in innate immunity through the detection of bacterial components derived from peptidoglycans (Cario, 2005). NOD2 responds to muramyl dipeptide, a specific motif of peptidoglycan, while NOD1 reacts to a Gram negative peptidoglycan derivative, y-D-glutamyl-meso-diamino-pimelic acid (Kim et al., 2004; Watanabe et al., 2004). Mutations in NOD2 have been associated with Crohn's disease, which suggest NOD2 may have an important role in regulating inflammatory diseases (Strober et al., 2006). However, the mechanisms by which this may occur are not yet fully understood. Nevertheless, studies using NOD2 deficient mice ($Card15^{-/-}$) have shown that stimulation of NOD2 inhibits proinflammatory responses mediated by TLR2 due to defective activation of the NF-κB signalling pathway (Watanabe et al., 2004). Wild type APCs stimulated by peptidoglycans show increased production of proinflammatory IL-12 compared to APCs from $Card15^{-/-}$ mice. Furthermore, cells from $Card15^{-/-}$ mice were shown to have elevated levels of NF-κB. Another study using $Card15^{-/-}$ mice showed an increased susceptibility to *Listeria monocytogenes* infection given orally, but not by intravenous or intraperitoneal delivery (Kobayashi et al., 2005). This result suggests that NOD2 is an important regulator of immunity in the intestine. While it is apparent that TLR and NOD-mediated sensing of bacterial molecular motifs is crucial for modulating inflammatory and homeostatic

responses to the intestinal microbiota, their exact role and mechanisms of action are not yet fully understood.

1.4.4 Regulation of mucosal barrier function by bacterial components

The epithelium of the large bowel forms a protective barrier that may be as little as a single cell thick. It is a site characterised by a high rate of cell turnover where the epithelium is replaced every five to seven days (Cliffe et al., 2005). A characteristic feature of germ-free rats is a reduction in epithelial cell proliferation compared to conventionally raised rats (Goodlad et al., 1989). Therefore, it would seem likely that bacterial-induced increases in cell proliferation in the large bowel may be mediated by TLR signalling. However, in the absence of intestinal injury, epithelial cell proliferation in MyD88 or TLR4 deficient mice is similar to that in wild-type mice, which suggests some other bacterial factor is involved in their proliferation (Fukata et al., 2005). In contrast, intestinal epithelial cell proliferation is reduced in MyD88, TLR4, or TLR2 deficient mice when intestinal injury is induced using DSS (Rakoff-Nahoum et al., 2004; Silva et al., 2008). Injury to colonic epithelial cells allows the resident microbiota access to the lamina propria which results in an acute inflammatory response. Surprisingly, mice which are deficient in MyD88, TLR2, or TLR4 are more susceptible to DSS-induced injury that wild-type mice, and show reduced epithelial cell proliferation alongside increased apoptosis (Rakoff-Nahoum et al., 2004). Moreover, MyD88$^{-/-}$ mice show increased mortality and morbidity after DSS administration compared to wild-type mice (Rakoff-Nahoum et al., 2004). This increase in mortality was not due to an overgrowth in commensal bacteria, and was found to be independent of T, B and NK cell activity (Rakoff-Nahoum et al., 2004). Wild-type mice given broad-spectrum antibiotics or antibodies targeting TLR2 or TLR4 resulted in similar DSS-induced injury severity in the colon (Rakoff-Nahoum et al., 2004; Silva et al., 2008). Administration of DSS to wild-type germ-free mice also produces greater colonic injury compared to mice that have a conventional microbiota (Maslowski et al., 2009).

At first, these findings seem counter-intuitive as it would be expected that mice which are unable to mount a TLR-dependent immune response to the resident bacterial community would exhibit reduced intestinal pathology following administration of DSS. These studies show that under normal conditions, a lack of TLR signalling is tolerated for normal intestinal epithelial cell proliferation. However, in the presence of injury, both the intestinal bacterial community and their detection by TLR-mediated signalling are required for optimal cell proliferation.

The mechanism by which TLR signalling influences epithelial cell proliferation is not fully understood. However, one possible factor driving the increased susceptibility of TLR deficient mice to intestinal injury is the production of IL-6, TNF and KC-1. In addition to their role in inflammation and immune regulation, these cytokines have been shown to have cytoprotective and restorative functions in a number of tissues (Bohan et al., 2003; Tebbutt et al., 2002; Ueland et al., 2004). Administration of DSS to wild-type mice was shown to increase colonic concentrations of IL-6 and KC-1, which could be inhibited by antibiotic treatment (Rakoff-Nahoum et al., 2004). In contrast, MyD88$^{-/-}$ mice had low concentrations of these cytokines in the uninjured state and were unable to up-regulate their expression levels following DSS administration (Rakoff-Nahoum et al., 2004). Similarly, expression of cytoprotective heat-shock proteins hsp25 and hsp72 was also impaired in MyD88$^{-/-}$ mice compared to wild-type mice following DSS administration (Rakoff-Nahoum et al., 2004).

Epithelial barrier function may also be influenced by products of bacterial metabolism. Butyrate has been shown to increase cell layer integrity in cultured epithelial colorectal adenocarcinoma (Caco-2) cells, as measured by transepithelial electrical resistance (TER) (Peng et al., 2009). This increase in barrier function was attributed to an increase in AMP-activated protein kinase K (AMPK) levels, which resulted in an accelerated assembly of tight junction proteins (Peng et al., 2009). Furthermore, the butyrate-induced activation of AMPK and increased TER was eliminated by the addition of a specific inhibitor of AMPK. Acetate has also been shown to play an important role in the amelioration of

intestinal injury following DSS administration in mice. Treatment with acetate following DSS administration was shown to reduce colonic inflammation (Maslowski et al., 2009). However, mice deficient in GPR43, a receptor that binds SCFA, displayed increased injury following DSS administration, which could not be abrogated by acetate treatment (Maslowski et al., 2009). DSS-induced intestinal injury in germ-free mice can be reduced by treatment with acetate, indicating the presence of a TLR-independent mechanism for protection against epithelial damage (Maslowski et al., 2009).

Studies using germ-free mice have also shown that colonisation with *B. thetaiotaomicron* increases expression levels of genes involved in enhancing barrier integrity in the intestinal epithelium (Hooper and Gordon, 2001). In further studies, confocal microscopy of cultured Caco-2 cells stimulated with a TLR2 ligand revealed an apical tightening and sealing of ZO-1, a tight junction molecule (Cario et al., 2004). Furthermore, stimulation of TLR2 resulted in enhanced TER, suggesting an increase in barrier function (Cario et al., 2004). These studies suggest that barrier integrity and repair in intestinal epithelial cells is mediated by receptors that sense bacterial components and metabolic products. Upon signalling, they activate downstream events which limit the extent of damage by increasing proliferation, reducing apoptosis, and regulating inflammatory pathways.

1.4.5 Systemic effects of microbiota metabolism

The effects of the intestinal microbiota are not restricted to the large bowel mucosa. Global metabolic profiling using mass spectrometry (MS) and nuclear magnetic resonance (NMR) based technologies have shown surprisingly large effects of the microbial community in a wide range of compartments including blood, urine, liver and faecal metabolites (Martin et al., 2007; Martin et al., 2008; Wikoff et al., 2009).

A study comparing blood metabolites in conventional and germ-free mice revealed extensive differences in plasma biochemistry (Wikoff et al., 2009). Analysis by liquid chromatography coupled with electrospray ionisation showed up to 11% of approximately 4000 peaks had significantly different signal intensities and up to 145 peaks were found to be unique to conventional mice (Wikoff et al., 2009). Plasma profiles revealed that amino acid metabolites, such as indole-containing compounds derived from bacterial-mediated metabolism of tryptophan, were particularly distinct (Wikoff et al., 2009). The antioxidant indole-3-propionic acid was present only in the plasma of conventional mice, and could be detected in germ-free mice following colonisation with *Clostridium sporogenes* (Wikoff et al., 2009).

The intestinal microbiota also play a key role in metabolism of conjugated bile acids (CBA), which are synthesised in the liver from cholesterol and are necessary for absorption of fats and lipid-soluble vitamins in the intestine (Jones et al., 2008). Many secondary bile acids, such as deoxycholic and lithocholic acids, are the result of host and microbial co-metabolism (Ridlon et al., 2006). Bacterial bile salt hydrolases deconjugate CBA to produce free and modified bile acids, some of which have been associated with the formation of gall stones and cancer (Baek et al., 2010; Payne et al., 2009; Ridlon et al., 2006). Bacterial modification of bile acids may also have important consequences on host energy harvest and balance as deconjugated bile acids are less efficient at emulsifying dietary fats, which may impact their absorption (Heuman, 1989; Tannock, 2004). Conversely, modified bile acids, such as tauro-conjugated bile acids are more effective at fat emulsification and micelle production (Heuman, 1989).

Metabolic profiling of human baby microbiota (HBM) associated mice show increased concentrations of tauro-conjugated bile acids in the ileum compared to conventional mice (Martin et al., 2007). In contrast, administration of *L. paracasei* and *L. rhamnosus* to HBM colonised mice resulted in decreased tauro-conjugated and unconjugated bile acids in the faeces (Martin et al., 2008). HBM

colonised mice were also found to have elevated concentrations of hepatic triglycerides compared to conventional mice, which suggests the microbiota may influence accumulation of lipids in the liver (Martin et al., 2007; Martin et al., 2008). Indeed, conventional mice have increased adiposity compared to germ-free mice, as measured by epididymal fat pad to body weight ratios (Backhed et al., 2004; Crawford et al., 2009). Moreover, germ-free mice fed a high fat diet show decreased obesity levels compared to their colonised counterparts (Backhed et al., 2007). Significant differences in plasma and urine metabolite profiles have also observed between conventional, HBM associated, and lactobacilli treated mice (Martin et al., 2007; Martin et al., 2008).

The influence of the microbiota on host metabolism has further been demonstrated in a recent study examining myocardial function and energy utilisation in germ-free mice (Crawford et al., 2009). Nutrient deprivation in the host induces a mobilisation and utilisation of lipids. Ketone bodies are one of the products of lipolysis from adipose stores, which are used as an energy source in tissues such as the liver and heart during fasting (Cahill, 2006). Serum concentrations of the ketone body β-hydroxybutyrate in fasted germ-free mice are significantly reduced compared to fasted conventional mice (Crawford et al., 2009). The elevated levels of β-hydroxybutyrate in conventional mice was attributed to a microbiota-induced increase in expression levels of Pparα, a nuclear receptor transcription factor required for lipid metabolism during fasting in various tissues (Crawford et al., 2009). Furthermore, isolated perfused hearts from germ-free mice utilised glucose more rapidly that those from conventional mice, indicating a microbiota-induced shift in metabolism (Crawford et al., 2009).

These studies show that there are extensive interactions occurring between the large bowel microbiota and host with consequences reaching beyond the intestinal mucosa. For example, the reduction of cholesterol levels and alterations in lipid metabolism induced by activity of the microbiota may potentially reduce the risk for cardiovascular diseases and obesity.

1.4.6 Microbiota and obesity

The large bowel microbiota has an important function in harvesting energy from food components that escape digestion and absorption in the small intestine. Human and animal studies have brought to attention the possible role of the resident microbial community in the regulation of obesity (Ley et al., 2005; Turnbaugh et al., 2006). A characteristic feature of germ-free mice is a lower body fat composition and metabolic activity compared to colonised mice (Backhed et al., 2004). However, conventionalisation of germ-free mice with a microbial community harvested from conventional mice results in a striking increase in adiposity, despite a reduction in food consumption (Backhed et al., 2004; Crawford et al., 2009). Colonisation of germ-free mice with a single strain of *B. thetaiotaomicron* is able to produce a similar increase in body fat (Backhed et al., 2004). The greater fat accumulation seen in colonised mice is facilitated by increased microbiota-derived SCFA metabolism, an increase in triglyceride concentrations in the liver and serum, and microbial regulation of pathways that promote adipocyte hypertrophy (Backhed et al., 2004; Martin et al., 2008). Expression of fasting-inducing adipocyte factor (Fiaf), a lipoprotein lipase (LPL) inhibitor, is suppressed in the intestinal epithelium of colonised mice, resulting in elevated LPL activity in adipocytes (Backhed et al., 2004). Furthermore, Fiaf has been shown to induce the expression of peroxisomal proliferator-activated receptor coactivator (Pgc-1α) and other regulators of fatty acid oxidation which are also up-regulated in germ-free mice (Backhed et al., 2007). Additionally, germ-free mice showed increased activity of AMP-activated protein kinase (AMPK), which respond to increases in intracellular AMP to ATP ratios by inducing ATP generating catabolic pathways and stimulating fatty acid oxidation (Backhed et al., 2007).

Several studies have also demonstrated the role of diet in interactions between the microbiota and host with regard to energy metabolism and lipid storage. Germ-free mice fed a diet high in fat and sucrose has been shown to be more resistant to diet-induced obesity than colonised mice (Backhed et al., 2007). Conventionally raised rats fed obesity-inducing diets also display lower total body and

wet fat weights when the diets were supplemented with konjac flour (Li et al., 2005). This reduced weight gain was associated with a decrease in blood triglyceride, glucose and high-density lipoprotein concentrations. In another study, wild-type mice fed high fat diets supplemented with DRC in the form of soluble guar gum fibre exhibited a greater weight gain and adiposity than rats fed DRC in the form of insoluble cereal fibre (Isken et al., 2010).

Alterations in the large bowel microbiota composition have been observed in obese humans and mice in a number of studies. A reduction in bacterial diversity and Bacteroidetes abundance, and a concomitant increase in Firmicutes numbers are characteristic features of the microbiota in obese humans and leptin deficient mice (*ob*/*ob*) characterised by an obese phenotype (Ley et al., 2005; Ley et al., 2006b; Turnbaugh et al., 2006). Feeding a high-fat diet to wild-type mice also results in a decreased Bacteroidetes/Firmicutes ratio, with an expansion of the Mollicutes class accounting for much of the changes seen in the Firmicutes abundance (Turnbaugh et al., 2008). This high-fat diet-induced change in Bacteroidetes and Mollicutes abundance is reversible using subsequent dietary manipulations, which are associated with a reduction in body weight and body fat (Turnbaugh et al., 2008). Metagenomic analysis of the microbiota in obese and normal twin pairs also reveal an enrichment of genes involved in metabolic pathways and nutrient harvest in obese individuals (Turnbaugh et al., 2009a). A possible causative role for the microbiota in producing an obese phenotype was demonstrated in studies where colonisation of germ-free mice with the microbiota from obese mice resulted in the development of the obese phenotype in the recipient mice (Turnbaugh et al., 2008; Turnbaugh et al., 2006). Results from these studies suggest the microbiota from obese mice have an increased capacity for energy harvest, which has consequences for host metabolism and energy balance. However, the relationship between microbiota and obesity is not clear-cut as several studies have shown no significant differences in Bacteroidetes/Firmicutes ratios in obese subjects compared to healthy individuals (Duncan et al., 2007a; Duncan et al., 2008; Schwiertz et al., 2010).

High-fat diet induced decreases in Bacteroidetes/Firmicutes ratio are also observed in mice deficient for RELMβ, an effector of T cell-mediated intestinal immune function expressed specifically in colonic goblet cells (Hildebrandt et al., 2009). However, RELMβ deficient mice remain relatively lean despite being fed a high-fat diet, highlighting the importance of diet in modifying microbiota composition. A group of obesity associated metabolic disorders, collectively known as metabolic syndrome, may also be associated with alterations in the resident community activity. Mice deficient in TLR5 have been shown to display numerous features related to metabolic syndrome, including hyperlipidemia, hypertension, insulin resistance, and increased adiposity (Vijay-Kumar et al., 2010). These characteristics were associated with alterations in the large bowel microbiota structure. Furthermore, transfer of the microbiota from $TLR5^{-/-}$ mice to wild-type germ-free mice resulted in development of many of the features of metabolic syndrome in the recipients, including hyperphagia, obesity, hyperglycemia and insulin resistance. Severe reduction of the microbial community using broad-spectrum antibiotics resulted in the elimination of many features associated with metabolic syndrome, indicating a role for the microbiota in the pathology of these disorders. Similarly, food restriction also prevented the occurrence of many of these metabolic abnormalities in $TLR5^{-/-}$ mice.

These recent studies have shown that obesity is associated with phylum level changes in microbial abundance and diversity, and alterations in gene and metabolic pathways representation. The broader implication of these findings is that deviations in microbiota function may be associated with, or even lead to altered host physiology.

1.5 Hypothesis and aims

The extensive and diverse collection of past studies examining interactions between diet, microbes and host provide a clear indication of the complexity of the large bowel ecosystem. Unravelling the interconnected web of mechanisms influencing microbe and host physiology remains a highly challenging task. It is apparent that many of the fundamental biological processes governing host and microbe responses to dietary DRC are not fully understood. The period encompassing weaning through to adulthood represents a period of great transitional change for both the host and microbial community. In light of the increasing awareness of disease associated shifts in microbial communities and the interest in dietary modification of the large bowel microbiota for improving health, an understanding of the biological processes that drive the interactions between diet, microbiota and host is highly important. Furthermore, there is evidence that exposure to an altered large bowel microbiota in the young may predispose individuals to an increased incidence of atopic diseases or obesity (Kalliomaki et al., 2008; Wang et al., 2008). Therefore, the ability to modify the microbiota in the young using food components such as DRC may provide a viable avenue for beneficially influencing health later in life.

The goal of this study was to gain a greater understanding of the biological processes occurring in the colon of newly weaned rats fed different forms of DRC. Moreover, the specific effects of each DRC and the changing microbiota on the host were defined by comparing the effects of feeding DRC to conventionally raised and germ-free rat. Investigative tools that were used included analysis of the host transcriptome by microarray and molecular methods for determining microbiota composition and diversity. Therefore, the two key hypotheses to be investigated are:

Hypothesis 1: Feeding DRC to newly weaned rats engineers the colonic microbiota composition towards one with an increased fermentative capacity.

Hypothesis 2: DRC induced changes in the colonic microbiota composition alters host gene transcription and physiology.

The major analytical approaches used in this thesis for testing the stated hypotheses are outlined in Figure 3. Therefore, the major aims of this study are to:

1. **Measure SCFA concentrations in the colon of newly weaned rats fed different forms and doses of DRC to assess changes in metabolic activity of the microbiota.** Colon digesta carboxylic acid concentrations were measured by gas chromatography equipped with a flame ionisation detector.

2. **Examine changes in the colonic mucosal architecture in response to DRC.** Alterations in colonic crypt length and goblet cells numbers in response to DRC feeding were assessed in transverse sections of colon tissue.

3. **Analyse changes in large bowel microbiota diversity and identify phylotypes that differ between DRC treatments.** Colonic microbiota profiles were determined by temporal temperature gradient gel electrophoresis (TTGE) and 454 pyrosequencing analysis of the V3 hypervariable region of the 16S rRNA gene.

4. **Assess changes in the host transcriptome induced by feeding DRC using microarrays.** DRC induced changes in host gene expression was measured by microarray and reverse transcription quantitative PCR (RT-qPCR). Analysis of biological functions and pathways associated with differentially expressed genes was performed using bioinformatic tools.

5. **Determine the effects of DRC on the host transcriptome in germ-free rats to identify changes in genes expression that are modulated by DRC and changes in gene expression modulated by the microbiota.** The contribution of the microbiota to changes in host gene expression was determined by comparing the transcriptomes of germ free and conventionally raised rats fed DRC. Transcriptome analysis was performed by microarray and RT-qPCR, and biological functions and pathways were analysed using bioinformatic tools.

6. **Correlate data from rat model of DRC feeding to extend the current understanding of diet, microbe and host interactions in the colon.** Transcriptomic, microbiota composition, SCFA concentration, and colonic mucosal morphology data were correlated to provide an overall picture of the interactions between DRC, microbiota and host in the colon.

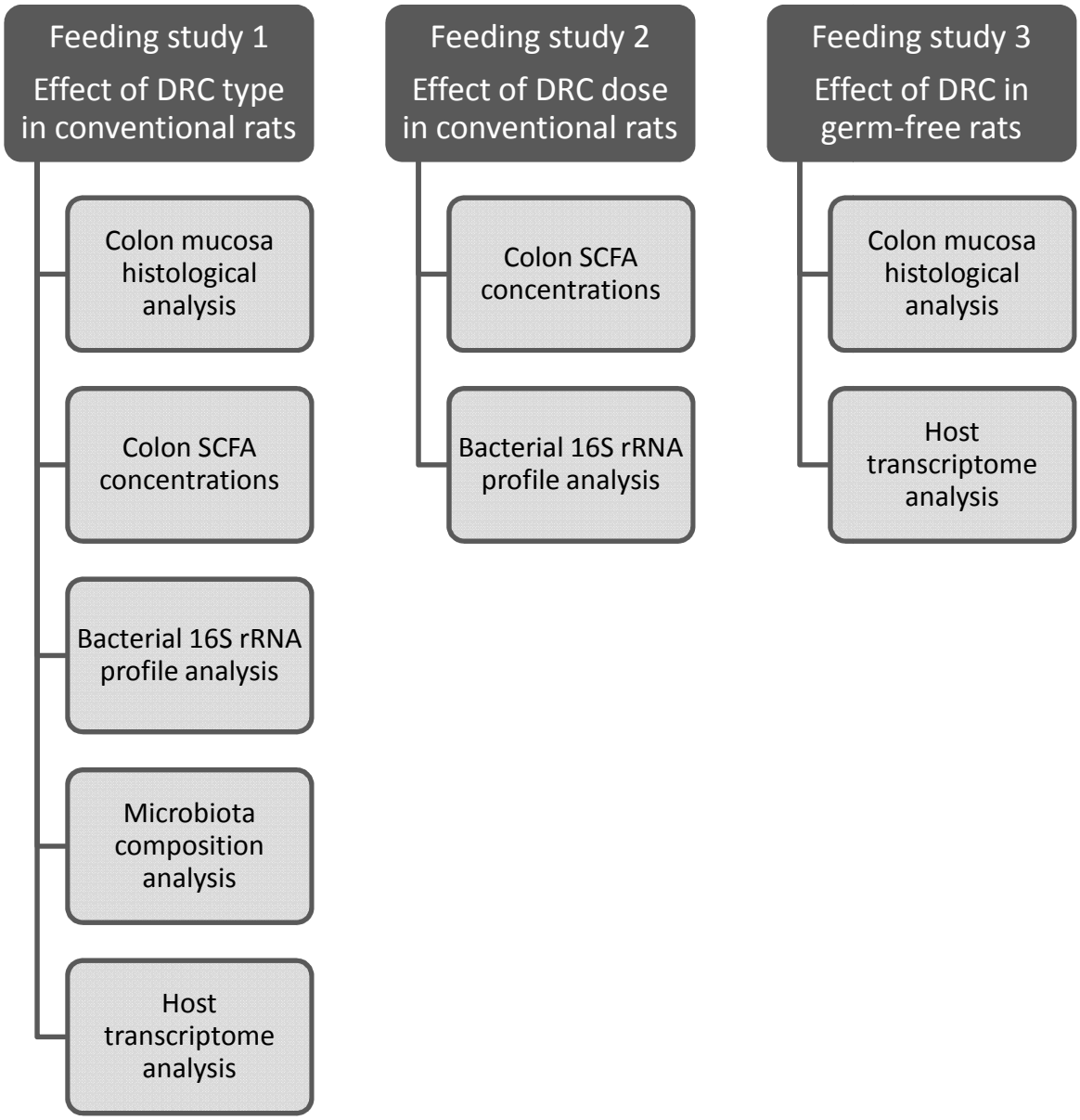

Figure 3. Overview of analytical approaches. Overview of analyses undertaken in this thesis to examine the effects of feeding DRC to newly weaned rats on microbiota composition and metabolism, and host transcription and mucosal morphology.

Chapter 2. Methods and Materials

2.1 Animals

A rat model was used to assess the effects of feeding DRC from early post weaning. The similarity of basic physiological mechanisms and metabolic processes between rats and humans makes the rat model a useful approximation of processes that may occur in humans. The large bowel microbiota in rats and humans are also similar with regard to the dominance of the Bacteroidetes and Firmicutes. However, there are major differences between rats and humans, which therefore require data generated from rat models to be carefully evaluated. For example, the caecum in rodents forms a substantial part of the large bowel and is the primary site for microbial fermentation. However, in humans, the primary site of microbial fermentation is the colon, with the caecum being a small rudimentary structure. Therefore, the contribution of fermentation products towards total energy uptake is likely to be different between rats and humans. Nevertheless, the ability to conduct highly controlled experiments and examine tissue samples not normally available in human studies makes rodent models an important research tool. Furthermore, the availability of germ-free rats provides a unique opportunity for investigating interactions between the host and the microbiota, or components of the microbiota. However, the use of germ-free animals also presents a number of technical challenges. Animals must be housed in a sterile isolator supplied with filtered air and all food, water and laboratory supplies which come in contact with the animals must be sterilised. Animals must also be constantly monitored for contamination to avoid invalidation of results. Furthermore, the absence of bacteria results in a number of physiological abnormalities itself, such as the enlarged fluid filled caecum and reduction in body fat associated with germ-free rats (Coates, 1975; Turnbaugh et al., 2008). Despite these limitations, germ-free rats are a valuable tool as they enable the manipulation of the microbiota to a degree that is not possible in human studies.

All rat experiments were approved by the AgResearch Grasslands Animal Ethics committee, Palmerston North, New Zealand (AEC applications 11952, 11410 and 10956). Newly weaned 21 day old conventionally raised (CR) male Sprague Dawley rats born at Plant and Food Research (Palmerston North, New Zealand) were individually housed in hanging wire mesh cages for the duration of feeding experiments. Twenty one to twenty eight day old germ-free (GF) male Sprague-Dawley rats, obtained from Taconic (Germantown, NY, USA), were housed individually in standard rat cages within a gnotobiotic isolator. All rats were kept under strict 12 hour light cycles and room temperatures were maintained at 22 ± 2 °C. Environmental enrichment was provided in the form of glass marbles and 100 mm diameter plastic tubing. Food and water was provided *ad libitum*. Rats were weighed weekly to track body weight. After 14 or 28 days of feeding, rats were euthanased by CO_2 overdose and colon tissues and contents were collected.

2.2 Diets

Rats were fed a lactic casein based basal diet (BD) or the basal diet supplemented with digestion resistant carbohydrates (DRC) in the form of inulin (IN), resistant starch (RS), konjac flour (KJ), freeze-dried *Undaria pinnatifida* seaweed (UN), or barley β-glucan (GL). RS used in this study was Hi-maize 1043 (National Starch and Chemical Company, Bridgewater, NJ, USA), a high amylose maize RS2 type resistant starch. KJ was produced from freeze dried *Amorphophallus konjac* corms grown at Plant and Food Research, Pukekohe, New Zealand. IN used in this study was Fibruline XL (Cosucra, Warcoing, Belgium), a long chain inulin (average degree of polymerisation >20). UN was freeze dried and ground at Plant and Food Research, Nelson, New Zealand. GL used in this study was Glucagel™ (GraceLinc Ltd, Christchurch, New Zealand). Formulation of diets supplemented with 5% by weight of IN, KJ, RS, UN or GL are shown in Table 1. Formulation of DRC dose response diets supplemented with RS or KJ at 1.25%, 2.5% or 5% by weight is shown in Table 2. The formulation of diets for GF rats is shown in Table 3. Diets for GF rats were produced and sterilised by gamma irradiation at 25 kGy by Research Diets (New Brunswick, NJ, USA). Following arrival in New Zealand, diets for GF rats were

again treated by gamma irradiation at 25 kGy at Schering-Plough Animal Health Limited (Upper Hutt, New Zealand). Treatment with 25-70 kGy has been shown to safely sterilise food with minimal nutrient loss (International Consultative Group on Food Irradiation, 1999). Food intake was measured weekly.

2.3 Study design

To determine the effects of a number of different DRC on colonic SCFA concentrations, microbiota composition, mucosal morphology and host gene expression, individually housed 21 day old CR newly weaned male Sprague-Dawley rats were fed BD, RS, KJ, UN, GL, or IN diets for 14 or 28 days (n=10) in study 1. Rack positions for hanging cages were randomised for all rats. Study 1 followed a 2 x 6 factor design, with feeding period (14 or 28 days) and form of DRC as factors, respectively. In study 2, the effects of DRC dose on colonic SCFA concentrations and microbiota composition were examined by feeding individually housed 21 day old CR male Sprague-Dawley rats BD, 1.25% RS, 2.5% RS, 5% RS, 1.25% KJ, 2.5% KJ, or 5% KJ diets for 28 days (n=10). RS was chosen as a representative example of a purified form of DRC and KJ was chosen as a representative of a 'crude' DRC preparation. Study 2 followed a 2 x 4 factor design, with DRC type (RS or KJ), and DRC dose (0%, 1.25%, 2.5% or 5%) as factors respectively. Rack positions for hanging cages were randomised for all rats. In study 3, the effects of DRC on host gene expression and colonic mucosal morphology in the absence of a microbiota was examined by feeding individually housed GF 21-28 day old male Sprague-Dawley rats BD, RS or KJ diets for 28 days. Study 3 followed a randomised design, with diets assigned to rats randomly. Rat cage positions in the germ-free isolator were also randomised for all rats. Statistical analyses of body weight and food intake were performed using ANOVA with the software packages GenStat version 12 (VSN International Ltd, Hemel Hempstead, United Kingdom), with $P<0.05$ regarded as statistically significant.

Table 1. Diet composition for study 1 (g/kg)

	Basal diet (BD)	Inulin diet (IN)	Konjac diet (KJ)	Resistant starch diet (RS)	Seaweed diet (UN)	β-glucan diet (GL)
Lactic casein	120	120	120	120	120	120
Vitamin mix[1]	50	50	50	50	50	50
Mineral mix[2]	50	50	50	50	50	50
Corn oil	65	65	65	65	65	65
Corn starch	650	600	600	600	600	600
Sucrose	40	40	40	40	40	40
Cellulose	25	25	25	25	25	25
IN[3]	-	50	-	-	-	-
KJ[4]	-	-	50	-	-	-
RS[5]	-	-	-	50	-	-
UN[6]					50	-
GL[7]						50

[1]Vitamin mixture contains the following components: Retinoic acid 0.08 g, ergocalciferol 0.0005 g, dl-α-tocopheryl acetate 4 g, menadione 0.06 g, thiamin hydrochloride 0.1 g, riboflavin 0.14 g, pyridoxine hydrochloride 0.16 g, D-pantothenic acid 0.4 g, folic acid 0.04 g, nicotinic acid 0.4 g, cyanocobalamin 0.001 g, d-biotin 0.02 g, myo-inositol 4 g, cholin chloride 30 g, sucrose 960.6 g.

[2]Mineral mixture contains the following components: Ferric citrate $3H_2O$ 756.7 g, manganous sulphate H_2O 80 g, zinc oxide 20 g, cupric carbonate $2H_2O$ 6.7 g, chromic potassium sulphate $12H_2O$ 6.3 g, sodium selenite 0.11 g, cobaltous chloride $6H_2O$ 0.039 g, potassium iodate 0.085 g, ammonium molybdate $4H_2O$ 0.093 g, sucrose 129.973 g.

[3]Inulin (Fibruline® XL, Cosucra, Warcoing, Belgium).

[4]Konjac flour (Plant and Food Research, Pukekohe, New Zealand).

[5]Resistant starch (Hi-maize 1043, National Starch and Chemical Company, Bridgewater, NJ, USA).

[6] Undaria pinnatifida seaweed (Plant and Food Research, Nelson, New Zealand).

[7]Glucagel barley β-glucan (GraceLinc, Christchurch, New Zealand).

Table 2. Diet composition for study 2 (g/kg)

	Basal diet (BD)	5% Konjac diet (KJ-5)	2.5% Konjac diet (KJ-2.5)	1.25% Konjac diet (KJ-1.25)	5% Resistant starch diet (RS-5)	2.5% Resistant starch diet (RS-2.5)	1.25% Resistant starch diet (RS-1.25)
Lactic casein	120	120	120	120	120	120	120
Vitamin mix[1]	50	50	50	50	50	50	50
Mineral mix[2]	50	50	50	50	50	50	50
Corn oil	65	65	65	65	65	65	65
Corn starch	650	600	625	637.5	600	625	637.5
Sucrose	40	40	40	40	40	40	40
Cellulose	25	25	25	25	25	25	25
KJ[3]	-	50	25	12.5	-	-	-
RS[4]	-	-	-		50	25	12.5

[1]Vitamin mixture contains the following components: Retinoic acid 0.08 g, ergocalciferol 0.0005 g, dl-α-tocopheryl acetate 4 g, menadione 0.06 g, thiamin hydrochloride 0.1 g, riboflavin 0.14 g, pyridoxine hydrochloride 0.16 g, D-pantothenic acid 0.4 g, folic acid 0.04 g, nicotinic acid 0.4 g, cyanocobalamin 0.001 g, d-biotin 0.02 g, myo-inositol 4 g, cholin chloride 30 g, sucrose 960.6 g.

[2]Mineral mixture contains the following components: Ferric citrate $3H_2O$ 756.7 g, manganous sulphate H_2O 80 g, zinc oxide 20 g, cupric carbonate $2H_2O$ 6.7 g, chromic potassium sulphate $12H_2O$ 6.3 g, sodium selenite 0.11 g, cobaltous chloride $6H_2O$ 0.039 g, potassium iodate 0.085 g, ammonium molybdate $4H_2O$ 0.093 g, sucrose 129.973 g.

[3]Konjac flour (Plant and Food Research, Pukekohe, New Zealand).

[4]Resistant starch (Hi-maize 1043, National Starch and Chemical Company, Bridgewater, NJ, USA.

Table 3. Diet composition for study 3 (g/kg)

	Basal diet (BD)	Konjac diet (KJ)	Resistant starch diet (RS)
Lactic casein	120	120	120
Vitamin mix[1]	10	10	10
Choline Bitartrate	2.5	2.5	2.5
Mineral mix[2]	35	35	35
Corn oil	65	65	65
Corn starch	525	475	475
Maltodextrin	125	125	125
Sucrose	92.5	92.5	92.5
Cellulose	25	25	25
KJ[3]	-	50	-
RS[4]	-	-	50

Diets were produced by Research Diets (Research Diets, New Brunswick, NJ, USA) and sterilised by gamma irradiation at 25 kGy.

[1]Vitamin mixture contains the following components: Vitamin A palmitate (500,000 IU/gm) 0.8 g, vitamin D3 (100,000 IU/gm) 1.0 g, vitamin E acetate (500 IU/gm) 10.0 g, menadione sodium bisulfite (62.5% menadione) 0.08 g, biotin (1.0%) 2.0 g, cyancocobalamin (0.1%) 1.0 g, folic acid 0.2 g, nicotinic acid 3.0 g, calcium pantothenate 1.6 g, pyridoxine-HCl 0.7 g, riboflavin 0.6 g, thiamin HCl 0.6 g, sucrose 978.4 g.

[2]Mineral mixture contains the following components: Calcium carbonate (40.0% Ca) 357 g, potassium phosphate, monobasic (28.7% K, 22.8% P) 250 g, potassium citrate $1H_2O$ (36.2% K) 28 g, potassium sulphate (44.9% K, 18.4% S) 46.6 g, magnesium oxide (60.3% Mg) 24 g, sodium chloride (39.3% Na, 60.7% Cl) 74 g, cupric carbonate (57.5% Cu) 0.3 g, potassium iodate (59.3% I) 0.01 g, ferric citrate (21.2% Fe) 6.06 g, manganous carbonate (47.8% Mn) 0.63 g, sodium selenate (41.8% Se) 0.01025 g, zinc carbonate (52.1% Zn) 1.65 g, chromium K sulphate $12H_2O$ 0.275 g, ammonium molybdate $4H_2O$ 0.00795 g, sodium silicate $9H_2O$ 1.45 g, lithium chloride 0.0174 g, boric acid 0.0815 g, sodium fluoride 0.0635 g, nickel carbonate 0.0318 g, ammonium vanadate 0.0066 g, sucrose 209.806 g.

[3]Konjac flour (Plant and Food Research, Pukekohe, New Zealand).

[4]Resistant starch (Hi-maize 1043, National Starch and Chemical Company, Bridgewater, NJ, USA.

2.4 Procedure for set up and use of germ-free isolators

In preparation for the use of GF rats, a gnotobiotic semi-rigid isolator (Charles River, Wilmington, MA, USA) and 18 rat cages placed within were sterilised by saturating internal surfaces with 1L of MB-10 chlorine dioxide solution at 200 ppm (BASF, Florham Park, NJ, USA). Following MB-10 application, all air vents in the gnotobiotic isolator were sealed for 24 hours, after which air vents were unsealed and the air-blower turned on to full for 3 days to the allow the gnotobiotic isolator to dry completely. To confirm sterilisation of the isolator, swabs of internal surfaces were taken and incubated in Hungate tubes containing 5 ml of Brain Heart Infusion (BHI) broth composed of 37 g of BHI powder (Becton Dickinson, Sparks, MD), 5 g of yeast extract (Becton Dickinson), 10 ml of haemin (0.05% weight/volume; Becton Dickinson), 1 ml of vitamin K (0.05% weight/volume; Becton Dickinson), and 2 g of L-cysteine-HCl (Becton Dickinson) per litre of broth. Swabs were incubated at room temperature and 37°C for 7 days, and under aerobic and anaerobic conditions. Anaerobic cultures were performed by purging the headspace of the Hungate tubes containing BHI broth with CO_2 and sealing the tubes closed with a cap containing a rubber septum.

Rodent bedding material and water was sterilised by autoclaving. Food and equipment for weighing rats and sample handling were sterilised by gamma irradiation at 25 kGy at Schering-Plough Animal Health Limited. Sterilised bedding material, food, water, and equipment were introduced in the gnotobiotic isolator by placing them within an entry chamber, after which the chamber and contents were thoroughly sprayed with MB-10. The outer door was then sealed and the contents of the closed entry chamber left for 10 minutes before the inner door was opened and the contents transferred into the gnotobiotic isolator.

GF rats were transitioned into the gnotobiotic isolator in closed plastic Nalgene jars, which were sprayed externally with MB-10 and left in the isolator entry chamber for 10 minutes before transfer

into the isolator. Once within the gnotobiotic isolator, rats were individually housed in standard rat cages.

2.4.1 Checking germ-free isolators and rats for contamination

On arrival of the GF rats and over the course of study 3, the GF status of rats were monitored by twice weekly cultures of faecal pellets in BHI broth in aerobic and anaerobic conditions at room temperature and 37°C, and Gram staining faecal material.

Gram staining to detect uncultivable bacteria was carried out by smearing faecal material on a glass slide. The slide was then briefly passed through a Bunsen flame to heat-fix any bacteria that may be present and then left to cool for 5 minutes. The slide was flooded with crystal violet solution (Sigma-Aldrich) for 60 seconds and then briefly washed with a gentle stream of water. The slide was then flooded with iodine solution (26 mM I, 40 mM KI, 120 mM $NaHCO_3$) and left to stand for 30 seconds. The iodine was poured off and the slide was gently rinsed in water. A few drops of decolourising solution (equal volume of 100% ethanol and acetone) was then added to each slide, which was then gently rinsed off in water. The slides were counterstained by flooding with safranin solution (Sigma-Aldrich) for 20 seconds to visualise Gram negative bacteria. The slides were then rinsed with water and left to dry, after which they were examined by light microscopy with a 100 X oil immersion objective lens. Over the course of the experiment, no growth was detected in any cultures. Isolated bacteria were observed occasionally in Gram stained faecal material, but these did not increase in frequency over the course of the experiment and were likely to be dead bacteria found in the food (Taylor et al., 1986).

2.5 Sample collection

Rats were euthanized by CO_2 overdose, after which the colon was removed and digesta collected for SCFA and microbiota analysis. Following digesta collection, 5 mm transverse sections of the colon at

1 cm from the start, 1 cm from the end, and from the centre of the colon were collected from each rat and placed in 10% formalin solution (LabServ, Auckland, New Zealand) for histological analysis. The remaining sections of colon were flushed with 10 ml of phosphate buffered saline (PBS) (Sigma-Aldrich, St Louis, MO, USA). 5 mm transverse sections of the remaining colon corresponding to approximately 1 cm from the start, 1 cm from the end, and from the centre of the colon were collected for gene expression analysis. All digesta and remaining tissue samples were snap frozen in liquid nitrogen and stored at -85°C.

2.6 Histology

Preparation and staining of histology slides was carried out by staff at the Institute of Veterinary, Animal & Biomedical Sciences, Massey University, Palmerston North, New Zealand.

Formalin fixed transverse, paraffin embedded sections of the colon from the central position and 1 cm from the starting and ending positions were stained with Haematoxylin and eosin (H&E) and counterstained with Alcian blue to visualise acidic mucins. Histological measurements were performed using bright field microscopy at 200 times magnification and Image-Pro Plus 4.0 (MediaCybernetics, Bethesda, MD, USA). Crypt lengths were determined by measuring an average of 80 random fully longitudinally sectioned crypts from the base of the crypt to the flat margin of the colon mucosa in all three colon sections for each rat. Similarly, numbers of goblet cells per crypt were determined by counting goblet cells in an average of 30 random fully longitudinally sectioned crypts per rat. Statistical analyses were performed using ANOVA in GenStat version 12 (VSN International Ltd), with $P<0.05$ regarded as statistically significant.

2.7 SCFA and carboxylic acid analysis

The quantity of acetic, propionic, butyric, lactic and succinic acids in the colon digesta of each rat was analysed by flame ionisation detector (FID) gas chromatography (GC) using a Shimadzu GC-17A gas chromatograph system (Nakagyo-ku, Kyoto, Japan) fitted with a Agilent HP-1 methyl silicone gum GC column (10 m × 0.53 mm × 2.65 µm) (Agilent Technologies, Santa Clara, CA, USA) using a method described by (Jensen et al., 1995)), with the following modifications. Colon digesta samples were thawed and mixed with 8 ml homogenisation medium (0.9% NaCl w/v, 0.1% Tween 20 v/v) per gram of sample and 1 ml of internal standard (100 mM 2-ethyl butyric acid) per gram of sample. The aqueous homogenate was centrifuged at 3000 X g for 5 minutes at 4°C to remove particulate material, following which 1 ml of supernatant was transferred to a glass tube. Extraction of SCFA into an organic solvent was performed by adding 0.5 ml hydrochloric acid and 2 ml diethyl ether followed by vortexing for 60 seconds. The samples were then centrifuged at 1600 X g for 15 minutes at 4°C to separate the aqueous and organic phases. The upper diethyl ether phase was collected and samples derivatised by adding 40 µL N-methyl-N-E-butyldimethylsilytrifluoracetamide (MTBSTFA) (Sigma-Aldrich) and incubating at 80°C for 20 minutes. The samples were then left at room temperature for 48 hours prior to GC analysis to allow for complete derivatisation of lactic acid (Jensen et al., 1995).

One µl of derivatised sample was injected at a 1:4 split ratio into the GC column with a helium carrier gas at 10 kPa for the first 6 minutes of the run, which increased to 15 kPa at 5 kPa per minute for the final 3 minutes. Detector and injector temperatures were both set to 260°C. The detector flame was maintained with a hydrogen/air mixture with both gases supplied at 50 psi. After an initial GC column temperature of 70°C at the time of sample injection, the temperature was increased to 80°C at 10°C per minute, followed by an increase to 260°C at 20°C per minute. After completion of the separation run, the GC column temperature was returned to 70°C. Data collection and chromatograph control was performed using GC solutions software (Shimadzu).

Identification and quantification of peaks was performed by running single standards of acetic, propionic, butyric, lactic and succinic acids, and a standards cocktail containing all acids at a final concentration of 10, 5, 2.5, 1.25, 0.625, and 0.313 mM to generate a standard curve. All peak areas were normalised with a 5 mM 2-ethyl butyric acid internal standard, which was added to all samples and standards.

Analysis of recovery of SCFA and carboxylic acids was performed by assaying samples spiked with known amounts of acids (Appendix A). Serial dilutions of known concentrations of SCFA and carboxylic acids were measured to determine linearity and minimal detectable concentrations (Appendix B). Statistical analyses were performed using ANOVA in GenStat version 12 (VSN International Ltd) on square root transformed data where necessary in cases of unequal variances, with $P<0.05$ regarded as statistically significant. Linear regression analysis for DRC dose response was performed using the statistical programming language R (R Development Core Team, Vienna, Austria), with $P<0.05$ indicating a linear regression slope significantly different to zero.

2.8 Isolation of DNA from colonic digesta

DNA was extracted from colonic digesta for microbiota composition analysis by qPCR and 454 pyrosequencing. DNA was isolated from colonic digesta by homogenising approximately 100 mg of digesta with 1 ml of TN150 buffer (10 mM Tris-HCl, 150 mM NaCl, pH 8), followed by centrifugation at 13000 X g for 5 minutes at 4°C. The supernatant was discarded and the pellet washed by adding 1 ml of TN150 buffer and centrifuging at 13000 X g for 5 minutes at 4°C. The supernatant was discarded and the pellet resuspended in 1 ml TN150 buffer. The samples were then transferred to a beadbeater tube containing 0.3 g of sterile 0.1 mm diameter zirconium beads (Sigma-Aldrich) and shaken in a mini-bead beater (Biospec Products, Bartlesville, OK, USA) set at maximum for 3 minutes. Samples were cooled on ice for 5 minutes, after which they were centrifuged at 13000 X g for 5 minutes at 4°C. Five hundred µl of the supernatant was transferred to a new microcentrifuge tube, to

which 500 µl of TE (10 mM Tris, 1 mM EDTA, ph 8.5)-saturated phenol was added. The samples were mixed by vortexing and then centrifuged at 13000 X g for 3 minutes at 4°C, after which the top layer was transferred to a new microcentrifuge tube. Five hundred µl of chloroform-isoamyl alcohol (24:1) was added to the top layer, which was mixed by vortexing, followed by centrifugation at 13000 X g for 3 minutes at 4°C. The top layer was again transferred to a new microcentrifuge tube with a further 500 µl of chloroform-isoamyl alcohol (24:1) added. The samples were mixed by vortexing and centrifuged at 13000 X g for 3 minutes at 4°C. The top layer was transferred to a new microcentrifuge tube and combined with 1 ml of ice cold 100% ethanol and 50 µl 3M sodium acetate. The samples were incubated overnight at -20°C to precipitate the DNA. Samples were then centrifuged at 13000 X g for 20 minutes at 4°C, after which the supernatant was discarded and the DNA pellet air dried for 20 minutes. The pellets were then dissolved in 25 ml of TE buffer (ph 8.5) and the DNA concentrations quantified using a using a NanoDrop ND-1000 UV-VIS Spectrophotometer (Thermo Fisher Scientific, Wilmington, DE, USA).

2.9 Isolation of RNA from colonic digesta

RNA was extracted from colonic digesta to determine the TTGE profile of the metabolically active members of the community. Approximately 100 mg of colonic digesta was placed into a beadbeater tube containing 0.3 g of sterile 0.1 mm diameter zirconium beads (Sigma-Aldrich). One ml of PBS was added to each tube, which was then vortexed and centrifuged at 13000 X g for 5 minutes at 4°C. The supernatant was discarded and a further 1 ml of PBS was added to the pellet and vortexed, followed by centrifugation at 13000 X g for 5 minutes at 4°C. The supernatant was discarded and 200 µl of lysis buffer (10 mM Tris-HCl, 10 mM EDTA, pH 7.9) containing lysozyme (10 mg/ml; Sigma-Aldrich) was added to the pellet. The samples were then homogenised by vortexing and incubated at room temperature for 30 minutes. After incubation, 50 µl of 20% sodium dodecyl sulphate (SDS), 300 µl of 50 mM sodium acetate/10 mM EDTA (pH 5.1), and 300 µl of TE (10 mM Tris, 1 mM EDTA, ph 8.5)-saturated phenol were added to the tubes. The tubes were then shaken in a mini-bead beater

(Biospec Products) set at maximum for 2 minutes, after which they were centrifuged at 14000 X g for 10 minutes at 4°C. The upper layer was transferred to a new microcentrifuge tube with 600 µl of TE-saturated phenol and vortexed for 1 minute, followed by centrifugation at 14000 X g for 10 minutes at 4°C. The upper layer was transferred to a new microcentrifuge tube and 600 µl of phenol:chloroform:isoamylalcohol (25:24:1) was added. The tube was vortexed for 1 minute and centrifuged 14000 X g for 10 minutes at 4°C. The upper layer was again transferred to a new microcentrifuge tube with 600 µl of phenol:chloroform:isoamylalcohol (25:24:1), vortexed for 1 minute and centrifuged 14000 X g for 10 minutes at 4°C. Phenol was removed by transferring the upper layer to a new microcentrifuge tube with 1 ml of chloroform:isoamylalcohol (24:1) and vortexing for 1 minute. The tubes were then centrifuged at 14000 X g for 5 minutes at 4°C and the upper layer transferred to a new microcentrifuge tube. RNA was precipitated by adding 1 ml of ice cold 100% isopropanol and incubating for 10 minutes on ice, followed by centrifugation at 14000 X g for 10 minutes at 4°C. The supernatant was discarded and 1 ml of 80% ice cold ethanol was added to the tube. The samples were centrifuged at 14000 X g for 5 minutes at 4°C, after which the supernatant was discarded and the pellets left to air dry for 20 minutes. The RNA pellets were then dissolved in 100 µl of H_2O.

To remove residual genomic DNA, 50 µl of RNA sample was added to a new microcentrifuge tube with 20 µl of DNase I buffer (30 mM $MgCl_2$, 10 mM NaCl, 200mM Tris-HCl, pH 7.9), 1.5 µl of DNase I (10 U/µl; Roche, Basel, Switzerland) and 28.5 µl of H_2O. The tubes were mixed by shaking and incubated at 37°C for 1 hour. To deactivate the DNase, tubes were incubated at 75°C for 10 minutes.

DNase treated RNA was purified using Qiagen RNA/DNA Midi kits (Qiagen, Valencia, CA, USA). Prior to use, QIAGEN-tip 100 columns (Qiagen) were equilibrated by adding 1 ml of Buffer QRE, which was allowed to drain by gravity. Buffer QRV2 was added to each DNase treated RNA sample at a volume of 1.35 ml, which was then vortexed and centrifuged at 5000 X g for 5 minutes at 4°C. The

supernatant was then transferred to the equilibrated column and allowed to drain by gravity. Columns were then washed twice by adding 1 ml of Buffer QRW, which was left to drain, followed by a further 1 ml of Buffer QRW, which was also allowed to drain by gravity. A new 2 ml microcentrifuge tube was placed beneath each column and the bound RNA eluted by adding 500 µl of Buffer QRU to each column, which was drained by gravity into the collecting tube. A further 500 µl of Buffer QRU was added to each column to give a total elution volume of 1 ml. Purified RNA was precipitated by adding 1 ml of ice cold 100% isopropanol to each tube, which was then mixed by inversion and centrifuged at 15000 X g for 30 minutes at 4°C. The supernatant was discarded and 500 µl of ice cold 100% ethanol was added to each tube. The tubes were then centrifuged at 15000 X g for 15 minutes at 4°C, after which the supernatant was discarded. The RNA pellet was washed once more by adding 500 µl of ice cold 100% ethanol and centrifuging at 15000 X g for 15 minutes at 4°C. The supernatant was then discarded and the pellet left to air dry for 20 minutes. The RNA pellet was then dissolved in 60 µl of H_2O. RNA concentrations were assessed using a NanoDrop ND-1000 UV-VIS Spectrophotometer (Thermo Fisher Scientific). RNA was stored at -85°C until use.

2.10 RT-PCR of colonic digesta RNA

RT-PCR amplification of colon digesta RNA using primers HDA1-GC (5'-CGC CCG GGG CGC GCC CCG GGC GGG GCG GGG GCA CGG GGGGAC TCC TAC GGG AGG CAG CAG T-3') and HDA2 (5'-GTA TTA CCG CGG CTG CTG GCA C-3') was performed for TTGE analysis of microbiota profiles. The primers HDA1-GC and HDA target the V3 hyper-variable region of the 16S rRNA, resulting in a PCR product approximately 200 bases in size (Tannock et al., 2004; Tannock et al., 2000).

Prior to analysis by RT-PCR, RNA samples were checked for DNA contamination by PCR using HDA1-GC/HDA2 primers. Each reaction mixture contained 1 µl of RNA, 10 mM final concentration Tris-HCl, 2.5 mM final concentration $MgCl_2$, 50 mM final concentration KCl, each deoxynucleoside triphosphate at a final concentration of 200 mM, 20 pmol of primers HDA1-GC and HDA2, and 2.5 U

of Taq DNA polymerase (Roche) in a total volume of 50 µl. The following program was used in a Hybaid Express thermal cycler (Thermo Fisher Scientific): 94°C for 3 minutes, 30 cycles consisting of 94°C for 30 seconds, 56°C for 30 seconds, and 68°C for 60 seconds, followed by 68°C for 7 minutes. PCR products were run on a 2% agarose gel and only RNA samples which were negative for amplification products, indicating the absence of contaminating DNA, were used in subsequent RT-PCR analysis.

RNA samples from rats fed BD, IN, RS and KJ from study 1, and RNA from rats fed BD, 1.25% RS, 2.5% RS, 5% RS, 1.25% KJ, 2.5% KJ, or 5% KJ diets from study 2 were reverse transcribed and amplified using Titan One Tube RT-PCR Kits (Roche). Each reaction mixture contained 1 µl of RNA template, 10 µl of 5 X RT-PCR reaction buffers, 32 µl of H_2O, 2.5 µl of DTT, each deoxynucleoside triphosphate at a final concentration of 200 mM, 1 µl Titan enzyme mix, and 20 pmol of primer HDA2 in a reaction volume of 50 µl. Reactions were performed using a Hybaid Express thermal cycler (Thermo Fisher Scientific) with the following program. The reactions were heated to 50°C for 30 minutes to synthesise cDNA, followed by heating to 95°C to deactivate the reverse transcriptase component of the Titan enzyme mix. The program was then paused and 20 pmol of primer HDA1-GC was added to each tube. The program was then resumed with the 35 cycles consisting of 94°C for 30 seconds, 56°C for 30 seconds, and 72°C for 45 seconds. RT-PCR products were then checked by running on a 2% agarose gel and only samples which showed amplification products approximately 200 bases in size were used for temporal temperature gradient gel electrophoretic (TTGE) separation of RT-PCR amplicons.

2.11 TTGE profile analysis

Analysis of microbiota composition was initially accomplished through culture based methods. However, these methods have inherent limitations as major a proportion of the microbiota remain unculturable (Eckburg et al., 2005; Rajilic-Stojanovic et al., 2007). Molecular based methods such as

TTGE can be used to address this problem. Similar in principal to DGGE, TTGE is a molecular fingerprinting method for the separation of PCR products generated from DNA or cDNA samples, which may be composed of differing sequences (Shaji et al., 2003). Amplification of the hypervariable regions of the bacterial 16S rRNA gene with primers that contain a high G+C 'CG clamp' provides a useful method for identifying the constituents of a mixed population of bacteria (Clarridge, 2004; Tannock et al., 2000). Due to the similar sized products resulting from PCR amplification, conventional gel electrophoresis is usually unable to discriminate between amplicons of different sequences. However, this limitation can be overcome by TTGE separation where PCR products are electrophoresed with increasing temperature over time. When the PCR product encounters a critical threshold temperature, the weaker melting regions of the double stranded PCR product which lie outside of the GC clamp denature, which considerably slows its migration. One limitation of 16S rRNA based DGGE for examining microbial ecology that requires consideration is that 16S rRNA gene copy numbers vary between the genomes of different bacterial species (Klappenbach et al., 2000), which may bias the representation of the microbial community towards species with a high gene copy number. Furthermore, heterogeneity in ribosomal RNA operon copy numbers and sequence can be found within some species, which would result in a single bacterial species producing more than one band (Crosby and Criddle, 2003). Other species may have near identical 16S rRNA gene sequences that migrate the same distance, resulting in an underestimation of community diversity (Simpson et al., 1999). However, despite these limitations, 16S rRNA fingerprinting techniques such as DGGE have been widely and successfully used to characterise alterations in composition of microbial communities. The primary difference with TTGE compared to DGGE is that DGGE relies on a gradient of increasingly high concentrations of a denaturing agent in the polyacrylamide gel in order to melt the PCR product. The primary advantage of TTGE over DGGE is that migration distances of PCR products between gels is more reproducible as fine grained control of temperature ramping is more easily accomplished than consistent casting of gradient gels (Shaji et al., 2003).

An outline of the methodology of TTGE separation is shown in Figure 4. TTGE analysis of RT-PCR products was performed using a DCode universal mutation detection system apparatus (Bio-Rad, Hercules, CA, USA) on a 6% polyacrylamide gel prepared by adding 6 ml of 40% acrylamide/bis solution (Bio-Rad), 1 ml of 50 X TAE buffer (2M Tris-acetate, 50mM EDTA, ph 8), and 16.8 g of urea (7M; Merck, Whitehouse Station, NJ, USA) made up to a total volume of 40 ml with H_2O. The polyacrylamide/urea gel solution was set by adding 40 µl of TEMED (Sigma-Aldrich) and 400 µl of 10% ammonium persulphate (Bio-Rad) prior to pouring. 35 µl of RT-PCR products were loaded in each well of the polyacrylamide gel, which was run at 20 volts at 63°C for 15 minutes. The voltage was then increased to 40 volts for 16 hours and the temperature increased from 63°C to a final temperature of 70°C with a ramp rate of 0.4°C h^{-1}. A single sample was selected as a common reference, which was run on all gels to allow for normalisation of fragment migration lengths between gels run on different days. Gels were stained with ethidium bromide solution (0.5 µg/ml) (Sigma-Aldrich) and photographed using a Kodak Gel Logic 2200 Imaging System (Kodak, Rochester, NY, USA).

Digital images of 16S rRNA TTGE profiles were analysed using the BioNumerics 4.01 software package (Applied Maths, Sint-Martens-Latem, Belgium). All visible bands were selected manually and the TTGE profiles were compared by principal component analysis (PCA), Unweighted Pair Group Method with Arithmetic Mean (UPGMA) cluster analysis using Dice's similarity coefficients with a migration distance sensitivity threshold of 2%, and multidimensional scaling (MDS) analysis of profile similarities. The internal stability of TTGE profiles within groups was examined with the Jackknife method using average similarities. Jackknife analysis is a method for estimating bias and standard error by systematically recomputing the statistical estimate from the sample set with one observation left out each time.

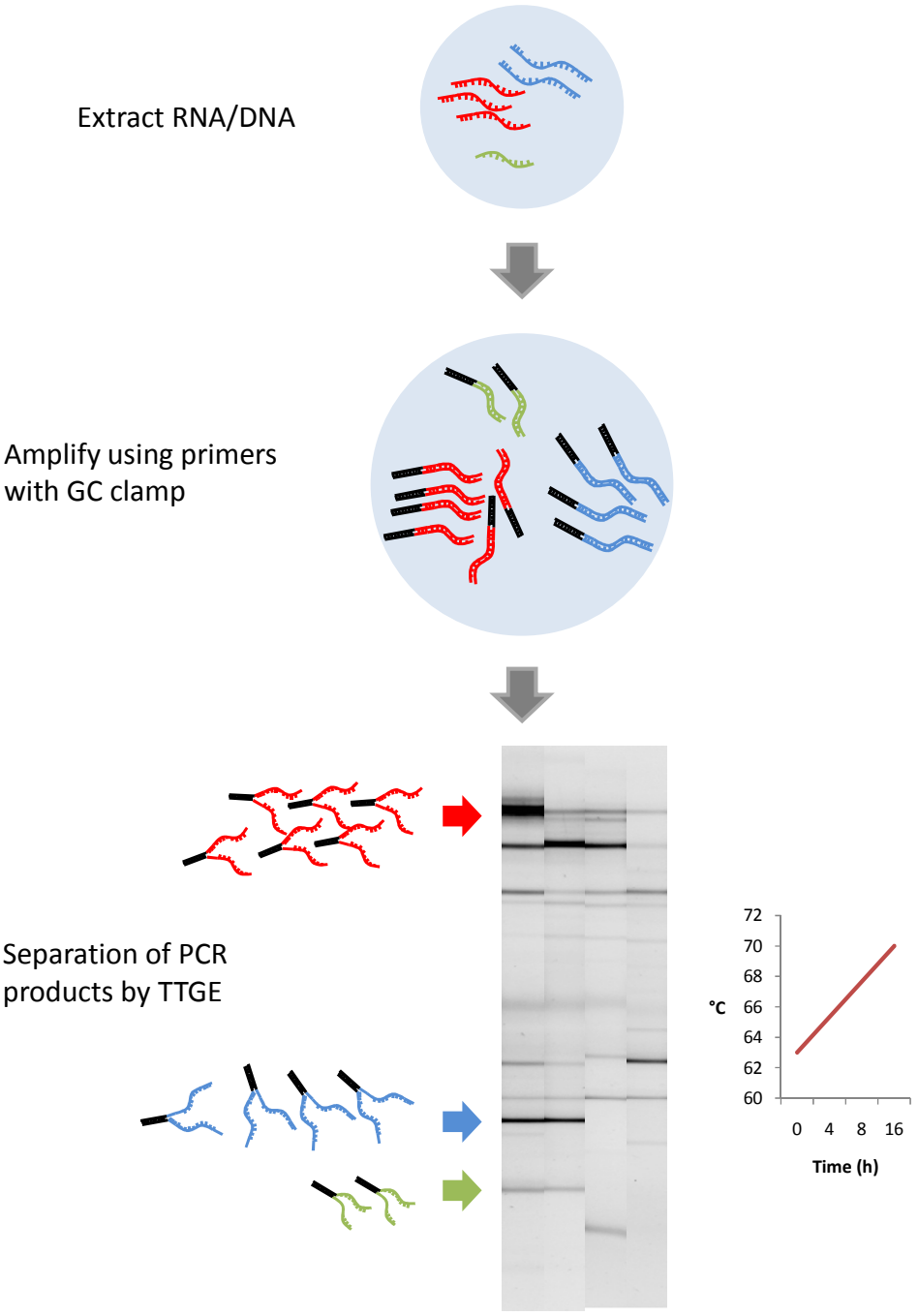

Figure 4. Principal of temperature gradient gel electrophoretic (TTGE) analysis. DNA or RNA is extracted from sample and amplified by PCR using primers containing a GC clamp. PCR products are then electrophoresed on a polyacrylamide gel with increasing temperature over time. PCR products of differing sequences melt at different temperatures, which determine their migration distance. The more abundance PCR products result in darker bands.

2.12 Cloning and identification of TTGE fragments

Selected TTGE fragments which showed variation across diets were excised from the polyacrylamide gel with a sterile scalpel blade and placed in 100 µl of diffusion buffer (0.5 M ammonium acetate, 10 mM magnesium acetate, 1 mM EDTA [pH 8.0], and 0.1% sodium dodecyl sulphate) and stored at -20°C.

2.12.1 Extraction of DNA from cut bands

To extract DNA from gels, cut bands were thawed on ice and then incubated at 50°C for 30 minutes. The tubes were then mixed by vortexing and centrifuged at 5600 X g for 1 minute. The supernatant containing DNA eluted from the gel was transferred to QIAquick gel extraction kit spin columns (Qiagen) on new microcentrifuge tubes. The spin columns were then centrifuged at 5600 X g for 1 minute. Three hundred µl of QXI Buffer was added to the flow through, followed by the addition of 10 µl of QIA II Solution to each sample. The tubes were then incubated at room temperature for 10 minutes and vortexed every 2 minutes during the incubation time. The samples were then centrifuged at 5600 X g for 1 minute, after which the supernatant was discarded. The pellets were washed by adding 500 µl of PE Buffer, followed by centrifugation at 5600 X g for 1 minute. The supernatant was discarded and the pellets washed again by adding a further 500 µl of PE Buffer, followed by centrifugation at 5600 X g for 1 minute. The supernatant was discarded and the DNA pellets air dried for 15 minutes. The DNA pellets was then dissolved in 36 µl of Elution Buffer and mixed by vortexing. The samples were incubated at room temperature for 5 minutes, after which they were centrifuged at 5600 X g for 1 minute. The supernatant containing the purified DNA fragments were then transferred to new microcentrifuge tubes.

2.12.2 S1 nuclease treatment of cut band DNA

Single stranded DNA was removed from the purified DNA extracted from cut bands by adding 3.6 µl of Reaction buffer (300 mM sodium acetate, 500 mM NaCl, 0.3 mM zinc sulphate, ph 4.5) and 1 µl of

S1 nuclease (Roche; catalogue number 818348) to each tube. The samples were then incubated at 37°C for 30 minutes. After incubation, the S1 nuclease was deactivated by heating the tubes at 95°C for 10 minutes.

2.12.3 Amplification of TTGE cut band DNA

The S1 nuclease treated purified DNA fragments were then amplified by PCR using HDA1-GC and HDA2 primers. Each reaction mixture contained 1 µl of S1 nuclease treated DNA template, 10 mM final concentration Tris-HCl, 2.5 mM final concentration $MgCl_2$, 50 mM final concentration KCl, each deoxynucleoside triphosphate at a final concentration of 200 mM, 20 pmol of primers HDA1-GC and HDA2, and 2.5 U of Taq DNA polymerase (Roche) in a total volume of 50 µl. The following program was used in a Hybaid Express thermal cycler (Thermo Fisher Scientific): 94°C for 3 minutes, 30 cycles consisting of 94°C for 30 seconds, 56°C for 30 seconds, and 68°C for 60 seconds, followed by 68°C for 7 minutes. The remaining S1 nuclease treated cut band DNA was stored at -80°C.

The resulting PCR products were cleaned using a QIAquick PCR purification kit (Qiagen) using the following protocol. PB Buffer was added at a volume of 225 µl to each PCR reaction tube and mixed by vortexing. The samples were transferred to QIAquick PCR purification kit spin columns on 5 ml centrifuge tubes. The spin columns were then centrifuged at 5600 X g for 1 minute. The flow through was discarded and the sample was then washed by adding 750 µl of PE Buffer to the column and centrifuging at 5600 X g for 1 minute. The spin columns were placed in new microcentrifuge tubes and the DNA eluted by adding 30 µl of buffer EB to each column. Samples were left to stand for 1 minute after which they were centrifuged at 5600 X g for 1 minute. The cleaned PCR products were stored at 4°C until used for ligation into a cloning vector.

2.12.4 Cloning of TTGE cut band DNA

Cleaned PCR products were cloned in *E. coli* DH5α with the pGEM-T Easy vector system (Promega, Madison, Wis.) using the following protocol. Cleaned PCR product was added at a volume of 1.5 µl to a new microcentrifuge tube containing 2.5 µl of 2X Rapid Ligation buffer (Promega), 0.5 µl of ligase (Promega), and 0.5 µl of pGEM-T Easy vector (Promega). The ligation reactions were then incubated at room temperature for 1 hour. Forty µl of competent *E. coli* DH5α cells was added to each ligation reaction. The total contents of each microcentrifuge tube was then transferred to an ice cold electroporation cuvette and incubated on ice for 1 minute. After incubation, the cuvette was placed in a Gene Pulser (Bio-Rad) and pulsed with a setting of 2.8 kV, 200 Ω resistance, and 25 µF capacitance. Once the pulse was completed, 1 ml of SOC broth (20 mg/ml Bacto Tryptone [Becton-Dickinson], 50 mg/ml Bacto Yeast Extract [Becton-Dickinson], 10 mM NaCl, 2.5 mM KCl, 10 mM $MgCl_2$, 10 mM $MgSO_4$, 20 mM glucose) was added to the cuvette. The contents of the cuvette was then transferred to a glass bijou bottle and incubated in a shaking water bath at 37°C for 1 hour.

After incubation, successfully transformed cells were selected by streaking cells on MacConkey Agar + ampicillin selection plates (50 mg/ml Difco MacConkey Agar [Becton-Dickinson] and 100 µg/ml of ampicillin [Sigma-Aldrich]) and incubating overnight at 37°C. After incubation, white colonies representing cells that were successfully transformed with a pGEM-T Easy vector containing the TTGE fragment DNA ligated into the α-peptide region of the β-galactosidase enzyme (lacZ), and one pink colony representing a negative control were purity plated on MacConkey Agar + ampicillin selection plates and incubated overnight at 37°C. Each transformant was then inoculated into 2 ml of LB + ampicillin broth (10 mg/ml Bacto Tryptone [Becton-Dickinson], 5 mg/ml Bacto Yeast Extract [Becton-Dickinson], 10 mg/ml NaCl, 100 µg/ml of ampicillin [Sigma-Aldrich], ph 7) and incubated overnight at 37°C.

Isolation of cloned plasmids containing the TTGE fragment DNA inserts was performed using QIAprep Spin Miniprep kits (Qiagen). Overnight cultures were centrifuged at 13000 X g for 5 minutes, following which the supernatant was discarded. The cell pellets were then resuspended in 1 ml of PI Buffer. Lysis of the cells was performed by adding 250 µl of P2 Buffer to each tube and inverting the tubes repeatedly for up to 5 minutes until the solutions became viscous and slightly clear. The lysis reaction was then stopped by adding 350 µl of N3 Buffer to each tube and mixing by inverting the tubes. The tubes were then centrifuged at 13000 X g for 10 minutes and the supernatant transferred to a QIAprep Spin column on a collection tube. The spin columns were centrifuged at 5600 X g for 1 minute after which the flow through was discarded. To remove any traces of nuclease activity, each spin column was washed with the addition of 500 µl of PB Buffer followed by centrifugation at 5600 X g for 1 minute. The flow through was discarded and the spin columns were washed with 750 µl of PE Buffer and centrifuged at 5600 X g for 2 minute. Each spin column was then placed into a new microcentrifuge tube and the bound plasmid DNA eluted by adding 50 µl of buffer EB and centrifuging at 5600 X g for 1 minute. Quantification of purified plasmid DNA was carried out by running DNA samples on a 1% agarose gel with a lane containing Molecular Weight Marker III (Roche). Purified plasmids were stored at 4°C.

The insertion of the TTGE fragment DNA into the pGEM-T Easy vector was confirmed by PCR using T7 (5'-TAA TAC GAC TCA CTA TAG GG-3') and SP6 (5'-ATT TAG GTG ACA CTA TAG-3') primers. Each reaction mixture contained 1 µl of plasmid DNA, 10 mM final concentration Tris-HCl, 2.5 mM final concentration $MgCl_2$, 50 mM final concentration KCl, each deoxynucleoside triphosphate at a final concentration of 200 mM, 20 pmol of primers T7 and SP6, and 2.5 U of Taq DNA polymerase (Roche) in a total volume of 50 µl. The PCR reactions were carried out using Hybaid Express thermal cycler (Thermo Fisher Scientific) with the following program: 94°C for 4 minutes, 15 cycles consisting of 94°C for 30 seconds, 45°C for 45 seconds, and 72°C for 60 seconds, followed by 68°C for 7 minutes.

The presence of approximately 360 base-pair sized PCR products on a 2% agarose gel indicated the 200 base-pair sized TTGE fragment DNA was correctly inserted into the pGEM-T Easy vector.

2.12.5 Sequence analysis of plasmids containing TTGE cut band DNA

Sequencing was performed by staff at the Alan Wilson Centre Genome Service, Massey University, Palmerston North, New Zealand.

Prior to sequence analysis, plasmid DNA was amplified by PCR using HDA1-GC and HDA2 primers and the PCR products were separated by TTGE using the previously described protocols. Only products which formed a single band that migrated to the same position with respect to the original excised TTGE fragments were used for sequencing. Purified plasmids were sequenced at the Alan Wilson Centre Genome Service by facility staff using an ABI3730 Genetic Analyzer (Applied Biosystems Inc., Foster City, CA, USA) with T7 and SP6 primers. Sequences from trace files were analysed using ABI Sequence Scanner v1.0 software (Applied Biosystems Inc.). To identify closest bacterial matches, sequences were then searched against the National Center for Biotechnology Information (NCBI) database using the BLASTN algorithm and the Ribosomal Database Project (RDP) (Center for Microbial Ecology, Michigan State University, East Lansing, MI, USA; http://rdp.cme.msu.edu/) database using the RDP Seqmatch tool.

2.13 Quantitative PCR of TTGE fragment sequences in colon digesta DNA

The abundance of successfully identified TTGE cut band DNA sequences in colon digesta DNA was analysed by quantitative PCR (qPCR). Primers targeting TTGE cut band sequences were designed using Primer3 and validated using purified plasmid DNA for sense and non-sense target sequences. qPCR analysis was performed using a LightCycler 480 Real Time PCR System (Roche) with the SYBR green detection method. Quantitative PCR reactions were carried using iQ SYBR Green Supermix (Bio-Rad). The qPCR reaction mixture components, primer sequences, and qPCR program

parameters are shown in Table 4. Serial dilutions of purified plasmid DNA was used to produced standard curves for qPCR analysis, with plasmid copy number calculated from the molecular weight of the pGEM-T Easy plasmid with the inserted TTGE cut band DNA. The specificity of primers and qPCR conditions was analysed by performing a melting curve analysis on the qPCR products using the following parameters: 95°C for 30 seconds, 65°C for 60 seconds followed by a final temperature of 95°C with a ramp rate of 0.11°C second^{-1}. Statistical analysis of gene copy numbers were performed using ANOVA in GenStat version 12 (VSN International Ltd) on log transformed data, with $P<0.05$ regarded as statistically significant. Linear regression analysis for DRC dose response was performed using the statistical programming language R (R Development Core Team).

Table 4. Primers and amplification conditions for quantitative analysis of TTGE fragment DNA

Band ID	Primers	qPCR conditions	Reaction mixture
1-1	1-1F (5'-CGCGTGAGTGAAGAAGGTTT-3') 1-1R (5'-CTTTCTGGTTGATTACCGTCAA-3')	95°C for 180 sec 95°C for 15 sec 62°C for 20 sec X 40 cycles 72°C for 20 sec	10 µl of Biorad Supermix 4 µl of H2O 2 µl of 1-1F (10mM) 2 µl of 1-1R (10mM) 2 µl of Template DNA (20ng total)
3-7	3-7F (5'-ATGGGGGAAACCCTGATG-3') 3-7R (5'-CGTGGCTTCCTCCTCAGGTA-3')	95°C for 180 sec 95°C for 15 sec 63°C for 20 sec X 40 cycles 72°C for 20 sec	10 µl of Biorad Supermix 7 µl of H2O 0.5 µl of 3-7F (10mM) 0.5 µl of 3-7R (10mM) 2 µl of Template DNA (20ng total)
9-2	9-2bF (5'-ATGGGCGGAAGCCTGATG-3') 9-2bR (5'-AGCCGGAGCTTCCTCCTAAG-3')	95°C for 180 sec 95°C for 15 sec 64°C for 20 sec X 40 cycles 72°C for 20 sec	10 µl of Biorad Supermix 6 µl of H2O 1 µl of 9-2bF (10mM) 1 µl of 9-2bR (10mM) 2 µl of Template DNA (20ng total)

Primers and qPCR conditions for the quantification of TTGE cut band fragment DNA sequences in colon digesta DNA. Band ID refers to identification number of TTGE fragment that was successfully cloned. Analysis was performed using a LightCycler 480 Real Time PCR System (Roche). Biorad Supermix (iQ SYBR Green Supermix, Bio-Rad) is a mastermix containing SYBR green I, 2X reaction buffer, and DNA polymerase.

2.14 Identification of colonic microbiota using next generation sequencing

PCR amplification and PCR product cleanup was performed by Dr. Blair Lawley, University of Otago, Dunedin, New Zealand. Sequencing was performed by staff at the University of Otago High-Throughput DNA Sequencing Unit, University of Otago, Dunedin, New Zealand.

Microbiota composition in colonic digesta was carried out using next generation sequencing (NGS). The major advantage offered by NGS technologies over traditional capillary sequencing platforms is the generation of much greater numbers of sequences without cloning bias by parallelising the sequencing process, enabling the production of thousands or millions of sequences at once. The recent use of NGS platforms such as the Roche 454 Genome Sequencer FLX (Roche) has transformed the study of microbial communities in the large bowel by providing detailed insights into the community structure and activity beyond what was possible with traditional Sanger sequencing. The Roche 454 platform is capable of generating up to one million sequences in one run, with a read length of 400 bases. However, the use of NGS platforms presents unique challenges. Analysis of the large datasets generated is computationally intensive and the error rate is higher than with traditional Sanger sequencing, which have been reported between 0.001% and 1%, while 454 sequencing has had reported error rates between 0.49% and 2.8% (Hoff, 2009). Due to the large number of sequences generated, an increase in error rate can result in a major overestimation of community diversity (Quince et al., 2009). Therefore, stringent filtering of sequences based on quality score or complex algorithms for minimising the effects of sequencing errors is often required (Johnson and Slatkin, 2008). However, despite these limitations, NGS platforms have been proven to be invaluable for the compositional and metagenomic analysis of the large bowel microbiota (Hildebrandt et al., 2009; Qin et al., 2010; Turnbaugh et al., 2010).

The colonic microbiota in rats fed BD, IN, RS and KJ diets for 28 days were identified by sequencing PCR products of the V3 region of the 16S rRNA gene amplified using HDA1 (5'-AC TCC TAC GGG AGG

CAG CAG T-3') and HDA-2 primers. Colon digesta DNA from rats fed BD, IN, RS and KJ in study 1 were pooled in equimolar amounts within their respective groups to provide an overview of microbiota compositional changes in rats fed the same diet. The pooled DNA sets were amplified by PCR with each reaction mixture containing 1 µl of pooled DNA template, 10 mM final concentration Tris-HCl, 2.5 mM final concentration $MgCl_2$, 50 mM final concentration KCl, each deoxynucleoside triphosphate at a final concentration of 200 mM, 20 pmol of primers HDA1 and HDA2, and 2.5 U of Taq DNA polymerase (Roche) in a total volume of 50 µl. The following program was used in a Hybaid Express thermal cycler (Thermo Fisher Scientific): 94°C for 3 minutes, 30 cycles consisting of 94°C for 30 seconds, 56°C for 30 seconds, and 68°C for 60 seconds, followed by 68°C for 7 minutes.

The PCR products were then cleaned using a QIAquick PCR purification kit (Qiagen) using the following protocol. PB Buffer at a volume of 225 µl was added to each PCR reaction tube and mixed by vortexing. The samples were transferred to QIAquick PCR purification kit spin columns on 5 ml centrifuge tubes. The spin columns were then centrifuged at 5600 X g for 1 minute. The flow through was discarded and the sample was then washed by adding 750 µl of PE Buffer to the column and centrifuging at 5600 X g for 1 minute. The spin columns were placed in new microcentrifuge tubes and the DNA eluted by adding 30 µl buffer EB to each column. Samples were left to stand for 1 minute after which they were centrifuged at 5600 X g for 1 minute.

The PCR products were then submitted to the University of Otago High-Throughput DNA Sequencing Unit where they were sequenced by the facility operators using a Roche 454 Genome Sequencer FLX (Roche). An outline of the principles of 454 pyrosequencing is shown in Figure 5. To summarise, biotinylated adapter sequences and a 5 nucleotide length barcode sequence were ligated to single stranded PCR products, which were immobilised onto DNA capture beads. The barcode sequence was used to identify the PCR products originating from the BD, IN, RS, or KJ fed rats, with a unique barcode sequence used for each group. Each capture bead was then emulsified with amplification

reagents in a water-in-oil mixture, resulting in microreactors containing one bead with one unique template DNA molecule. The captured DNA templates were then amplified by emulsion PCR on the beads. The beads were then transferred to a sequencing plate containing wells of a size that allow for only one bead per well. The clonally amplified PCR products on each bead then act as a template for DNA polymerase. Each individual nucleotide is then flowed across the plate, and then washed away. If a nucleotide complementary to the template is introduced, then that nucleotide is added to an extending DNA strand produced by the DNA polymerase. This results in the release of a pyrophosphate from the phosphate-sugar-phosphate backbone of the extending DNA strand. The presence of pyrophosphate in each well was then determined by the reaction of pyrophosphate with sulfurylase, resulting in the release of ATP. The released ATP is then used in the oxidation of luciferin by luciferase, resulting in the production of a chemiluminescent signal, which is recorded by a digital camera. If a template DNA has a sequence of identical nucleotides, this is represented by the presence of multiple pyrophosphate molecules, which in turn results in a longer and more intense chemiluminescent signal.

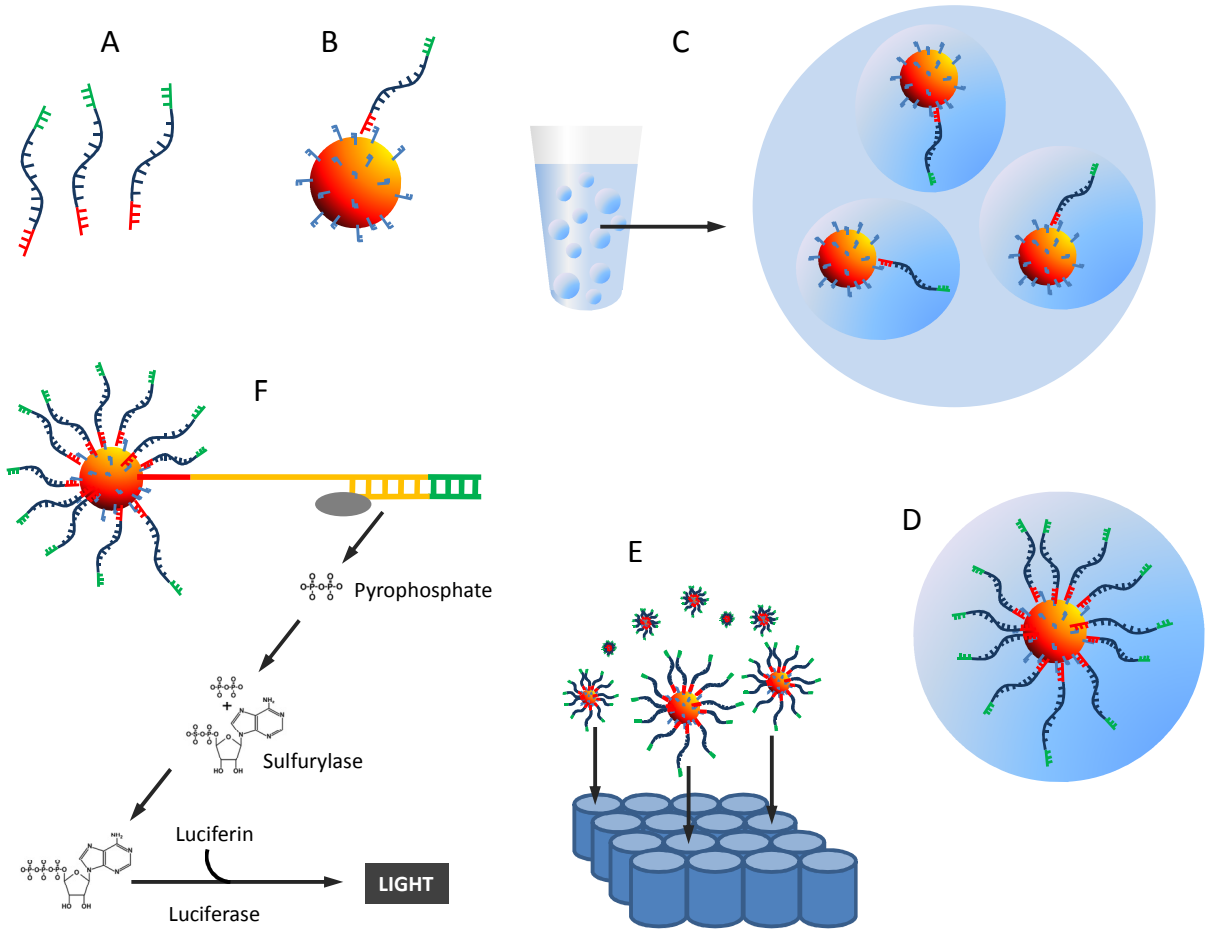

Figure 5. Roche 454 Sequencing workflow. (A) DNA samples are ligated with A and B adapters specific to the 5' and 3' ends. (B) Ligated DNA fragments are captured on microbeads. Concentrations of microbeads and DNA are optimised such that one microbead will have one captured DNA fragment. (C) Microbeads are suspended in a water-in-oil emulsion with amplification reagents, such that each microbead is contained within its own mini-reactor. (D) Each captured DNA fragment is amplified by emulsion PCR. (E) Microbeads with clonally amplified DNA are loaded onto a sequencing plate with a well diameter that allows only one microbead to fit in each well. Individual nucleotides are flowed across the plate in a fixed order to facilitate sequencing-by-synthesis. (F) Within each well, the introduction of a nucleotide complementary to the microbead bound DNA template results on the extension of a DNA strand by DNA polymerase. This results in the release of pyrophosphate, which is detected as a light signal following a chain of chemical reactions involving sulfurylase and luciferase. Diagram adapted from Roche 454 Genome Sequencer product information (www.454.com).

2.14.1 Analysis of 454 sequence data

The data files produced by the Roche 454 Genome Sequencer FLX were then processed using the RDP Pyrosequencing Pipeline (http://pyro.cme.msu.edu/), which is a collection of online tools that enable the data processing and analysis of large 16S rRNA sequence libraries. Sequences originating from the BD, IN, RS and KJ groups were separated based on the unique barcode sequenced assigned to each group, the HDA1/HDA2 primer sequences were trimmed, and sequences containing any ambiguous bases were removed from further analyses using the RDP Pyrosequencing Pipeline Initial Processor tool. Sequences were assigned to a bacterial taxonomy with a confidence threshold of 80% using the RDP Pyrosequencing Pipeline Classifier tool, which uses a naïve Bayesian rRNA classifier (Wang et al., 2007). The microbial community composition of rats fed BD, IN, RS and KJ diets were compared using the RDP Pyrosequencing Pipeline Library Compare tool, which estimates the statistical significance of observed differences in the abundance of a given taxon between two communities.

To examine microbial diversity in rats fed BD, IN, RS and KJ, sequences were clustered at the 3% maximum cluster distance using the RDP Pyrosequencing Pipeline Complete Linkage Clustering tool. This groups together all sequences which have a 97% or greater sequence similarity, which is commonly regarded as representing the similarity observed at the species level (Bohannan and Hughes, 2003; McCaig et al., 1999). Microbial diversity at the 3% maximum cluster distance was then estimated using the RDP Pyrosequencing Pipeline Shannon and Chao1 Index tool. The Chao1 index estimates the diversity of a community by examining the numbers of clusters represented by only one sequence and numbers of clusters represented by two sequences (Bohannan and Hughes, 2003).

Comparative phylogenetic analysis of sequences was performed to identify proportions of bacteria most closely related to bacteria from clostridial clusters IV and XIVa, which are the major butyric acid producing groups in the large bowel (Barcenilla et al., 2000). Colonic digesta sequences from rats fed

BD, IN, RS and KJ were grouped at 3% maximum cluster distance using the RDP Pyrosequencing Pipeline Complete Linkage Clustering tool. Grouped sequences were aligned in combination with representative sequences from bacteria belonging to clostridial clusters IV and XIVa (Table 5) using the RDP Pyrosequencing Pipeline Aligner tool. A phylogram of aligned sequences was constructed using the Neighbour-Joining method in the MEGA4 software package (Center for Evolutionary Medicine and Informatics, Tempe, AZ, USA). Sequences clustering on the same branches as representative RDP clostridial cluster IV and XIVa sequences were identified to determine proportions of total sequences from BD, IN, RS and KJ fed rats which were most similar to bacteria from the clostridial cluster IV and XIVa groups. Tests for significance of sequence abundance differences between groups at major branches were performed using the Unifrac Lineage Specific Analysis (Department of Chemistry and Biochemistry, University of Colorado at Boulder, Boulder, CO, USA).

Table 5. RDP sequences used for comparative phylogenetic analysis

	RDP ID	Name
Clostridial cluster XIVa	S000088221	Anaerostipes caccae (T)
	S000087730	Roseburia intestinalis (T)
	S000414442	Roseburia cecicola (T)
	S000000080	Clostridium indolis (T)
	S000012710	Clostridium xylanolyticum (T)
	S000012715	Eubacterium cellulosolvens (T)
	S000015326	Clostridium populeti (T)
	S000260075	Clostridium sphenoides (T)
	S000260335	Clostridium aerotolerans (T)
	S000381879	Eubacterium ruminantium (T)
	S000414260	Clostridium aminophilum (T)
	S000414599	Eubacterium eligens (T)
	S000414610	Eubacterium hallii (T)
	S000414616	Eubacterium rectale (T)
	S000414617	Eubacterium xylanophilum (T)
	S000428723	Clostridium algidixylanolyticum (T)
	S000436013	Ruminococcus gnavus
	S000436018	Ruminococcus lactaris (T)
	S000436454	Clostridium clostridioforme (T)
	S001199960	Blautia coccoides
	S001199961	Blautia hansenii DSM 20583
Clostridial cluster IV	S000436012	Ruminococcus callidus (T)
	S000436014	Ruminococcus albus (T)
	S000128478	Faecalibacterium prausnitzii (T)
	S000014612	Clostridium methylpentosum (T)
	S000004442	Clostridium leptum
	S000436479	Clostridium sporosphaeroides (T)

Sequences obtained from RDP database of members from Clostridial clusters IV and XIVa for comparative phylogenetic analysis. These sequences were aligned with the 16S rRNA sequences from the colonic microbiota to construct a phylogenetic tree.

2.15 Isolation of RNA from colon tissue

Total RNA for host transcriptome analysis was isolated by homogenising colon tissue, obtained from studies 1 and 3, in 2 ml of Trizol (Invitrogen Corporation, Carlsbad, California, USA). After homogenisation, samples were incubated on ice for 10 minutes, followed by centrifugation at 12000 X g for 10 minutes at 4°C. The supernatant was transferred to a new microcentrifuge tube and 200 µl of chloroform was added. Samples were shaken by hand for 15 seconds, followed by centrifugation at 12000 X g for 15 minutes at 4°C. The upper aqueous layer was transferred to a new microcentrifuge tube and 500 µl of 100% isopropanol was added to precipitate the RNA. Samples were incubated at room temperature for 10 minutes and then centrifuged at 12000 X g for 10 minutes at 4°C. Following centrifugation, the supernatant was discarded and the remaining pellet washed by adding 500 µl 75% ethanol. Samples were centrifuged at 7500 X g for 5 minutes at 4°C, after which the supernatant was discarded and the remaining pellet air dried for 15 minutes. The RNA pellet was then dissolved in 20 µl of H_2O.

The resuspended RNA was then further purified using RNeasy mini spin columns (Qiagen) using the following protocol. The RNA sample was adjusted to 100 µl with H_2O and 350 µl of Buffer RLT was added and mixed by pipetting. One hundred percent ethanol was added to each tube at a volume of 250 µl and mixed by pipetting. The sample was then transferred to an RNeasy mini spin column sitting in a collection tube and centrifuged at 8000 X g for 15 seconds. The flow-through was discarded and the RNeasy mini spin column placed in a new collection tube. The RNeasy mini spin column was washed by adding 500 µl of Buffer RPE followed by centrifugation at 8000 X g for 15 seconds. The flow-through was discarded and the RNeasy mini spin column was washed again with 500 µl of Buffer RPE followed by centrifugation at 8000 X g for 2 minutes. The RNeasy mini spin column was placed into a new collection tube and the bound RNA eluted by adding 30 µl H_2O followed by centrifuging at 8000 X g for 1 minute. The RNA was then quantified using a NanoDrop ND-1000 UV-VIS Spectrophotometer (Thermo Fisher Scientific). RNA quality was assessed with an

Agilent 2100 Bioanalyzer (Agilent Technologies). Only RNA samples with an RNA integrity number (RIN) > 8 were used for subsequent microarray analysis. A reference RNA for use as a common reference in two colour microarray analyses was made by pooling equimolar amounts of RNA from the 10 rats in the BD group. RNA samples were stored at -85°C prior to transcriptome analysis by microarray.

2.16 Microarray Analysis

Microarrays are a high throughput technology that enables the expression levels of thousands of genes to be measured simultaneously. Microarrays are produced by immobilising oligonucleotides probes corresponding to gene sequences on a solid substrate. Gene expression levels are measured by the capture of fluorescently labelled cDNA or cRNA transcribed from sample RNA onto the microarray. Measurement of the fluorescent signal intensities from each immobilised probe therefore indicates the relative abundance of each gene. Compared to single gene methods such as Northern blot or RT-qPCR, microarrays more easily allow the expression of multiple genes within biologically meaning pathways and processes to be measured. Despite the advantages, microarrays technologies do have some drawbacks compared to single gene methods. For example, RT-qPCR is generally considered to be a more sensitive method for detecting expression level changes. The effects of dye biases and non-specific or cross hybridisation of labelled targets to array probes are also issues characteristic of microarrays (Morey et al., 2006). Furthermore, many traditional statistical methods do not perform well with microarray data due to the large number of genes being analysed. Therefore, complex mathematical approaches are required for microarray analysis, which in combination with the large datasets generated from microarray experiments, results in computationally intensive analyses. Nevertheless, the ability to measure expression level changes in thousands of genes at once makes microarray technologies a highly valuable tool for transcriptome analyses.

In this study, a common reference design was chosen for 2 colour microarray analysis as the number of groups included in the studies precluded the use of a loop design. Transcript abundance for all samples was therefore compared to a common reference RNA.

2.16.1 Microarray hybridisation

Total RNA extracted from colon tissue from CR-BD, CR-RS, CR-KJ, CR-IN, GF-BD, GF-RS, GF-KJ rats were analysed individually by 4x44K Agilent Whole Rat Genome Oligo Microarrays (Agilent Technologies, catalogue number G4131F), with RNA from one rat presenting one biological replicate (n=6). Agilent Low RNA Input Linear Amplification Kit (Agilent Technologies, catalogue number 5188-5340) was used to generate Cyanine 3 (Cy3) and Cyanine 5 (Cy5) labelled cRNA for microarray hybridisation using the following protocol:

Sample cDNA from was generated from 200 ng of total RNA of individual rats by adding 2 µl Agilent Spike-In mix (Agilent Technologies), 4 µl 5X First Strand Buffer, 2µl 0.1M DTT, 1 µl 10mM dNTP mix, 1 µl MMLV-RT enzyme, and 0.5 µl RNaseOUT in a total volume of 20 µl and incubating at 40°C for 2 hours. The MMLV-RT enzyme was then deactivated by incubating the mixture at 65°C for 15 minutes, after which the tube was placed at 4°C prior to transcription of fluorochrome labelled cRNA. Reference cDNA was generated from 500 ng of pooled reference RNA using the procedure and reagents listed in the previous step.

Cy3 labelled sample cRNA was generated from sample cDNA templates by adding 15.3 µl H_2O, 20 µl 4X transcription buffer, 6 µl 0.1M DTT, 8 µl NTP mix, 6.4 µl 50% PEG, 0.5 µl RNaseOUT, 0.6 µl Inorganic pyrophosphatase, 0.8 µl T7 RNA Polymerase, and 2.4 µl Cyanine 3-CTP, followed by incubation at 40°C for 2 hours. Cy5 labelled reference cRNA was generated from reference cDNA templates using the procedure and all reagents listed in the previous step except for the inclusion of 2.4 µl Cyanine 5-CTP instead of 2.4 µl Cyanine 3-CTP.

Cy3 labelled sample cRNA and Cy5 labelled reference cRNA were purified with Qiagen RNeasy mini spin columns (Qiagen) using the following procedure. Twenty µl of H_2O, 350 µl of Buffer RLT, and 250 µl of ethanol were added to each cRNA tube. The contents of each tube was then transferred to an RNeasy mini column in a 2 ml collection tube and centrifuged at 8000 X g for 30 seconds at 4°C. The flow-through was discarded and 500 µl Buffer RPE was added to each mini column, which was then centrifuged at 8000 X g for 60 seconds at 4°C. A further 500 µl of Buffer RPE was added to each mini column, which was then centrifuged at 8000 X g for 60 seconds at 4°C. The cleaned cRNA bound to each mini column was then eluted by placing the mini column into a new tube and adding 30 µl H_2O, followed by centrifugation at 8000 X g for 30 seconds at 4°C. The yield and specific Cy3 or Cy5 activity in each cRNA reaction was examined using a NanoDrop ND-1000 UV-VIS Spectrophotometer (Thermo Fisher Scientific). cRNA reactions which yielded > 8.0 pmol Cy3 or Cy5 per µg cRNA were used for microarray hybridisation.

Hybridisation reactions were set up consisting of 825 ng of each Cy3 labelled sample cRNA, 825 ng of Cy5 labelled reference cRNA, 50 µl 10X Blocking Agent, 10 µl 25X Fragmentation Buffer, and H_2O to bring the total volume to 250 µl. The reaction tube was then incubated at 60°C for 60 minutes to fragment unlabelled RNA. After incubation, 250 µl 2X Hybridization Buffer was added to each tube to stop the fragmentation reaction. Each hybridization reaction was dispensed into a single chamber on a SureHyb gasket slide at a volume of 490 µl (Agilent Technologies), which was then placed within a SureHyb chamber base (Agilent Technologies). The active side of a 4x44K Agilent Whole Rat Genome Oligo Microarray slide (Agilent Technologies) was then placed onto the SureHyb gasket slide. The SureHyb chamber cover was placed on top of the sandwiched slides and the assembled chamber secured shut. The assembled slide chamber was then incubated at 65°C for 17 hours on a rotating platform set to 4 rpm.

After incubation, the slide chambers were disassembled while submerged in GE Wash Buffer 1 (Agilent Technologies) and the microarray slides placed in a slide staining-dish. The slides were then submerged in fresh GE Wash Buffer 1 for 1 minute at room temperature. The slides were then submerged in GE Wash Buffer 2 for 1 minute at 37°C. To prevent Cy5 degradation by ozone, the slides were submerged in acetonitrile for 10 seconds at room temperature, after which the slides were washed in Stabilizing and Drying Solution (Agilent Technologies) for 30 seconds at room temperature.

2.16.2 Microarray data acquisition

Microarrays were scanned with an Agilent DNA Microarray Scanner G2565CA (Agilent Technologies) immediately after they were dried. Slides were scanned with a 5 μm scanning resolution using the extended dynamic range setting. Fluorescent intensities of the Cy3 and Cy5 signals from the microarray spots were calculated from the scanned images of the microarray slides using Agilent Feature Extraction 9.0 Image Analysis software (Agilent Technologies). A generalised representation of the workflow for the generation of fluorescently labelled cRNA probes and microarray hybridisation is shown in Figure 6. Preprocessing, quality checking, normalisation, and determination of differentially expressed genes was performed using Bioconductor (Gentleman et al., 2004), a freely available set of tools for the analysis of microarrays implemented in the statistical programming language R (R Development Core Team). Bioconductor and R are open source and highly customisable, and are widely used as full access to algorithms and their implementation is readily available.

2.16.3 Microarray quality checking and normalisation

Expression of each microarray probe was calculated by comparing the Cy3 (green) signal intensity, representing the transcript abundance in the sample RNA, to the Cy5 (red) signal intensity, which represents the transcript abundance in the reference RNA. An overview of the microarray analysis

pipeline is shown in Figure 7. Red and green signal intensities were normalised within microarrays by loess normalisation using the limma package of Bioconductor (Gentleman et al., 2004; Smyth, 2004). After normalisation, the red and green intensities were summarised as log-ratios (M-values) and log-averages (A-values); $M=\log_2(R/G)$ and $A=½(\log_2R + \log_2G)$. Following loess normalisation, Aquantile normalisation was performed to normalise A-values between microarrays without altering M-values (Smyth, 2004). Therefore, in a common reference 2 colour microarray design such as that used in this study, the expression levels of all genes are expressed as the ratio of red (reference) signal vs. green signal (sample). Comparisons in gene expression levels are performed by comparing the red/green ratios of the gene between arrays.

Microarray quality was assessed using image plots showing the physical distribution of red and green signals on each microarray, boxplots showing distribution of un-normalised red and green intensities, MA plots showing distribution of M-values compared to A-values of each microarray, and intensities plots showing frequency of red and green signals (Appendix F - Appendix L). Examination of microarray quality resulted in the removal of one microarray of the IN group from subsequent analyses due to an irregular distribution of the red signal intensities compared to all other arrays.

2.16.4 Determination of differentially expressed genes

A number of experimental comparisons between dietary treatments in CR and GF rats were performed to identify differentially expressed genes: (i) CR-BD vs. CR-IN; (ii) CR-BD vs. CR-RS; (iii) CR-BD vs. CR-KJ; (iv) GF-BD vs. GF-KJ; (v) GF-BD vs. GF-RS; (vi) CR-BD vs. GF-BD; (vii) CR-RS vs. GF-RS; and (viii) CR-KJ vs. GF-KJ. For each comparison, a list of differentially expressed genes was generated by calculating an empirical Bayes moderated t-statistic for each gene using a linear model implemented in the software package limma (Smyth, 2004), which is a component of Bioconductor. Genes were determined to be differentially expressed within a comparison if they showed > 1.2 fold change in expression and a Benjamini and Hochberg false discovery rate adjusted P value (FDR) < 0.05 (Smyth,

2004). Hierarchical clustering, principal component analysis (PCA) and class predictions of gene expression profiles were performed using the Bioconductor packages limma, MADE4 (Culhane et al., 2005), and Prediction Analysis of Microarrays for R (PAMR) (Hastie et al., 2010).

2.16.5 Biological processes associated with differentially expressed genes

Analysis of biological processes from the Gene Ontology (GO) Consortium database (Ashburner et al., 2000) associated with differentially expressed genes was performed using the GOstats package (Falcon and Gentleman, 2007) in R. The GO Consortium database is a bioinformatic resource with the purpose of standardising descriptions of gene and gene products across species and databases. Lists of differentially expressed genes were tested for significant over-representation using a hypergeometric test where biological processes were considered to be over-represented if genes within a list were associated with a biological process in greater proportions than would be expected through chance alone.

2.16.6 Biological network analysis using IPA

Analysis of gene interaction networks among differentially expressed genes was performed using Ingenuity Pathway Analysis (IPA) (Ingenuity Systems, Redwood City, CA, USA). IPA is a bioinformatic software package which correlates genes with biological functions and pathways curated from the literature and databases including the Kyoto Encyclopedia of Genes and Genomes (KEGG) database (Kanehisa and Goto, 2000) and the GO database.

Gene data sets containing gene identifiers, fold changes in expression within comparisons and corresponding significance values were uploaded to the IPA server. Each gene identifier was mapped to its corresponding network eligible molecule in the IPA database, which were overlaid onto a global molecular network developed from information contained in IPA database. Networks of genes and gene products were then generated based on their connectivity, which is their interconnectedness

with each other relative to all molecules that they are connected to in the IPA database (Calvano et al., 2005). Networks generated from gene lists were scored based on the number of molecules in the network in comparison to the total number of network eligible molecules analysed and the total number of network eligible molecules within the IPA database. The network score was calculated using the right-tailed Fisher's Exact Test.

2.16.7 KEGG pathways analysis using GSEA

Gene set enrichment analysis (GSEA) of genes belonging to KEGG pathways was performed with a permutation based approach using the Category package in Bioconductor (Jiang and Gentleman, 2007; Subramanian et al., 2005). Because phenotypic changes may be associated with small but coherent changes in the expression of a biologically linked set of genes, GSEA may be used for interpreting microarray data by aggregating the per gene statistics across genes within a predetermined gene set, thereby enabling the detection of situations where all genes in a pathway change in a small, but consistent way (Jiang and Gentleman, 2007). The KEGG database is a bioinformatic resource that maps genes and gene products to biological pathways that include metabolic processes and diseases drawn from published literature.

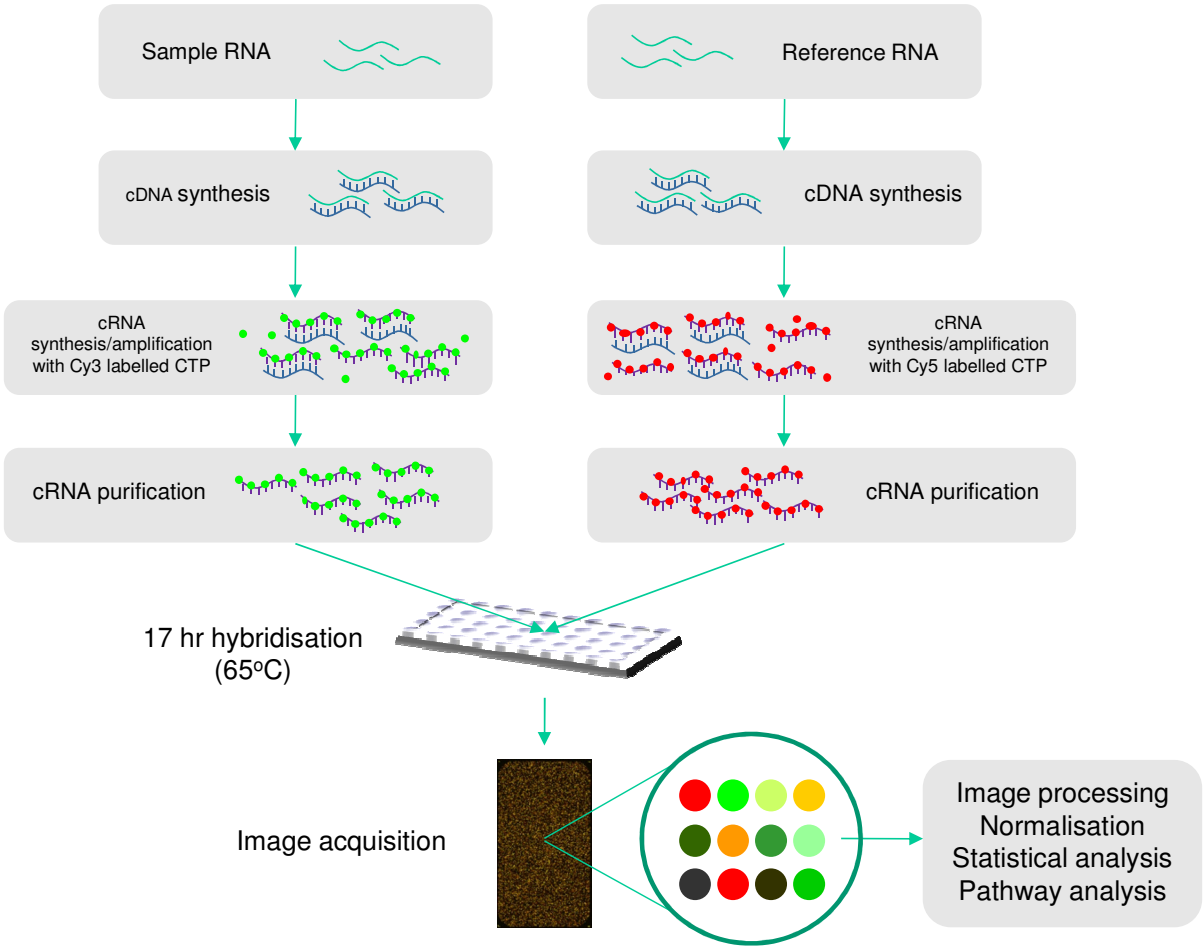

Figure 6. Microarray hybridisation workflow. cDNA is synthesised from sample and reference RNA. Cy3 labelled cRNA is then synthesised from the sample cDNA, and Cy5 labelled cRNA is synthesised from the reference cDNA. Purified Cy3 labelled sample cRNA and Cy5 labelled reference cRNA is co-hybridised to the same microarray. After overnight hybridisation, the microarrays are washed and then scanned. The green and red fluorescent signals for each spot is then determined, indicating the proportion of bound Cy3 and Cy5 cRNA, respectively.

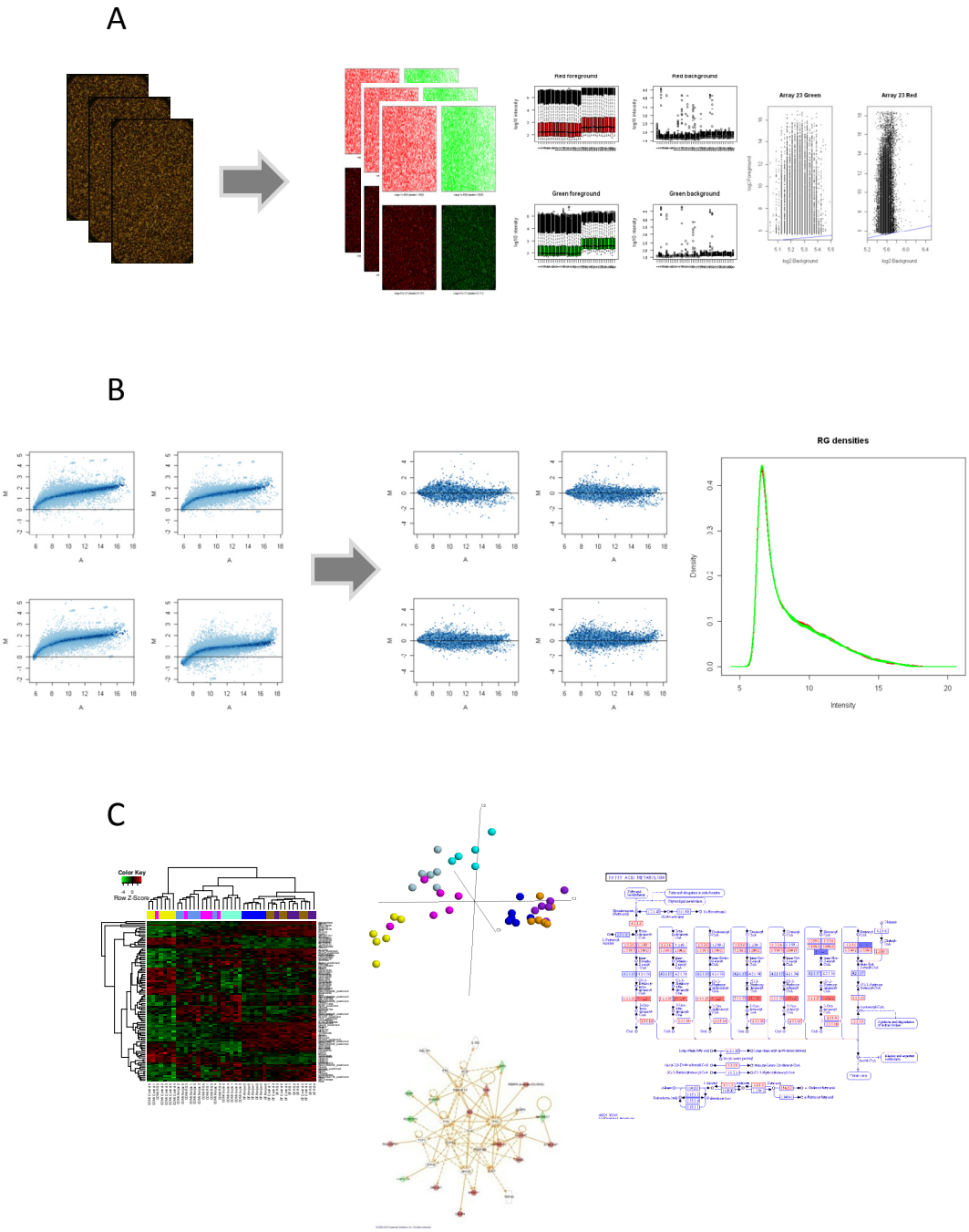

Figure 7. Analysis of microarray data. (A) Quality checking of microarrays. Raw green and red signal, and background intensities are evaluated for spatial biases, bad spots are flagged for removal from further analyses, and distribution of red and green signals between arrays is determined. (B) Microarrays are normalised to scale signal intensities and red/green signal ratios within and between arrays. (C) Differentially expressed genes between treatments are determined, which can then be analysed using a variety of methods including hierarchical clustering, principal component analysis, network analysis, and pathway analysis.

2.17 RT-qPCR analysis of rat gene expression

Results from the microarray analysis of host gene expression was validated by RT-qPCR analysis of colon tissue RNA from study 1 (CR-BD, CR-RS, CR-KJ and CR-IN) and study 3 (GF-BD, GF-RS, and GF-KJ). Six biological replicates were measured by RT-qPCR for each group, except for CR-IN, which consisted of 5 biological replicates. Transcription of cDNA from colon tissue RNA was performed using an Applied Biosystems High Capacity RNA-to-cDNA Kit (Applied Biosystems Inc.). A transcription mixture consisting of 10 µl of 2X RT buffer, 1 µl of 20X RT Enzyme Mix, 2 µg of RNA, and H_2O up to a total volume of 20 µl was incubated at 37°C for 60 minutes, followed by 95°C for 5 minutes. Samples were then stored at -20°C until RT-qPCR analysis.

Quantitative PCR reactions were carried out using Applied Biosystems TaqMan Gene Expression Master Mix (Applied Biosystems Inc.) with a Corbett Rotor-Gene 6000 real-time thermal cycler (Qiagen). Predesigned and prevalidated Applied Biosystems TaqMan Gene Expression Assays (Applied Biosystems Inc.) for genes *Galntl4*, *Galnt2*, *Hspca*, *Mcpt1*, *Mrps31*, and *Uba52* were used for comparative gene expression analysis and microarray validation. Genes were selected to include those that showed significant differential expression by microarray. Each reaction mix consisted of 10 µl of 2X TaqMan Gene Expression Master Mix, 1 µl of cDNA template, 1 µl of TaqMan Gene Expression Assay, and 8 µl of H_2O. The reactions were carried out using the following program; 50°C for 2 minutes, 95°C for 10 minutes, followed by 40 cycles of 95°C for 15 seconds and 60°C for 60 seconds. Relative expression between groups was determined by comparing mean cycle thresholds (Ct) normalised against 60S ribosomal protein L40 encoding *Uba52*, which was chosen as a normalisation reference as it showed low and non significant variation in expression levels across all samples. Data acquisition and Ct values were calculated using Rotor-Gene 6000 Series software version 1.7 (Qiagen). Statistical significance of fold changes was tested using ANOVA and correlation between microarray and RT-qPCR results was tested by Spearman rho correlation analysis in R (R Development Core Team).

Chapter 3. Results

3.1 Diet intake

All rats were of good health before and during the feeding studies and all rats survived until the termination of the studies when they were euthanased by CO_2 overdose. In study 1, total diet intake for CR rats fed GL were significantly lower than that for BD fed rats after 28 days of feeding (P=0.05; GL=336 ± 37, BD=368 ± 24, g ± s.d.). No significant differences in food intake were observed between other groups of rats from feeding study 1 (Table 6). No significant differences in food intake between rats fed different diets were observed in study 2, which examined the effects of RS or KJ dose. Similarly, no significant differences in food intake were seen in GF rats fed for 28 days (Table 7). However, GF rats had significantly higher food intakes than CR rats (P<0.01; GF=649 ± 49, CR=363 ± 35, g ± s.d.).

3.2 Rat weights

Treatment groups were balanced for body weight at the beginning of each study. Final weight and percentage of starting weight after 28 days of feeding in rat study 1 was significantly lower in GL fed CR rats compared to BD fed rats (P=0.04 and P=0.01, respectively) (Table 6). This result, in conjunction with the reduced food intake observed in GL fed rats, suggests a possible satiety effect of GL. Therefore GL may be influencing weight gain through effects on diet palatability and/or alterations in metabolism. However, due to the possibility of adverse effects beyond the reduced weight gain, GL was not examined in subsequent feeding studies. CR Rats fed IN, KJ, RS, or UN in study 1 showed no significant changes in final weight or weight gain after 28 days compared to BD fed rats. Similarly, no significant differences in rat weight or weight gain were observed between dietary groups in CR rats in feeding study 2, or GF rats in feeding study 3. GF rats gained significantly less weight than CR counterparts after 28 days of feeding (P<0.01; GF=211 ± 15, CR=368 ± 39, % ± s.d.), despite consuming more food.

Table 6. Study 1 – Body weights of conventionally raised rats after 28 days of feeding

Diet	Start weight (g)	Final weight (g)	Percent start weight	Total food intake (g)
BD	49 ± 9	177 ± 22	370 ± 35	368 ± 24
RS	52 ± 10	188 ± 22	368 ± 50	387 ± 31
KJ	47 ± 8	171 ± 27	366 ± 36	365 ± 37
UN	45 ±7	178 ± 17	405 ± 55	365 ± 31
GL	49 ± 11	157 ± 23*	325 ± 47*	336 ± 37*
IN	45 ± 6	167 ± 17	378 ± 42	361 ± 37
P value	0.38	*0.04	*0.01	*0.05
LSD	8	19	40	30

Mean gross body weight at start of study and final weight after 28 days of feeding, g ± s.d., n=10. Percent start weight indicates mean percentage of final rat weight after 28 days of feeding compared to start of study (% ± s.d.). Mean total food intake after 28 days of feeding (g ± s.d.). *Significantly different from BD group (P<0.05). LSD = least significant difference at P=0.05.

Table 7. Study 3 – Body weights of germ free rats after 28 days of feeding

Diet	Start weight (g)	Final weight (g)	Percent start weight	Total food intake (g)
BD	171 ± 22	352 ± 24	208 ± 19	623 ± 32
RS	178 ± 30	367 ± 42	209 ± 15	645 ± 43
KJ	175 ± 28	375 ± 46	215 ± 37	677 ± 60
P value	0.90	0.60	0.68	0.15

Mean gross body weight at start of study and final weight after 28 days of feeding, g ± s.d., n=6. Percent start weight indicates mean percentage of final rat weight after 28 days of feeding compared to start of study (% ± s.d.). Mean total food intake after 28 days of feeding (g ± s.d.).

3.3 DRC induced changes in colon mucosal morphology

Crypt lengths were measured in transverse sections of colon tissue to assess changes in growth of the colonic mucosa after feeding DRC (Table 8). Crypt lengths of CR rats from study 1 fed for 28 days showed a tendency to be longer than those fed for 14 days (P=0.06). After 14 days of feeding, no significant differences in crypt length were observed between rats fed different diets. However, significant differences in crypt length between groups were observed after 28 days of feeding (P=0.02). CR rats from study 1 fed KJ, UN, and GL showed significantly longer crypts than BD fed rats (P=0.02; KJ=233.7 ± 10.6, UN=240.7 ± 28.0, GL=229.0 ± 22.3, BD=206.7 ± 19.0 μm ± s.d.). Overall, CR rats fed BD, RS and KJ had significantly longer crypt lengths than those in their GF counterparts (P=0.01; CR=219 ± 22.6, GF=205.7 ± 14.8, μm ± s.d.) after 28 days of feeding. No significant differences in colon crypt length were observed between GF rats fed BD, KJ, or RS. These results show the interaction of DRC and the microbiota may have an important role for stimulating the growth of the colonic mucosa.

Numbers of mucus containing goblet cells were counted to measure DRC induced changes in the mucus producing potential of the colonic crypts (Table 9). Goblet cell counts per colon crypt in rats from study 1 fed for 28 days were significantly higher than those fed for 14 days (P<0.01; 14 days =21.5 ± 2.5, 28 days=23.7 ± 2.9, cells/crypt ± s.d.). No significant differences in goblet cell frequencies between diets were observed in rats fed for 14 days. However, CR rats fed for 28 days showed significant differences in goblet cell counts between rats fed KJ, UN, GL and IN compared to rats fed BD (P<0.01; KJ=24.2 ± 2.1, UN=24.1 ± 3.1, GL=24.5 ± 2.0, IN=25.6 ± 1.9, BD=20.9 ± 1.5, cells/crypt ± s.d.). Goblet cell numbers in colonic crypts were significantly higher in GF rats compared to their CR counterparts (P=0.05; GF=25.7 ± 0.7, CR=23.4 ± 0.6, cells/crypt ± s.e.m.), which is consistent with the increased mucus accumulation and distended caecums characteristic of germ-free rodents. GF rats fed KJ also showed significantly increased goblet cell abundance compared to those fed BD (P<0.01; GF-KJ=28.5 ± 2.9, GF-BD=24 ± 1.2, cells/crypt ± s.d.).

Table 8. Colon crypt length in rats from studies 1 and 3

		BD	RS	KJ	UN	GL	IN	P value	LSD
CR	Day 14	208.6 ± 19.3	220.1 ± 15.9	220.5 ± 16.4	227.3 ± 24.6	220.2 ± 22.7	208.4 ± 24.2	0.28	18.7
CR	Day 28	206.7 ± 19.0	216.6 ± 21.2	233.7 ± 10.6*	240.7 ± 28.0*	229.0 ± 22.3*	223.9 ± 29.2	*0.02	20.2
GF	Day 28	201.2 ± 14.1	205.6 ± 17.3	210.3 ± 14.1				0.60	18.8

Crypt length after 14 and 28 days of feeding in CR and GF rats from feeding studies 1 and 3,mean µm ± s.d., n=10 (CR), n=6 (GF). *Significantly different to BD group (P<0.05). LSD = least significant difference at P=0.05.

Table 9. Colon crypt goblet cell frequency in rats from studies 1 and 3

		BD	RS	KJ	UN	GL	IN	P value	LSD
CR	Day 14	20.4 ± 1.1	21.8 ± 1.3	21.4 ± 2.3	21.8 ± 3.2	21.4 ± 4.3	22.0 ± 1.8	0.78	2.3
CR	Day 28	20.9 ± 1.45	23.0 ± 4.1	24.2 ± 2.1*	24.1 ± 3.1*	24.5 ± 2.0*	25.6 ± 1.9*	*0.01	2.3
GF	Day 28	24 ± 1.2	25.3 ± 2.8	28.5 ± 2.9*				*0.02	3.0

Numbers of goblet cells per colon crypt after 14 and 28 days of feeding in CR and GF rats from feeding studies 1 and 3, mean number of cells ± s.d., n=10 (CR), n=6 (GF). *Significantly different to BD group (P<0.05). LSD = least significant difference at P=0.05.

3.4 DRC induced alterations in colonic SCFA concentrations

Analysis of SCFA and carboxylic acid concentrations in colon digesta was carried out by FID capillary GC to measure changes in bacterial metabolism (Table 10). After 14 days of feeding, CR rats fed RS and KJ showed significantly higher concentrations of colonic acetic acid than BD fed rats (P=0.008; RS=37.1 ± 13.7, KJ=32.7 ± 8.1, BD=21.6 ± 8.3, μmol/g ± s.d.). Similarly, CR rats fed IN, KJ, RS, or GL for 14 days showed elevated levels of butyric acid compared to BD rats (P<0.001; IN=5.8 ± 3.7, KJ=9.5 ± 3.7, RS=5.6 ± 1.8, GL=5.8 ± 2.4, BD=2.1 ± 1.2, μmol/g ± s.d.). Alterations in colonic SCFA concentrations were also observed between dietary groups in CR rats fed for 28 days and levels of acetic and butyric acids were significantly higher in rats fed for 28 days compared to 14 days (P<0.01 and P<0.01, respectively). Acetic acid levels in CR rats fed RS and KJ for 28 days were significantly higher than that observed in BD fed rats (P=0.01; RS= 53 ± 16.1, KJ=44.4 ± 16.7, BD=31.6 ± 12.4, μmol/g ± s.d.). Propionic acid concentrations were significantly increased in rats fed IN or RS for 28 days compared to BD fed rats (P<0.01; IN=6.3 ± 5.1, RS=6.0 ± 3.0, BD=1.7 ± 0.7, μmol/g ± s.d.). Significant changes in colonic butyric acid concentrations were also observed after 28 days in all DRC fed groups except those fed UN (P<0.001; IN=12.8 ± 8.8, KJ=11.8 ± 6.5, RS=11.6 ± 3.4, GL=9.3 ± 4.0, BD=3.8 ± 1.7, μmol/g ± s.d.). Whereas no changes were observed in lactic acid concentrations after 14 days of feeding, rats fed RS showed significantly higher colonic lactic acid levels after 28 days (P=0.02; RS=9.2 ± 6.4, BD=4.0 ± 2.1, μmol/g ± s.d.). Although succinic acid levels were highly variable between rats, feeding IN for 28 days resulted in significantly higher colonic succinic acid concentrations compared to BD fed rats (P=0.05; IN=11.4 ± 9.9, BD=5.4 ± 2.1, μmol/g ± s.d.). No significant differences were seen in carboxylic acid concentrations after feeding UN compared to BD fed rats. The differential effects of DRC on SCFA and carboxylic acid concentrations point to a differential effect of DRC on the composition and/or metabolism of the microbiota, depending on the form of DRC. A notable observation was that UN did not alter SCFA concentrations, despite increasing both colonic crypt depths and goblet cell counts. This suggests that UN exerts effects on colon mucosal morphology without altering microbiota metabolism or composition. Therefore, the

effects of UN on the microbiota was not subsequently examined, and UN was excluded from studies 2 and 3.

Principal component analysis showed colonic SCFA profiles of rats fed IN, RS, KJ and GL for 28 days were distinct from those fed BD (Figure 8). The DRC induced changes to SCFA profiles also tended to vary depending on the form of DRC. SCFA profiles from rats fed UN overlapped with those from rats fed BD, as expected considering UN did not significantly alter SCFA or carboxylic acid concentrations.

Results from study 2 also showed feeding DRC altered colonic SCFA and carboxylic acid concentrations. The lowest dose of RS or KJ which resulted in significant differences in SCFA concentrations was 2.5% (Table 11), which increased butyric acid concentrations in both RS and KJ fed rats compared to BD fed rats ($P<0.001$; RS [2.5%] 12.1 ± 7.7, KJ [2.5%] 11.7 ± 7.5, BD 5.6 ± 5.9, μmol/g ± s.d.). Linear regression analysis showed colonic SCFA concentrations responded with a significant linear relationship with increasing DRC dose. A significant linear relationship was observed with acetic ($P<0.01$), propionic ($P=0.01$) and butyric ($P<0.01$) concentrations with increasing RS dose after 28 days of feeding (Figure 9). Concentrations of colonic acetic ($P=0.03$) and butyric ($P<0.01$) acid also showed a significant linear relationship with increasing doses of KJ (Figure 9).

Table 10. SCFA concentrations in colonic digesta of rats from study 1

		BD	RS	KJ	UN	GL	IN	P value	LSD
	Acetic	21.6 ± 2.8	37.1 ± 13.7*	32.7 ± 8.1*	25.5 ± 6.1	27.0 ± 10.0	29.4 ± 6.7	*0.01	8.3
	Propionic	1.3 ± 1.45	5.2 ± 3.9	3.6 ± 4.4	1.9 ± 1.3	3.6 ± 5.0	4.9 ± 5.3	0.17	3.5
Day 14	Butyric	2.1 ± 1.2	5.6 ± 1.8*	9.5 ± 3.7*	3.2 ± 0.7	5.8 ± 2.4*	5.9 ± 3.7*	*<0.01	2.4
	Lactic	3.6 ± 1.4	8.3 ± 6.9	5.6 ± 1.7	3.8 ± 1.4	10.1 ± 13.0	4.1 ± 1.0	0.15	5.8
	Succinic	6.3 ± 3.9	9.6 ± 9.7	10.2 ± 3.5	5.4 ± 4.0	14.4 ± 17.8	7.9 ± 5.5	0.34	8.5
	Acetic	31.6 ± 12.4	53.0 ± 16.0*	44.4 ± 16.7*	30.4 ± 13.1	41.3 ± 7.0	40.8 ± 15.9	*0.01	12.5
	Propionic	1.7 ± 0.7	6.0 ± 3.0*	2.2 ± 1.3	1.6 ± 1.2	2.6 ± 2.4	6.3 ± 5.1*	*<0.01	2.4
Day 28	Butyric	3.8 ± 1.7	11.6 ± 3.4*	11.8 ± 6.5*	6.0 ± 0.9	9.3 ± 4.0*	12.8 ± 8.8*	*<0.01	4.5
	Lactic	4.0 ± 2.2	9.2 ± 6.4*	7.1 ± 2.8	3.7 ± 2.3	4.8 ± 2.4	6.4 ± 4.6	*0.02	3.4
	Succinic	5.4 ± 2.1	7.0 ± 4.1	9.6 ± 6.7	4.0 ± 2.4	7.5 ± 3.8	11.5 ± 9.9*	*0.01	4.9

Colonic SCFA and carboxylic acid concentrations in CR rats after 14 and 28 days of feeding, mean µmol/g colon contents ± s.d. (n=10). *Significantly different to BD group (P<0.05). LSD = least significant difference (P=0.05).

Table 11. Colonic SCFA concentration response to increasing doses of RS or KJ

	Dose	Acetic	Propionic	Butyric	Lactic	Succinic
BD		20.4 ± 9.2	6.9 ± 4.1	5.6 ± 5.9	3.3 ± 1.6	2.3 ± 0.7
	1.25 %	20.6 ± 5.6	6.0 ± 2.3	6.4 ± 3.7	2.7 ± 1.1	2.8 ± 0.8
RS	2.5 %	26.8 ± 9.5	9.4 ± 3.4	12.1 ± 7.7*	3.6 ± 1.2	4.3 ± 5.5
	5 %	32.5 ± 7.2*	10.1 ± 4.0*	16.3 ± 9.5*	6.0 ± 7.1*	9.9 ± 16.3*
	1.25 %	18.3 ± 8.1	6.1 ± 4.9	7.0 ± 4.7	2.9 ± 1.1	2.5 ± 0.7
KJ	2.5 %	24.6 ± 11.8	6.3 ± 3.7	11.7 ± 7.5*	3.3 ± 1.2	2.6 ± 0.8
	5 %	28.8 ± 6.1*	8.1 ± 4.0	17.1 ± 9.2*	4.9 ± 6.1	3.6 ± 2.0*
P value		* <0.01	* 0.04	* <0.01	* 0.05	* 0.04

Colonic SCFA and carboxylic acid concentrations with increasing RS or KJ dose (1.25, 2.5 and 5%) in CR rats fed for 28 days, mean µmol/g colon contents ± s.d. (n=10). *Significantly different to BD group (P=0.05).

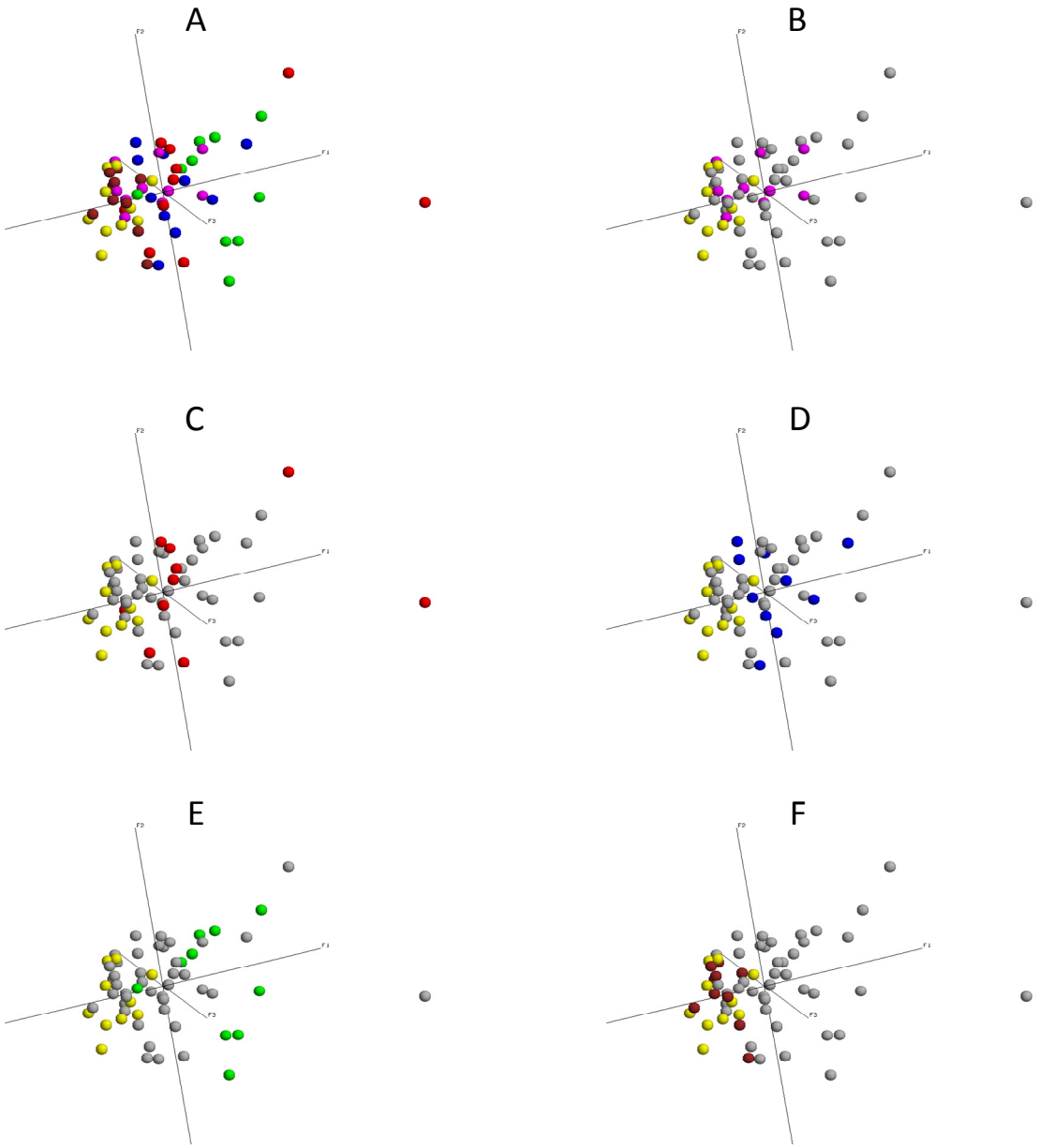

Figure 8. Principal component analysis of SCFA profiles. PCA plots of colonic SCFA profiles in rats fed DRC for 28 days from study 1, with each sphere representing the profile of one rat. (A) Profiles from rats fed BD (yellow), GL (magenta), IN (red), KJ (blue), RS (green) and UN (brown). Other plots show SCFA profiles from all rats with coloured spheres indicating profiles from; (B) BD and GL; (C) BD and IN; (D) BD and KJ; (E) BD and RS; and (F) BD and UN.

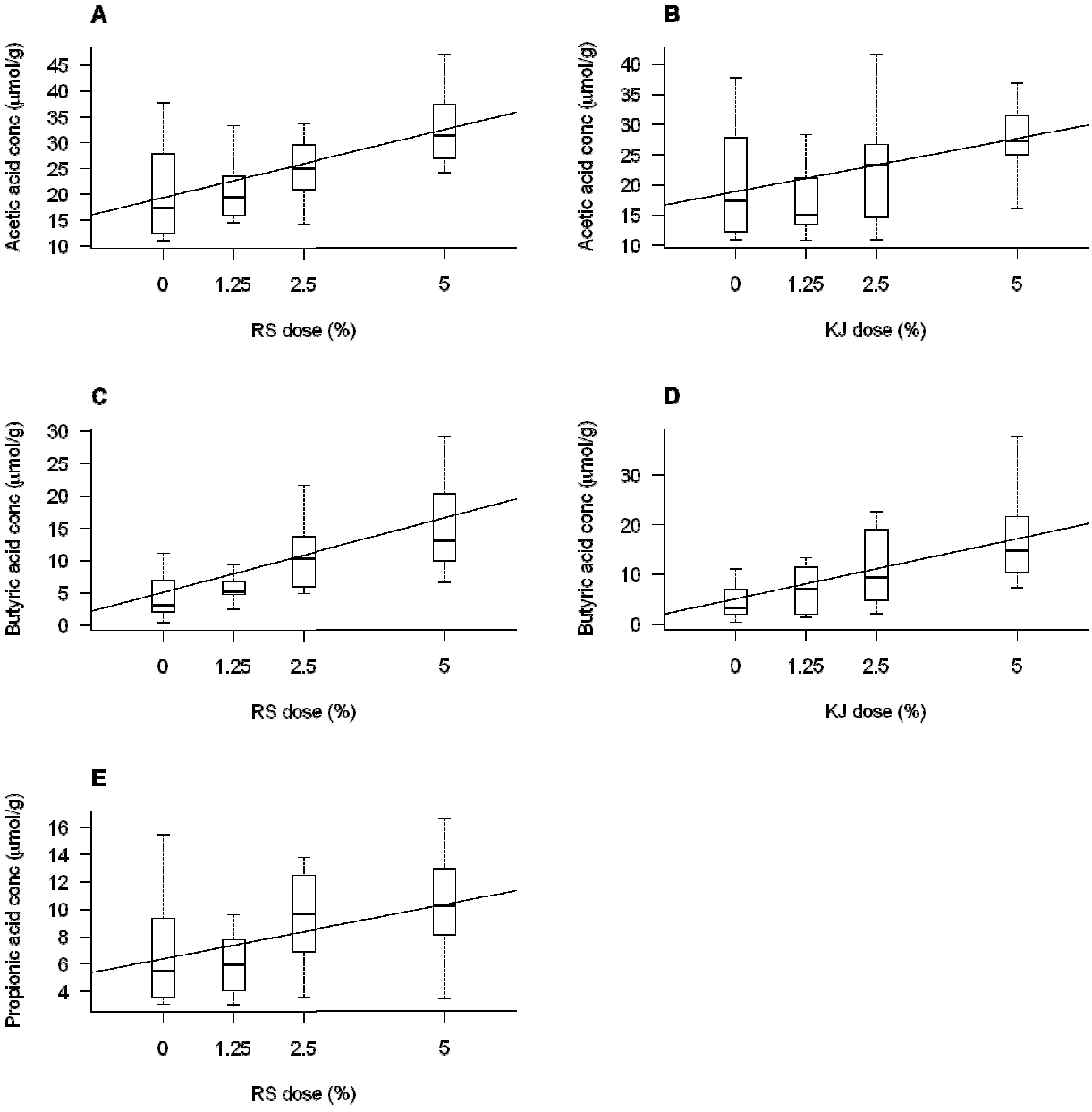

Figure 9. Effect of DRC dose on colonic SCFA concentrations. Colonic acetic acid concentrations in rats fed RS (A) and KJ (B), butyric acid concentrations in rats fed RS (C) and KJ (D), and propionic acid concentrations in rats fed RS (E). Boxplots show median, 25^{th}/75^{th} percentile, and 5^{th}/95^{th} percentile, µmol/g colon contents (n=10). Lines show linear regression of SCFA concentration vs. dose. Significance of slopes; (A) P<0.01; (B) P=0.03; (C) P<0.01; (D) P<0.01; and (E) P=0.01.

3.5 DRC induced changes in bacterial TTGE profiles

Bacterial 16S rRNA microbial community profiling of colon digesta from CR rats fed BD, KJ, RS and IN diets was performed by TTGE separation of RT-PCR products amplified from RNA using HDA1-GC/HDA2 primers. RNA TTGE profiles were used to characterise the structure of metabolically active members of the community. Unweighted pair group method with arithmetic mean (UPGMA) cluster analysis and PCA plots of TTGE profiles by Dice's similarity coefficient indicated a clear separation of profiles corresponding with diet (Figure 10). Jackknife analysis of similarity values correctly placed BD fed rats within the BD group 75% of the time, IN fed rats within the IN group 91.7% of the time, and KJ and RS fed rats within their respective groups 100% of the time (Table 12). In addition to showing distinct DRC induced shifts in microbiota profile, Jackknife analysis showed that variation in TTGE profiles between rats within the BD group were higher than rats fed IN, KJ and RS.

3.6 Microbiota composition in DRC fed rats

The microbiota composition of CR rats fed for 28 days from study 1 was examined by high throughput 454 pyrosequencing of the bacterial 16S rRNA gene. PCR products amplified from pooled DNA extracted from colon digesta using HDA1/HDA2 primers generated 10303, 8458, 10660, and 10590 sequences from BD, IN, KJ and RS fed rats, respectively, with an average product length of 200 bp. Taxonomic classification of sequences using the RDP pyrosequencing pipeline at an 80% confidence threshold showed significant differences in colonic microbiota community composition in all dietary groups (Table 13). Similar to TTGE community profile analysis, sequence identification showed that different diets produced distinct alterations in community structure.

IN fed rats showed phylum wide alterations in the colon digesta community compared to BD fed rats, with significantly lower proportions of Actinobacteria (IN=5.0%, BD=7.9% total sequences; $P<0.01$) and Firmicutes (IN=66.1%, BD=72.3%; $P<0.01$), whereas Bacteroidetes numbers were increased

(IN=21.7%, BD=14.5%; P<0.01). Changes in Bacteroidetes abundance were primarily due to increased proportions of *Bacteroides* spp. (IN=16.2%, BD=4.5%, P<0.01). Although the decrease in Firmicutes proportions in rats fed IN were mostly division wide, there was a large increase in the percentage of the Lachnospiraceae family which represented 38.0% of all sequences in the IN group, compared to 13.8% in the BD fed rats. Rats fed IN showed significant decreases in proportions of *Bifidobacterium* spp. (IN=2.2%, P<0.01) and *Lactobacillus* spp. (IN=8.97%, P<0.01) compared to controls (BD=4.8% and 19.5%, respectively).

Rats fed KJ diets had significantly lower proportions of Firmicutes sequences (62.9%, P<0.0001) and higher abundance of Bacteroidetes (16.9%, P<0.0001) compared to BD fed rats (72.3% and 14.5%, respectively). In contrast to the IN group, KJ fed rats had significantly higher proportions of Actinobacteria (12.7%, P<0.0001) compared to the BD group (7.9%). This expansion of Actinobacteria was mainly comprised of increases in *Bifidobacterium* spp. (KJ=6.6%, BD=4.8%; P<0.01) and Coriobacteriaceae (KJ=5.9%, BD=3.0%; P<0.01). *Lactobacillus* spp. proportions were also significantly lower in KJ fed rats (KJ=10.9%, BD=19.5%; P<0.01).

Rats fed RS showed an increase of Actinobacteria proportions compared to BD fed rats (RS=19.1%, BD=7.9%; P<0.01). Expansion of this division in RS fed rats occurred primarily through increased *Bifidobacterium* spp. abundance (RS=16.4%, BD=4.8%). RS fed rats showed phylum wide decreases in Firmicutes proportions compared to the BD group (RS=42.6%, BD=72.3%; P<0.01). In particular, a marked decrease in *Lactobacillus* spp. was observed (RS=9.6%, BD=19.5%; P<0.01). Proportions of Bacteroidetes sequences in RS fed rats were significantly higher compared to BD fed rats (RS=33.1%, BD=14.5%; P<0.0001). The majority of this increase was due to an expansion of unclassified Bacteroidetes (RS=17.3%, BD=8.5%). Although each diet resulted in a unique community structure, a common element shared by all DRC fed groups was an increase in Bacteroidetes to Firmicutes ratios compared to the BD fed group (IN=0.32, KJ=0.27, RS=0.78, BD=0.20). In light of the association of

obesity with a decrease in Bacteroidetes to Firmicutes ratio (Ley et al., 2005), the use of DRC may have a potentially useful role in strategies for addressing obesity. Each distinctive community composition induced by feeding DRC was also associated with an increase in fermentative capacity as shown by the increased SCFA and carboxylic acid concentrations in rats fed IN, RS and KJ.

3.6.1 Phylogenetic analysis of bacterial 16S rRNA sequences

Phylogenetic analysis of bacterial 16S rRNA gene sequences showed feeding DRC altered proportions of sequences that clustered most closely with sequences from bacterial belonging to clostridial clusters IV and XIVa (Figure 11). Unifrac Lineage-specific analyses showed significant differences in sequences belonging to clostridial cluster IV (BD=0.9%, IN=0.6%, KJ=4.7%, RS=0.6%; $P<0.0001$), and clostridial cluster XIVa (BD=14.1%, IN=38.1%, KJ=16.4%, RS=10.2%; $P<0.0001$) in rats fed for 28 days from study 1. Increased proportions of sequences clustering with bacterial sequences from clostridial clusters IV and XIVa may explain the increased colonic butyric acid observed in rats fed IN and KJ, as clostridial clusters IV and XIVa include prominent butyric acid producing bacteria (Barcenilla et al., 2000).

3.6.2 Species diversity estimate

Microbial diversity of sequences from colon contents DNA clustered at the 97% similarity threshold was similar between all groups except for rats fed KJ (Figure 12). The Chao1 index of estimated operational taxonomic units (OTUs) was significantly higher in CR rats fed KJ compared to IN, RS and BD groups at the 95% confidence interval (KJ=967, IN=564, RS=642, BD=576).

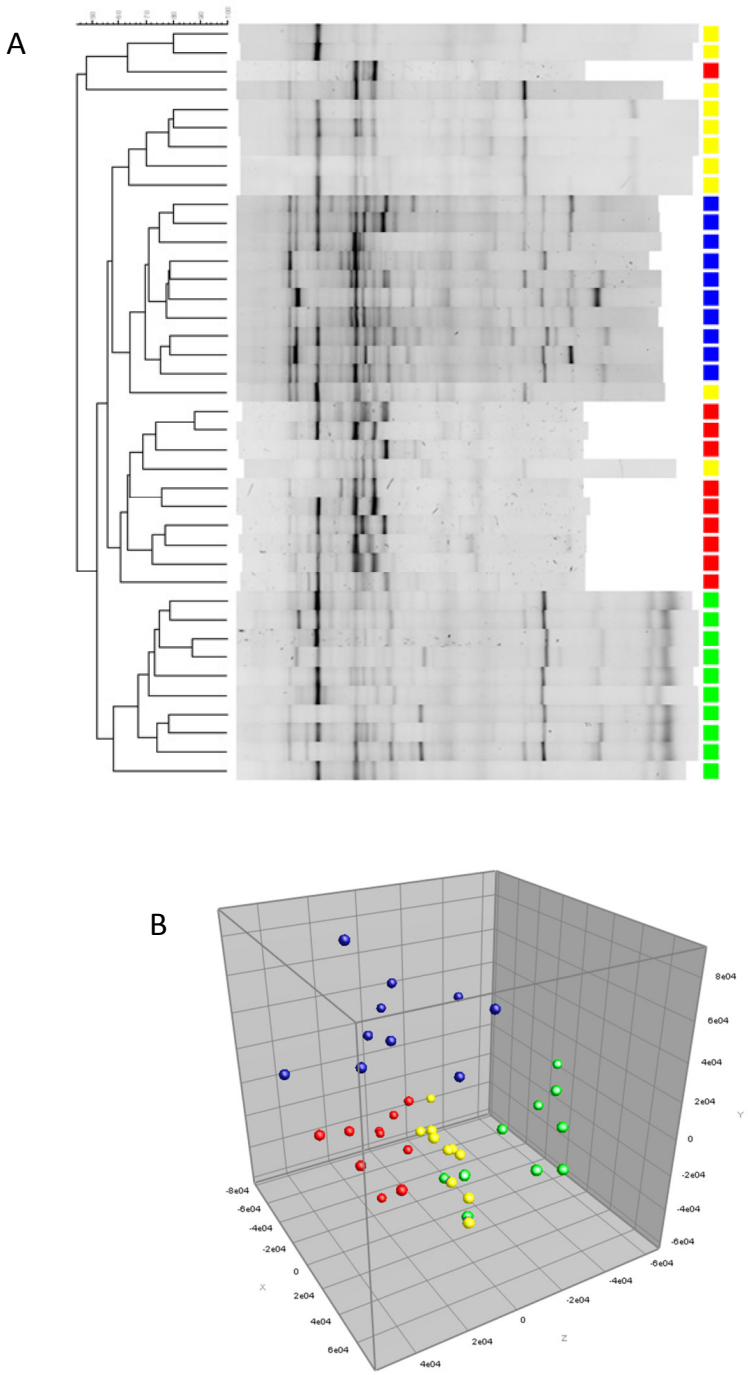

Figure 10. Bacterial 16S rRNA TTGE Profiles. (A) UPGMA clustering of Dice's similarity coefficient showing similarity of bacterial 16S rRNA TTGE profiles from RNA extracted from colon contents of rats fed BD (yellow), IN (red), KJ (blue) and RS (green) for 28 days from study 1. Scale bar indicates percentage similarity of profiles. (B) PCA plot of 16S rRNA TTGE profiles from study 1. Each sphere indicates bacterial 16S rRNA TTGE profile from one rat; BD (yellow), IN (red), KJ (blue) and RS (green).

Table 12. Group prediction of bacterial 16S rRNA TTGE profiles

	Actual groups			
Predicted	BD	IN	KJ	RS
BD	**75**	8.3	0	0
IN	16.7	**91.7**	0	0
KJ	8.3	0	**100**	0
RS	0	0	0	**100**

Confusion matrix showing distribution of predicted and actual group membership of bacterial 16S rRNA TTGE profiles from CR rats fed for 28 days in study 1. Columns indicate actual groups, rows represent predicted group membership, and values denote percentage of profiles. For example, of the profiles from BD fed rats (first column), 75% are predicted as belonging to group BD, 16.67% are incorrectly assigned to group IN, and 8.33% are incorrectly placed within group KJ. In contrast, 100% of KJ profiles are correctly assigned to the KJ group.

Table 13. Percentage of total bacterial 16S rRNA sequences

Depth	Identification	BD	IN	KJ	RS
Phylum	Actinobacteria	7.95	4.99*	12.74*	19.07*
	Verrucomicrobia	0.13	0.095	0.29*	0.24
	Firmicutes	72.35	66.07*	62.90*	42.56*
	Proteobacteria	1.21	1.41	0.98	0.48*
	Bacteroidetes	14.47	21.74*	16.91*	33.11*
Family	unclassified Actinobacteria	0.06	0.05	0.18	0.09
	Bifidobacteriaceae	4.82	2.21*	6.59*	16.41*
	Coriobacteriaceae	3.03	2.64	5.94*	2.54
Family	unclassified Firmicutes	10.01	8.29	14.15	6.07
	Clostridiaceae	7.84	0.01*	1.18*	1.12*
	Lachnospiraceae	13.83	37.95*	15.83*	9.94*
	Peptostreptococcaceae	4.35	0.70*	1.83*	0.52*
	Erysipelotrichaceae	15.51	9.59*	18.34*	14.52
	Lactobacillaceae	19.98	9.06*	10.90*	9.69*
	Streptococcaceae	0.51	0.28	0.24*	0.48
	Ruminococcaceae	0.37	0.19	0.42	0.20
Family	unclassified Bacteroidetes	8.52	4.47	10.32	17.34
	Bacteroidaceae	4.46	16.17*	5.03	2.77*
	Rikenellaceae	0.77	0.11*	0.48*	0.22*
	Porphyromonadaceae	0.70	0.99	0.87	0.80
	Prevotellaceae			0.22*	
Genus	*Lachnospiraceae Incertae Sedis*	0.65	6.07*	2.22*	0.87*
	Peptostreptococcaceae Incertae Sedis	4.33	0.70*	1.81*	0.52*
	Allobaculum	5.46	2.26*	6.13	7.97*
	Bacteroides	4.46	16.17*	5.03	2.77*
	Bifidobacterium	4.82	2.21*	6.59*	16.37*
	Clostridium	0.71	0*	0.08*	0.06*
	Lactobacillus	19.47	8.97*	10.45*	9.57*
	Turicibacter	3.46	0.37*	3.53	2.51*

Proportions of total bacterial 16S rRNA sequences (%) in colon DNA of rats fed BD, IN, KJ or RS for 28 days from study 1 identified at the phylum, family and genus level. Genera shown correspond to sequences identified at the genus level that represent > 0.5% of total bacterial 16S rRNA sequences in at least one dietary group. *Significantly different to BD group (P<0.01).

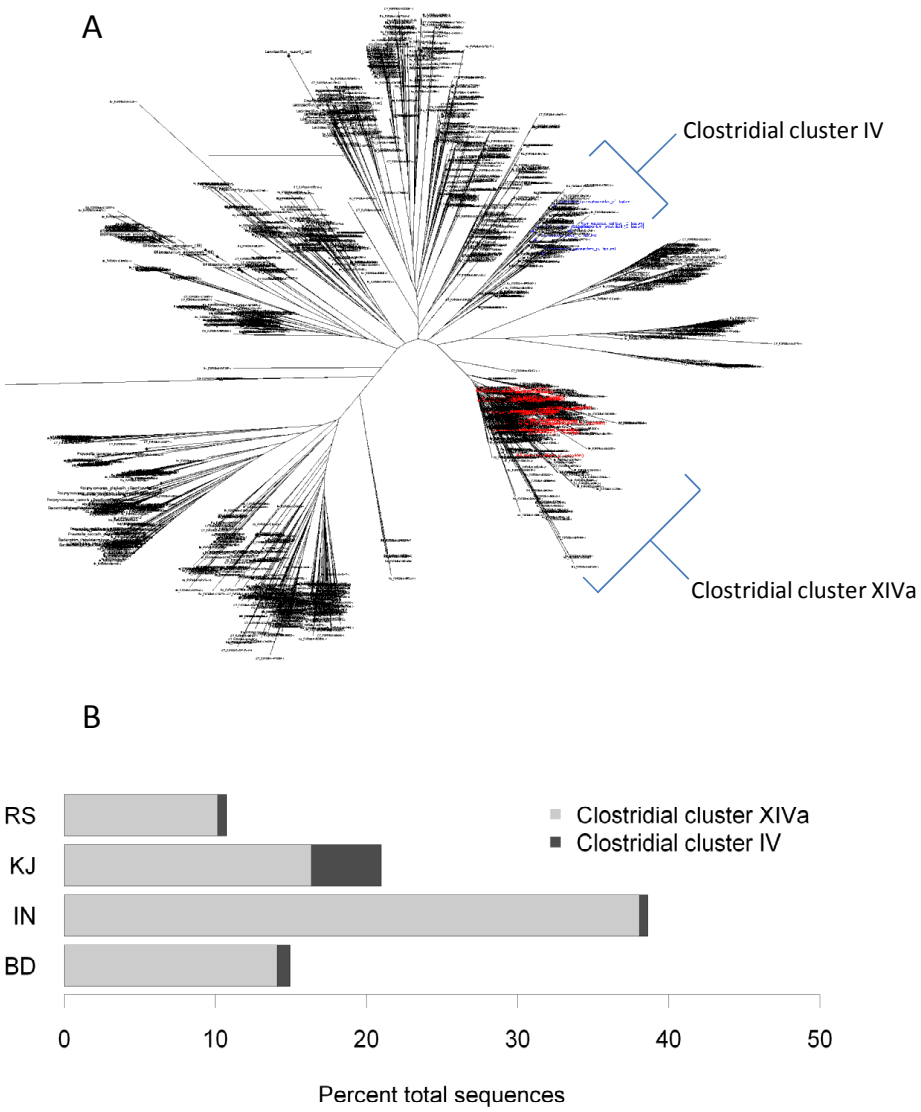

Figure 11. Phylogenetic analysis of bacterial 16S rRNA sequences. (A) Phylogenetic tree of bacterial 16S rRNA sequences in colon digesta DNA of rats fed BD, RS, KJ and IN for 28 days. Phylogram constructed using Neighbour Joining method with aligned sequences clustered at 97% similarity. Highlighted clusters show branches that include sequences from bacteria belonging to clostridial cluster IV and Clostridial cluster XIVa obtained from RDP database, as indicated by blue and red text, respectively. (B) Percentage of total sequences of BD, RS, KJ and IN fed rats clustered within clostridial clusters IV and XIVa branches.

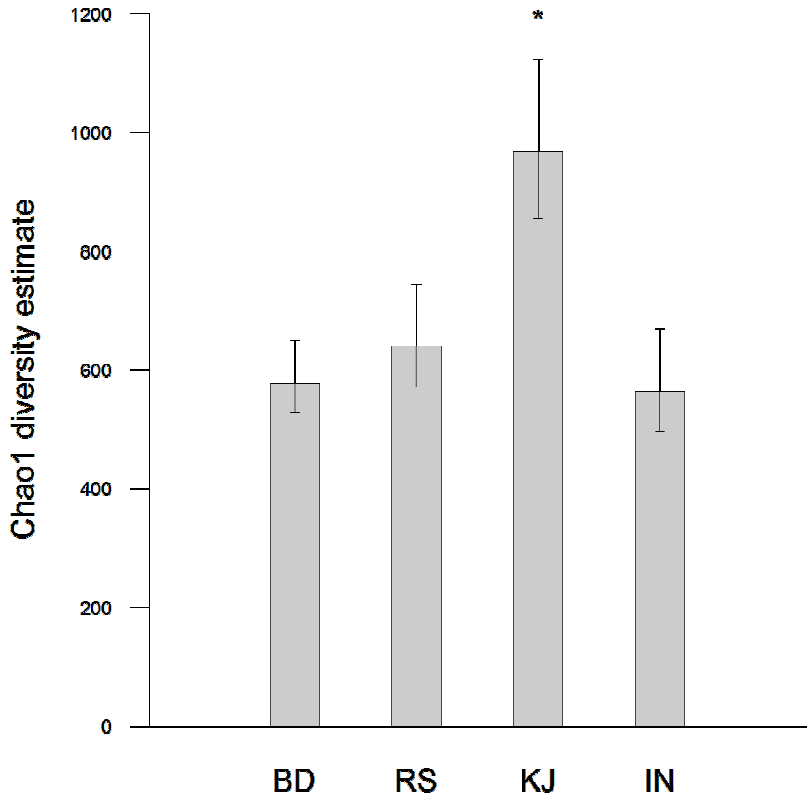

Figure 12. Microbiota diversity estimate. Chao1 diversity index of estimated numbers of OTUs (at 97% identity) in colon of rats fed BD, RS, KJ and IN diets for 28 days in study 1. Error bars represent 95% confidence interval. *Significantly higher diversity compared to BD, RS and KJ groups, $P<0.05$.

3.7 Alterations in 16S rRNA TTGE profiles in response to DRC dose

The effect of DRC dose on the microbiota community was investigated by feeding varying doses of KJ or RS to 21 day old male Sprague-Dawley rats in study 2. A basal diet was supplemented with KJ or RS at 5% (KJ-5, RS-5), 2.5% (KJ-2.5, RS-2.5), 1.25% (KJ-1.25, RS1-1.25) or 0% (BD). Multidimensional scaling (MDS) analysis of bacterial 16S rRNA TTGE profile similarities, as measured by Dice's coefficient, showed profiles from rats fed the highest dose of KJ or RS (5%) tended to segregate furthest from profiles of rats fed BD (Figures 13A and 13B). UPGMA cluster analysis of 16S rRNA TTGE profiles of pooled RNA of each group using HDA1/HDA2-GC primers showed a clearer tendency for groups to cluster together depending on type of DRC, particularly at the 5% and 2.5% dosages (Figure 14). MDS analysis showed profiles from rats fed BD or diets with 5% KJ or 5% RS also tended to segregate according diet (Figure 13C), which reconfirms results of the 16S rRNA TTGE profile analysis in study 1 (Figure 10).

Several bands were excised from the dose response TTGE gels and identified by sequence analysis using the RDP SeqMatch tool (Table 14). Specific primers were successfully designed targeting sequences from bands 1, 4 and 6, which were then used to quantify the abundance of these sequences in DNA extracted from colon digesta from each rat by qPCR. Band 1 was identified as a member of the *Lactobacillus* genus with a seqmatch (S_ab) score of 1, representing an identical match to a known sequence in the RDP database. Band 4 was identified as a member of the *Ruminococcus* genus and band 6 was identified as a member of the *Clostridium* genus with S_ab scores of 0.896 and 1, respectively.

Quantitative PCR analysis of 16S rRNA gene copy numbers in colonic bacterial DNA, corresponding to TTGE band positions 1, 4, and 6 (Figure 14), were altered by feeding DRC (Table 15) in study 2. Rats fed KJ at a dose of 5% had significantly lower *Lactobacillus* spp. 16S rRNA gene copy numbers ($P=0.01$; KJ [5%] 4.94 ± 1.31, BD 6.22 ± 0.94, $\log_{10}$ gene copies ± s.d) and significantly higher

Ruminococcus spp. 16S rRNA gene copy number (P=0.01; KJ [5%] 2.60 ± 0.76, BD 1.90 ± 0.17, $\log_{10}$ gene copies ± s.d) compared to rats fed BD. Rats fed RS at a dose of 5% show significantly lower *Clostridium* spp. 16S rRNA gene copy numbers compared to rats fed BD (P<0.01; RS [5%] 4.21 ± 0.66, BD 5.14 ± 0.23, $\log_{10}$ gene copies ± s.d.).

Although RS or KJ fed at doses lower than 5% did not significantly alter 16S rRNA gene copy numbers, linear regression analysis showed 16S rRNA copy numbers from several bands responded with a significant linear or inverse linear relationship with increasing DRC dose (Figure 15). Copy numbers of the 16S rRNA gene corresponding to *Lactobacillus* spp. (band 1) decreased with a significant inverse linear relationship with increasing KJ dose (P=0.01) (Figure 15). Similarly, 16S rRNA gene copy numbers corresponding to *Clostridium* spp. (band 6) and *Ruminococcus* spp. (band 4) also showed significant inverse linear relationships with increasing RS dose (P<0.01 and P=0.03, respectively) (Figure 15). Copy numbers of the 16S rRNA gene corresponding to the *Ruminococcus* spp. (band 4) increased with a significant linear relationship with increasing KJ dose (P=0.02) (Figure 15). *Lactobacillus* and *Clostridium* 16S rRNA gene copy numbers did not show significant linear relationships with increasing RS dose and KJ dose respectively (P>0.05).

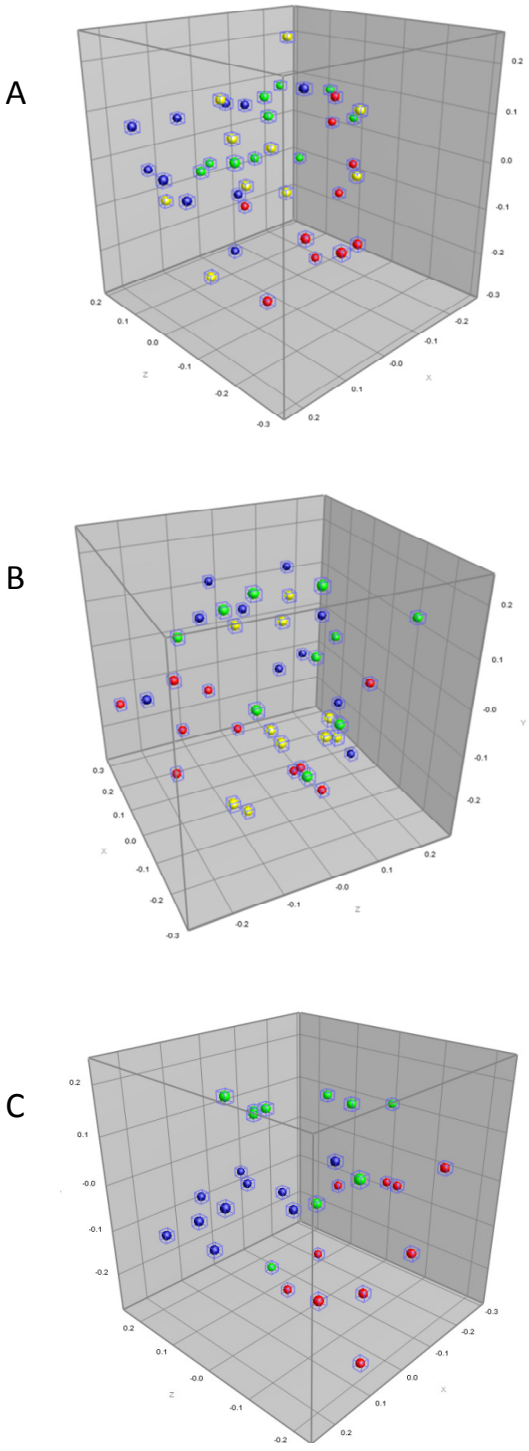

Figure 13. Multidimensional scaling analysis of TTGE profile in response to DRC dose. MDS plots of bacterial 16S rRNA TTGE profile similarities in rats fed KJ (A) and RS (B). Coloured points indicate profile of one rat, with colours indicating DRC dose; 0% (red), 1.25% (yellow), 2.5% (green), 5% (blue). (C) MDS plot of TTGE profile similarities in rats fed BD (red), 5% KJ (blue), and 5% RS (green).

Table 14. Identification of excised TTGE bands

Band	ID Match	Sequence name	Phylum	Family/Genus	S_ab Score
1	S000389901	*Lactobacillus jensenii*	Firmicutes	*Lactobacillus*	1
	S000436393	*Lactobacillus acidophilus* (T)	Firmicutes	*Lactobacillus*	1
	S000566924	*Lactobacillus kitasatonis*	Firmicutes	*Lactobacillus*	1
2	S000578499	uncultured bacterium	Firmicutes	Lachnospiraceae Incertae Sedis	1
	S000578680	uncultured bacterium	Firmicutes	Unclassified Lachnospiraceae	1
3	S000247984	*Allobaculum stercoricanis* (T)	Firmicutes	*Allobaculum*	0.678
	S000584266	uncultured bacterium	Firmicutes	*Allobaculum*	0.792
4	S001126333	uncultured bacterium	Firmicutes	Lachnospiraceae Incertae Sedis	0.888
	S000582212	uncultured bacterium	Firmicutes	*Ruminococcus*	0.896
	S000149090	*Ruminococcus* sp. 25F8	Firmicutes	*Ruminococcus*	0.840
5	S001012211	uncultured bacterium	Bacteroidetes	*Tannerella*	0.910
	S001011736	uncultured bacterium	Bacteroidetes	Unclassified Porphyromonadaceae	0.910
6	S000001564	*Clostridium aurantibutyricum*	Firmicutes	*Clostridium*	1
	S000015682	*Clostridium disporicum* (T)	Firmicutes	*Clostridium*	1
	S000260250	*Clostridium quinii* (T)	Firmicutes	*Clostridium*	1
7	S001199283	*Bifidobacterium pseudolongum*	Actinobacteria	*Bifidobacterium*	1
	S000002498	*Bifidobacterium animalis*	Actinobacteria	*Bifidobacterium*	0.930

Closest matches and classifications for sequenced TTGE bands from study 2 using RDP seqmatch. Band numbers indicate band positions as shown in Figure 14. S_ab score represents number of unique 7-base oligomers shared between sample sequence and RDP database sequence divided by lowest number of unique oligomers in either sequence. An S_ab score of 1 indicates an exact match between sample sequence and RDP database sequence.

Table 15. TTGE band bacterial 16S rRNA gene copy numbers in response to RS dose

		Lactobacillus	*Clostridium*	*Ruminococcus*
	BD	6.22 ± 0.94	5.14 ± 0.23	1.90 ± 0.17
	1.25 %	6.05 ± 0.73	4.96 ± 0.38	1.85 ± 0.29
RS	2.5 %	6.29 ± 0.62	4.75 ± 0.26	1.83 ± 0.25
	5 %	5.64 ± 0.67	4.21 ± 0.66*	1.62 ± 0.35
	1.25 %	5.98 ± 0.85	4.54 ± 0.82	2.06 ± 0.36
KJ	2.5 %	5.57 ± 1.18	4.83 ± 0.31	2.46 ± 0.62
	5 %	4.94 ± 1.31*	4.78 ± 0.37	2.60 ± 0.76*
P value		0.013	0.004	0.011

Mean Log_{10} 16S rRNA gene copy numbers (± s.d.) of excised TTGE bands in colon digesta DNA of rats fed BD or 1.25%, 2.5%, or 5% of RS or KJ from feeding study 2 (n=10). *Significantly different to BD group, P <0.05.

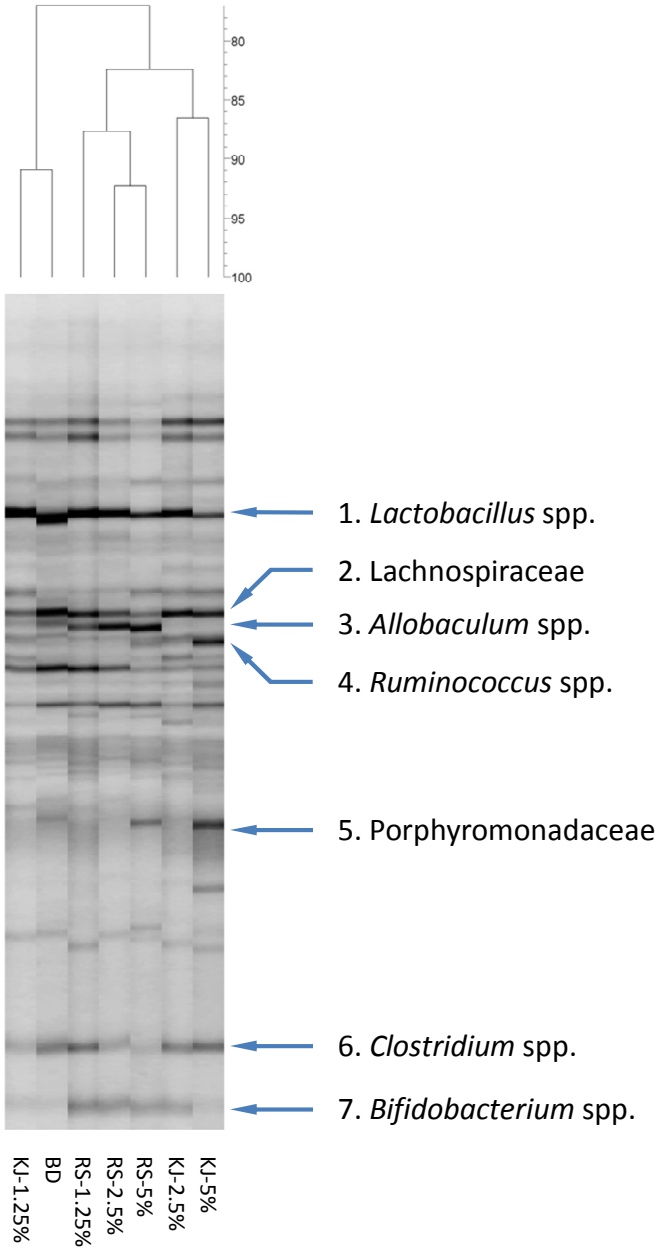

Figure 14. DRC dose response of bacterial 16S rRNA TTGE profiles from pooled DNA. 16S rRNA TTGE profiles of colon bacterial community from pooled colon contents DNA of rats fed BD, or RS or KJ at 1.25%, 2.5%, or 5% for 28 days (10 rats per group). Dendrogram constructed from UPGMA cluster analysis of Dice's similarity coefficient of TTGE profiles based on all visible bands. Scale bar indicates percentage similarity of profiles. Arrows indicate band position of sequences identified using RDP seqmatch.

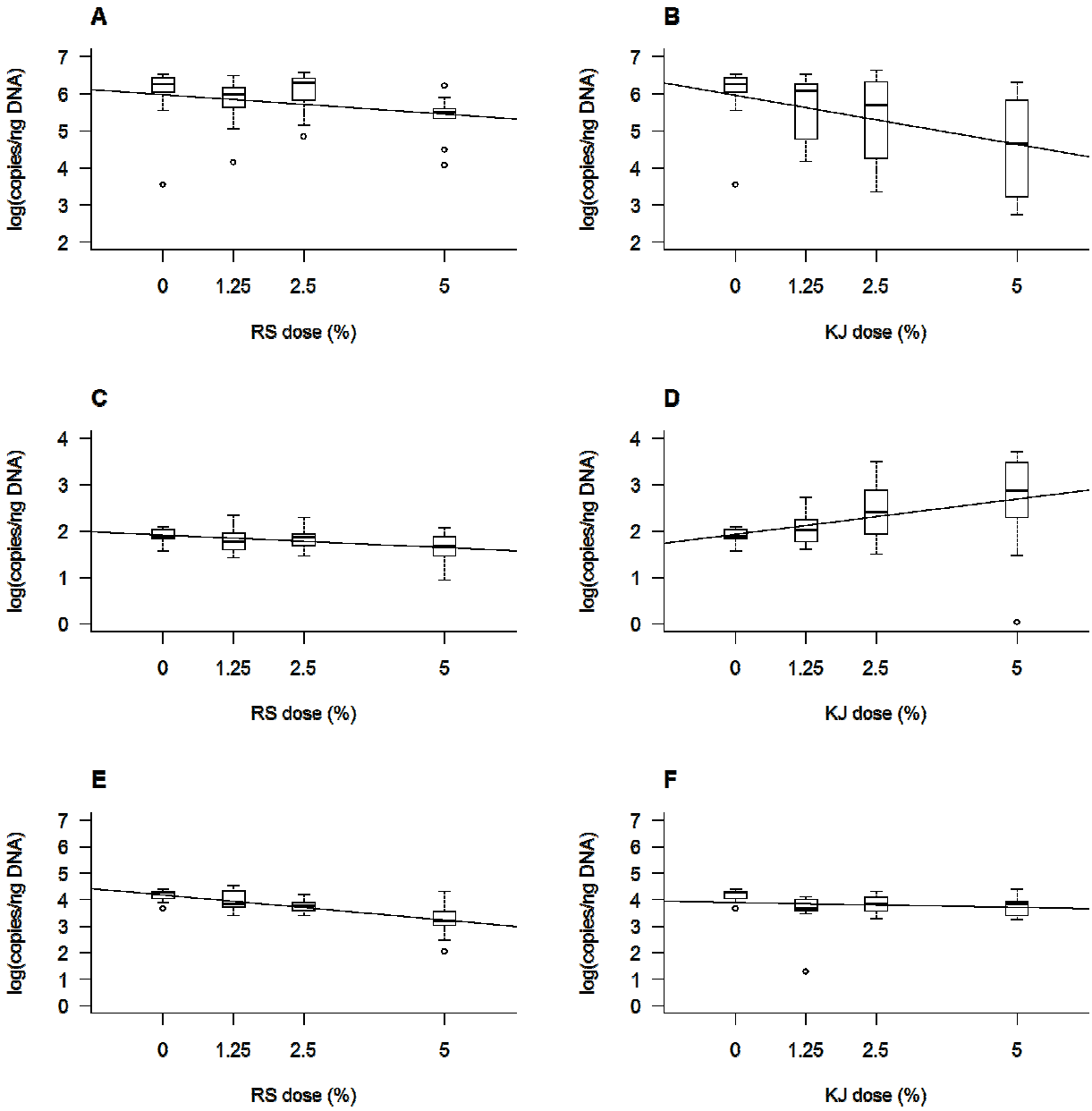

Figure 15. Response of bacterial 16S rRNA gene copy numbers to DRC dose. Log_{10} 16S rRNA gene copy numbers per ng DNA corresponding to; *Lactobacillus* spp. in rats fed RS (A) and KJ (B); *Ruminococcus* spp. in rats fed RS (C) and KJ (D); and *Clostridium* spp. in rats fed RS (E) and KJ (F). X axis indicates RS or KJ dose (%). Boxplots show median, $25^{th}/75^{th}$ percentile, and $5^{th}/95^{th}$ percentile log_{10} gene copy numbers (n=10). Open circles indicate outliers. Line indicates linear regression of gene copy numbers with RS or KJ dose. Significance of linear regression; (A) P=0.13; (B) P=0.01; (C) P=0.03; (D) P=0.02; (E) P<0.01; and (F) P=0.46.

3.8 DRC and microbiota induced alterations in colon gene expression

Host transcriptional responses to DRC supplemented diets was determined by microarray analysis of RNA extracted from the colon of CR 21 day old male Sprague-Dawley rats fed IN, RS, KJ, or BD and 21-28 day old GF rats fed BD, RS or KJ diets. Analysis of host gene expression was carried out using Agilent Whole Rat Genome microarrays using a common reference design, with 6 biological replicates per dietary group, except for the CR-IN group which consisted of 5 biological replicates due to the removal of one microarray that did not pass quality control criteria. The magnitude of gene expression differences were small for dietary comparisons between CR rats, with the largest observed difference of 3.3 fold change (FC) in expression for Ela1, a protease that targets elastin, between IN and BD fed rats. Differences in gene expression between CR rats were expected to be subtle as the rats were physiologically normal and dietary intervention with DRC was not expected to shift host physiology into a disease state. Therefore, a low FC and stringent P value cut off was implemented for determining differential expression. Genes with >1.2 FC between comparisons and Benjamini and Hochberg false discovery rate adjusted P values (FDR) < 0.05 were determined to be differentially expressed. Comparisons within CR rats showed 465 differentially expressed genes between CR-IN and CR-BD groups, 64 differentially expressed genes between CR-RS and CR-BD groups, and 52 differentially expressed genes between CR-KJ and CR-BD rats (Table 16). Within the GF rats, 360 differentially expressed genes were identified between GF-KJ and GF-BD groups. However, no differentially expressed genes were found between the GF-RS and GF-BD fed rats.

Comparisons between CR-BD vs. GF-BD, CR-KJ vs. GF-KJ, and CR-RS vs. GF-RS groups revealed 9098, 8969, and 9038 differentially expressed genes, respectively, highlighting the broad influence of the microbiota on colonic gene expression. The magnitude of fold changes were also substantially higher than that of comparisons between CR rats, with the largest observed difference in expression of 39 fold for neurotensin, a brain and gastrointestinal peptide that is secreted into the circulation following food intake.

Table 16. Numbers of differentially expressed genes in colon tissue

Contrast	Up	No change	Down
CR-BD vs. CR-IN	282	35116	183
CR-BD vs. CR-RS	48	35517	16
CR-BD vs. CR-KJ	28	35529	24
GF-BD vs. GF-RS	0	35581	0
GF-BD vs. GF-KJ	72	35221	288
CR-BD vs. GF-BD	4953	26397	4231
CR-RS vs. GF-RS	4766	26461	4354
CR-KJ vs. GF-KJ	4602	26551	4428

Numbers of differentially expressed genes induced by feeding DRC to CR and GF rats, and numbers of differentially expressed genes (FDR<0.05, FC>1.2) between CR and GF rats fed the same diets. *Contrast* indicates comparison, *Up* indicates number of genes more highly expressed in first coefficient of contrast, *Down* indicates number of genes more highly expressed in second coefficient of contrast, *No change* indicates number of genes that did not show significant changes in gene expression levels. For example, 282 genes showed significantly higher expression levels in CR-BD rats compared to CR-IN rats, while 183 genes were more highly expressed in CR-IN rats compared to CR-BD rats.

3.8.1 Differentially expressed genes vary with type of DRC

The distinctive influence of DRC on colonic gene expression patterns in CR rats was evident by the small overlap of differentially expressed genes shared between comparisons of the various DRC diets to BD rats. Only 5 genes were shared in common within differentially expressed genes between CR-IN compared to CR-BD, CR-RS compared to CR-BD, and CR-KJ compared to CR-BD rats (Figure 16). Differentially expressed genes between GF-BD and GF-KJ groups were also distinctive compared with dietary treatments within CR groups, with 326 of 360 differentially expressed genes unique to that comparison. All of the 20 differentially expressed genes with the highest FC for each DRC group of CR rats compared with the CR-BD group were unique to that particular DRC.

Expression profiles of the top 100 differentially expressed genes between CR-IN and CR-BD groups across all rats tended to cluster together for several groups (Figure 17). As expected, CR-IN and CR-BD groups were clearly separated as the list of genes was selected based on differential expression between the two groups. However, profiles from several groups also showed a tendency to cluster together, without *a priori* gene selection for differential expression between these groups. Gene expression profiles for CR-BD rats formed a distinct cluster separate from all other profiles except for that of one CR-RS rat. Profiles from CR-RS and CR-KJ fed rats tended to cluster within their respective groups. Profiles from the GF-KJ group also formed a clearly defined cluster distinct from the profiles of GF-BD and GF-RS rats. Overall, three distinct groups of profiles were observed; BD fed CR rats; DRC fed CR rats; and GF rats. PCA plots of expression profiles also showed profiles from rats within the same group tended to cluster together (Figure 18). Class prediction using the PAMR software package for Bioconductor, which assigns individual rats to groups based upon their gene expression profiles, confirmed the distinctive influence each form of DRC exerted on host gene expression (Table 17). Once again, because the selection of genes which were differentially expressed between CR-BD and CR-IN rats, class prediction based on expression profiles of those genes placed CR-BD and CR-IN rats within groups clearly delineated from each other. However, profiles from CR-BD and CR-IN rats

were also always accurately placed within their respective groups in comparison to all other experimental groups. Class prediction showed expression profiles of rats other than CR-BD and CR-IN also tended to be correctly predicted. Gene expression profiles from GF and CR rat were always correctly assigned to their microbiota status. Profiles from rats fed KJ also tended to show good predictive ability, with CR-KJ rats accurately classified for 4 out 6 profiles, and GF-KJ rats accurately classified for 5 out 6 profiles.

A feature of the differentially expressed genes with the highest FC between CR-IN and CR-BD rats was the presence of 5 genes regulating Mast cell protease activity, all of which were expressed at lower levels in rats fed IN: *Mcpt1* (2.6 FC, FDR=0.02), *Mcpt9* (1.9 FC, FDR=0.05), predicted mast cell protease 8 (1.9 FC, FDR=0.03), predicted mast cell protease 1-like 3 precursor (1.8 FC, FDR=0.03), and *Mcpt8l2* (1.7 FC, FDR=0.03) (Table 18). Other genes showing significant reductions in expression levels induced by feeding IN to CR rats include *Gcnt3* (1.9 FC, FDR=0.01), a glucosaminyl transferase involved in the production of O-glycans on mucin-type glycoproteins, and a predicted low density lipoprotein receptor-related protein binding protein (1.8 FC, FDR=0.03). Genes that were significantly increased in expression levels in CR rats resulting from feeding IN include *G6pc* (1.8 FC, FDR<0.01), a glucose-6-phosphotase, and *Ela1* (3.3 FC, FDR=0.01), an elastase that breaks down elastin, a protein in connective tissue.

Feeding RS to CR rats resulted in decreased expression levels of *Tac1* (1.5 FC, FDR<0.01), *Calcb* (1.6 FC, FDR=0.01), and *Gdf15* (1.4 FC, FDR=0.02), which all play a role in regulating cell proliferation and differentiation (Table 19). Two genes regulating muscle function were also differentially expressed. *Myh11*, a smooth muscle myosin heavy peptide, and a homolog of tropomyosin 1 were both expressed at lower levels in RS fed rats (1.4 FC, FDR<0.01). Other differentially expressed genes with a relatively high FC include the glucose transporter *Slc2a4*, which is expressed 1.4 fold lower in CR-RS

rats (FDR<0.01), and the carbohydrate response element binding protein *Wbscr14*, which is has a 1.6 fold higher expression in RS fed rats (FDR<0.01).

The differentially expressed genes with the largest fold changes resulting from feeding KJ to CR rats included genes that encode heat shock proteins; *Hspca* (1.4 FC, FDR=0.02), and a homolog to HSP-60 (1.3 FC, FDR=0.03), which both show lower expression levels in CR-KJ compared to CR-BD groups (Table 20). Expression of predicted *Slc16a11*, a monocarboxylic acid transporter, and an acetyl-coA dehydrogenase homolog were significantly increased in KJ fed rats (1.4 FC, FDR<0.05). *Slc16a11* catalyses the transport of monocarboxylates, such as lactate and pyruvate, across the plasma membrane, and acetyl-coA dehydrogenases are involved in the oxidation of fatty acids in the mitochondria.

No differentially expressed genes were observed between GF rats fed RS and BD diets. However, feeding KJ to GF rats resulted in a number of differentially expressed genes (Table 21). Genes that were more highly expressed in GF-KJ rats included *Cyp1a1* (3.1 FC, FDR<0.01), a member of the cytochrome P450 superfamily involved in the detoxification of endogenous and exogenous compounds, and the mast cell protease *Mcpt1* (2.4 FC, FDR=0.04). In contrast, *Mcpt1* showed lower expression levels in CR rats fed IN. Among the differentially expressed genes that showed lower expression in GF-KJ rats with the largest FC was the defensin *Defcr4* (3.6 FC, FDR<0.01), and *RatNP-3b* (2.4 FC, FDR=0.01), a predicted precursor to the defensin NP-3. Other differentially expressed genes that showed lower expression levels in the GF-KJ group were *Cyp3a18* (2.0 FC, FDR<0.01), another member of the cytochrome P450 superfamily, and *Batt* (1.8 FC, FDR<0.01), a bile acid Coenzyme A: amino acid N-acyltransferase involved in the conjugation of glycine or taurine to bile acids.

Differentially expressed genes that were more highly expressed in CR compared to GF rats fed BD, KJ or RS diets included several procollagen genes, *Col1a1*, *Col1a2*, and *Col3a1* (2.8 – 3.4 FC, FDR<0.01)

(Tables 22 - 24). A number of genes involved in muscle function were also more highly expressed compared to CR rats. *Myh11*, encoding myosin 11, was expressed 2.9 – 4.4 fold higher in CR rats fed BD, RS, or KJ compared to their GF counterparts (P<0.01). *MGC109519*, a homolog of tropomyosin 1, *Myl9*, a predicted myosin light chain polypeptide, and *Actg2*, a smooth muscle gamma actin had higher expression levels in CR-BD compared to GF-BD rats (3.3, 3.2, and 3.1 FC, respectively; FDR<0.01). Furthermore, the gene encoding haemoglobin beta chain complex, *Hbb*, was more highly expressed in CR rats fed BD, RS, and KJ compared to GF counterparts (11.1 – 26.0 FC, FDR<0.01). A gene encoding a predicted neurotensin showed large differences in expression levels between CR and GF rats, with 34.5, 36.2 and 39.2 FC increases in transcription levels for CR rats fed BD, KJ, and RS diets respectively (FDR<0.01). Neurotensin is produced in the enteric nervous system and may play a dual role of promoting acute intestinal inflammation, and stimulating epithelial cell proliferation and tissue healing. Other genes with significantly higher expression levels in all groups of GF rats which may have important roles in regulating cell growth and differentiation included *Reg4*, which showed 4.4 - 5.9 FC increased expression levels (FDR<0.01), and *Akr1b8*, an aldo-keto reductase, which was increased 5.1 – 5.8 fold (FDR<0.01).

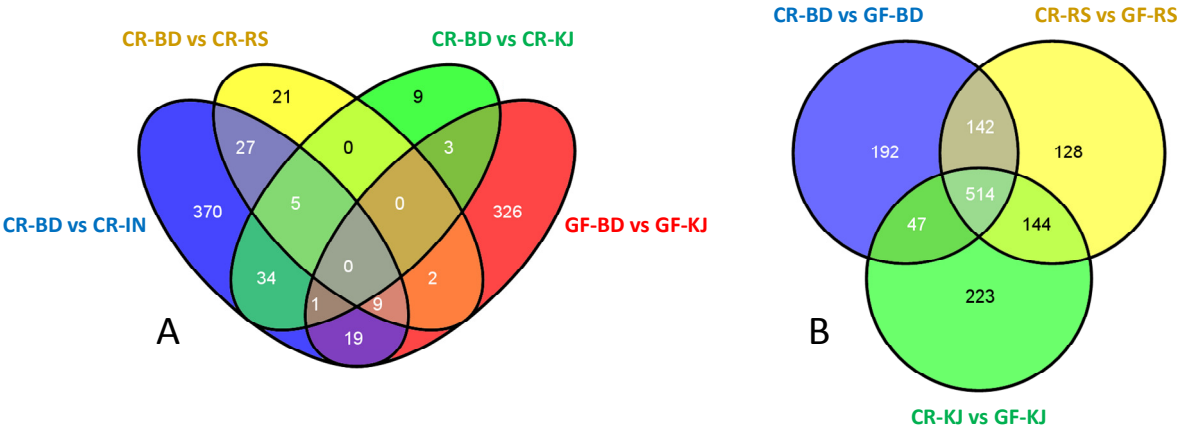

Figure 16. Numbers of unique and shared differentially expressed genes. (A) Venn diagram showing unique and common differentially expressed genes in the colon between comparisons of CR-BD vs. CR-IN, CR-BD vs. CR-RS, CR-BD vs. CR-KJ and GF-BD vs. GF-KJ. (B) Venn diagram showing unique and common differentially expressed genes between contrasts CR-BD vs. GF-BD, CR-RS vs. GF-RS, and CR-KJ vs. GF-KJ.

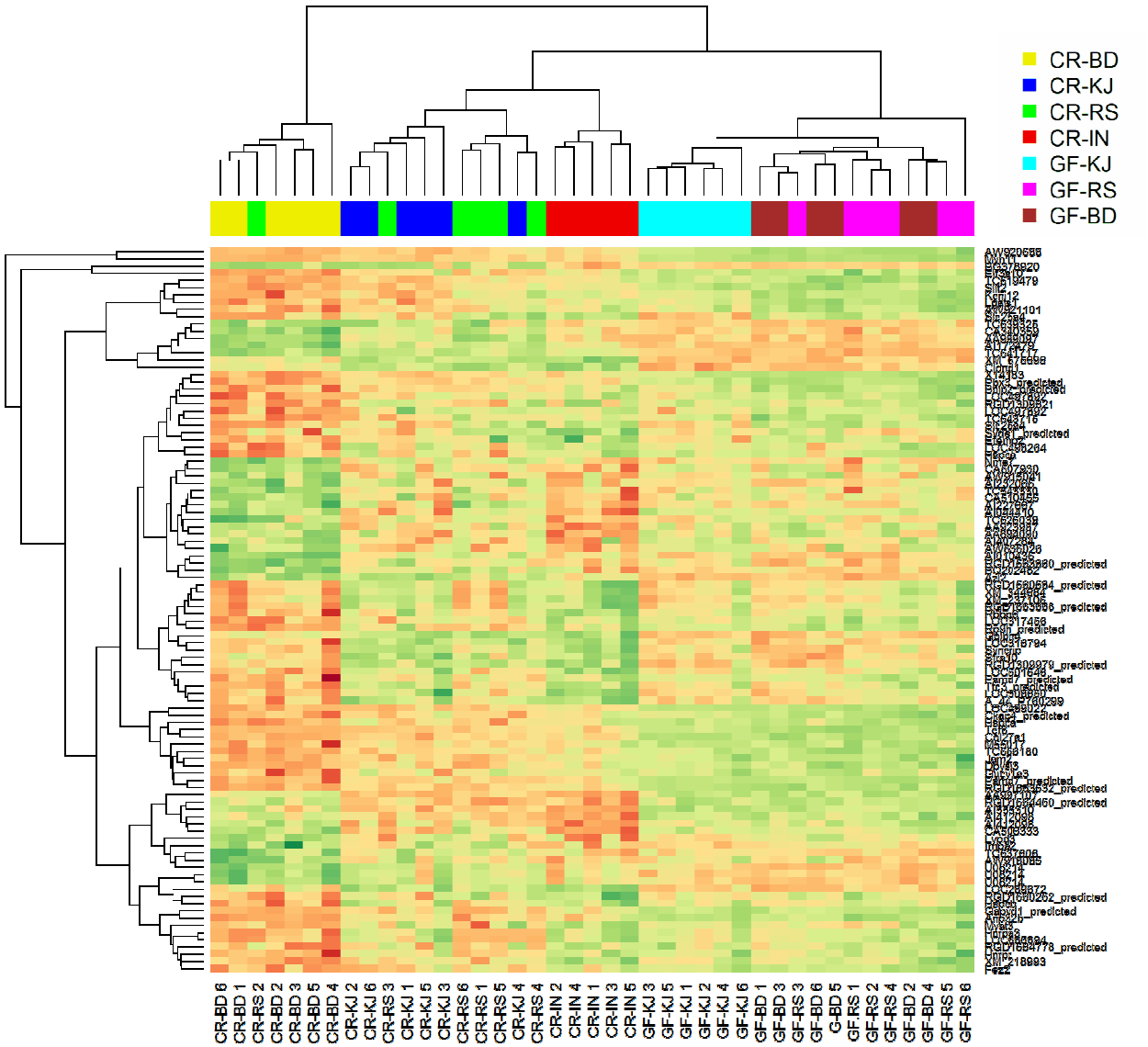

Figure 17. Heatmap of colonic gene expression profiles. Heatmap showing expression profiles of top 100 differentially expressed genes in colon tissue between CR-BD and CR-IN groups across all rats fed for 28 days. Columns represent profile of one rat. Coloured markers at top of heatmap represents dietary group, as indicated by colour key. Rows represent genes and colour of cells indicates expression of gene relative to reference RNA, with red indicating lower expression relative to reference RNA and green indicating higher expression relative to reference RNA.

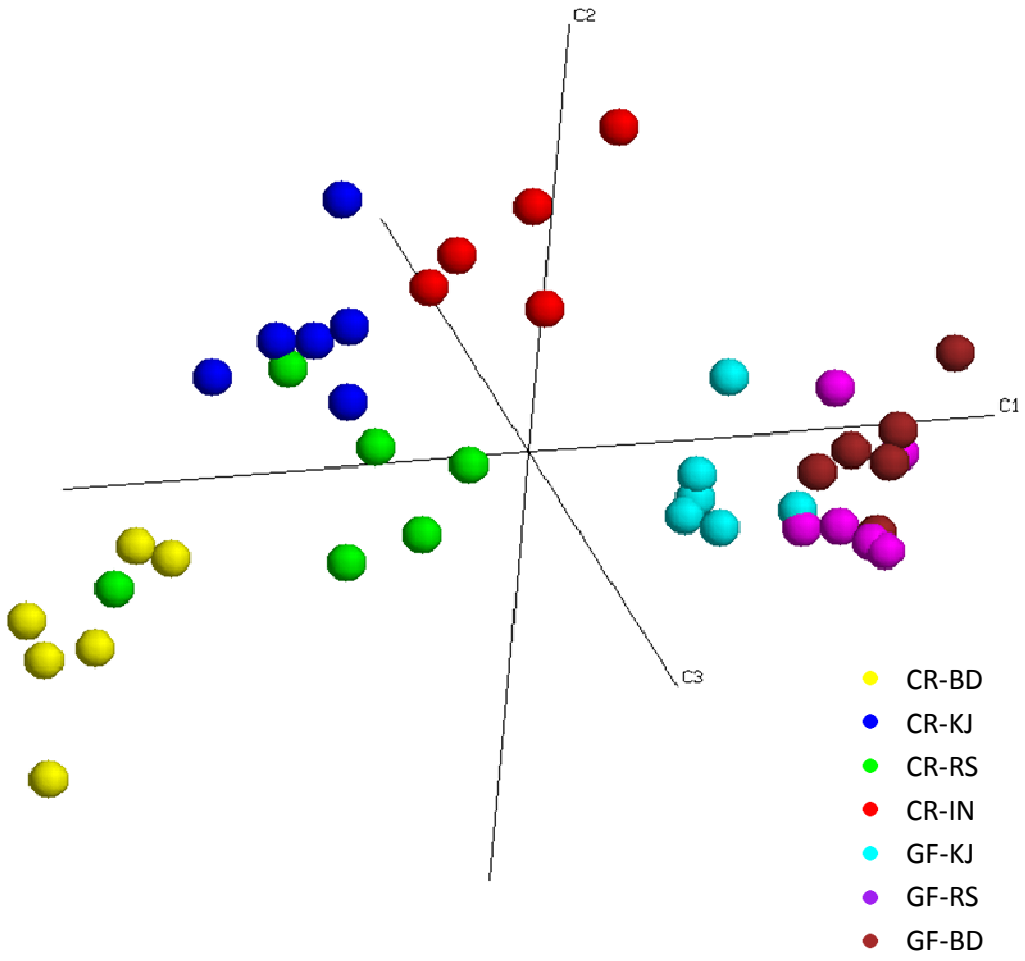

Figure 18. PCA plot of colonic gene expression profiles. PCA plot of variation in colonic gene expression profiles comprised of genes that form the top 100 differentially expressed genes between CR-BD and CR-IN groups, in all rats. Each sphere represents profile from one rat. Colour represents group, as indicated by colour key.

Table 17. Distribution of predicted and actual group membership of colonic gene expression profiles

	Actual groups						
Predicted	CR-BD	CD-IN	CR-KJ	CR-RS	GF-BD	GF-KJ	GF-RS
CR-BD	6		1	1			
CR-IN		5		1			
CR-KJ			4	2			
CR-RS			1	2			
GF-BD					3	1	2
GF-KJ						5	
GF-RS					3		4

Confusion matrix showing distribution of predicted and actual group membership of colon tissue gene expression profiles from rats fed for 28 days in study 1. Columns indicate actual groups, rows represent predicted group membership, and values denote number of profiles. For example, of the profiles from CR-KJ rats (third column), 1 is incorrectly predicted as belonging to group CR-BD, 4 are correctly assigned to group CR-KJ, and 1 is incorrectly placed within group CR-RS. In contrast, all CR-BD profiles are correctly assigned to the CR-BD group.

Table 18. Differentially expressed genes in colon tissue between CR rats fed BD and IN

Accession number	Gene symbol	Description	Fold change	FDR
NM_017145	Mcpt1	Rattus norvegicus mast cell protease 1 (Mcpt1), mRNA	2.58	0.02
AY212271	Nat8	Rattus norvegicus endogenous retrovirus mRNA, partial sequence	2.49	<0.01
XM_341549	Akr1c12_predicted	PREDICTED: Rattus norvegicus aldo-keto reductase family 1, member C12 (predicted) (Akr1c12_predicted), mRNA	2.04	0.03
TC525536	TC525536	Q6YT31 (Q6YT31) ATPase subunit 6, partial (6%)	1.90	0.04
NM_019323	Mcpt9	Rattus norvegicus mast cell protease 9 (Mcpt9), mRNA	1.86	0.05
NM_173312	Gcnt3	Rattus norvegicus glucosaminyl (N-acetyl) transferase 3, mucin type (Gcnt3), mRNA	1.86	0.01
XM_573787	RGD1565970_predicted	PREDICTED: Rattus norvegicus similar to mast cell protease 8 (predicted) (RGD1565970_predicted), mRNA	1.85	0.03
XM_341434	RGD1565715_predicted	PREDICTED: Rattus norvegicus similar to low density lipoprotein receptor-related protein binding protein (predicted) (RGD1565715_predicted), mRNA	1.76	0.03
XM_224209	RGD1562035_predicted	PREDICTED: Rattus norvegicus similar to mast cell protease 1-like 3 precursor (predicted) (RGD1562035_predicted), mRNA	1.76	0.03
XM_573782	Mcpt8l2	PREDICTED: Rattus norvegicus mast cell protease 8-like 2 (Mcpt8l2), mRNA	1.71	0.03
NM_012552	Ela1	Rattus norvegicus elastase 1, pancreatic (Ela1), mRNA	-3.29	0.01
NM_012674	Spink1	Rattus norvegicus serine protease inhibitor, Kazal type 1 (Spink1), mRNA	-2.80	0.05
NM_173339	Ceacam10	Rattus norvegicus CEA-related cell adhesion molecule 10 (Ceacam10), mRNA	-2.57	0.03
NM_130401	Pdzk1ip1	Rattus norvegicus PDZK1 interacting protein 1 (Pdzk1ip1), mRNA	-2.09	0.05
XM_234755	XM_234755	Rattus norvegicus similar to immunoglobulin heavy chain (LOC299475), mRNA	-1.96	0.01
NM_013098	G6pc	Rattus norvegicus glucose-6-phosphatase, catalytic (G6pc), mRNA	-1.85	<0.01
NM_133295	Ces3	Rattus norvegicus carboxylesterase 3 (Ces3), mRNA	-1.81	0.03
NM_017188	Unc119	Rattus norvegicus UNC-119 homolog (C. elegans) (Unc119), mRNA	-1.79	0.03
NM_001014092	Paqr5	Rattus norvegicus progestin and adipoQ receptor family member V (Paqr5), mRNA	-1.78	0.03
XM_341584	Mocos_predicted	PREDICTED: Rattus norvegicus molybdenum cofactor sulfurase (predicted) (Mocos_predicted), mRNA	-1.75	0.04

Highest ranked differentially expressed genes in colon tissue with known functions between conventionally raised rats fed BD or IN. Fold change value indicates fold difference in expression between treatments. Positive value indicates higher expression levels in BD fed rats and negative value indicates lower expression levels in BD fed rats. FDR indicates multiple testing adjusted P value for significance of fold change.

Table 19. Differentially expressed genes in colon tissue between CR rats fed BD and RS

Accession number	Gene symbol	Description	Fold change	FDR
TC542800	TC542800	BC031479 Als2 protein (Mus musculus;) , partial (5%)	1.62	0.02
XM_001055031	LOC680102	PREDICTED: Rattus norvegicus similar to mab-21-like 2 (LOC680102), mRNA	1.61	0.01
NM_138513	Calcb	Rattus norvegicus calcitonin-related polypeptide, beta (Calcb), mRNA	1.60	0.03
NM_012666	Tac1	Rattus norvegicus tachykinin 1 (Tac1), mRNA	1.51	<0.01
NM_080902	Hig1	Rattus norvegicus hypoxia induced gene 1 (Hig1), mRNA	1.46	0.02
XM_573030	Myh11	PREDICTED: Rattus norvegicus myosin, heavy polypeptide 11, smooth muscle (Myh11), mRNA	1.40	<0.01
NM_012751	Slc2a4	Rattus norvegicus solute carrier family 2 (facilitated glucose transporter), member 4 (Slc2a4), mRNA	1.38	<0.01
NM_001024345	MGC109519	Rattus norvegicus similar to tropomyosin 1, embryonic fibroblast - rat (MGC109519), mRNA	1.37	0.01
NM_019216	Gdf15	Rattus norvegicus growth differentiation factor 15 (Gdf15), mRNA	1.36	0.02
NM_013002	Pcp4	Rattus norvegicus Purkinje cell protein 4 (Pcp4), mRNA	1.35	0.03
NM_017013	Gsta2	Rattus norvegicus glutathione-S-transferase, alpha type2 (Gsta2), mRNA	-2.45	0.01
NM_153623	Cdig1l	Rattus norvegicus cadmium-inducible gene 1L (Cdig1l), mRNA	-1.73	0.02
NM_133552	Wbscr14	Rattus norvegicus Williams-Beuren syndrome chromosome region 14 homolog (human) (Wbscr14), mRNA	-1.63	<0.01
XM_341168	RGD1310587	PREDICTED: Rattus norvegicus similar to hypothetical protein FLJ14146 (RGD1310587), mRNA	-1.57	<0.01
XM_220362	RGD1559575_predicted	PREDICTED: Rattus norvegicus similar to novel protein (predicted) (RGD1559575_predicted), mRNA	-1.47	<0.01
XM_215059	Eraf_predicted	PREDICTED: Rattus norvegicus erythroid associated factor (predicted) (Eraf_predicted), mRNA	-1.47	0.05
XM_238442	RGD1311019_predicted	PREDICTED: Rattus norvegicus similar to hypothetical protein DKFZp434H2010 (predicted) (RGD1311019_predicted), mRNA	-1.43	0.04
NM_130404	Serpinb7	Rattus norvegicus serine (or cysteine) proteinase inhibitor, clade B, member 7 (Serpinb7), mRNA	-1.38	0.03
NM_022505	Rhced	Rattus norvegicus Rhesus blood group CE and D (Rhced), mRNA	-1.27	0.03
BC059161	RGD1311196	Rattus norvegicus similar to hypothetical protein, mRNA (cDNA clone MGC:72982 IMAGE:6887770), complete cds	-1.26	0.02

Highest ranked differentially expressed genes in colon tissue with known functions between conventionally raised rats fed BD or RS. Fold change value indicates fold difference in expression between treatments. Positive value indicates higher expression levels in BD fed rats and negative value indicates lower expression levels in BD fed rats. FDR indicates multiple testing adjusted P value for significance of fold change.

Table 20. Differentially expressed genes in colon tissue between CR rats fed BD and KJ

Accession number	Gene symbol	Description	Fold change	FDR
NM_031798	Slc12a2	Rattus norvegicus solute carrier family 12, member 2 (Slc12a2), mRNA	1.43	<0.01
NM_175761	Hspca	Rattus norvegicus heat shock protein 1, alpha (Hspca), mRNA	1.37	0.02
NM_131911	Anp32b	Rattus norvegicus acidic nuclear phosphoprotein 32 family, member B (Anp32b), mRNA	1.36	<0.01
XM_219278	XM_219278	Rattus norvegicus similar to 60 kDa heat shock protein, mitochondrial precursor (Hsp60) (HSP-65) (LOC308950), mRNA	1.34	0.03
XM_238649	Eif3s10	PREDICTED: Rattus norvegicus eukaryotic translation initiation factor 3, subunit 10 (theta) (Eif3s10), mRNA	1.32	0.01
XM_343189	Ckap4_predicted	PREDICTED: Rattus norvegicus cytoskeleton-associated protein 4 (predicted) (Ckap4_predicted), mRNA	1.32	0.03
NM_057119	Sfrs10	Rattus norvegicus splicing factor, arginine/serine-rich 10 (transformer 2 homolog, Drosophila) (Sfrs10), mRNA	1.30	<0.01
XM_343446	Syncrip	PREDICTED: Rattus norvegicus synaptotagmin binding, cytoplasmic RNA interacting protein (Syncrip), mRNA	1.30	<0.01
M55017	M55017	RATNUCIA2 Rat nucleolin gene	1.29	<0.01
XM_217254	Ifrd2_predicted	PREDICTED: Rattus norvegicus interferon-related developmental regulator 2 (predicted) (Ifrd2_predicted), mRNA	1.29	0.03
NM_053686	Trpv6	Rattus norvegicus transient receptor potential cation channel, subfamily V, member 6 (Trpv6), mRNA	-1.71	0.05
AF220557	AF220557	Rattus norvegicus clone 8C12 murine complement receptor 1-specific monoclonal antibody Ig light chain variable region mRNA	-1.61	0.05
NM_133595	Gchfr	Rattus norvegicus GTP cyclohydrolase I feedback regulator (Gchfr), mRNA	-1.48	0.02
XM_213334	Slc16a11_predicted	PREDICTED: Rattus norvegicus solute carrier family 16 (monocarboxylic acid transporters), member 11 (predicted), mRNA	-1.43	0.01
NM_001030025	Upp1	Rattus norvegicus uridine phosphorylase 1 (Upp1), mRNA	-1.39	0.04
AF232668	Kalrn	AF232668 Rattus norvegicus Kalirin-9a (Kalirin) mRNA, complete cds, alternatively spliced	-1.38	0.05
XM_222190	RGD1310159_predicted	Rattus norvegicus similar to acetyl-coA dehydrogenase -related (111.6 kD) (5G231) (LOC304500), mRNA	-1.35	0.05
NM_053953	Il1r2	Rattus norvegicus interleukin 1 receptor, type II (Il1r2), mRNA	-1.35	0.01
NM_133578	Dusp5	Rattus norvegicus dual specificity phosphatase 5 (Dusp5), mRNA	-1.28	0.05
NM_001037788	Styxl1	Rattus norvegicus serine/threonine/tyrosine interacting-like 1 (Styxl1), mRNA	-1.27	0.02

Highest ranked differentially expressed genes in colon tissue with known functions between conventionally raised rats fed BD or KJ. Fold change value indicates fold difference in expression between treatments. Positive value indicates higher expression levels in BD fed rats and negative value indicates lower expression levels in BD fed rats. FDR indicates multiple testing adjusted P value for significance of fold change.

Table 21. Differentially expressed genes in colon tissue between GF rats fed BD and KJ

Accession number	Gene symbol	Description	Fold change	FDR
NM_001013053	Defcr4	Rattus norvegicus defensin related cryptdin 4 (Defcr4), mRNA	3.59	<0.01
NM_017046	Scnn1g	Rattus norvegicus sodium channel, nonvoltage-gated 1 gamma (Scnn1g), mRNA	2.94	0.01
XM_001074118	RatNP-3b	PREDICTED: Rattus norvegicus defensin RatNP-3 precursor (RatNP-3b), mRNA	2.39	0.01
XM_235330	Colec10_predicted	PREDICTED: Rattus norvegicus collectin sub-family member 10 (C-type lectin) (predicted) (Colec10_predicted), mRNA	2.29	<0.01
NM_022251	Enpep	Rattus norvegicus glutamyl aminopeptidase (Enpep), mRNA	2.17	0.03
NM_031651	Slc13a1	Rattus norvegicus solute carrier family 13 (sodium/sulfate symporters), member 1 (Slc13a1), mRNA	2.14	<0.01
NM_173295	Udpgtr2	Rattus norvegicus liver UDP-glucuronosyltransferase, phenobarbital-inducible form (Udpgtr2), mRNA	2.06	<0.01
NM_020538	Aadac	Rattus norvegicus arylacetamide deacetylase (esterase) (Aadac), mRNA	2.06	<0.01
NM_145782	Cyp3a18	Rattus norvegicus cytochrome P450, 3a18 (Cyp3a18), mRNA	1.99	<0.01
NM_017300	Baat	Rattus norvegicus bile acid-Coenzyme A: amino acid N-acyltransferase (Baat), mRNA	1.80	<0.01
NM_001025116	RGD1565230_predicted	Rattus norvegicus pancreatic ribonuclease gamma (predicted) (RGD1565230_predicted), mRNA	-4.82	<0.01
NP516897	NP516897	pancreatic ribonuclease gamma [Rattus fuscipes]	-3.31	<0.01
NM_012540	Cyp1a1	Rattus norvegicus cytochrome P450, family 1, subfamily a, polypeptide 1 (Cyp1a1), mRNA	-3.10	<0.01
NM_019183	Actc1	Rattus norvegicus actin alpha cardiac 1 (Actc1), mRNA	-2.92	<0.01
NM_017272	Aldh1a4	Rattus norvegicus aldehyde dehydrogenase family 1, subfamily A4 (Aldh1a4), mRNA	-2.89	<0.01
NP516904	NP516904	pancreatic ribonuclease beta [Rattus rattus]	-2.52	<0.01
NM_017145	Mcpt1	Rattus norvegicus mast cell protease 1 (Mcpt1), mRNA	-2.36	0.04
XM_001079728	LOC691810	PREDICTED: Rattus norvegicus similar to phospholipase A2, group IVC (cytosolic, calcium-independent) (LOC691810), mRNA	-2.26	0.02
X76996	Gzmb	R.norvegicus mRNA for granzyme-like protein III	-2.11	<0.01
NM_001013232	Rnase1_predicted	Rattus norvegicus ribonuclease, RNase A family, 1 (pancreatic) (predicted) (Rnase1_predicted), mRNA	-2.08	<0.01

Highest ranked differentially expressed genes in colon tissue with known functions between germ-free rats fed BD or KJ. Fold change value indicates fold difference in expression between treatments. Positive value indicates higher expression levels in BD fed rats and negative value indicates lower expression levels in BD fed rats. FDR indicates multiple testing adjusted P value for significance of fold change.

Table 22. Differentially expressed genes in colon tissue between CR and GF fed BD

Accession number	Gene symbol	Description	Fold change	FDR
XM_001064395	LOC689116	PREDICTED: Rattus norvegicus similar to nuclear cap binding protein subunit 2, transcript variant 1 (LOC689116), mRNA	20.71	<0.01
Y17323	Y17323	Rattus norvegicus CDK109 mRNA.	13.70	<0.01
NM_033234	Hbb	Rattus norvegicus hemoglobin beta chain complex (Hbb), mRNA	11.08	<0.01
XM_219938	Mrpl43_predicted	PREDICTED: Rattus norvegicus mitochondrial ribosomal protein L43 (predicted) (Mrpl43_predicted), mRNA	6.57	<0.01
XM_214441	Ogn_predicted	PREDICTED: Rattus norvegicus osteoglycin (predicted) (Ogn_predicted), mRNA	6.19	<0.01
XM_001053321	Myh11	PREDICTED: Rattus norvegicus myosin, heavy polypeptide 11, smooth muscle, transcript variant 1 (Myh11), mRNA	4.42	<0.01
XM_213925	Dpt_predicted	PREDICTED: Rattus norvegicus dermatopontin (predicted) (Dpt_predicted), mRNA	3.72	<0.01
NM_001014125	Pdia5	Rattus norvegicus protein disulfide isomerase-associated 5 (Pdia5), mRNA	3.71	<0.01
NM_022665	Alpi	Rattus norvegicus Alkaline phosphatase 1, intestinal, defined by SSR (Alpi), mRNA	3.66	<0.01
NM_001024345	MGC109519	Rattus norvegicus similar to tropomyosin 1, embryonic fibroblast - rat (MGC109519), mRNA	3.26	<0.01
XM_216884	Nts_predicted	PREDICTED: Rattus norvegicus neurotensin (predicted) (Nts_predicted), mRNA	-34.52	<0.01
NM_001012118	Osr2	Rattus norvegicus odd-skipped related 2 (Drosophila) (Osr2), mRNA	-17.24	<0.01
XM_001074118	RatNP-3b	PREDICTED: Rattus norvegicus defensin RatNP-3 precursor (RatNP-3b), mRNA	-12.96	<0.01
NM_031651	Slc13a1	Rattus norvegicus solute carrier family 13 (sodium/sulfate symporters), member 1 (Slc13a1), mRNA	-12.95	<0.01
XM_001062312	LOC685106	PREDICTED: Rattus norvegicus similar to ribosomal protein L6 (LOC685106), mRNA	-7.92	<0.01
XM_237242	Abca12_predicted	PREDICTED: Rattus norvegicus ATP-binding cassette, sub-family A (ABC1), member 12 (predicted) (Abca12_predicted), mRNA	-7.53	<0.01
NM_053791	Prlpm	Rattus norvegicus prolactin-like protein M (Prlpm), mRNA	-7.10	<0.01
NM_001000257	Olr357_predicted	Rattus norvegicus olfactory receptor 357 (predicted) (Olr357_predicted), mRNA	-6.61	<0.01
XM_001079728	LOC691810	PREDICTED: Rattus norvegicus similar to phospholipase A2, group IVC (cytosolic, calcium-independent) (LOC691810), mRNA	-6.08	<0.01
XM_220804	RGD1310166_predicted	Rattus norvegicus similar to Chromodomain-helicase-DNA-binding protein 1 (CHD-1) (LOC303395), mRNA	-5.86	<0.01

Highest ranked differentially expressed genes in colon tissue with known functions between conventionally raised and germ-free rats fed BD. Fold change value indicates fold difference in expression between treatments. Positive value indicates higher expression levels in conventionally raised rats and negative value indicates lower expression levels in conventionally raised rats. FDR indicates multiple testing adjusted P value for significance of fold change.

Table 23. Differentially expressed genes in colon tissue between CR and GF fed KJ

Accession number	Gene symbol	Description	Fold change	FDR
NM_033234	Hbb	Rattus norvegicus hemoglobin beta chain complex (Hbb), mRNA	14.70	<0.01
XM_001064395	LOC689116	PREDICTED: Rattus norvegicus similar to nuclear cap binding protein subunit 2, transcript variant 1 (LOC689116), mRNA	14.21	<0.01
Y17323	Y17323	Rattus norvegicus CDK109 mRNA. [Y17323]	9.02	<0.01
NM_198776	MGC72973	Rattus norvegicus beta-glo (MGC72973), mRNA	6.04	<0.01
XM_214441	Ogn_predicted	PREDICTED: Rattus norvegicus osteoglycin (predicted) (Ogn_predicted), mRNA	4.80	<0.01
BF290512	BF290512	BF290512 EST455103 Rat Gene Index, normalized rat, Rattus norvegicus cDNA Rattus norvegicus cDNA clone RGIHW28 5' sequence, mRNA sequence	4.56	<0.01
XM_219938	Mrpl43_predicted	PREDICTED: Rattus norvegicus mitochondrial ribosomal protein L43 (predicted) (Mrpl43_predicted), mRNA	4.35	<0.01
NM_031531	Serpina3n	Rattus norvegicus serine (or cysteine) peptidase inhibitor, clade A, member 3N (Serpina3n), mRNA	4.19	<0.01
NM_022665	Alpi	Rattus norvegicus Alkaline phosphatase 1, intestinal, defined by SSR (Alpi), mRNA	3.63	<0.01
XM_213440	Col1a1	PREDICTED: Rattus norvegicus procollagen, type 1, alpha 1 (Col1a1), mRNA	3.37	<0.01
XM_216884	Nts_predicted	PREDICTED: Rattus norvegicus neurotensin (predicted) (Nts_predicted), mRNA	-36.21	<0.01
NM_012556	Fabp1	Rattus norvegicus fatty acid binding protein 1, liver (Fabp1), mRNA	-32.04	<0.01
NM_173305	Hsd17b9	Rattus norvegicus hydroxysteroid (17-beta) dehydrogenase 9 (Hsd17b9), mRNA	-15.47	<0.01
NM_001012118	Osr2	Rattus norvegicus odd-skipped related 2 (Drosophila) (Osr2), mRNA	-15.06	<0.01
NM_017272	Aldh1a4	Rattus norvegicus aldehyde dehydrogenase family 1, subfamily A4 (Aldh1a4), mRNA	-12.66	<0.01
XM_001079728	LOC691810	PREDICTED: Rattus norvegicus similar to phospholipase A2, group IVC (cytosolic, calcium-independent) (LOC691810), mRNA	-12.21	<0.01
XM_237242	Abca12_predicted	PREDICTED: Rattus norvegicus ATP-binding cassette, sub-family A (ABC1), member 12 (predicted) (Abca12_predicted), mRNA	-7.46	<0.01
XM_001062312	LOC685106	PREDICTED: Rattus norvegicus similar to ribosomal protein L6 (LOC685106), mRNA	-6.72	<0.01
NM_031651	Slc13a1	Rattus norvegicus solute carrier family 13 (sodium/sulfate symporters), member 1 (Slc13a1), mRNA	-6.66	<0.01
XM_220804	Olr357_predicted	Rattus norvegicus olfactory receptor 357 (predicted) (Olr357_predicted), mRNA	-6.39	<0.01

Highest ranked differentially expressed genes in colon tissue with known functions between conventionally raised and germ-free rats fed KJ. Fold change value indicates fold difference in expression between treatments. Positive value indicates higher expression levels in conventionally raised rats and negative value indicates lower expression levels in conventionally raised rats. FDR indicates multiple testing adjusted P value for significance of fold change.

Table 24. Differentially expressed genes in colon tissue between CR and GF fed RS

Accession number	Gene symbol	Description	Fold change	FDR
NM_033234	Hbb	Rattus norvegicus hemoglobin beta chain complex (Hbb), mRNA	25.10	<0.01
XM_001064395	LOC689116	PREDICTED: Rattus norvegicus similar to nuclear cap binding protein subunit 2, transcript variant 1 (LOC689116), mRNA	17.65	<0.01
Y17323	Y17323	Rattus norvegicus CDK109 mRNA.	11.18	<0.01
NM_198776	MGC72973	Rattus norvegicus beta-glo (MGC72973), mRNA	9.84	<0.01
XM_214441	Ogn_predicted	PREDICTED: Rattus norvegicus osteoglycin (predicted) (Ogn_predicted), mRNA	5.77	<0.01
NM_001013853	LOC287167	Rattus norvegicus globin, alpha (LOC287167), mRNA	5.17	<0.01
NM_013197	Alas2	Rattus norvegicus aminolevulinic acid synthase 2 (Alas2), mRNA	4.39	<0.01
XM_001064621	LOC689116	PREDICTED: Rattus norvegicus similar to nuclear cap binding protein subunit 2, transcript variant 4 (LOC689116), mRNA	4.38	<0.01
XM_219938	Mrpl43_predicted	PREDICTED: Rattus norvegicus mitochondrial ribosomal protein L43 (predicted) (Mrpl43_predicted), mRNA	4.24	<0.01
NM_022665	Alpi	Rattus norvegicus Alkaline phosphatase 1, intestinal, defined by SSR (Alpi), mRNA	4.11	<0.01
XM_216884	Nts_predicted	PREDICTED: Rattus norvegicus neurotensin (predicted) (Nts_predicted), mRNA	-39.20	<0.01
NM_001012118	Osr2	Rattus norvegicus odd-skipped related 2 (Drosophila) (Osr2), mRNA	-16.38	<0.01
XM_001079728	LOC691810	PREDICTED: Rattus norvegicus similar to phospholipase A2, group IVC (cytosolic, calcium-independent) (LOC691810), mRNA	-14.37	<0.01
NM_173305	Hsd17b9	Rattus norvegicus hydroxysteroid (17-beta) dehydrogenase 9 (Hsd17b9), mRNA	-13.70	<0.01
NM_031651	Slc13a1	Rattus norvegicus solute carrier family 13 (sodium/sulfate symporters), member 1 (Slc13a1), mRNA	-12.26	<0.01
XM_001074118	RatNP-3b	PREDICTED: Rattus norvegicus defensin RatNP-3 precursor (RatNP-3b), mRNA	-10.30	<0.01
XM_237242	Abca12_predicted	PREDICTED: Rattus norvegicus ATP-binding cassette, sub-family A (ABC1), member 12 (predicted) (Abca12_predicted), mRNA	-9.91	<0.01
NM_001000257	Olr357_predicted	Rattus norvegicus olfactory receptor 357 (predicted) (Olr357_predicted), mRNA	-7.12	<0.01
XM_001062312	LOC685106	PREDICTED: Rattus norvegicus similar to ribosomal protein L6 (LOC685106), mRNA	-6.24	<0.01
XM_235330	Colec10_predicted	PREDICTED: Rattus norvegicus collectin sub-family member 10 (C-type lectin) (predicted) (Colec10_predicted), mRNA	-6.20	<0.01

Highest ranked differentially expressed genes in colon tissue with known functions between conventionally raised and germ-free rats fed RS. Fold change value indicates fold difference in expression between treatments. Positive value indicates higher expression levels in conventionally raised rats and negative value indicates lower expression levels in conventionally raised rats. FDR indicates multiple testing adjusted P value for significance of fold change.

3.8.2 RT-qPCR confirmation of microarray gene expression results

Expression levels of *Galntl4*, *Galnt2*, *Hspca*, *Mcpt1*, and *Mrps31*, normalised against *Uba52*, were examined by RT-qPCR to validate microarray gene expression results (Tables 25 - 29). *Galntl4* and *Galnt2* encode polypeptide N-acetylgalactosaminyltransferases which are involved in the initial steps of O-linked oligosaccharide biosynthesis, which can result in the formation of mucin type molecules (Varki et al., 1999). *Mcpt1* encodes a mast cell protease, *Hspca* encodes for heat shock protein 90aa1, and *Mrps31* encodes mitochondrial ribosomal protein S31. Feeding IN to CR rats resulted in significantly higher expression levels of *Galntl4* compared to BD fed CR rats by microarray and RT-qPCR. Microarray and RT-qPCR results showed feeding IN or KJ to CR rats significantly lowered expression levels of *Hspca* compared to CR rats fed BD. Similarly, expression levels of *Mcpt1*, measured by microarray and RT-qPCR, were significantly lower in CR rats fed IN compared to those fed BD. Furthermore, levels of *Mcpt1* by microarray and RT-qPCR analyses were significantly higher in KJ fed GF rats compared to GF rats fed BD. Expression of *Mrps31*, as measured by microarray or RT-qPCR, was not altered by feeding DRC to CR or GF rats. However, some differences were observed in *Galnt2* expression when measured by microarray compared to RT-qPCR. For example, CR rats fed IN showed significantly lower expression levels of *Galnt2* compared to CR rats fed BD by RT-qPCR, but not by microarray. Conversely, GF rats fed KJ showed significantly higher levels of *Galnt2* compared to GF rats fed BD by microarray analysis, but not when measured by RT-qPCR. Although significance values of fold changes in *Galnt2* expression did not show agreement in CR-IN compared to CR-BD or GF-KJ compared to GF-BD rats, the direction of fold changes were similar. Furthermore, fold changes between microarray and RT-qPCR results for *Galntl4*, *Galnt2*, *Hspca* and *Mcpt1* showed strong correlation (Spearman rho=0.94). Similarly, microarray FDR and RT-qPCR P values were also strongly correlated (Spearman rho=0.87). Although some differences in microarray and RT-qPCR results are generally expected, Spearman rho correlation values >0.8 indicate a high level of agreement between microarray and RT-qPCR data (Morey et al., 2006).

Table 25. Validation of *Galntl4* microarray gene expression results by RT-qPCR

Contrast	Microarray FC	Microarray FDR	RT-qPCR FC	RT-qPCR P value
CR-BD vs. CR-IN	-1.42	0.01	-1.64	<0.01
CR-BD vs. CR-RS	-1.21	0.49	-1.47	0.08
CR-BD vs. CR-KJ	-1.14	0.83	-1.26	0.11
GF-BD vs. GF-RS	-1.05	0.99	1.02	0.88
GF-BD vs. GF-KJ	1.17	0.53	1.37	0.02

Expression levels of *Galntl4* in the colon by microarray and RT-qPCR. Contrast indicates comparison. FC value indicates fold difference in expression between treatments. Positive FC value indicates higher expression levels in first coefficient of contrast and negative FC value indicates higher expression levels in second coefficient. Microarray FDR indicates multiple testing adjusted P value for significance of fold change. RT-qPCR P value indicates significance of fold change determined by ANOVA.

Table 26. Validation of *Galnt2* microarray gene expression results by RT-qPCR

Contrast	Microarray FC	Microarray FDR	RT-qPCR FC	RT-qPCR P value
CR-BD vs. CR-IN	1.11	0.57	1.52	0.04
CR-BD vs. CR-RS	-1.01	0.99	1.08	0.76
CR-BD vs. CR-KJ	1.11	0.72	1.22	0.26
GF-BD vs. GF-RS	-1.13	0.99	1.07	0.69
GF-BD vs. GF-KJ	-1.32	<0.01	-1.12	0.53

Expression levels of *Galnt2* in the colon by microarray and RT-qPCR. Contrast indicates comparison. FC value indicates fold difference in expression between treatments. Positive FC value indicates higher expression levels in first coefficient of contrast and negative FC value indicates higher expression levels in second coefficient. Microarray FDR indicates multiple testing adjusted P value for significance of fold change. RT-qPCR P value indicates significance of fold change determined by ANOVA.

Table 27. Validation of *Hspca* microarray gene expression results by RT-qPCR

Contrast	Microarray FC	Microarray FDR	RT-qPCR FC	RT-qPCR P value
CR-BD vs. CR-IN	1.50	<0.01	2.66	0.04
CR-BD vs. CR-RS	1.18	0.37	1.07	0.66
CR-BD vs. CR-KJ	1.37	0.02	2.08	0.04
GF-BD vs. GF-RS	1.06	0.99	1.14	0.68
GF-BD vs. GF-KJ	-1.01	0.99	-1.12	0.96

Expression levels of *Hspca* in the colon by microarray and RT-qPCR. Contrast indicates comparison. FC value indicates fold difference in expression between treatments. Positive FC value indicates higher expression levels in first coefficient of contrast and negative FC value indicates higher expression levels in second coefficient. Microarray FDR indicates multiple testing adjusted P value for significance of fold change. RT-qPCR P value indicates significance of fold change determined by ANOVA.

Table 28. Validation of *Mcpt1* microarray gene expression results by RT-qPCR

Contrast	Microarray FC	Microarray FDR	RT-qPCR FC	RT-qPCR P value
CR-BD vs. CR-IN	2.58	0.02	3.14	<0.01
CR-BD vs. CR-RS	1.44	0.74	1.25	0.52
CR-BD vs. CR-KJ	1.18	0.99	1.28	0.64
GF-BD vs. GF-RS	-1.12	0.99	1.08	0.79
GF-BD vs. GF-KJ	-2.36	0.04	-2.12	0.02

Expression levels of *Mcpt1* in the colon by microarray and RT-qPCR. Contrast indicates comparison. FC value indicates fold difference in expression between treatments. Positive FC value indicates higher expression levels in first coefficient of contrast and negative FC value indicates higher expression levels in second coefficient. Microarray FDR indicates multiple testing adjusted P value for significance of fold change. RT-qPCR P value indicates significance of fold change determined by ANOVA.

Table 29. Validation of *Mrps31* microarray gene expression results by RT-qPCR

Contrast	Microarray FC	Microarray FDR	RT-qPCR FC	RT-qPCR P value
CR-BD vs. CR-IN	1.06	0.32	-1.16	0.35
CR-BD vs. CR-RS	1.05	0.88	-1.16	0.20
CR-BD vs. CR-KJ	1.04	0.85	-1.21	0.13
GF-BD vs. GF-RS	-1.03	0.99	1.19	0.34
GF-BD vs. GF-KJ	1.03	0.99	1.45	0.44

Expression levels of *Mrps31* in the colon by microarray and RT-qPCR. Contrast indicates comparison. FC value indicates fold difference in expression between treatments. Positive FC value indicates higher expression levels in first coefficient of contrast and negative FC value indicates higher expression levels in second coefficient. Microarray FDR indicates multiple testing adjusted P value for significance of fold change. RT-qPCR P value indicates significance of fold change determined by ANOVA.

3.8.3 Biological processes associated with differentially expressed genes

Analysis of the biological processes associated with differentially expressed genes between experimental groups was carried out using the GOstats package in R. Hypergeometric testing showed 201 biological processes associated with differentially expressed genes between CR-BD and CR-IN fed rats were significantly over-represented (P<0.05), the top 20 of which included *glucose homeostasis*, *cell motion*, *metal ion transport*, and *response to reactive oxygen species* (P<0.01) (Table 30). Significantly over-represented biological processes associated with differentially expressed genes between CR-BD and CR-RS fed rats included *cell development*, *cell differentiation*, *glycolysis*, and *integrin-mediated signaling pathway* (P<0.01) (Table 31). In total, 75 biological processes were significantly over-represented (P<0.05) in differentially expressed genes between CR rats fed BD and RS. Differentially expressed genes between KJ and BD fed CR rats were associated with 19 significantly over-represented biological processes (P<0.05) including *cellular metabolic process*, *nitric oxide metabolic process*, and *membrane organization* (Table 32).

Over-represented biological processes associated with differentially expressed genes between GF rats fed BD and KJ included *lipid metabolic process*, *cytoskeleton organization*, and *regulation of hormone levels* (P<0.01) (Table 33). Overall, 345 significantly over-represented biological processes were associated with differentially expressed genes between GF-BD and GF-KJ rats (P<0.05). Differentially expressed genes between CR and GF rats were significantly over-represented for biological processes including *collagen fibril organization* and *vasculature development*, *lipid transport*, and *anatomical structure morphogenesis* (P<0.01) (Tables 34 -36).

Table 30. Significantly over-represented biological processes between CR rats fed BD and IN

GO ID	Term	P value	Exp Count	Count	Size
GO:0009612	response to mechanical stimulus	<0.01	0.93	6	77
GO:0065008	regulation of biological quality	<0.01	17.30	32	1436
GO:0000302	response to reactive oxygen species	<0.01	1.05	6	87
GO:0043269	regulation of ion transport	<0.01	1.05	6	87
GO:0006936	muscle contraction	<0.01	1.63	7	135
GO:0030029	actin filament-based process	<0.01	2.65	9	220
GO:0043086	negative regulation of catalytic activity	<0.01	2.65	9	220
GO:0042493	response to drug	<0.01	3.84	11	319
GO:0044092	negative regulation of molecular function	<0.01	3.28	10	272
GO:0006928	cell motion	<0.01	7.00	16	581
GO:0051674	localization of cell	<0.01	7.00	16	581
GO:0042542	response to hydrogen peroxide	<0.01	0.88	5	73
GO:0003012	muscle system process	<0.01	1.75	7	145
GO:0007638	mechanosensory behavior	<0.01	0.07	2	6
GO:0006575	cellular amino acid derivative metabolic process	<0.01	2.30	8	191
GO:0030001	metal ion transport	<0.01	5.22	13	433
GO:0048666	neuron development	<0.01	4.60	12	382
GO:0033500	carbohydrate homeostasis	<0.01	0.57	4	47
GO:0042593	glucose homeostasis	<0.01	0.57	4	47
GO:0010959	regulation of metal ion transport	<0.01	0.95	5	79

Significantly over-represented Gene Ontology biological processes associated with differentially expressed genes in the colon between conventionally raised rats fed BD and IN determined using GOstats. P value indicates significance of over-representation. *Exp Counts* indicate the expected number of genes associated with biological process through chance alone and *Counts* indicate actual number of genes. *Size* indicates all genes in genome associated with biological process.

Table 31. Significantly over-represented biological processes between CR rats fed BD and RS

GO ID	Term	P value	Exp Count	Count	Size
GO:0048468	cell development	<0.01	2.11	8	913
GO:0007517	muscle organ development	<0.01	0.50	4	218
GO:0007275	multicellular organismal development	<0.01	5.61	13	2431
GO:0030154	cell differentiation	<0.01	3.55	10	1539
GO:0048731	system development	<0.01	5.02	12	2178
GO:0048869	cellular developmental process	<0.01	3.69	10	1601
GO:0022008	neurogenesis	<0.01	1.45	6	627
GO:0030705	cytoskeleton-dependent intracellular transport	<0.01	0.08	2	34
GO:0048856	anatomical structure development	<0.01	5.25	12	2279
GO:0032502	developmental process	<0.01	6.84	14	2966
GO:0007229	integrin-mediated signaling pathway	<0.01	0.09	2	39
GO:0042311	vasodilation	<0.01	0.09	2	41
GO:0000904	cell morphogenesis involved in differentiation	<0.01	0.69	4	300
GO:0007399	nervous system development	0.01	2.22	7	961
GO:0031175	neuron projection development	0.01	0.72	4	313
GO:0014706	striated muscle tissue development	0.01	0.40	3	173
GO:0060537	muscle tissue development	0.01	0.42	3	180
GO:0006096	glycolysis	0.01	0.14	2	60
GO:0048699	generation of neurons	0.01	1.33	5	578
GO:0003013	circulatory system process	0.01	0.46	3	201

Significantly over-represented Gene Ontology biological processes associated with differentially expressed genes in colon tissue between conventionally raised rats fed BD and RS determined using GOstats. P value indicates significance of over-representation. *Exp Counts* indicate the expected number of genes associated with biological process through chance alone and *Counts* indicate actual number of genes. *Size* indicates all genes in genome associated with biological process.

Table 32. Significantly over-represented biological processes between CR rats fed BD and KJ

GO ID	Term	P value	Exp Count	Count	Size
GO:0045428	regulation of nitric oxide biosynthetic process	<0.01	0.03	2	23
GO:0006809	nitric oxide biosynthetic process	<0.01	0.04	2	30
GO:0044403	symbiosis, encompassing mutualism through parasitism	<0.01	0.04	2	30
GO:0046209	nitric oxide metabolic process	<0.01	0.04	2	31
GO:0044419	interspecies interaction between organisms	<0.01	0.05	2	35
GO:0043933	macromolecular complex subunit organization	0.01	0.84	4	592
GO:0044237	cellular metabolic process	0.01	8.44	14	5969
GO:0016044	membrane organization	0.01	0.45	3	319
GO:0006470	protein amino acid dephosphorylation	0.01	0.16	2	111
GO:0006396	RNA processing	0.01	0.50	3	353
GO:0006457	protein folding	0.01	0.19	2	131
GO:0016311	dephosphorylation	0.02	0.21	2	146
GO:0044271	nitrogen compound biosynthetic process	0.02	0.24	2	170
GO:0008380	RNA splicing	0.02	0.25	2	175
GO:0006397	mRNA processing	0.03	0.29	2	203
GO:0065003	macromolecular complex assembly	0.04	0.76	3	536
GO:0016071	mRNA metabolic process	0.04	0.34	2	238
GO:0044238	primary metabolic process	0.05	8.83	13	6247
GO:0008152	metabolic process	0.05	9.95	14	7042

Significantly over-represented Gene Ontology biological processes associated with differentially expressed genes in colon tissue between conventionally raised rats fed BD and KJ determined using GOstats. P value indicates significance of over-representation. *Exp Counts* indicate the expected number of genes associated with biological process through chance alone and *Counts* indicate actual number of genes. *Size* indicates all genes in genome associated with biological process.

Table 33. Significantly over-represented biological processes between GF rats fed BD and KJ

GO ID	Term	P value	Exp Count	Count	Size
GO:0006629	lipid metabolic process	<0.01	7.65	24	724
GO:0065008	regulation of biological quality	<0.01	15.17	35	1436
GO:0003013	circulatory system process	<0.01	2.12	11	201
GO:0008015	blood circulation	<0.01	2.12	11	201
GO:0046456	icosanoid biosynthetic process	<0.01	0.38	5	36
GO:0006636	unsaturated fatty acid biosynthetic process	<0.01	0.39	5	37
GO:0044255	cellular lipid metabolic process	<0.01	6.75	19	639
GO:0010033	response to organic substance	<0.01	9.40	23	890
GO:0009719	response to endogenous stimulus	<0.01	5.82	17	551
GO:0044057	regulation of system process	<0.01	3.14	12	297
GO:0007010	cytoskeleton organization	<0.01	3.88	13	367
GO:0015837	amine transport	<0.01	1.54	8	146
GO:0051240	positive regulation of multicellular organismal process	<0.01	2.44	10	231
GO:0006690	icosanoid metabolic process	<0.01	0.54	5	51
GO:0033559	unsaturated fatty acid metabolic process	<0.01	0.55	5	52
GO:0010817	regulation of hormone levels	<0.01	2.53	10	240
GO:0032787	monocarboxylic acid metabolic process	<0.01	3.55	12	336
GO:0006800	oxygen and reactive oxygen species metabolic process	<0.01	0.57	5	54
GO:0035150	regulation of tube size	<0.01	0.89	6	84
GO:0050880	regulation of blood vessel size	<0.01	0.89	6	84

Significantly over-represented Gene Ontology biological processes associated with differentially expressed genes in colon tissue between germ-free rats fed BD and KJ determined using GOstats. P value indicates significance of over-representation. *Exp Counts* indicate the expected number of genes associated with biological process through chance alone and *Counts* indicate actual number of genes. *Size* indicates all genes in genome associated with biological process.

Table 34. Significantly over-represented biological processes between CR and GF rats fed BD

GO ID	Term	P value	Exp Count	Count	Size
GO:0016043	cellular component organization	<0.01	49.04	94	2010
GO:0030199	collagen fibril organization	<0.01	0.54	9	22
GO:0030198	extracellular matrix organization	<0.01	2.15	14	88
GO:0043062	extracellular structure organization	<0.01	3.59	17	147
GO:0001568	blood vessel development	<0.01	6.54	20	268
GO:0001944	vasculature development	<0.01	6.68	20	274
GO:0051179	localization	<0.01	68.70	101	2816
GO:0048858	cell projection morphogenesis	<0.01	6.39	19	262
GO:0032990	cell part morphogenesis	<0.01	6.61	19	271
GO:0032502	developmental process	<0.01	72.36	103	2966
GO:0045112	integrin biosynthetic process	<0.01	0.10	3	4
GO:0009653	anatomical structure morphogenesis	<0.01	29.40	51	1205
GO:0051128	regulation of cellular component organization	<0.01	9.44	23	387
GO:0030029	actin filament-based process	<0.01	5.37	16	220
GO:0006810	transport	<0.01	55.57	82	2278
GO:0048731	system development	<0.01	53.13	79	2178
GO:0051234	establishment of localization	<0.01	55.89	82	2291
GO:0007009	plasma membrane organization	<0.01	0.29	4	12
GO:0032989	cellular component morphogenesis	<0.01	10.54	24	432
GO:0048812	neuron projection morphogenesis	<0.01	6.20	17	254

Significantly over-represented Gene Ontology biological processes associated with differentially expressed genes in colon tissue between conventionally raised and germ-free rats fed BD determined using GOstats. P value indicates significance of over-representation. *Exp Counts* indicate the expected number of genes associated with biological process through chance alone and *Counts* indicate actual number of genes. *Size* indicates all genes in genome associated with biological process.

Table 35. Significantly over-represented biological processes between CR and GF rats fed KJ

GO ID	Term	P value	Exp Count	Count	Size
GO:0030199	collagen fibril organization	<0.01	0.59	9	22
GO:0016043	cellular component organization	<0.01	54.12	87	2010
GO:0030198	extracellular matrix organization	<0.01	2.37	12	88
GO:0043062	extracellular structure organization	<0.01	3.96	15	147
GO:0001568	blood vessel development	<0.01	7.22	21	268
GO:0001944	vasculature development	<0.01	7.38	21	274
GO:0010627	regulation of protein kinase cascade	<0.01	6.49	19	241
GO:0001501	skeletal system development	<0.01	8.35	21	310
GO:0007265	Ras protein signal transduction	<0.01	5.71	16	212
GO:0007507	heart development	<0.01	5.76	16	214
GO:0043408	regulation of MAPKKK cascade	<0.01	3.04	11	113
GO:0007167	enzyme linked receptor protein signaling pathway	<0.01	9.53	22	354
GO:0007242	intracellular signaling cascade	<0.01	33.44	54	1242
GO:0016048	detection of temperature stimulus	<0.01	0.16	3	6
GO:0009605	response to external stimulus	<0.01	22.83	40	848
GO:0032964	collagen biosynthetic process	<0.01	0.38	4	14
GO:0006869	lipid transport	<0.01	3.26	11	121
GO:0048762	mesenchymal cell differentiation	<0.01	1.43	7	53
GO:0010033	response to organic substance	<0.01	23.96	41	890
GO:0001503	ossification	<0.01	4.44	13	165

Significantly over-represented Gene Ontology biological processes associated with differentially expressed genes in colon tissue between conventionally raised and germ-free rats fed KJ determined using GOstats. P value indicates significance of over-representation. *Exp Counts* indicate the expected number of genes associated with biological process through chance alone and *Counts* indicate actual number of genes. *Size* indicates all genes in genome associated with biological process.

Table 36. Significantly over-represented biological processes between CR and GF rats fed RS

GO ID	Term	P value	Exp Count	Count	Size
GO:0030199	collagen fibril organization	<0.01	0.58	9	22
GO:0016043	cellular component organization	<0.01	52.77	91	2010
GO:0043062	extracellular structure organization	<0.01	3.86	16	147
GO:0030198	extracellular matrix organization	<0.01	2.31	12	88
GO:0001503	ossification	<0.01	4.33	16	165
GO:0001501	skeletal system development	<0.01	8.14	23	310
GO:0060348	bone development	<0.01	4.59	16	175
GO:0050961	detection of temperature stimulus involved in sensory perception	<0.01	0.11	3	4
GO:0050965	detection of temperature stimulus involved in sensory perception of pain	<0.01	0.11	3	4
GO:0006810	transport	<0.01	59.81	88	2278
GO:0007264	small GTPase mediated signal transduction	<0.01	10.13	24	386
GO:0051234	establishment of localization	<0.01	60.15	88	2291
GO:0045453	bone resorption	<0.01	0.79	6	30
GO:0001944	vasculature development	<0.01	7.19	19	274
GO:0070647	protein modification by small protein conjugation or removal	<0.01	3.83	13	146
GO:0046849	bone remodeling	<0.01	2.86	11	109
GO:0007265	Ras protein signal transduction	<0.01	5.57	16	212
GO:0048771	tissue remodeling	<0.01	3.94	13	150
GO:0009966	regulation of signal transduction	<0.01	18.40	35	701
GO:0051051	negative regulation of transport	<0.01	3.49	12	133

Significantly over-represented Gene Ontology biological processes associated with differentially expressed genes in colon tissue between conventionally raised and germ-free rats fed RS determined using GOstats. P value indicates significance of over-representation. *Exp Counts* indicate the expected number of genes associated with biological process through chance alone and *Counts* indicate actual number of genes. *Size* indicates all genes in genome associated with biological process.

3.8.4 Biological interaction networks associated with differentially expressed genes

Differentially expressed genes between dietary comparisons were examined for networks of biological interaction relationships using IPA. The highest ranked interaction network generated from differentially expressed genes between CR rats fed BD and IN involved genes associated with *Cellular assembly and organization*, *Cellular compromise*, and *Nervous system development and function* (Figure 19). The biological interaction network with the highest score generated from differentially expressed genes between CR rats fed BD and KJ involved genes associated with *Cellular development*, *Cellular growth and proliferation*, and *Hematological system development and function* (Figure 20). The highest ranked network constructed from differentially expressed genes between CR rats fed BD and RS included genes associated with *Inflammatory response*, *Organ morphology*, and *Renal and urological system development and function* (Figure 21). Network analysis of differentially expressed genes between GF rats fed BD and KJ generated an interaction network that included genes associated with *Lipid metabolism*, *Molecular transport*, and *Small molecule biochemistry* (Figure 22).

3.8.4.1 Network of differentially expressed genes between CR-BD and CR-IN

Genes within the network generated from differentially expressed genes between CR-BD and CR-IN rats generally showed a higher expression in BD fed rats compared to IN fed rats (Figure 19). Genes that showed higher expression in BD fed rats within this network included the glucose transporter *Slc2a4* (FC=1.32, FDR<0.01), small GTPase *RhoA* (FC=1.24, FDR<0.01), heat shock protein *Hspd1* (FC=1.35, FDR<0.01) and beta-galactoside binding lectin *Lgals1* (FC=1.43, FDR<0.01). Genes that showed increased expression levels in rats fed IN included *Acot2*, an acyl-CoA thioesterase (FC=1.26, FDR=0.03) and *Spink1*, a serine peptidase inhibitor (FC=2.8, FDR=0.05)

3.8.4.2 Network of differentially expressed genes between CR-BD and CR-KJ

Genes within the network generated from differentially expressed genes between CR-BD and CR-KJ rats (Figure 20) included *Il1r2* (FC=1.35, FDR=0.01), a receptor for IL-1, and the lipid receptor *Scarb1* (FC=1.23, FDR=0.03), both of which showed higher expression levels in KJ fed rats. Genes that expressed at lower levels in KJ fed rats included the heat shock protein *Hsp90aa1* (FC=1.37, FDR=0.02) and the DNA topoisomerase *Top1* (FC=1.22, FDR=0.01).

3.8.4.3 Network of differentially expressed genes between CR-BD and CR-RS

Most genes within the biological interaction network constructed from differentially expressed genes between CR rats fed BD and RS showed lower expression levels in RS fed rats, including *Slc2a4* (FC=1.38, FDR<0.01) and *Lgals1* (FC= 1.32, FDR=0.05) (Figure 21). Expression levels of the solute carrier *Slc25a4* (FC=1.27, FDR=0.01), neuropeptide encoding *Tac1* (FC=1.51, FDR<0.01), and urokinase plasminogen activator receptor *Plaur* (FC=1.3, FDR=0.02) was also lower in RS fed rats. Genes within this network that were more highly expressed in RS fed rats included the alpha haemoglobin stabilising protein *AHSP* (FC=1.47, FDR=0.05) and serpin peptidase inhibitor, clade B (ovalbumin), member 7 encoding *Serpinb7* (FC=1.38, FDR=0.03).

3.8.4.4 Network of differentially expressed genes between GF-BD and GF-KJ

The highest ranked network generated from differentially expressed genes between GF-BD and GF-KJ rats (Figure 22) included *Pparα*, encoding peroxisome proliferator-activated receptor alpha, which showed significantly higher expression levels in BD fed germ-free rats (FC=1.46, FDR=0.01) and *Slc10a2* (FC=1.64, FDR<0.01), a sodium/bile acid co-transporter. Genes within this interaction network that were more highly expressed in GF rats fed KJ included *Tac1* (FC=1.35, FDR=0.04), the growth factor *Fgf2* and its receptor *Fgfr2* (FC=1.26, FDR<0.01 for both), and *Rxrg* (FC=1.57, FDR<0.01), a retinoid nuclear receptor.

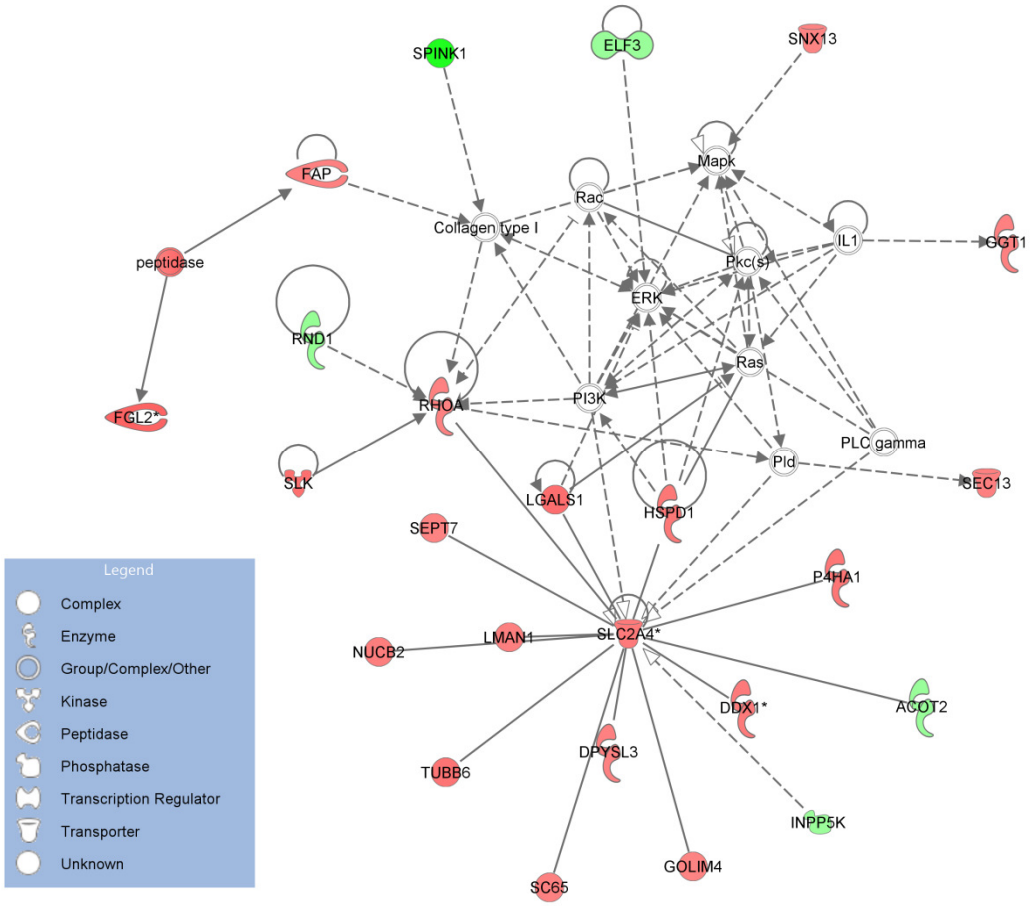

Figure 19. Network of differentially expressed genes in colon tissue between CR-BD and CR-IN rats. Genes are represented by nodes and interactions represented by edges (solid = direct interaction, dashed = indirect interaction). Coloured nodes indicate differentially expressed genes, with red showing genes more highly expressed in CR rats fed BD, and green showing genes more highly expressed in CR rats fed IN. Intensity of colour indicates degree of fold change, with greater intensity signifying higher expression level. Node shape indicates functional class of gene product as indicated in legend.

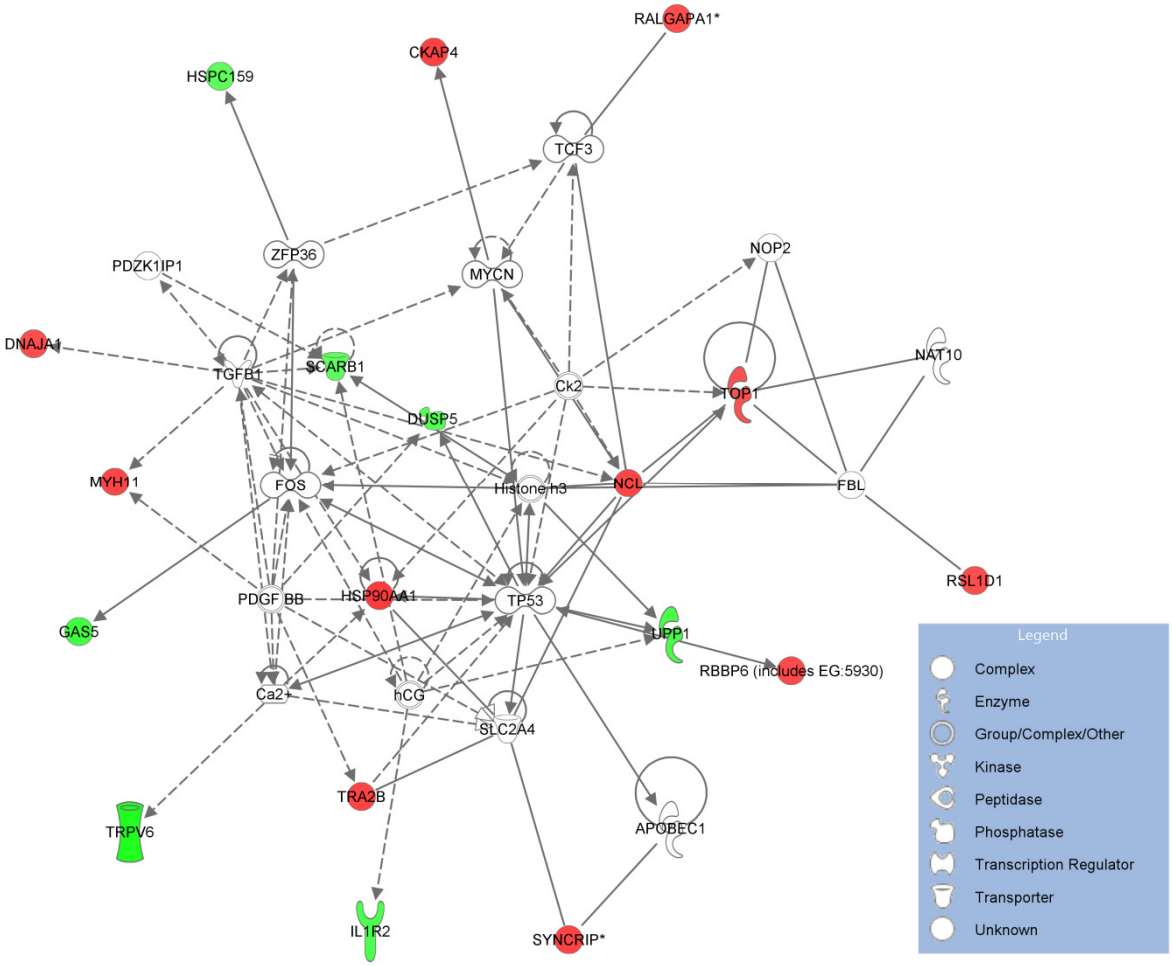

Figure 20. Network of differentially expressed genes in colon tissue between CR-BD and CR-KJ rats. Genes are represented by nodes and interactions represented by edges. Coloured nodes indicate differentially expressed genes, with red showing genes more highly expressed in CR rats fed BD, and green showing genes more highly expressed in CR rats fed KJ. Intensity of colour indicates degree of fold change, with greater intensity signifying higher expression level. Node shape indicates functional class of gene product as indicated in legend.

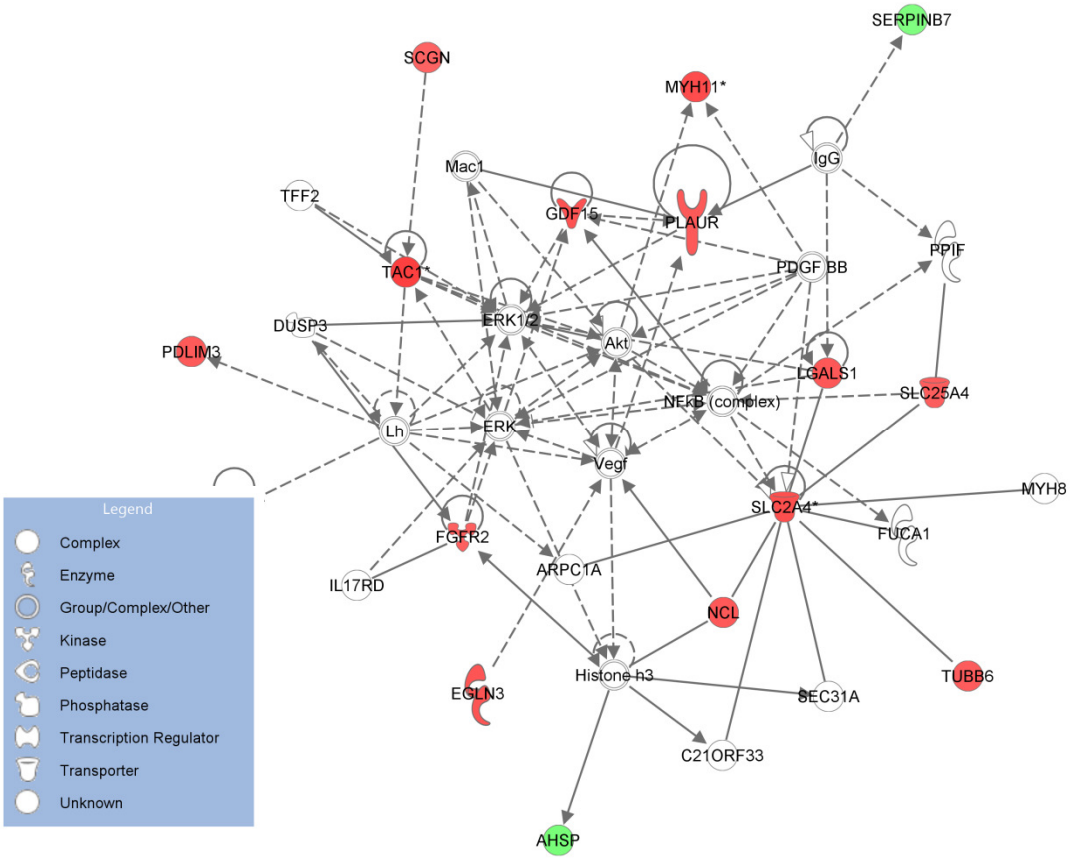

Figure 21. Network of differentially expressed genes in colon tissue between CR-BD and CR-RS rats. Genes are represented by nodes and interactions represented by edges. Coloured nodes indicate differentially expressed genes, with red showing genes more highly expressed in CR rats fed BD, and green showing genes more highly expressed in CR rats fed RS. Intensity of colour indicates degree of fold change, with greater intensity signifying higher expression level. Node shape indicates functional class of gene product as indicated in legend.

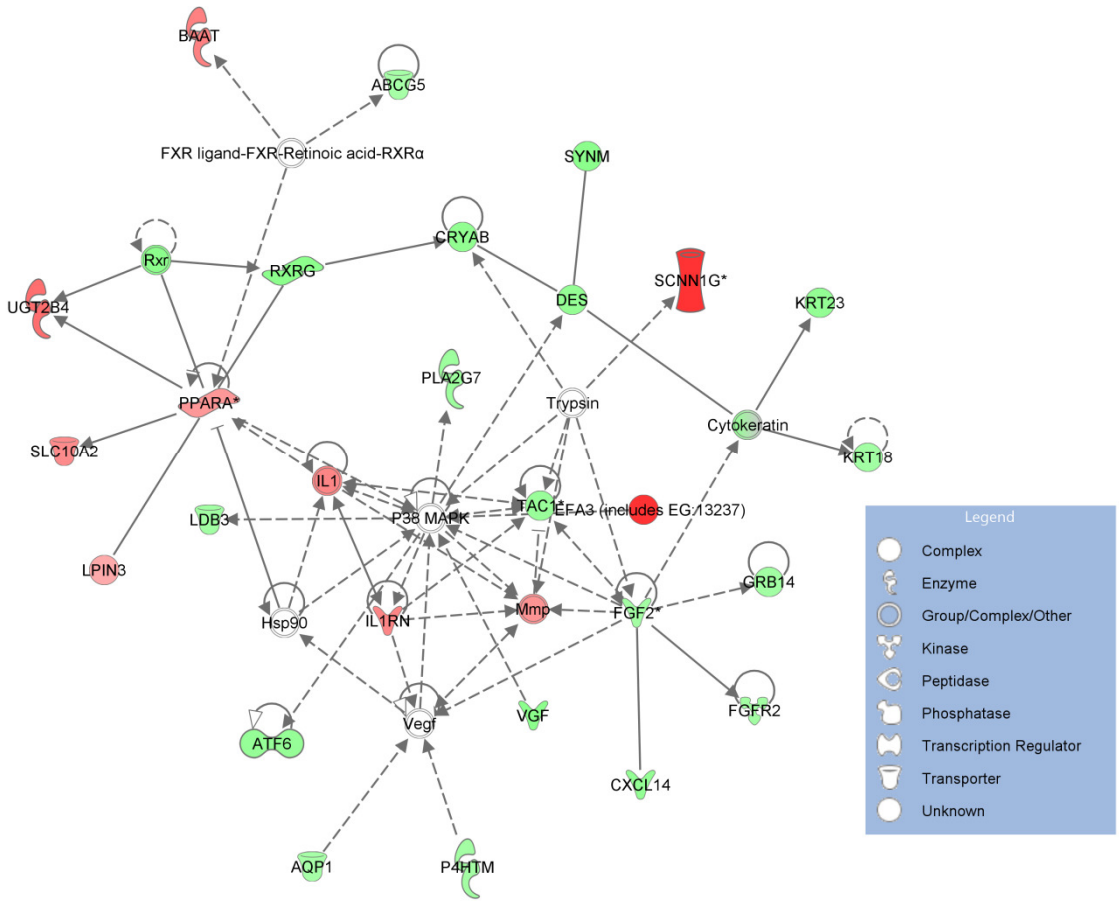

Figure 22. Network of differentially expressed genes in colon tissue between GF-BD and GF-KJ rats. Genes are represented by nodes and interactions represented by edges. Coloured nodes indicate differentially expressed genes, with red showing genes more highly expressed in GF-BD rats, and green showing genes more highly expressed in GF rats fed KJ. Intensity of colour indicates degree of fold change, with greater intensity signifying higher expression level.

3.9 Expression of KEGG pathway gene sets altered by DRC

Analysis of biological pathways that were significantly altered by feeding DRC in the presence or absence of a microbial community were examined by GSEA of rat KEGG pathways (Tables 37 - 39). GSEA tests for significance of differences in expression levels between treatments of all genes within *a priori* biological pathways, rather than examining individual genes. CR rats fed IN, KJ or RS showed significant alterations in expression levels of genes in the metabolic KEGG pathways *Fatty acid metabolism* (IN P=0.04), *Linoleic acid metabolism* (IN, KJ and RS; P=0.01 – 0.03), and *Retinol metabolism* (IN and KJ, P=0.03 and P=0.03). Genes within the KEGG pathway *Linoleic acid metabolism* were generally up-regulated in CR rats fed KJ, RS or IN compared to those fed BD, indicating a higher activity of this pathway in DRC fed rats in the presence of a microbiota. Similarly, CR rats fed IN or KJ also showed higher expression levels of genes within the KEGG pathway *Retinol metabolism* than rats fed BD. Genes within the *Fatty acid metabolism* pathway in CR rats fed IN tended to be more highly expressed than CR-BD rats (Figure 23).

Processes relating to the clearance of exogenous compounds were also differentially expressed by feeding IN or KJ to CR rats compared to BD fed CR rats; *Drug metabolism - other enzymes* (IN P=0.01), *Metabolism of xenobiotics by cytochrome P450* (IN P=0.04 and KJ P=0.03), and *Drug metabolism - cytochrome P450* (IN P=0.04 and KJ P=0.04). However, these pathways were not altered in GF rats by feeding KJ or RS, indicating a role for the large bowel microbial community in mediating these host responses to DRC.

Feeding KJ to GF rats resulted in the differential expression of pathways that were not differentially expressed in KJ fed CR rats with the exception of *Histidine metabolism* (P=0.03). Differentially expressed pathways between GF-KJ and GF-BD rats included processes relating to cell signalling, immune function, and mucosal barrier function. The latter included KEGG pathways *Tight junction* (P=0.04) and *O-glycan biosynthesis* (P<0.01). Genes within the *O-glycan biosynthesis* pathway

tended to be more highly expressed in GF rats fed KJ (Figure 24), while genes within the *Tight junction* pathway were generally expressed at a lower level in GF-KJ rats compared with GF rats fed BD (Figure 25).

Feeding KJ and RS to GF rats also resulted in the differential expression of the *Complement and coagulation cascades* pathway (P=0.04 for both), which showed no change in CR rats. In contrast to KJ, feeding RS to GF rats had minimal impact on the differential expression of KEGG pathways, which is consistent with the absence of differentially expressed genes between GF-RS and GF-BD rats. As expected, a wide range of metabolic pathways were differentially expressed between CR and GF rats, demonstrating the extensive influence of the microbiota in host physiology (Table 39). Cluster analysis showed differentially expressed pathways significances between comparisons were most similar between CR rats fed DRC, GF rats fed DRC, and between comparisons of GF to CR rats (Figure 26).

Table 37. Differentially expressed KEGG pathways in colon tissue of CR rats fed DRC

Pathway ID	Pathway name	BD vs. IN	BD vs. KJ	BD vs. RS
rno00983	Drug metabolism - other enzymes	0.01		
rno00591	Linoleic acid metabolism	0.01	0.02	0.03
rno00760	Nicotinate and nicotinamide metabolism	0.02		
rno04120	Ubiquitin mediated proteolysis	0.03		0.03
rno00830	Retinol metabolism	0.03	0.03	
rno00350	Tyrosine metabolism	0.04	0.02	
rno00980	Metabolism of xenobiotics by cytochrome P450	0.04	0.03	
rno04622	RIG-I-like receptor signaling pathway	0.04		0.04
rno00071	Fatty acid metabolism	0.04		
rno00982	Drug metabolism - cytochrome P450	0.04	0.04	
rno00340	Histidine metabolism		0.03	

Gene set enrichment analysis (GSEA) P values for differential expression of pathways in colon tissue between conventionally raised rats fed IN, KJ, or RS compared to BD. P values < 0.05 indicate all genes within a particular KEGG pathways show significant differences in expression between dietary comparisons.

Table 38. Differentially expressed KEGG pathways in colon tissue of GF rats fed DRC

Pathway ID	Pathway name	BD vs. KJ	BD vs. RS
rno00512	O-Glycan biosynthesis	<0.01	
rno00590	Arachidonic acid metabolism	<0.01	
rno00340	Histidine metabolism	<0.01	
rno04810	Regulation of actin cytoskeleton	<0.01	
rno04260	Cardiac muscle contraction	<0.01	
rno05410	Hypertrophic cardiomyopathy (HCM)	<0.01	
rno05412	Arrhythmogenic right ventricular cardiomyopathy (ARVC)	<0.01	
rno04920	Adipocytokine signaling pathway	<0.01	
rno04270	Vascular smooth muscle contraction	<0.01	
rno04010	MAPK signaling pathway	<0.01	
rno04080	Neuroactive ligand-receptor interaction	<0.01	
rno04510	Focal adhesion	<0.01	
rno04512	ECM-receptor interaction	<0.01	
rno05218	Melanoma	<0.01	
rno04020	Calcium signaling pathway	<0.01	
rno04350	TGF-beta signaling pathway	<0.01	
rno04130	SNARE interactions in vesicular transport	0.01	
rno05222	Small cell lung cancer	0.01	
rno04720	Long-term potentiation	0.01	
rno04360	Axon guidance	0.01	
rno05211	Renal cell carcinoma	0.01	
rno04670	Leukocyte transendothelial migration	0.02	
rno04530	Tight junction	0.04	
rno04610	Complement and coagulation cascades	0.04	0.04
rno04330	Notch signaling pathway		0.04

Gene set enrichment analysis (GSEA) P values for differential expression of pathways in colon tissue between germ-free rats fed KJ or RS compared to BD. P values < 0.05 indicate all genes within a particular KEGG pathways show significant differences in expression between dietary comparisons.

Table 39. Differentially expressed KEGG pathways in colon tissue between CR and GF rats

Pathway ID	Pathway name	KJ	RS	BD
rno00983	Drug metabolism - other enzymes	<0.01	<0.01	<0.01
rno00980	Metabolism of xenobiotics by cytochrome P450	<0.01	<0.01	<0.01
rno00982	Drug metabolism - cytochrome P450	<0.01	<0.01	<0.01
rno00361	gamma-Hexachlorocyclohexane degradation	<0.01	<0.01	<0.01
rno00340	Histidine metabolism	<0.01	<0.01	<0.01
rno01040	Biosynthesis of unsaturated fatty acids	<0.01	<0.01	<0.01
rno00360	Phenylalanine metabolism	<0.01	<0.01	<0.01
rno00650	Butanoate metabolism	<0.01	<0.01	<0.01
rno00512	O-Glycan biosynthesis	<0.01		
rno00480	Glutathione metabolism	<0.01	<0.01	<0.01
rno03050	Proteasome	<0.01	0.02	0.08
rno04950	Maturity onset diabetes of the young	<0.01	<0.01	<0.01
rno00860	Porphyrin and chlorophyll metabolism	<0.01		<0.01
rno00410	beta-Alanine metabolism	<0.01		
rno00150	Androgen and estrogen metabolism	<0.01	<0.01	0<0.01
rno03410	Base excision repair	<0.01	<0.01	<0.01
rno04330	Notch signaling pathway	0.01		
rno00380	Tryptophan metabolism	0.02		
rno00240	Pyrimidine metabolism	0.02		
rno00591	Linoleic acid metabolism	0.02	<0.01	<0.01
rno00030	Pentose phosphate pathway	0.02	<0.01	<0.01
rno00601	Glycosphingolipid biosynthesis - lacto and neolacto series	0.03		
rno00970	Aminoacyl-tRNA biosynthesis	0.03	0.02	0.01
rno03320	PPAR signaling pathway		0.01	
rno00640	Propanoate metabolism		0.02	0.02
rno00100	Steroid biosynthesis		0.02	0.04
rno05310	Asthma			<0.01
rno04115	p53 signaling pathway			<0.01
rno00350	Tyrosine metabolism			0.05

Gene set enrichment analysis (GSEA) P values for differential expression of pathways in colon tissue between conventionally raised and germ-free rats fed KJ, RS or BD. P values < 0.05 indicate all genes within a particular KEGG pathways show significant differences in expression between dietary comparisons.

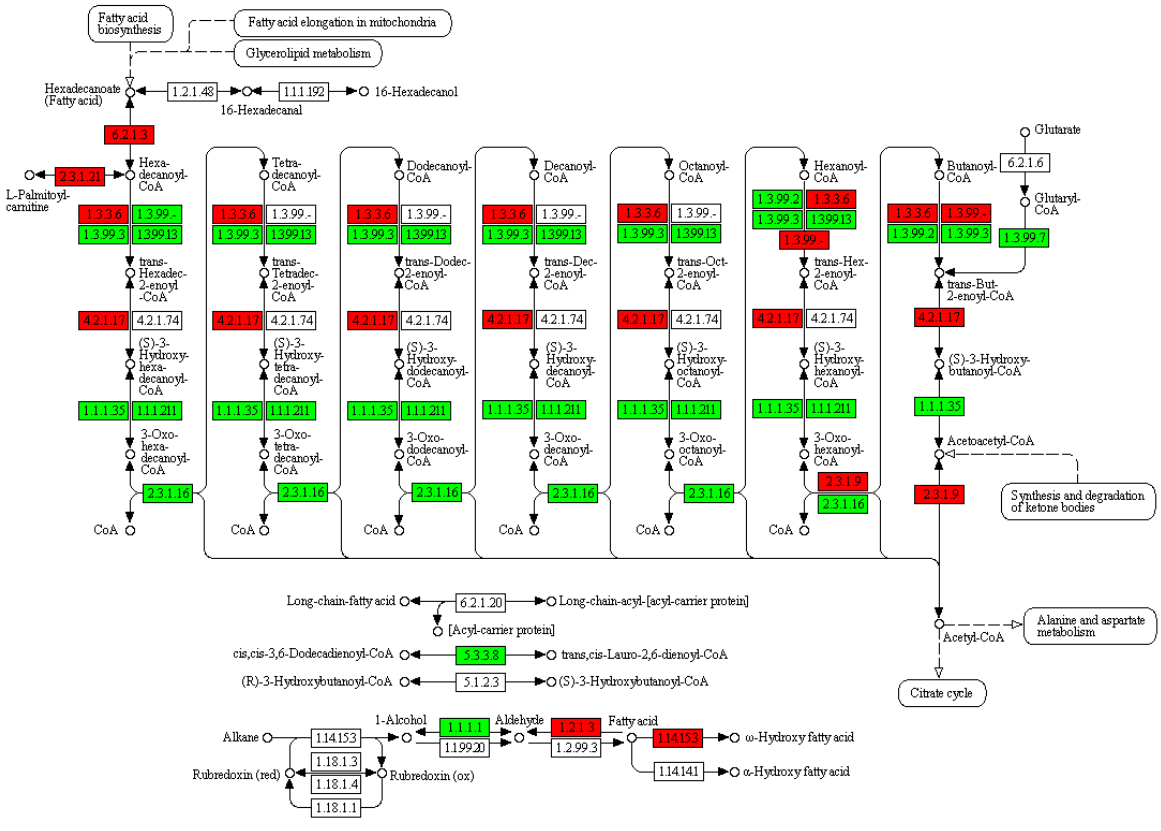

Figure 23. KEGG Fatty acid metabolism pathway. Fatty acid metabolism pathway schematic showing direction of gene expression changes between CR-BD and CR-IN rats. Genes and gene products are indicated by nodes and interactions indicated by arrows. Red nodes indicate genes more highly expressed in conventionally raised BD fed rats and green nodes indicate genes more highly expressed in rats fed IN.

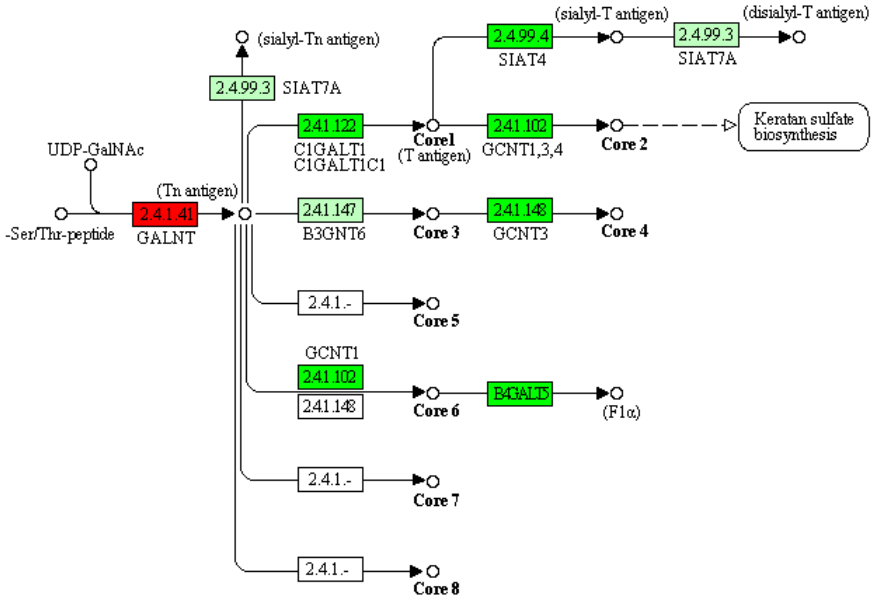

Figure 24. KEGG O-glycan biosynthesis pathway. O-glycan biosynthesis pathway schematic showing direction of gene expression changes between GF-BD and GF-KJ rats. Genes and gene products are indicated by nodes and interactions indicated by arrows. Red nodes indicate genes more highly expressed in GF rats fed BD and green nodes indicate genes more highly expressed in GF rats fed KJ.

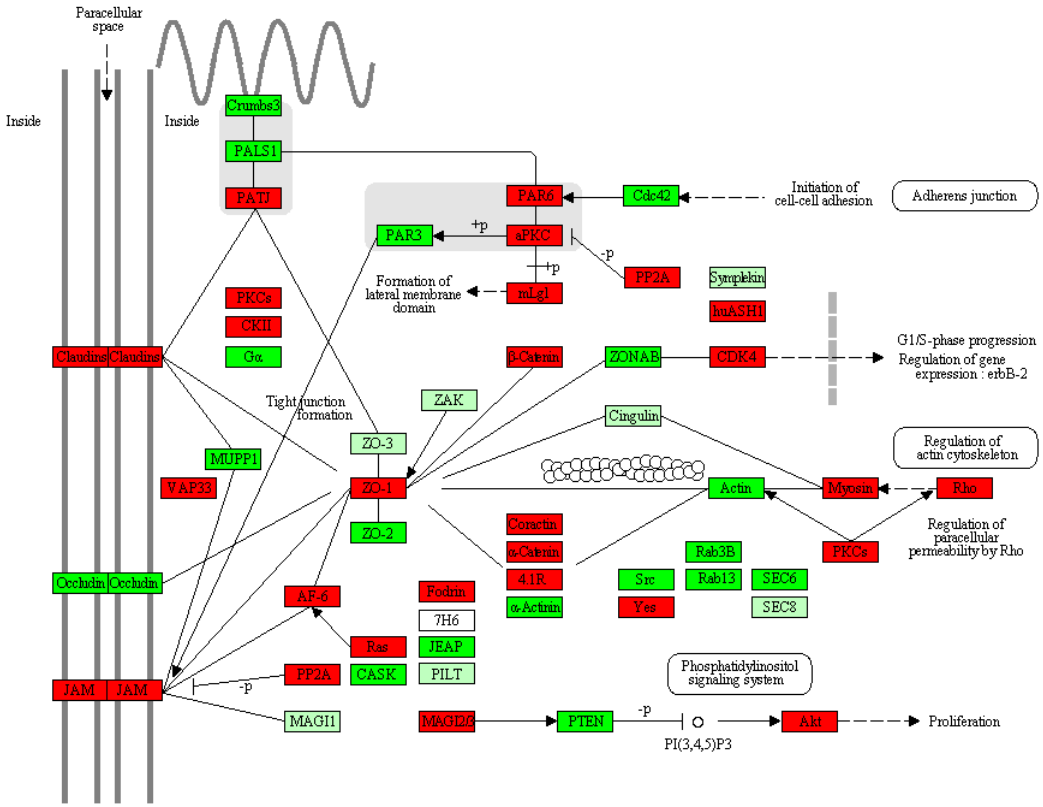

Figure 25. KEGG Tight junction pathway. Tight junction pathway schematic showing direction of gene expression changes between GF-BD and GF-KJ rats. Genes and gene products are indicated by nodes and interactions indicated by arrows. Red nodes indicate genes more highly expressed in GF rats fed BD and green nodes indicate genes more highly expressed in GF rats fed KJ.

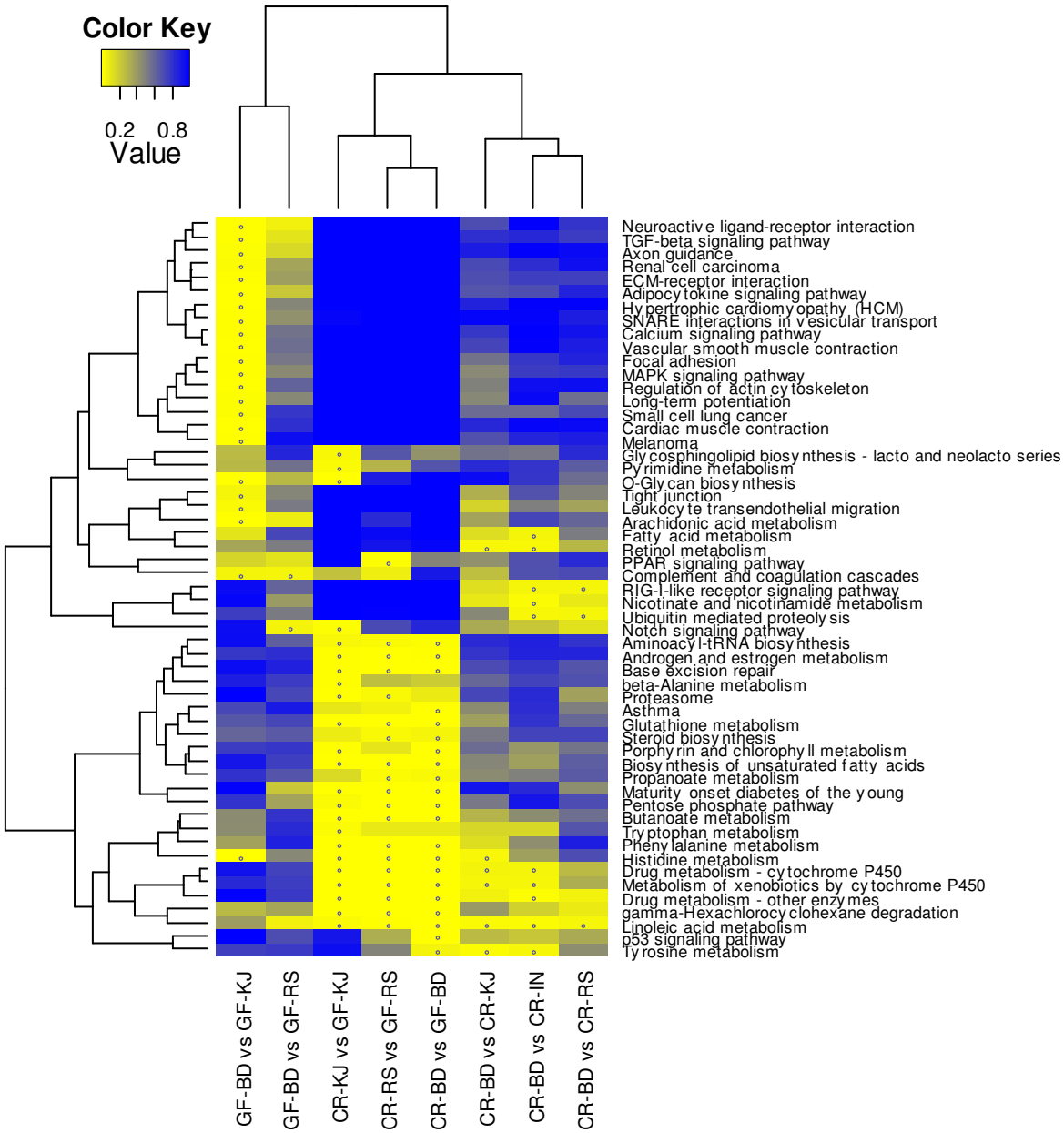

Figure 26. Differentially expressed KEGG pathways. Heatmap showing distribution of differentially expressed KEGG pathways from GSEA. Columns represent comparisons between diets and presence/absence of the microbiota. Cell colour indicates significance, with yellow representing low P values and blue representing high P values, as indicated by colour key. Cells marked with circles indicate significantly differentially expressed pathways ($P<0.05$).

Chapter 4. Discussion

The goal of this study was to characterise the effects of feeding DRC to newly weaned rats, which was represented by the hypotheses; *Feeding DRC to newly weaned rats engineers the colonic microbiota composition towards one with an increased fermentative capacity*; and *DRC induced changes in the colonic microbiota composition alters host gene transcription and physiology.*

Increased colonic SCFA concentrations in CR rats were identified after 14 and 28 days of feeding DRC, but changes in colon mucosal morphology were only observed after 28 days. Alterations in the colonic microbiota structure as measured by 16S rRNA TTGE and DNA pyrosequencing were also observed after 28 days of feeding DRC. The effect of DRC on microbiota profiles varied depending on the type of DRC, indicating the chemical form of DRC is an important factor in characterising the effects of DRC. Similarly, colonic SCFA concentrations and 16S rRNA TTGE profiles were also shown to be influenced by the dose of DRC supplementation in the diet. Alterations in the microbiota structure were accompanied by changes in host gene expression in the colon, the pattern of which also varied according to the type of DRC. Analysis of the colonic transcriptome in GF rats confirmed that DRC induced changes in host gene expression was modulated by the microbiota, as the pattern of DRC induced transcriptional changes in GF rats was different to those in CR rats. Therefore, results from this study confirm the first hypothesis that feeding DRC to newly weaned rats shifts the colonic microbiota composition towards one with an increased fermentative capacity. Furthermore, analyses of DRC induced colon transcriptional and mucosal morphological changes in CR and GF rats confirm the second hypothesis that DRC induced alterations in the colonic microbiota influences host gene expression and physiology. By using high throughput technologies and bioinformatic tools to identify changes in the colonic microbiota and colonic gene expression in response to DRC, this study contributes to the understanding of the complex interactions between food, microbe and host.

4.1 Rat body weight and food intake

Comparisons of body weights between CR and GF rats in this study are difficult because of differences in starting age (CR=21 days, GF=21-28 days) and the enlarged fluid filled caecum which comprises up to 30% or more of the gross weight of GF rats (Coates, 1975). Nevertheless, GF rats were shown to eat more food, but gain less weight than their CR counterparts. This result indicates an important role for the microbiota in modulating energy metabolism and balance, which is supported by findings reported by Bäckhed et al (2004).

The results from all three studies showed that with the exception of GL, the presence of up to 5% DRC in the diet did not have any effects on body weight over 14 or 28 days of feeding in youngling male Sprague-Dawley rats. Other than the GL supplemented diets, no differences were observed in food intake for rats fed the DRC supplemented diets compared to those fed the basal diet. These results indicate that the DRC used, with the exception of GL, were tolerated to the same degree by all rats, with no adverse effects on diet palatability or body weight gain. However, rats fed the GL diet ate significantly less food after 28 days of feeding and had significantly lower body weights compared to rats fed BD. Due to possible adverse effects of GL on rat growth, GL was only examined in study 1. However, these results also raise the possibility that GL may exert a satiety effect through either reduced palatability, a reduction in appetite, or through alterations in host energy metabolism. Therefore, the reduction in food intake and weight gain observed with GL suggests further study examining its mechanism of action may be useful for developing GL as a functional food ingredient. With the increasing prevalence of obesity and obesity-related diseases worldwide, the development of dietary ingredients that contribute to viable weight control strategies warrants further investigation.

4.2 DRC induced changes in colon mucosal morphology

Histological analysis of colon tissue collected from studies 1 and 3 showed differential effects of DRC on colon mucosal morphology. Colonic crypt lengths were measured as an indicator for cell proliferation and growth (Jacobs and Lupton, 1984), and colonic goblet cells were counted to provide a measure of mucin production as higher numbers of goblet cells have been associated with increased mucin layer thickness in the colon (Kleessen et al., 2003).

Differences in colonic crypt length and goblet cell numbers between dietary treatments were not observed at 14 days of feeding. However, the presence of KJ, UN or GL in the diet after 28 days of feeding resulted in longer colon crypts in CR rats, whereas crypt lengths were not altered in DRC fed GF rats. This result indicates the proliferative effects of DRC in the colon are most likely mediated by the resident microbiota, which is consistent with results from previous studies (Goodlad et al., 1989; McCullogh et al., 1998). These results also show that there is a lag period between measureable changes in the mucosal morphology parameters examined in this study, and alterations in SCFA concentrations, which by extension, indicates changes in activity of the microbiota. Therefore, alterations in host physiology resulting from feeding DRC may not be apparent until some weeks after changes in the microbiota activity is detected, even though diet induced changes in the microbiota may occur remarkably quickly; Turnbaugh et al. (Turnbaugh et al., 2009b) showed that feeding mice a high fat, high sugar diet resulted in a rapid shift in the faecal microbiota that was detectable after only one day of feeding.

Consistent with previous reports, colon crypts lengths in CR rats were significantly longer than those in GF rats (Banasaz et al., 2002; Kleessen et al., 2003). An increase in crypt length results in a higher surface area for the absorption of water and ions, which has been shown to occur throughout the length of the colonic crypt (Geibel, 2005). Alterations in crypt cell proliferation may also influence host exposure to pathogens as increased epithelial cell turnover in the large bowel has been shown

to reduce the intestinal burden of *Trichuris trichuria*, a parasitic nematode, in mice (Cliffe et al., 2005).

Rats fed RS did not show altered colonic crypt lengths or goblet cell numbers compared to those fed BD. However, goblet cell numbers per crypt were significantly higher in CR rats fed IN, KJ, UN and GL compared those fed BD, indicating a potential increase in mucin production. The mucus layer is an important component of the mucosal barrier which forms a protective layer against both mechanical stresses and bacterial infection (Meyer-Hoffert et al., 2008). Goblet cell counts in GF rats fed KJ were also higher compared to GF rats fed BD. This finding suggests that KJ, a strong gel forming DRC, may also influence goblet cell proliferation through physical or chemical interactions with the colon mucosa, as extracellular pressure has been shown to stimulate proliferation in cultured intestinal epithelial cells (Hirokawa et al., 1997). These results show that DRC induced changes in the colonic morphology are the result of interactions between the host, specific types of DRC, and the microbiota.

4.3 DRC induced changes in colonic fermentation

Diets supplemented with 5% of all forms of DRC except UN was shown to increase the concentration of fermentation products in colonic digesta compared to the basal diet. In contrast, the addition of UN to the diet did not significantly alter the concentration of colonic fermentation products. The lack of effect of UN on colonic fermentation may be due to the absence of microbiota that have evolved to degrade UN in Sprague Dawley rats, as UN would not be a food ingredient that laboratory rats would commonly have been exposed to. Alternatively, the presence of UN in the diet may modify the microbiota composition, but in a way that does not increase bacterial fermentation. A previous study has shown caecal inocula from rats fed UN have a decreased fermentative capacity for a number of substrates, such as lactulose and citrus pectin, compared to inocula from rats fed a cellulose control diet (Goni et al., 2001). The high concentrations and particular structural

arrangement of fucose and sulphate in brown seaweeds such as UN may also contribute to their resistance to bacterial fermentation in the large bowel (Michel et al., 1996). Although SCFA concentrations were unaltered, rats fed UN had significantly longer colonic crypts and higher goblet cell numbers than BD fed rats, which suggests that these morphological changes may be the result of physicochemical properties of UN in the colon. The addition of seaweed to the diet has been shown to increase the weight of the caecum and contents in rats due to the high water holding capacity and viscosity of seaweeds such as UN (Goni et al., 2001; Jiménez-Escrig and Sánchez-Muniz, 2000). The increased intraluminal pressure resulting from the strong gel forming properties of UN may therefore be responsible for the alteration in colon crypt length and goblet cell numbers in UN fed rats compared to those fed BD.

Overall, concentrations of total colonic SCFA were significantly higher after 14 and 28 days of feeding in rats fed IN, RS, KJ or GL compared to rats fed BD. Furthermore, total colonic SCFA levels were significantly higher after 28 days compared to 14 days of feeding. It is possible that this increase in total colonic SCFA concentrations observed between 14 and 28 days of feeding may be due to alterations in the colonic microbiota composition or metabolic activity during this period. Concentrations of butyric acid were also increased in the colon digesta of rats fed IN, RS, KJ, or GL diets for 14 days compared to those fed BD. Moreover, concentrations of colonic butyric acid in rats fed IN, RS, KJ or GL for 28 days were significantly higher compared to rats fed for 14 days.

Microbial production of SCFA may play an important role in regulating appetite and energy balance. GF mice have been shown to require additional energy expenditure in order to utilise food compared to CR mice (Wostmann et al., 1982). This is manifested by an increase in food intake, with a lower gain in body weight in GF mice compared to CR mice (Wostmann et al., 1982). The influence of the microbiota and products of microbial polysaccharide breakdown on host energy balance is perhaps most strikingly demonstrated by studies that show a rapid gain in body weight and fat deposition

despite a reduction in food intake in GF mice following conventionalisation with a normal microbiota (Backhed et al., 2004; Turnbaugh et al., 2008). Concentrations of acetic, propionic and butyric acid in portal blood are several times higher than that found in peripheral venous blood, which indicate the bowel is the major source of SCFA (Cummings et al., 1987). Microbial fermentation products are utilised by the host through a number of routes; butyric acid is primarily utilised by the colonic epithelia, while intestinally absorbed propionic acid is converted into more complex lipids in the liver and acetate is utilised primarily in muscle tissue (Cummings and Macfarlane, 1997; Roediger, 1980). Monosaccharides released from polysaccharide break down are also taken up by the colon, which is facilitated by an increase in mucosal blood flow stimulated by increased SCFA concentrations (Backhed et al., 2004; Scheppach, 1994). The resident microbiota is also able to direct the host to increase hepatic production of triglycerides by stimulating the increased expression of genes encoding acetyl-CoA carboxylase and fatty acid synthase, which are important enzymes involved in *de novo* synthesis of fatty acids (Backhed et al., 2004). Furthermore, activation of GPR41, a G protein-coupled receptor for SCFA, has been shown to stimulate production of leptin in mouse adipose tissue (Xiong et al., 2004). Leptin plays a key role in energy homeostasis and defects in leptin signalling are associated with numerous conditions in rodents and humans, including severe obesity, hyperphagia and immunological pathologies (Fernandez-Riejos et al., 2010; Morris and Rui, 2009). Propionic acid, which was significantly higher in the colon of CR rats fed IN and RS for 28 days compared to those fed BD, has been shown to stimulate leptin production in human adipose tissue through activation of GPR41 and GPR43, a SCFA receptor which is also expressed in the ileum and colon (Al-Lahham et al., 2010; Karaki et al., 2006). The effect of bacterial fermentation on satiety has also been demonstrated in humans where feeding diets supplemented with a chicory oligofructose resulted in reduced hunger scores, which were associated with increased secretion of the gastrointestinal peptides plasma glucagon-like peptide 1 and peptide YY (Cani et al., 2009).

Butyric acid has also been shown to inhibit the production of inflammatory cytokines in isolated lamina propria cells and PBMCs in humans, and reduce the severity of TNBS induced colitis in rats (Segain et al., 2000). An increase in butyric acid from feeding resistant starch has been positively correlated with an increase in apoptotic response in colonic epithelial cells after azoxymethane induced DNA damage in rats (Le Leu et al., 2009). Butyric acid also increases tight junction assembly in Caco-2 cells, indicating a possible function for the enhancement of intestinal barrier function (Peng et al., 2009). Acetate signalling through GPR43 has been shown to be important for the resolution of DSS induced colitis in mice (Maslowski et al., 2009). The addition of acetate to the drinking water reduces the severity of DSS induced colitis in wild-type mice, but has no beneficial effects in GPR43$^{-/-}$ mice, which also exhibit more severe inflammation (Maslowski et al., 2009). GPR43 expression in neutrophils and eosinophils is also closely regulated with expression of TLR2 and TLR4, indicating a possible role for the microbiota in protection against inflammatory diseases (Maslowski et al., 2009). Indeed, DSS induced colitis has been shown to be more severe in GF mice compared to CR mice (Maslowski et al., 2009).

The effect of DRC dose on colonic SCFA concentrations was examined in study 2, where rats were fed BD or the basal diet supplemented with 1.25%, 2.5% or 5% RS or KJ. Linear regression analysis showed a significant positive linear relationship of colonic SCFA concentrations and dose of RS and KJ after 28 days of feeding. Concentrations of colonic SCFA for the 5% RS and 5% KJ in study 2 were similar to those observed in feeding study 1, indicating a good reproducibility of results from studies conducted at different times. Analysis of variance showed the minimum DRC dose that produced significantly different concentrations of colonic SCFA compared to that produced by the basal diet was 2.5%. Results from the New Zealand 2002 National Children's Nutrition Survey indicated that the mean daily dietary fibre intake of 5-14 year old children was 18.4 g, which represented 4.3% of their daily food consumption by weight (Parnell et al., 2003). Therefore, the dosages of DRC

examined in this study were an appropriate approximation of the typical DRC intake that may occur in humans.

Principal component analysis of colonic SCFA profiles showed that feeding IN, RS, KJ and GL resulted in profiles that tended to segregate from those of BD fed rats. Of the different forms of DRC examined, feeding IN, RS and KJ resulted in SCFA profiles which showed the largest differences compared to those from BD fed rats, while SCFA profiles from UN fed rats were most similar to those of BD fed rats after 14 and 28 days of feeding. Following analysis of colonic SCFA concentrations, identification of the microbiota community in rats fed IN, RS and KJ was undertaken as these DRC induced the largest differences in SCFA profiles compared to rats fed BD. The analysis of the microbiota in rats fed IN, RS, and KJ also enables the effects of purified DRC, such as IN and RS, to be compared to a crude DRC preparation, such as KJ, which may be composed of up to 76.6% konjac glucomannan, 2.1% fibre, 8.3% starch, 1.4% crude protein, 0.8% soluble sugars, and 2.1% ash (Li et al., 2005).

These results show that colonic SCFA concentrations, and therefore metabolic activity of the microbiota, are altered by feeding DRC and that colonic SCFA profiles tend to be associated with specific forms of DRC. The SCFA results also support the results obtained from histological analysis, which showed that DRC induced changes in the colonic mucosa are dependent on the chemical form of DRC. The particular arrangement of glycosidic linkages may dictate which particular groups of bacteria are most suitable for degrading a specific type of DRC. Carbohydrates that may normally be readily fermentable may also be protected from degradation by structural arrangements with other carbohydrates which are not readily broken down.

4.4 Effects of DRC on colonic microbiota profiles

4.4.1 TTGE profiling

The use of rRNA to produce TTGE profiles enabled the generation of a molecular fingerprint of the metabolically active members of the colonic microbiota. TTGE microbiota profiling was performed using rRNA as it has also been shown to highlight alterations in the community which may not be apparent when using DNA, indicating RNA-TTGE analysis may resolve more changes in the microbiota than DNA-TTGE in some situations (Tannock et al., 2004).

Analysis of 16S rRNA TTGE profiles in rats fed BD, IN, RS and KJ diets from study 1 indicated a distinct colonic microbiota profile was associated with each diet. This was confirmed by Jackknife analysis of profile similarities which placed BD fed rats within the CR-BD group 75% of the time, IN fed rats within the CR-IN group 92% of the time, and KJ and RS fed rats within their respective groups 100% of the time. Although other studies have shown DRC induced alterations in the large bowel microbiota of normal rodents under non-pathological conditions (Abnous et al., 2009; Snart et al., 2006), the clear separation of microbiota profiles associated with diet in this study was surprising. Previous studies examining dietary DRC treatments in rodents have not generally shown such distinctive differences except when using higher doses of DRC. For example, markedly different faecal DGGE profiles have been observed in mice fed inulin and oligofructose in a study by Licht et al. (2006), but the diets were supplemented with 15% of inulin or oligofructose. In comparison, the diets examined here were supplemented with up to 5% DRC. It is possible that the distinctive nature of the colonic microbiota profiles induced by feeding diets with 5% IN, RS or KJ is a result of the age of the rats examined in this study. Weaning is a period that is characterised by dramatic changes in the large bowel community (Stark and Lee, 1982) and disturbances in the microbial ecology through alterations in the diet during this time may results in greater differences than would be seen by feeding DRC at a later stage in life.

These results show that the microbiota composition may be directed towards a distinct profile dependant on the type of DRC, and that these profiles are associated with an increased fermentative capacity. UPGMA clustering analysis of 16S rRNA TTGE profiles also show increased uniformity in profiles between rats fed the same DRC diet in comparison to rats fed BD. The increase in microbiota uniformity is an important feature of DRC, as this may enable a more consistent characterisation of each type of DRC to be made, which in turn may make predictions of biological effects that each DRC may exert more consistent.

The DRC induced alterations in TTGE profiles were mirrored by altered SCFA profiles observed in rats fed IN, RS and KJ. This indicates that feeding DRC not only alters the microbiota composition, but that it also modifies the metabolic activity of community members. Therefore, feeding DRC to weanling rats will also impact upon host physiology, which is confirmed by the alterations observed in colon mucosal morphology in DRC fed CR rats.

The impact of DRC dose on the colonic microbiota was examined by analysing 16S rRNA TTGE profiles from colon digesta RNA samples of rats fed BD, or the basal diet supplemented with 1.25%, 2.5% or 5% RS or KJ from rat feeding study 2. RS and KJ were chosen as representative examples of purified DRC and 'crude' DRC preparations, respectively. TTGE profiles from rats fed 5% RS or 5% KJ showed the greatest differences compared to profiles of BD fed rats, while profiles from rats fed intermediate doses of KJ or RS were more similar to those of BD fed rats. The effect of RS or KJ dose on colonic microbiota profiles was confirmed by UPGMA cluster analysis of the TTGE profiles from pooled RNA, which showed three clusters of profiles; (1) rats fed 1.25%, 2.5% and 5% RS; (2) rats fed 2.5% and 5% KJ; and (3) rats fed BD and 1.25% KJ. The effect of RS and KJ dose on colonic microbiota profiles also mirrored their effect on colonic SCFA concentrations, which suggests that any DRC induced effects on host physiology that might occur may also be dose dependant. These results may be important considering the average daily intake of dietary fibre of 5-14 year old New Zealand children is 18.4 g

(Parnell et al., 2003), but the recommended daily intake from the United States National Academy of Sciences for this age group is 25 – 31 g (National Academy of Sciences, 2002).

4.4.2 Identification and qPCR analysis of TTGE bands

Bands from TTGE gels that appeared to differ in staining intensity between dietary treatments in study 2 were excised and sequenced for the purposes of bacterial identification and to design primers for qPCR analysis of identified 16S rRNA gene copy numbers in colon digesta DNA. Gene copy numbers of the 16S rRNA genes identified to *Lactobacillus*, *Clostridium* and *Ruminococcus* genera varied according to RS or KJ dose, which was consistent with the observed band intensities from the TTGE profiles from the pooled RNA. The changes in gene copy numbers from different RS and KJ doses also corresponded with DRC dose dependant changes observed in SCFA and TTGE profiles. The decreased observed in *Lactobacillus spp.* 16S rRNA gene copy numbers in rats fed RS and KJ was unexpected given results from other studies which showed enrichment in large bowel *Lactobacillus* from feeding RS or KJ (Chen et al., 2008; Snart et al., 2006). However, the different effects of RS and KJ on *Lactobacillus* numbers in this study compared to other studies may be a function of the age of rats, as previous studies have examined effects in older rats. A study examining the effects of inulin in post-weaning infants also found a significant decrease in faecal *Lactobacillus* numbers following dietary supplementation with inulin (Yap et al., 2008). Other studies examining diet induced changes in the microbiota of growing pigs found no effect of inulin or barley β-glucan supplemented diets on *Lactobacillus* abundance in the colon (Loh et al., 2006; Pieper et al., 2008).

4.5 Identification of microbiota using next generation sequencing

Identification of the colonic microbiota composition was undertaken by 454 pyrosequencing of pooled DNA amplified with the universal bacterial primers HDA-1 and HDA-2. Analysis of DNA was performed to determine the proportions of bacterial taxa present in each dietary group. Because of

the similarity of TTGE profiles between rats fed the same diets, the DNA from individual rats fed BD, IN, RS, and KJ was pooled within their respective dietary groups. The primary advantage of next generation sequencing platforms such as the Roche 454 Genome Sequencer FLX is that they provide far greater sequence coverage without cloning bias compared to traditional sequencing platforms. Approximately 35 to 43 percent of 16S rRNA sequences in each dietary group examined could be identified at the genus level, while over 83 to 95 percent of sequences could be identified at the family level. However, due to the PCR product length resulting from the use of HDA1 and HDA2 primers, taxonomic classification at the species level was not possible. In future, the use of other primers which amplify longer portions of the 16S rRNA gene may be able to address this limitation. Nevertheless, the use of next generation sequencing provided a detailed catalogue of the microbial community members to an extent not possible from TTGE separation of amplified bacterial 16S rRNA and cloning and sequencing of excised bands.

4.5.1 DRC induced changes in Bacteroidetes to Firmicutes ratios

Analysis of 16S rRNA amplicon sequences showed broad phylum wide changes in the colonic community composition or rats fed IN, RS and KJ compared to rats fed BD. Each DRC modified the microbiota in a manner specific to the type of DRC, which was consistent with the DRC induced changes seen in colonic 16S rRNA TTGE profiles. Although each type of DRC resulted in a distinct microbiota composition, a common element shared by IN, RS and KJ fed rats was an increase in Bacteroidetes to Firmicutes ratios compared to BD fed rats.

Feeding DRC in early post-weaning life may have important consequences for health, as studies have shown obese mice and humans are characterised by decreased Bacteroidetes to Firmicutes ratios (Turnbaugh et al., 2006). Obesity related changes in the microbial community have been shown to alter the metabolic potential of the microbiota and are associated with an increased capacity for energy harvest (Turnbaugh et al., 2006). Although no significant differences were observed in body

weight between BD, IN, RS, and KJ fed youngling rats, exposure to different bacterial communities at an early age may still have important consequences later in life. Incidence of childhood atopic eczema has been associated with reduced faecal community diversity in 18 month old infants (Wang et al., 2008) and newly weaned pigs raised in microbial isolators have also shown increased expression of inflammatory genes compared to pigs raised outdoors (Mulder et al., 2009). Furthermore, a prospective follow-up study of 7 year old obese and overweight children showed a strong correlation with faecal community composition at 6 months of age and later childhood obesity (Kalliomaki et al., 2008).

4.5.2 DRC induced alterations in *Lactobacillus* and *Bifidobacterium* proportions

Rats fed IN, RS, and KJ had lower proportions of *Lactobacillus* after 28 days of feeding than rats fed BD. This result was consistent with the abundance of sequences corresponding to the *Lactobacillus spp.* TTGE band in colon digesta DNA of rats fed RS and KJ as measured by qPCR. Although this result contrasts with previously studies that that show increases in large bowel *Lactobacillus* numbers following DRC feeding (Kleessen et al., 2001; Snart et al., 2006), the impact of DRC on *Lactobacillus* numbers may vary depending on age, as the effects of DRC on early post weaning life have not been extensively studied. A possible explanation for the decreased observed in proportions of *Lactobacillus* is that the particular *Lactobacillus* species prevalent in the large bowel of youngling rats examined in this study were not able to degrade the types of DRC used. In a study examining the faecal microbiota of rats that were of a similar age to those used in this study, 28-42 day old rats fed oat bran or wheat bran supplemented diets for 28 days showed no differences in *Lactobacillus* numbers (Abnous et al., 2009). A further possibility is that the diets supplemented with IN, RS or KJ contained less corn starch than the BD diet, which may have negatively affected *Lactobacillus* numbers as starch is readily utilised by *Lactobacillus* (Reddy et al., 2008). Although corn starch is readily digested, it has been shown to reach the large bowel and modify the resident microbiota composition (Licht et al., 2006).

Proportions of bifidobacteria in the colon were significantly increased by feeding RS and KJ, but were decreased in rats fed IN. Bifidobacteria proportions were highest in RS fed rats, which was more than 2 fold higher in RS fed rats compared to any other group. The combined proportions of lactic acid producing lactobacilli and bifidobacteria were also highest in RS fed rats. This result may explain the significantly increased concentrations of colonic lactic acid in RS fed rats compared to rats fed BD. Furthermore, rats fed RS were the only group which showed significantly higher colonic concentrations of lactic acid compared to BD fed rats in both study 1 and 2. The marked decrease in bifidobacteria proportions observed in rats fed IN may be explained in part by reports showing long-chain inulin, such as that used in this study, does not exhibit bifidogenic properties characteristic of FOS and short-chain inulin (Bouhnik et al., 2004; Kleessen et al., 2001).

4.5.3 DRC induced alteration in proportions of clostridial cluster IV and XIVa

Phylogenetic analysis of sequences showed that rats fed IN, RS and KJ had altered proportions of bacteria belonging to clostridial cluster IV and XIVa, many of which are prominent butyric acid producers (Barcenilla et al., 2000) (Louis and Flint, 2009).

Rats fed IN showed a large 2.7 fold increase in the proportion of bacteria belonging to clostridial cluster XIVa, much of which was due to an expansion of bacteria from the Lachnospiraceae family, which comprised 38% of the total colonic population. A small increase in proportions of bacteria from clostridial cluster XIVa was also observed in rats fed KJ. However, KJ fed rats also showed a significant increase in the abundance of bacteria belonging to clostridial cluster IV. The numbers of clostridial cluster IV bacteria in the microbiota may have important consequences for health. Studies have shown that patients with Crohn's disease and ulcerative colitis have a lower abundance of clostridial cluster IV (Manichanh et al., 2006; Sokol et al., 2009). Furthermore, oral administration of *F. prausnitzii*, a prominent member of clostridial cluster IV, has been shown to reduce the severity of

TNBS induced colitis in mice and restore the microbiota composition to one that more closely resembles that of non-colitic mice (Sokol et al., 2008).

The increase in clostridial cluster IV and XIVa corresponded with higher concentrations of colonic butyric acid in rats fed IN and KJ, which suggests these bacterial groups were responsible for the increase in butyric acid. This also indicates that IN and KJ induced increases in butyric acid may occur through the stimulation of different bacterial populations. Colonic butyric acid concentrations were also increased by feeding RS, although no expansion in clostridial cluster IV or XIVa were observed. Therefore, it is possible that the RS induced increase in butyric acid is due to increased metabolic activity of bacteria from these groups without alterations in bacterial abundance. Alternatively, the elevated butyric acid concentrations in RS fed CR rats may be mediated by another group such as the unclassified Bacteroidetes that were increased in RS fed rats compared to those fed BD.

4.5.4 Microbial diversity

Chao1 diversity estimates of colonic microbiota sequences showed increased microbial diversity in rats fed KJ compared to those fed BD. However, microbial diversity in rats fed IN or RS did not differ significantly from those fed BD. The increased diversity observed in KJ fed rats suggests KJ may be a useful substrate for improving colonic microbial composition, which may have important consequences for the host. Increased microbiota diversity and diets high in dietary fibre have been associated with decreased incidences of bowel diseases in studies comparing populations in western and developing countries (Burkitt, 1973; De Filippo et al., 2010). Furthermore, higher bacterial diversities have also been observed in healthy individuals compared to those with Crohn's disease (Dicksved et al., 2008; Manichanh et al., 2006). It is possible that a reduced microbial diversity may allow a single pathogenic strain to more easily dominant the community, which may negatively impact the health of the individual. A study of neonatal necrotising enterocolitis among preterm

infants has showed a greatly restricted bacterial diversity in colitic infants, with Proteobacteria comprising over 90% of the faecal microbiota (Wang et al., 2009).

4.5.5 Comparisons with human microbiota

Analysis of the microbiota composition showed that microbial communities at the phylum level were similar between young rats used in this study and adult humans, with Bacteroidetes and Firmicutes dominating in both communities, with Proteobacteria and Actinobacteria representing minor populations (Bibiloni et al., 2006; Costello et al., 2009; De Filippo et al., 2010; Turnbaugh et al., 2009a). However, differences in microbiota composition were observed at lower taxonomic levels. Proportions of *Lactobacillus* were higher in rats (9-19.5%) than that reported in humans (less than 3%) (Lay et al., 2005; Mariat et al., 2009). On the other hand, bacteria from clostridial cluster IV form a large component of the microbiota in humans, comprising 10-20% of the community (Lay et al., 2005; Sokol et al., 2009), compared to less than 5% in the rat colonic microbiota. Similarly, *Prevotella* species are commonly found members of the Bacteroidetes in humans (Hopkins and Macfarlane, 2002), but were not detected in rats from this study. However, a direct comparison of the microbiota between humans and rats is sometimes difficult as samples from humans are usually faecal samples or colon biopsies. Faecal samples may not always reflect the microbiota composition or activity in the large bowel due to changes in pH, water content and substrates as the faecal material is excreted (Mai et al., 2010). Similarly, the bacterial composition of colon biopsies is also not representative of the large bowel microbiota in the normal state as the extensive preparation procedure prior to biopsies sampling alters the colon environment (Mai et al., 2010). However, despite the differences in human and rat large bowel microbial communities, there are sufficient parallels between the two to make the rat a viable model of human responses to DRC.

4.6 DRC induced changes in colonic gene expression

Microarray analysis showed each type of DRC produced distinct effects on colon tissue gene expression, which corresponded with the distinct effects each DRC had on colonic microbiota composition, mucosal morphology and SCFA profiles. Microarray results were confirmed in general by comparative expression analysis of selected genes by RT-qPCR. Through examining the effects of feeding DRC to GF and CR rats, this study has also demonstrated that the effects of DRC on colonic gene expression are modulated by the resident microbiota.

The increase in goblet cell numbers in CR rats fed IN was associated with altered expression levels of *Galntl4* and *Galnt2*, which belong to the family of GalNAc-transferases that initiate mucin-type O-linked glycosylation, leading to the formation of secreted mucins (Varki et al., 1999). Interestingly, the shift in expression of *Galntl4* depended on the presence of the microbiota. Expression levels of *Galntl4* in CR rats fed IN were significantly higher than those of CR rats fed BD. Microarray and RT-qPCR analysis showed feeding RS or KJ to CR rats also increased *Galntl4* expression levels compared to those of CR-BD rats, although the differences were not statistically significant ($P>0.05$). However, KJ fed GF rats showed significantly lower expression levels of *Galntl4* compared to GF-BD rats. A possible explanation for the increase in *Galntl4* expression in DRC fed CR rats, but not GF rats, is the presence of bacterial community members, such as *B. thetaiotaomicron*, which are able to stimulate the host to increase mucin secretion depending on the activity of other members of the microbiota (Mahowald et al., 2009). Alterations in expression of GalNAc-transferases may also explain differences in diet induced changes in mucin distribution and composition between CR and GF rats (Fontaine et al., 1996; Meslin et al., 1993; Sharma et al., 1995).

Analysis of significantly over-represented GO biological processes associated with differentially expressed genes resulting from feeding DRC confirmed the unique effects each DRC had on colonic gene expression. Although the biological processes over-represented for each DRC treatment could

be broadly classified into processes relating to various aspects of metabolism, cell signalling, and cellular proliferation and differentiation, the specific biological processes varied depending on the type of DRC. These findings show that not all DRC produce the same response and therefore claims in support of different dietary supplements may need to be specific to each supplement. These findings also raise the possibility that dietary supplements may be formulated to produce personalised effects.

Feeding IN, a purified DRC preparation, resulted in 465 differentially expressed genes in CR rats, which was the largest number of differentially expressed genes of all the DRC tested. On the other hand, feeding KJ, a crude DRC preparation, resulted in only 52 differentially expressed genes in CR rats. Therefore, any effects that the non carbohydrate components of KJ may exert on host gene expression appear to be minor, and are not reflected by the numbers of differentially expressed genes. However, to definitively characterise the effects of the non carbohydrate components of KJ on colonic gene expression, experiments using purified konjac glucomannan supplemented diets would be required.

The presence of a microbiota was shown to have wide ranging effects on host gene expression, both in terms of numbers of differentially expressed genes and the magnitude of fold changes in the colon. For example, neurotensin, a gastrointestinal peptide, was expressed up to 39 fold higher in GF rats compared to CR rats. Neurotensin is involved in a wide range of processes that regulate intestinal motility, intestinal secretion, and mucosal growth and repair (Zhao et al., 2007), which points to the important role that the resident microbiota has on mammalian physiology.

The effects of RS on host gene expression were absent when fed to GF rats, which indicate RS induced changes in transcription are mediated by the presence of the microbiota. This result was mirrored by the histological analysis of the colon mucosa, where RS had no significant effects on

goblet cell numbers and crypt length in both CR and GF rats. In contrast, feeding KJ to GF rats resulted in a large number of differentially expressed genes, of which only 4 also showed differential expression in CR rats fed KJ, suggesting distinct effects of KJ on colonic physiology in CR and GF states. It is likely that the microbiota mediated differential effects of KJ on colonic gene expression is due to metabolic activity of the microbiota, which results in the breakdown of KJ and the production of metabolites that would not otherwise be present.

4.6.1 Biological interaction networks

The biological interaction networks of differentially expressed genes between CR rats fed IN, RS, KJ, and BD were examined using IPA. Interaction networks were assembled based on known functional interactions of gene products. It is important to note that the networks do not necessarily describe actual processes in any particular biological system, but instead provide insight into potential interaction that may be occurring between products of differentially expressed genes.

4.6.1.1 Biological interaction network: CR-BD vs. CR-IN

The biological interaction network constructed from differentially expressed genes between CR rats fed IN and BD included the glucose transporter, *Slc2a4*, which directly interacts with 13 other genes within the network. *Slc2a4*, which was down-regulated in rats fed IN, has been shown to be suppressed in the adipose tissue of insulin resistant obese rats (Seraphim et al., 2007). Genes within this network that have known interactions with *Slc2a4* and were down-regulated in rats fed IN included *RhoA, Hspd1 and Lgals1. RhoA* is a member of a family of small GTPases involved in a number of cellular processes including actin filament reorganisation. Activation of *RhoA* has been shown to increase transepithelial electrical resistance (TER) in kidney cell lines (Fujita et al., 2000). *Hspd1*, a gene encoding heat shock protein 1, has been shown to induce apoptosis through binding with TLR4 (Kim et al., 2009) and up-regulate expression of TLR2 in bone marrow macrophages (Koh et al., 2009). *Lgals1*, a gene encoding galectin-1, a beta-galactoside binding lectin, has been shown to

increase proliferation and the production of several chemokines through activation of NF-κB in pancreatic fibroblast cells (Masamune et al., 2006). Genes that showed increased expression in rats fed IN included *Acot2*, a *Ppar-α* regulated gene encoding an acyl-CoA thioesterase, which has an important role in regulating lipid metabolism by promoting fatty acid oxidation (Stavinoha et al., 2004). Increased expression of *Acot2* may be explained by the increased concentrations of colonic SCFA in rats fed IN. This network therefore suggests feeding IN has the potential to modulate energy metabolism and innate immune function through a number of interconnected mechanisms.

4.6.1.2 Biological interaction network: CR-BD vs. CR-KJ

The interaction network constructed from differentially expressed genes induced by feeding KJ to CR rats included *Il1r2*, which was increased in rats fed KJ. *Il1r2* is a decoy receptor that blocks signalling of the pro-inflammatory cytokines IL1α and IL1β (Chang et al., 2009). Expression of *Scarb1*, a scavenger receptor involved in enterocyte absorption of dietary lipids (Beaslas et al., 2009), was also higher in KJ fed rats. KJ fed rats showed a lower expression of *Hsp90aa1*, a heat shock protein that is critical for the induction of type I and II interferon pathways (Shang and Tomasi, 2006), and is up-regulated in colorectal cancer cells (Milicevic et al., 2008; Park et al., 2007). This network indicates feeding KJ may also modulate energy metabolism and influence inflammation pathways through interconnected mechanisms.

4.6.1.3 Biological interaction network: CR-BD vs. CR-RS

Most genes within the highest ranked biological interaction network generated from differentially expressed genes between CR rats fed RS and BD showed lower expression levels in RS fed rats, which included the glucose transporter *Slc2a4* and galectin-1 encoding *Lgals1*. Expression of *Slc25a4*, a solute carrier that catalyses the exchange of ADP and ATP within the mitochondria, also showed reduced expression in RS fed rats compared to rats fed BD. *Tac1*, which encodes the neuropeptides substance P, neurokinin A, neuropeptide K, and neuropeptide gamma, showed lower expression in

the colon of RS fed rats. Substance P has been shown to play an important role in regulating intestinal motility, mucosal permeability, and the development and progress of intestinal inflammation (Koon and Pothoulakis, 2006). Substance P has also been shown to prevent apoptosis in colonic mucosa and promote mucosal healing during colitis in mice (Koon et al., 2007). Furthermore, neuropeptide Y and substance P may play an important role in regulating obesity through appetite stimulation and modulation of energy balance (Arora and Anubhuti, 2006; Karagiannides et al., 2008). Inhibition of substance P signalling using a receptor antagonist has been shown to reduce blood glucose levels and increase insulin sensitivity (Karagiannides et al., 2008). Expression of *Plaur*, which encodes the receptor for urokinase plasminogen activator, was also lower in RS fed rats. Concentrations of neutrophil secreted soluble urokinase plasminogen activator receptor have been shown to be elevated during inflammation (Pliyev and Menshikov, 2010). Genes within this network that were more highly expressed in RS fed rats include *AHSP*, encoding alpha haemoglobin stabilising protein, and *Serpinb7*, encoding serpin peptidase inhibitor, clade B (ovalbumin), member 7. Mutations in *Serpinb7* have been associated with IgA mediated autoimmune pathology (Li et al., 2004). Similar to the effects of feeding IN or KJ, the biological interaction network of differentially expressed genes induced by feeding RS indicated that RS may influence important processes that regulate energy metabolism, gastrointestinal function and inflammatory pathways.

4.6.1.4 Biological interaction network: GF-BD vs. GF-KJ

The biological interaction network generated from differentially expressed genes between GF rats fed BD or KJ included *Pparα*, encoding peroxisome proliferator-activated receptor alpha, which showed significantly lower expression in GF rats fed KJ compared to GF rats fed BD. *Pparα* is an important regulator of lipid metabolism (Rakhshandehroo et al., 2009) and immune system activity (Jones et al., 2002). Furthermore, *Pparα* has been shown to induce expression of *Cyp1a1* (Rakhshandehroo et al., 2009), which was expressed at a lower level in GF rats fed KJ compared to

those fed BD. *Slc10a2*, a sodium/bile acid co-transporter also regulated by *Pparα (Jung et al., 2002)*, showed lower expression in GF rats fed KJ. Genes within this interaction network that were more highly expressed in GF rats fed KJ included *Tac1*, the growth factor *Fgf2* and its receptor *Fgfr2*, and *Rxrg* a nuclear receptor activated by retinoic acid. Familial combined hyperlipidemia, a disease characterised by increased HDL and triglyceride levels, has been associated with a genetic variant of *Rxrg* (Nohara et al., 2007). Interestingly, the biological interaction network associated with KJ induced differentially expressed genes in GF rats indicated that KJ may also influence aspects energy metabolism and immune function in the absence of a microbiota.

4.6.1.5 Summary of biological interaction networks

The biological interaction networks associated with each DRC demonstrated the distinctive potential effects each microbiota has on host mucosal physiology. The IN associated microbiota was shown to modify expression of the carbohydrate transporter *Slc2a4*, which has a role in the regulation of several other genes involved in cell proliferation, apoptosis, immune function and lipid metabolism, which were also differentially expressed in rats fed IN. The biological interaction network associated with the KJ and RS microbiota similarly included differentially expressed genes involved in immune regulation and lipid metabolism. Associated with the increased expression of *Scarb1* in KJ fed rats and *Acot2* in rats fed IN, and decreased expression of neuropeptides encoded by *Tac1* in RS fed rats was an increase in Bacteroidetes to Firmicutes ratios in all DRC fed groups. These observations indicate a possible mechanism for the altered energy balance seen in obese humans and rodents characterised by a decrease in Bacteroidetes to Firmicutes ratios (Turnbaugh et al., 2009a; Turnbaugh et al., 2006).

4.7 DRC induced changes in expression of KEGG pathways

Changes in the expression pattern of genes within the KEGG pathways as a set, rather than individually, were analysed using GSEA. A cluster analysis of the profiles of differentially expressed

pathways induced by different DRC showed that the presence or absence of a microbiota plays a crucial role in determining the host response to DRC.

Analysis of pathways showed that IN and KJ induced changes in CR rats included alterations in the expression of metabolic pathways such as *Metabolism of xenobiotics by cytochrome P450*, and *Drug metabolism – cytochrome P450*. These pathways are involved in the clearance of endogenous and exogenous organic compounds and were unaffected by feeding KJ or RS to GF rats, confirming DRC induced effects on cytochrome P450 metabolism are mediated by the resident microbiota. Expression of the *Linoleic acid metabolism* and *Retinol metabolism* pathways in the mucosa were also altered by the specific microbiota associated with feeding IN and KJ. Linoleic acid is an essential fatty acid that is unable to be synthesised in animals and retinoids have important roles in a number of processes including nervous system development, epithelial surface maintenance, and immune function (Blomhoff and Blomhoff, 2006). Altered expression of the *Fatty acid metabolism* pathway induced by feeding IN to CR rats further points to the importance of the resident microbial community in regulating host energy balance.

While changes in transcription do not necessarily equate to changes in the proteome or metabolome, alterations in colonic mucosal phenotype were also observed in KJ and IN fed CR rats. Feeding KJ or IN to CR rats resulted in increased colonic goblet cell numbers, and KJ fed CR rats displayed increased colonic crypt lengths. IN and KJ induced alterations in colonic mucosal morphology of CR rats were associated with changes in the expression of diverse metabolic KEGG pathways, including *Tyrosine metabolism*, *Histidine metabolism*, and *Nicotinate and nicotinamide metabolism*. In contrast, mucosal morphology was unchanged in CR rats fed RS, which corresponded with the altered expression of only one metabolic pathway, *Linoleic acid metabolism*. Expression of numerous KEGG pathways were also altered in GF rats by feeding KJ. With the exception of *Histidine metabolism*, the pathways altered in GF rats fed KJ were different to those altered in CR rats fed KJ.

Interestingly, GF rats fed KJ exhibited the highest colonic goblet cell numbers and also showed altered expression of the *O-glycan biosynthesis* pathway. This result provides further support that KJ, a strong gel-forming DRC, may also influence goblet cell proliferation through physical or chemical interactions with the colon mucosa.

Although changes in the transcription of pathways related to cell growth and proliferation were not observed in CR rats fed IN or KJ, the altered transcription of numerous metabolic pathways and increased crypt length in KJ fed CR rats, and goblet cell numbers in KJ and IN fed CR rats, provides further evidence that the resident microbiota plays an important role in the regulation of cell proliferation in the colon. Indeed, the ability of the microbiota to stimulate epithelial growth in the large bowel has been demonstrated in previous studies examining the effects of microbial colonisation in GF rats (Banasaz et al., 2002; Goodlad et al., 1989). However, results from this study also show that the degree of cellular proliferation induced by the microbiota may depend on the particular microbiota composition.

4.8 Perspective on variation observed between rats

The microbiota community is highly diverse between individuals. Factors which contribute to the variation include diet, environmental factors, genetic makeup and health status of the host. However, the relative contributions of these factors to explaining the variation observed between individuals are still unknown. Furthermore, it seems likely that interactions between factors also play a role in defining the microbiota composition. For example, faecal community profiles in humans are more similar in structure between related individuals, regardless of whether they live together or in separate residences (Turnbaugh et al., 2009a). However, the degree of similarity in microbiota composition between monozygotic and dizygotic twins has been shown to be comparable, indicating the importance of factors other than genotype in dictating microbiota structure (Turnbaugh et al., 2009a).

Analysis of 16S rRNA TTGE profiles showed that the variation in microbiota profiles between rats fed the same diets was less than the variation in profiles between rats fed different diets. Because of the strictly controlled environmental variables and dietary regime that is possible when performing animal experiments such as those carried out in this study, it seems likely some of the microbiota variation that was observed between rats fed the same diet can be attributed to host genotype variation as Sprague-Dawley rats are an outbred strain of genetically variable composition. However, variation in the microbiota composition is still apparent with age matched inbred mice housed in controlled environments and fed controlled diets (Mai et al., 2007). This suggests that factors other than age, genotype, health status, and environmental conditions contribute towards microbiota dynamics. It is possible that chance may play a role in shaping the microbiota as colonisation events shortly after birth may shape the microbiota composition later in life.

Although 16S rRNA TTGE profiles in rats fed DRC were shifted towards one that showed less rat to rat variation than rats fed the basal diet, qPCR of excised TTGE bands showed a large variation in 16S rRNA gene copy numbers in DRC fed rats. For example, gene copy numbers corresponding to the *Lactobacillus* TTGE band varied by over 3 orders of magnitude in KJ fed rats. Variation in SCFA concentrations were also observed between rats fed the same diets, which suggests that even though similar bacteria may be present, their metabolic activity may differ. Equally, the variation in colonic SCFA concentrations may reflect a variation in mucosal SCFA uptake in the host.

Physiological differences between rats are a likely source of variation of the host response to DRC. Residual variation in host gene expression unexplained by dietary treatment may be large depending on the gene. Therefore, the innate variation in microbial communities and heterogeneity in host physiology and genotype often necessitates the use of large numbers of biological replicates to ensure sufficient statistical power for measuring *in vivo* responses. This is particularly true in dietary intervention studies when using healthy, non-disease state subjects where responses may be subtle.

Although there is often considerable variation in biological response in animal studies such as those performed in this study, the variation observed in human clinical studies is often far greater as experimental conditions cannot be so tightly controlled. To overcome this, human clinical studies often require large experimental groups that may number in the thousands. Therefore, animal studies have an important role in at least the initial stages of investigations into the biological effects of dietary supplements. However, care must always be taken when extrapolating findings from animal studies and applying them to humans because of the considerable differences in physiology. Furthermore, the diversity in human genetic makeup and environmental situations should also be taken into consideration when considering the findings from highly controlled animal studies as a dietary ingredient may affect different groups of people in different ways.

4.9 Conclusion

Results from this study have revealed some of the complex interactions that occur between DRC, colonic microbiota, and the host. This study has shown for the first time the potential of DRC to engineer the bacterial ecosystem of the colon in weanling rats towards one with an increased fermentative capacity and increased uniformity. The DRC induced changes in the resident microbial community has also been shown to modulate host gene expression responses. The changes in host expression of KEGG pathways associated with different microbiota showed the importance of the colonic microbial community in regulating metabolic processes in weanling rats even in the absence of disease or obesity. The findings from this study provide new insights into these fundamental biological processes, which is important in light of the increasing awareness of disease associated shifts in microbial communities and the interest in modifying the colonic microbiota for improving health.

4.10 Future directions

The global market for functional foods is a multi-billion dollar industry. Sales within the United States alone are estimated at $US 20 billion to 30 billion per year, which represents between 35 and 50 percent of worldwide sales (PricewaterhouseCoopers, 2009). Despite the tremendous market value of the functional foods industry, claims of efficacy are often not supported by the scientific evidence. In particular, it is now recognised that additional studies are required to support many of the health claims attributed to prebiotics and probiotics (Sanders et al., 2005). Indeed, the European Food Safety Authority (EFSA) issued negative opinions on the health claims of 416 products in 2010, including claims for the use of several probiotic products for maintaining digestive health, and β-glucans for maintaining healthy blood glucose levels (EFSA Panel on Dietetic Products, 2010a, b, c). Therefore, studies which investigate the biological mechanisms of action have a crucial role in providing information to enable informed decisions to be made on supplement use.

The marked effects of DRC supplementation that have been shown in early post-weaning life suggests dietary supplementation early in life may have important consequences for health, as exposure to different microbial community compositions at an early age may predispose individuals to a number of conditions such as atopic diseases, obesity and metabolic syndrome. The effect of DRC on the transcription of genes relating to metabolism raise the possibility of developing novel dietary supplements that may be used to address obesity and obesity related diseases. DRC induced alterations in genes that regulate aspects of the immune system may also support the development of dietary products to alleviate symptoms of inflammatory bowel diseases. Apart from the potential for developing novel functional foods with health claims backed by scientific evidence, a more thorough understanding of the effects of food ingredients may have an important role for health education and formulating health recommendations. Average daily dietary fibre intakes are thought to be half the recommended levels in the United States (Anderson et al., 2009), and approximately two thirds in New Zealand (Ministry of Health, 2003; National Health and Medical Research Council,

2005). However, results from this study show that the effects of DRC are dose dependant. Therefore, lower than recommended intakes of DRC may have important consequences for health.

The distinct effects of different types of DRC on the colonic microbiota and host responses that have been identified provide future scope for the development of different dietary supplements that target different parameters of large bowel function. Through the use of a rat model, results from this study have added to the understanding of the complex matrix of interactions between food, resident microbial community, and the host. This study has shown that not all DRC elicits the same response and therefore careful consideration needs to be given to claims in support of various supplement use. Due to the diverse range of DRC examined, findings from this study may also eventually contribute towards the design of mathematical models that are able to predict the effects of novel DRC supplements.

Although this thesis has provided new insights into the effects of DRC, there are several aspects that limit the conclusions that can be drawn from this study. Alterations in the transcriptome may not always result in changes in the proteome or metabolome. Analysis of the metabolite profile in urine or blood using technologies such as liquid chromatography/mass spectrometry or nuclear magnetic resonance spectroscopy may further elucidate the interactions between microbiota and host (Martin et al., 2007; Velagapudi et al., 2010). High-resolution mass spectrometric methods for characterising host or microbiota proteomes may also reveal changes in gene products that cannot be explained by alterations in transcription, such as those resulting from post-translational modifications or alternate splicing of transcripts. Metagenomic analysis of the bacterial genes present in the colon may provide useful information regarding the selection pressures exerted in the large bowel ecosystem by determining which genes are enriched under certain situations (Turnbaugh et al., 2008). There is also scope for identifying specific responses from components of the colon using methods such as laser microdissection to isolate specific groups of cells, such as epithelial cells, goblet cells or lamina

propria lymphocytes. Characterisation of responses in other tissue compartments such as the mesenteric lymph nodes or the metabolite profile of the portal and hepatic system may also help to provide a more complete picture of the effects of feeding DRC. Questions also remain about whether DRC induced changes in the microbiota of young rats persist into later life without requiring further dietary supplementation. However, the decreasing costs associated with high throughput technologies and the advent of new single molecule sequencing platforms provide great potential for extending the knowledge gained in this study.

Appendices

Appendix A. SCFA sample spiking

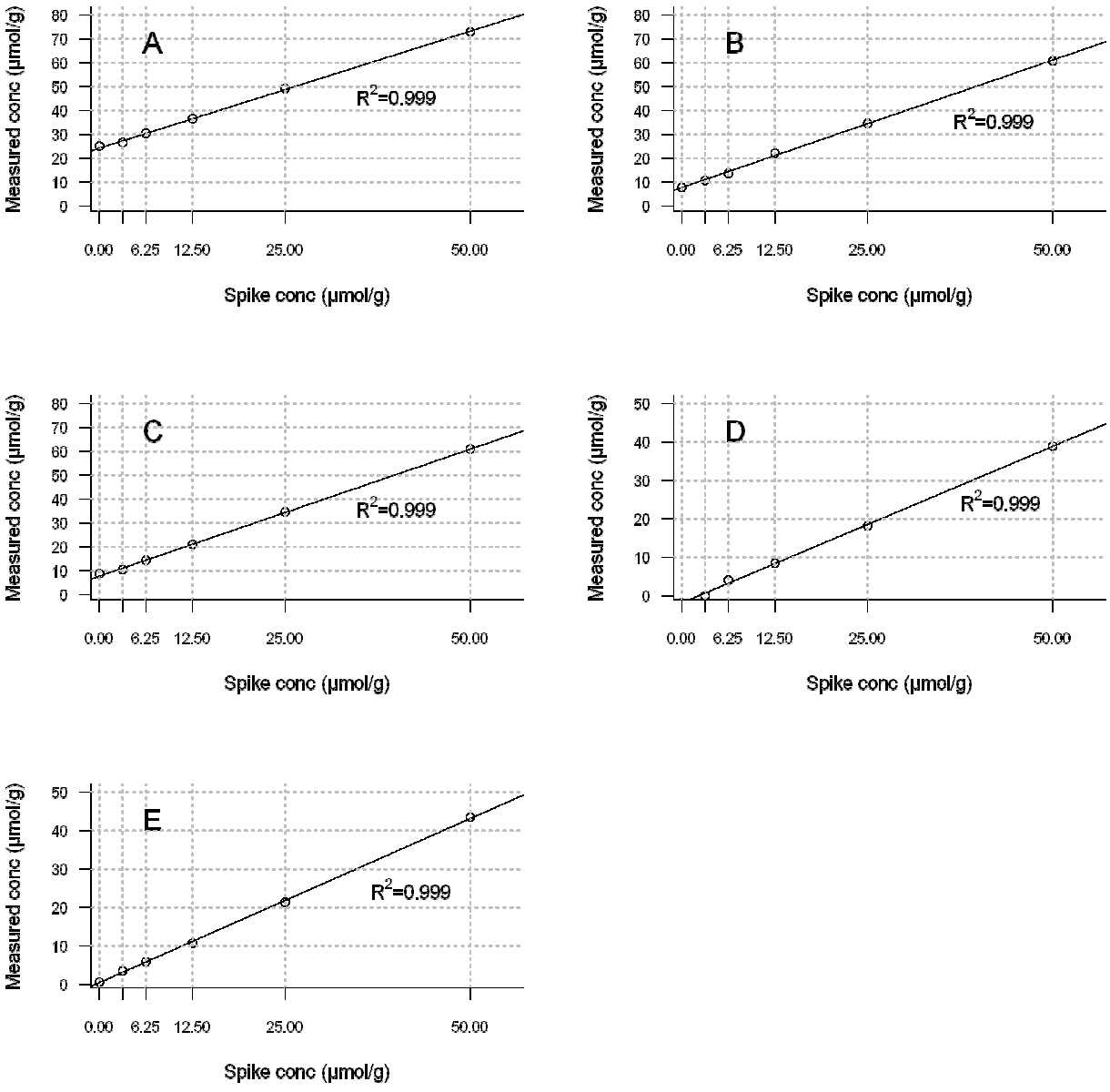

Sample spiking with known concentration of acids for (A) acetic, (B) propionic, (C) butyric, (D) lactic, and (E) succinic acids measured by gas chromatography. Each point indicates mean of 3 replicates. X-axis indicates concentration of each acid added to sample and Y-axis indicates the measured concentration. Line indicates linear regression fit and R^2 indicates goodness-of-fit.

Appendix B. SCFA standard curves

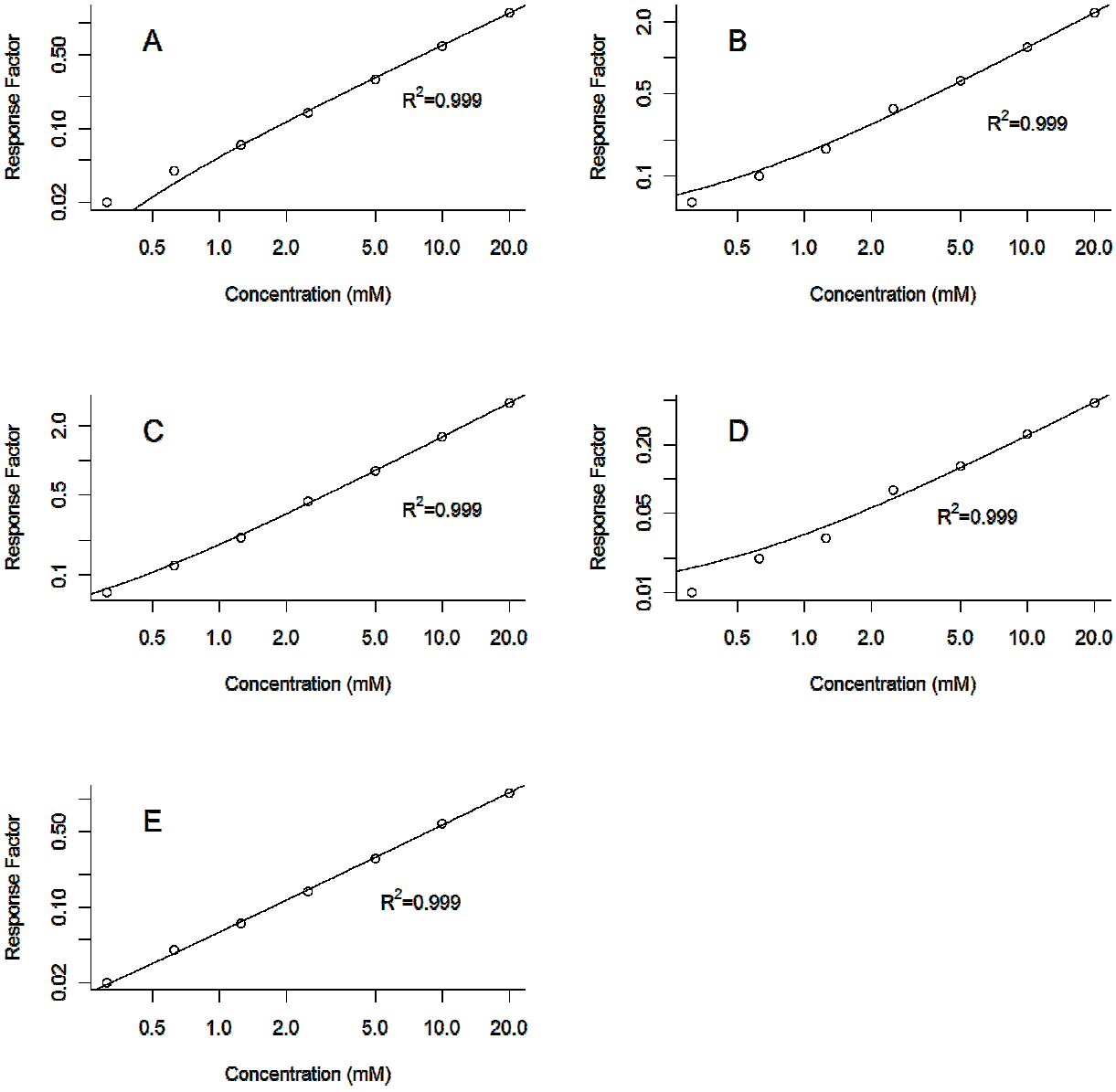

Standard curves for (A) acetic, (B) propionic, (C) butyric, (D) lactic, and (E) succinic acids measured by gas chromatography. Each point indicates mean of 3 replicates. Response factor equals the ratio of the acid peak area divided by the peak area of the internal standard. Line indicates linear regression fit and R^2 indicates goodness-of-fit.

Appendix C. Standard curves for qPCR analysis of TTGE cut bands

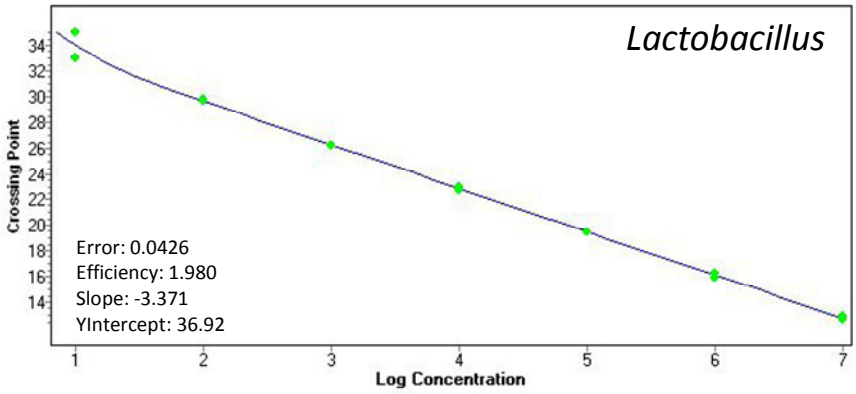

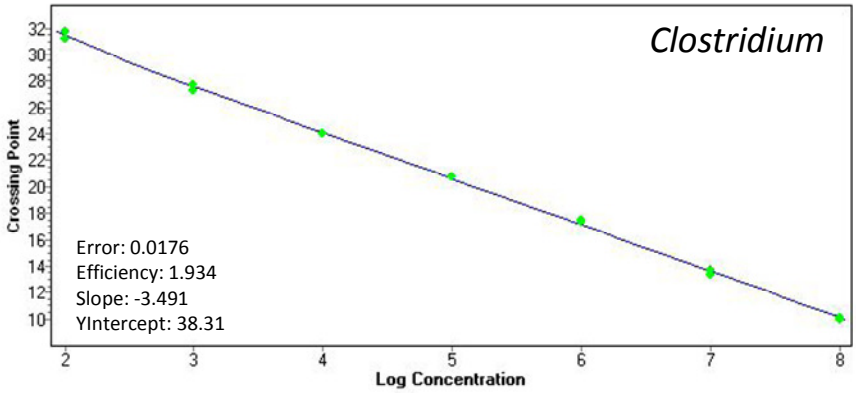

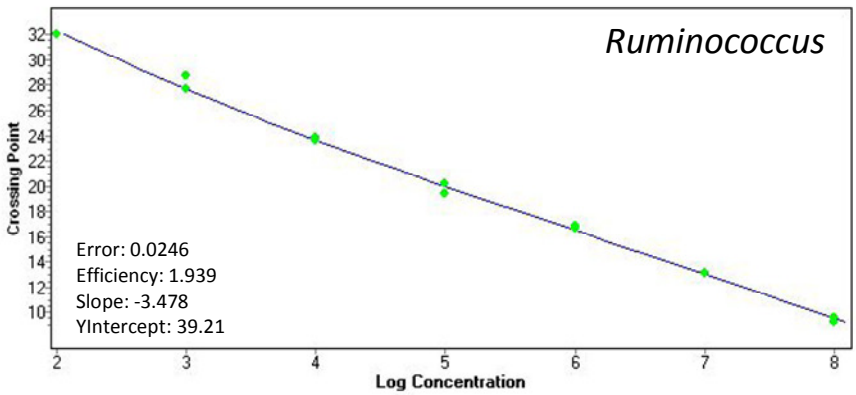

Standard curves for qPCR analysis of TTGE cut band sequences corresponding to the *Lactobacillus*, *Clostridium* and *Ruminococcus* 16S rRNA genes (bands 1, 6, and 4, respectively). Standard curves were generated from serial dilutions of plasmid DNA with inserted 16S rRNA sequence.

Appendix D. Melting curves for qPCR analysis of TTGE cut bands

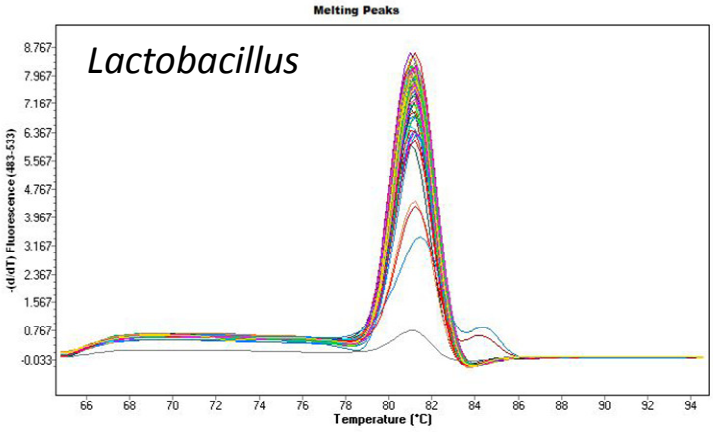

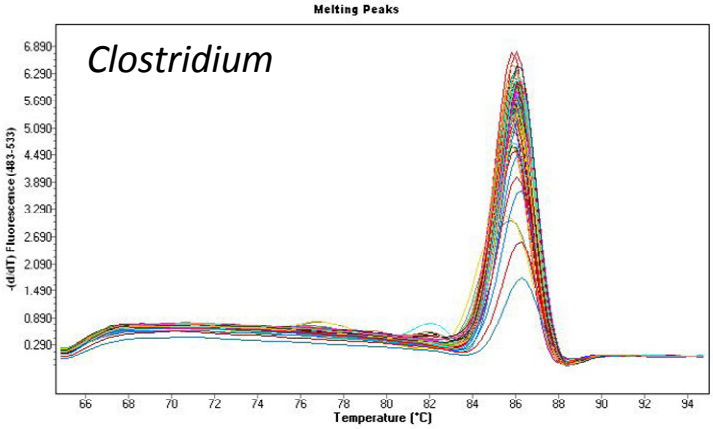

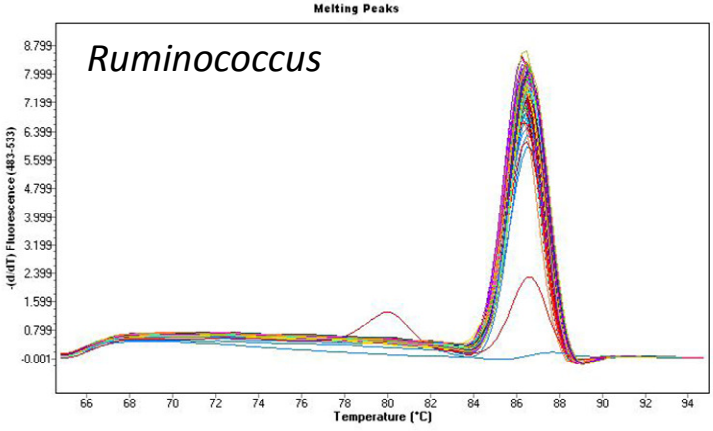

Representative melting curves for qPCR analysis of TTGE cut band sequences corresponding to the *Lactobacillus*, *Clostridium* and *Ruminococcus* 16S rRNA genes (bands 1, 6, and 4, respectively)..

Appendix E. TTGE cut band sequences

Band	Sequence
1	5'-AGGGAATCTTCCACAATGGACGAAAGTCTGATGGAGCAACGCCGCGTGAGTGAAGAAGGTTTTCGGATCGTAAAGCTCTGTTGTTGGTGAAGAAGGATAGAGGTAGTAACTGGCCTTTATTTGACGGTAATCAACCAGAAAGTCACGGCTAACTAC-3'
2	5'-GGGGAATATTGCACAATGGGGGGAACCCTGATGCAGCGACGCCGCGTGAGTGAAGAAGTATTTCGGTATGTAAAGCTCTATCAGCAGGGAAGAAAATGACGGTACCTGACTAAGAAGCCCCGGCTAACTAC-3'
3	5'-AGGAATTTTCGTCAATGGGCGCAAGCCTGAACGARCAATGCCGCGTGAACGARGAAGGKCTTCGGATCGTAAAGTTCTGTTGARAGGGAAAAAGGGTCACCAGARGAAATGCTGGKGAAGTGATATTACCTTTCGAGGAAGTCACGGCTAACTAC-3'
4	5'-GGGGAATATTGCACAATGGGCGGAAGCCTGATGCAGCGATGCCGCGTGAGGGAAGAAGGTTTTCGGATTGTAAACCTCTGTCTTAAGGGACGATAATGACGGTACCTTAGGAGGAAGCTCCGGCTAACTAC-3'
5	5'-GAGGAATATTGGTCAATGGGCGAGAGCCTGAACCAGCCAAGTCGCGTGAGGGAAGACGGCCCTACGGGTTGTAAACCTCTTTTGTCAGGGAGCAAGAACAGGCACGAGTGCCTGACTGAGAGTACCTGAAGAAAAAGCATCGGCTAACTAC-3'
6	5'-GGGGAATATTGCACAATGGGGGAAACCCTGATGCAGCAACGCCGCGTGAGTGATGACGGCCTTCGGGTTGTAAAGCTCTGTCTTCAGGGACGATAATGACGGTACCTGAGGAGGAAGCCACGGCTAACTAC-3'
7	5'-GGGGAATATTGCACAATGGGCGCAAGCCTGATGCAGCGACGCCGCGTGCGGGATGGAGGCCTTCGGGTTGTAAACCGCTTTTGTTCAAGGGCAAGGCACGGTCTTTGGCCGTGTTGAGTGGATTGTTCGAATAAGCACCGGCTAACTAC-3'

Sequences for TTGE bands from feeding study 2. Band numbers indicate band positions as shown in Figure 14.

Appendix F. Boxplots of microarray red and green signal intensities

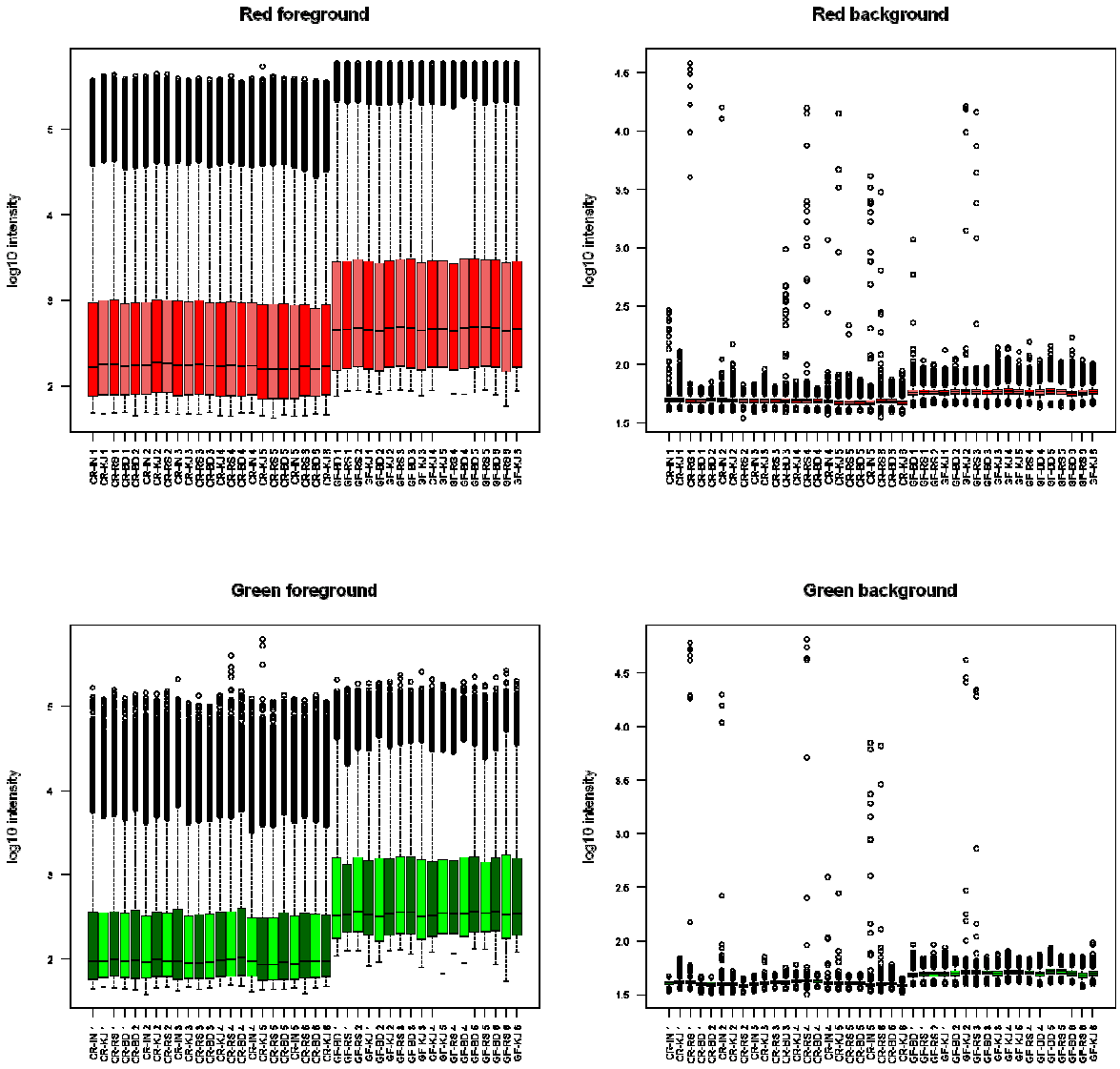

Unprocessed foreground and background red and green signal intensities for each microarray. Boxplots show median, 25th/75th percentile, and 5th/95th percentile for signal intensities. Points indicate outliers.

Appendix G. Boxplots of raw microarray red/green ratios

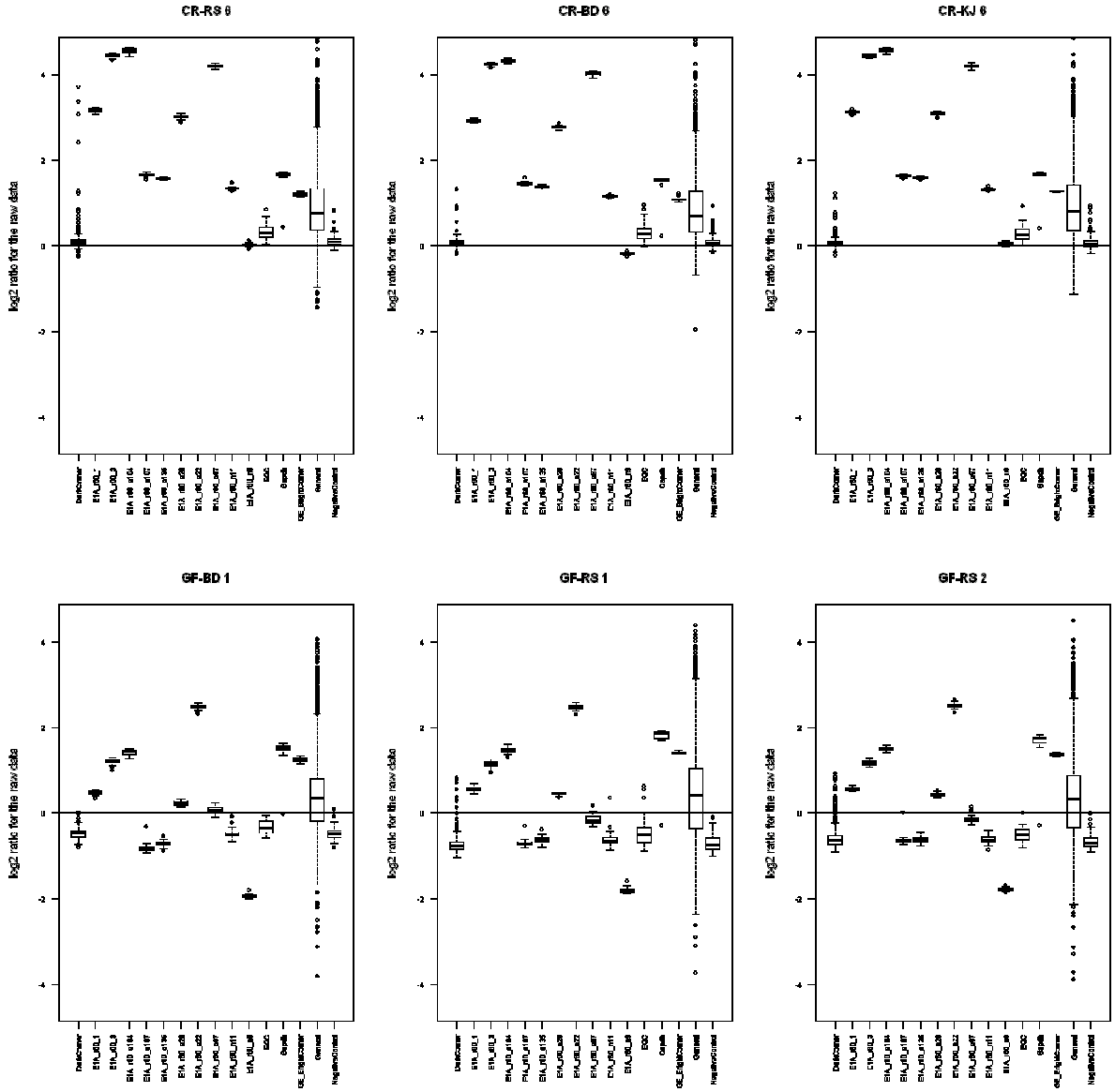

Boxplots of raw red/green signal ratios for control probes and non-control probes in representative arrays. Y-axis indicates $\log_2$(red signal/green signal). *General* indicates all non-control probes in array. Boxplots show median, 25^{th}/75^{th} percentile, and 5^{th}/95^{th} percentile for signal intensities. Points indicate outliers.

Appendix H. Boxplots of loess normalised microarray red/green ratios

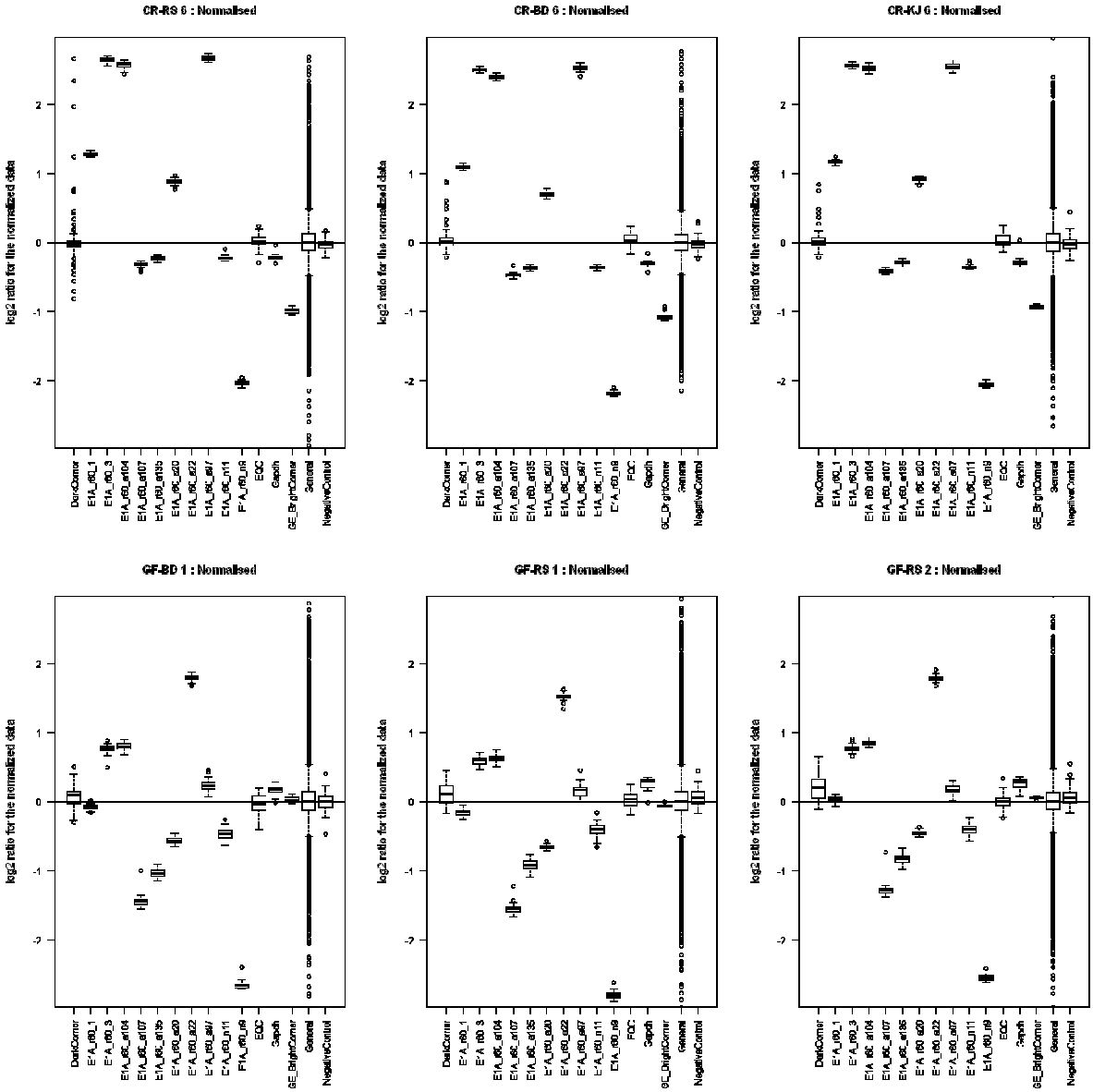

Boxplots of normalised red/green signal ratios for control probes and non-control probes in representative arrays. Y-axis indicates $\log_2$(red signal/green signal). General indicates all non-control probes in array. Boxplots show median, 25^{th}/75^{th} percentile, and 5^{th}/95^{th} percentile for signal intensities. Points indicate outliers.

Appendix I. MA plots of raw microarray red/green ratios

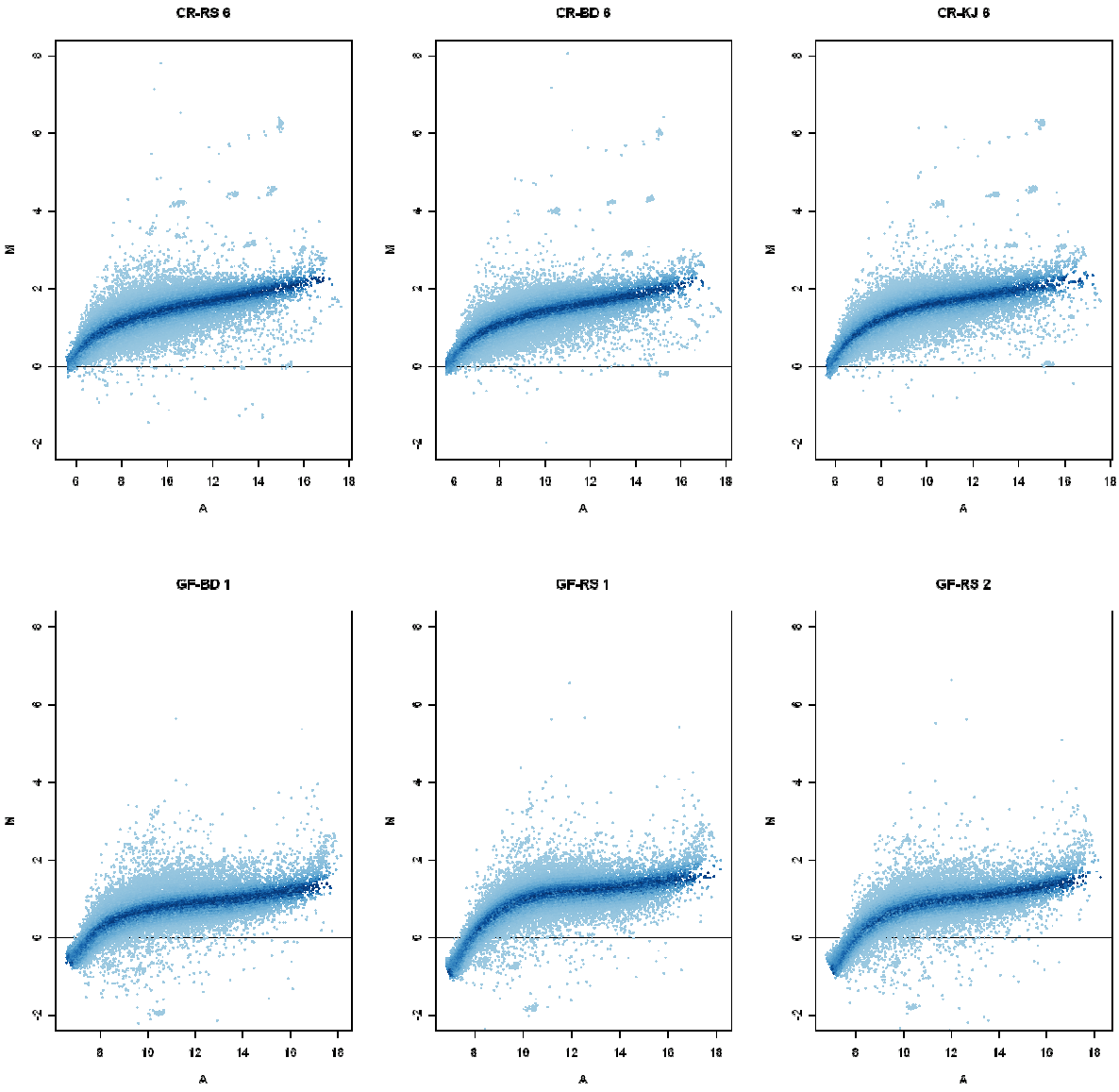

MA plots showing raw red/green signal ratios for each probe in representative arrays. M (Y-axis) indicates $\log_2$(red signal/green signal), A (X-axis) indicates ½($\log_2$R signal + $\log_2$G signal).

Appendix J. MA plots of loess normalised microarray red/green ratios

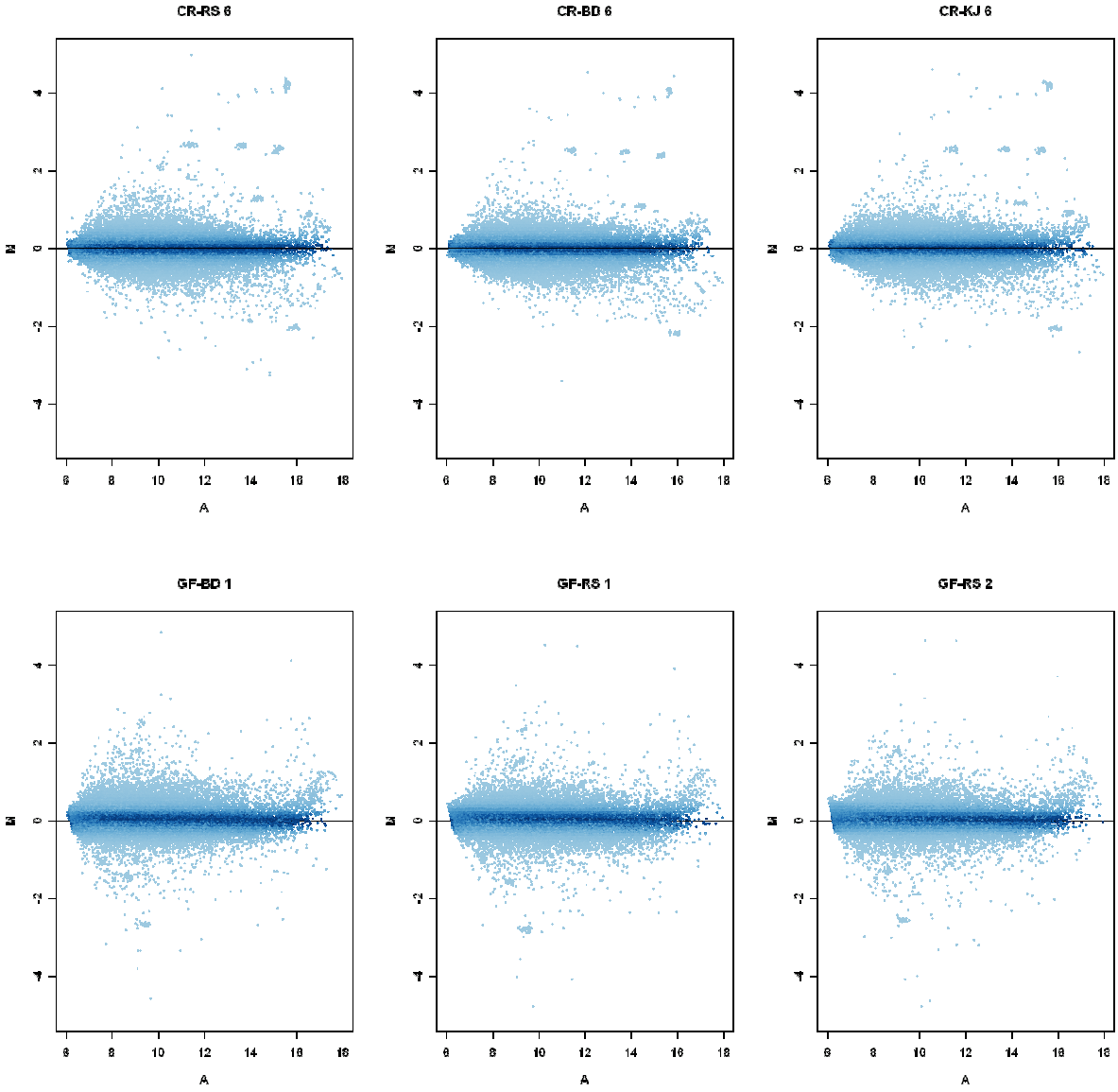

MA plots showing normalised red/green signal ratios for each probe in representative arrays. M (Y-axis) indicates $\log_2$(red signal/green signal), A (X-axis) indicates ½($\log_2$R signal + $\log_2$G signal).

Appendix K. Within-array normalised red and green signal densities

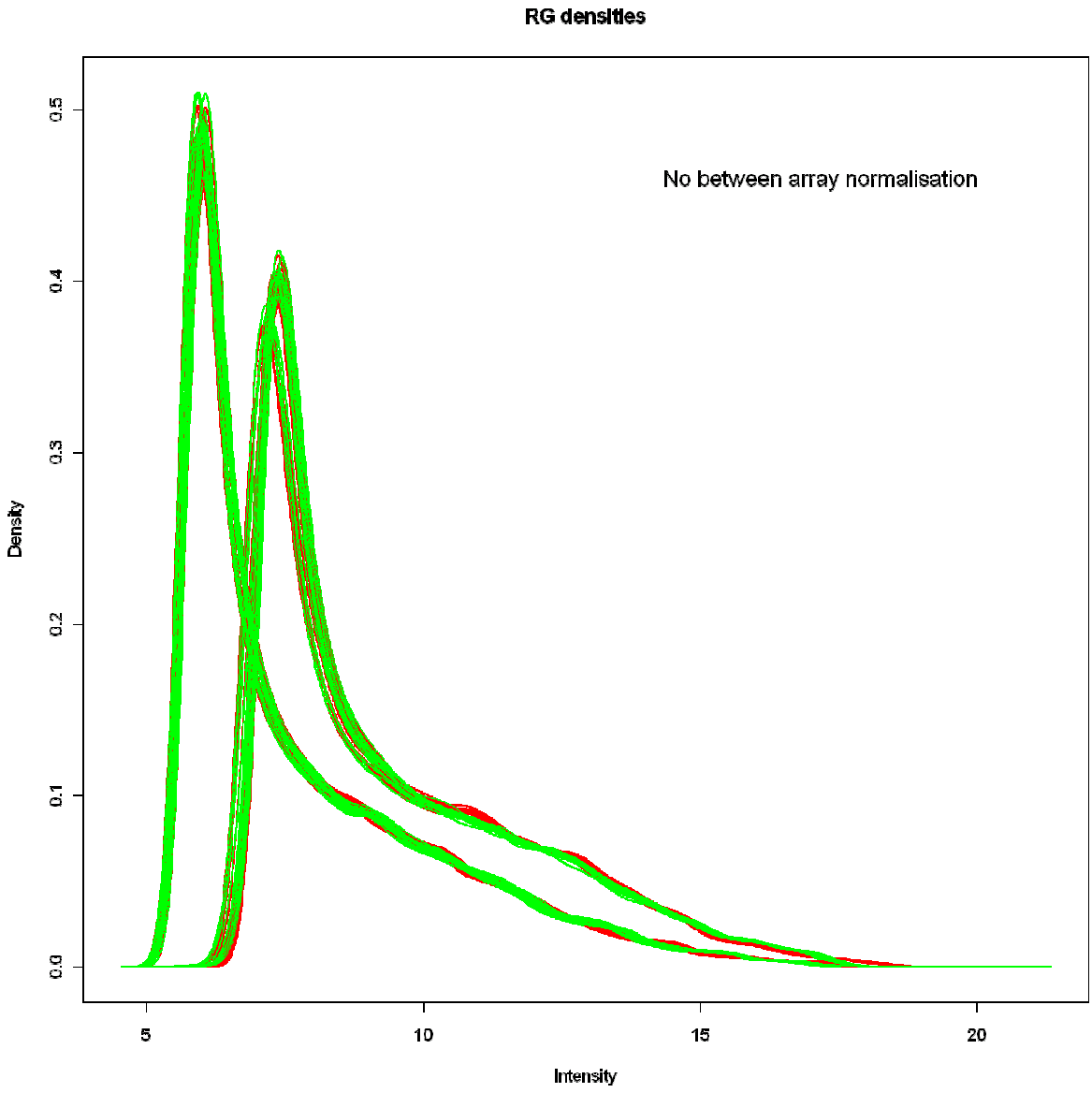

Plot of densities of red and green channel densities of all microarrays following within array loess normalisation. Green line indicates green signal densities and red line indicates red signal densities

Appendix L. Between-array normalised red and green signal densities

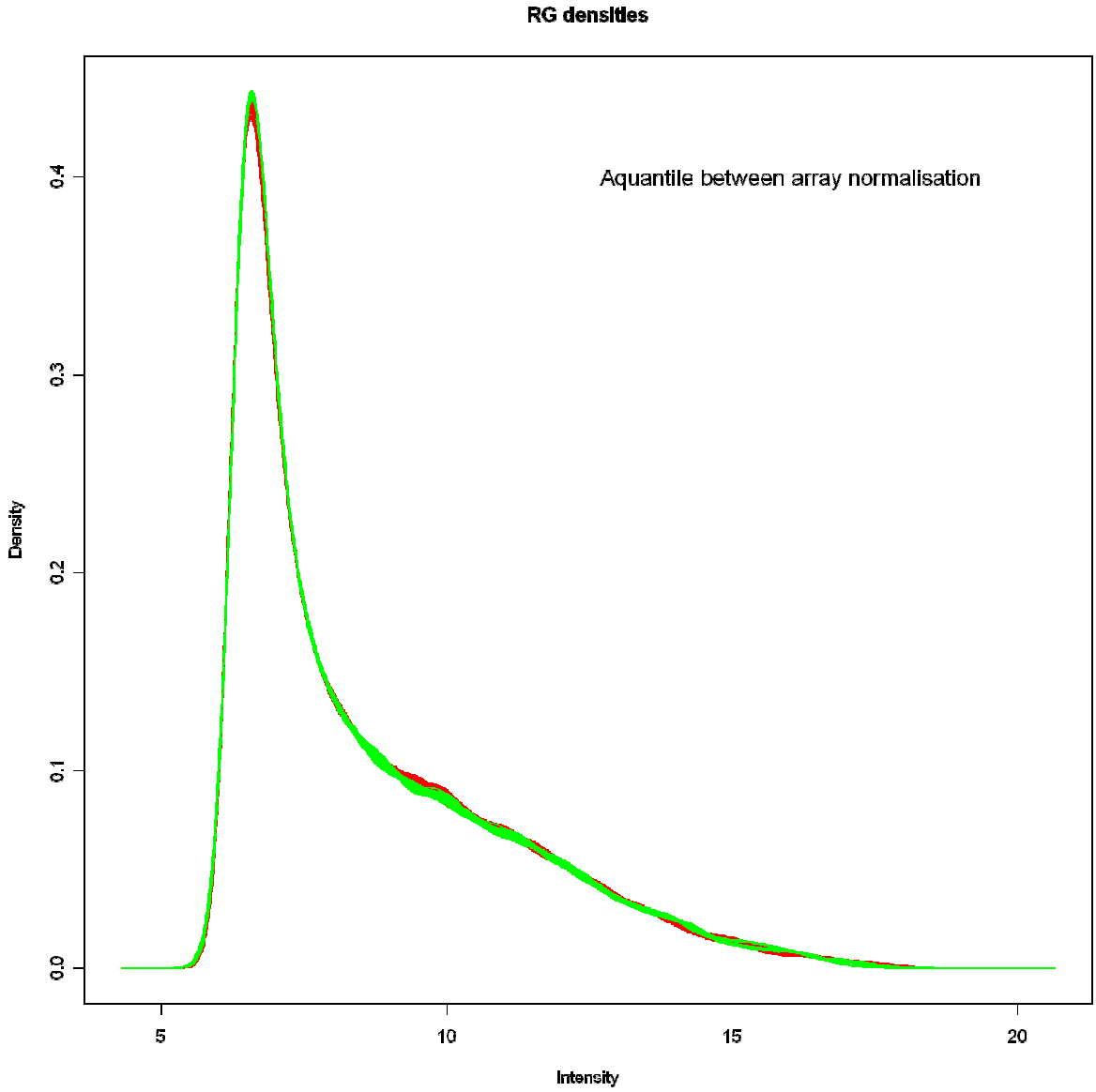

Plot of densities of red and green channel densities of all microarrays following within array loess normalisation and Aquantile between array normalisation. Green line indicates green signal densities and red line indicates red signal densities

References

Abnous, K., Brooks, S.P.J., Kwan, J., Matias, F., Green-Johnson, J., Selinger, L.B., Thomas, M., and Kalmokoff, M. (2009). Diets Enriched in Oat Bran or Wheat Bran Temporally and Differentially Alter the Composition of the Fecal Community of Rats. J Nutr *139*, 2024-2031.

Adlerberth, I., and Wold, A.E. (2009). Establishment of the gut microbiota in Western infants. Acta Paediatr *98*, 229-238.

Al-Lahham, S.H., Roelofsen, H., Priebe, M., Weening, D., Dijkstra, M., Hoek, A., Rezaee, F., Venema, K., and Vonk, R.J. (2010). Regulation of adipokine production in human adipose tissue by propionic acid. Eur J Clin Invest.

Aminov, R.I., Walker, A.W., Duncan, S.H., Harmsen, H.J., Welling, G.W., and Flint, H.J. (2006). Molecular diversity, cultivation, and improved detection by fluorescent in situ hybridization of a dominant group of human gut bacteria related to Roseburia spp. or Eubacterium rectale. Appl Environ Microbiol *72*, 6371-6376.

Anderson, J.W., Baird, P., Davis, R.H., Jr., Ferreri, S., Knudtson, M., Koraym, A., Waters, V., and Williams, C.L. (2009). Health benefits of dietary fiber. Nutr Rev *67*, 188-205.

Ardawi, M.S., and Newsholme, E.A. (1985). Fuel utilization in colonocytes of the rat. Biochem J *231*, 713-719.

Arora, S., and Anubhuti (2006). Role of neuropeptides in appetite regulation and obesity - A review. Neuropeptides *40*, 375-401.

Ashburner, M., Ball, C.A., Blake, J.A., Botstein, D., Butler, H., Cherry, J.M., Davis, A.P., Dolinski, K., Dwight, S.S., Eppig, J.T.*, et al.* (2000). Gene ontology: tool for the unification of biology. The Gene Ontology Consortium. Nat Genet *25*, 25-29.

Backhed, F., Ding, H., Wang, T., Hooper, L.V., Koh, G.Y., Nagy, A., Semenkovich, C.F., and Gordon, J.I. (2004). The gut microbiota as an environmental factor that regulates fat storage. Proceedings of the National Academy of Sciences of the United States of America *101*, 15718-15723.

Backhed, F., Ley, R.E., Sonnenburg, J.L., Peterson, D.A., and Gordon, J.I. (2005). Host-bacterial mutualism in the human intestine. Science (New York, NY *307*, 1915-1920.

Backhed, F., Manchester, J.K., Semenkovich, C.F., and Gordon, J.I. (2007). Mechanisms underlying the resistance to diet-induced obesity in germ-free mice. Proceedings of the National Academy of Sciences of the United States of America *104*, 979-984.

Baek, M.K., Park, J.S., Park, J.H., Kim, M.H., Kim, H.D., Bae, W.K., Chung, I.J., Shin, B.A., and Jung, Y.D. (2010). Lithocholic acid upregulates uPAR and cell invasiveness via MAPK and AP-1 signaling in colon cancer cells. Cancer Lett *290*, 123-128.

Banasaz, M., Norin, E., Holma, R., and Midtvedt, T. (2002). Increased enterocyte production in gnotobiotic rats mono-associated with Lactobacillus rhamnosus GG. Appl Environ Microbiol *68*, 3031-3034.

Barcenilla, A., Pryde, S.E., Martin, J.C., Duncan, S.H., Stewart, C.S., Henderson, C., and Flint, H.J. (2000). Phylogenetic relationships of butyrate-producing bacteria from the human gut. Appl Environ Microbiol *66*, 1654-1661.

Bauer-Marinovic, M., Florian, S., Muller-Schmehl, K., Glatt, H., and Jacobasch, G. (2006). Dietary resistant starch type 3 prevents tumor induction by 1,2-dimethylhydrazine and alters proliferation, apoptosis and dedifferentiation in rat colon. Carcinogenesis *27*, 1849-1859.

Beaslas, O., Cueille, C., Delers, F., Chateau, D., Chambaz, J., Rousset, M., and Carriere, V. (2009). Sensing of dietary lipids by enterocytes: a new role for SR-BI/CLA-1. PLoS One *4*, e4278.

Belenguer, A., Duncan, S.H., Calder, A.G., Holtrop, G., Louis, P., Lobley, G.E., and Flint, H.J. (2006). Two routes of metabolic cross-feeding between Bifidobacterium adolescentis and butyrate-producing anaerobes from the human gut. Appl Environ Microbiol *72*, 3593-3599.

Biasucci, G., Benenati, B., Morelli, L., Bessi, E., and Boehm, G. (2008). Cesarean delivery may affect the early biodiversity of intestinal bacteria. J Nutr *138*, 1796S-1800S.

Bibiloni, R., Mangold, M., Madsen, K.L., Fedorak, R.N., and Tannock, G.W. (2006). The bacteriology of biopsies differs between newly diagnosed, untreated, Crohn's disease and ulcerative colitis patients. Journal of medical microbiology *55*, 1141-1149.

Blomhoff, R., and Blomhoff, H.K. (2006). Overview of retinoid metabolism and function. J Neurobiol *66*, 606-630.

Boekhorst, J., Helmer, Q., Kleerebezem, M., and Siezen, R.J. (2006). Comparative analysis of proteins with a mucus-binding domain found exclusively in lactic acid bacteria. Microbiology (Reading, England) *152*, 273-280.

Bohan, A., Chen, W.S., Denson, L.A., Held, M.A., and Boyer, J.L. (2003). Tumor necrosis factor alpha-dependent up-regulation of Lrh-1 and Mrp3(Abcc3) reduces liver injury in obstructive cholestasis. J Biol Chem *278*, 36688-36698.

Bohannan, B.J., and Hughes, J. (2003). New approaches to analyzing microbial biodiversity data. Curr Opin Microbiol *6*, 282-287.

Boot, R., Koopman, J.P., Kruijt, B.C., Lammers, R.M., Kennis, H.M., Lankhorst, A., Mullink, J.W., Stadhouders, A.M., De Boer, H., Welling, G.W*., et al.* (1985). The 'normalization' of germ-free rabbits with host-specific caecal microflora. Laboratory animals *19*, 344-352.

Bouhnik, Y., Raskine, L., Simoneau, G., Vicaut, E., Neut, C., Flourie, B., Brouns, F., and Bornet, F.R. (2004). The capacity of nondigestible carbohydrates to stimulate fecal bifidobacteria in healthy humans: a double-blind, randomized, placebo-controlled, parallel-group, dose-response relation study. Am J Clin Nutr *80*, 1658-1664.

Bourriaud, C., Robins, R.J., Martin, L., Kozlowski, F., Tenailleau, E., Cherbut, C., and Michel, C. (2005). Lactate is mainly fermented to butyrate by human intestinal microfloras but inter-individual variation is evident. J Appl Microbiol *99*, 201-212.

Bry, L., Falk, P.G., Midtvedt, T., and Gordon, J.I. (1996). A model of host-microbial interactions in an open mammalian ecosystem. Science (New York, NY *273*, 1380-1383.

Burkitt, D.P. (1973). Epidemiology of large bowel disease: the role of fibre. Proc Nutr Soc *32*, 145-149.

Cahill, G.F., Jr. (2006). Fuel metabolism in starvation. Annu Rev Nutr *26*, 1-22.

Calvano, S.E., Xiao, W., Richards, D.R., Felciano, R.M., Baker, H.V., Cho, R.J., Chen, R.O., Brownstein, B.H., Cobb, J.P., Tschoeke, S.K*., et al.* (2005). A network-based analysis of systemic inflammation in humans. Nature *437*, 1032-1037.

Cani, P.D., Lecourt, E., Dewulf, E.M., Sohet, F.M., Pachikian, B.D., Naslain, D., De Backer, F., Neyrinck, A.M., and Delzenne, N.M. (2009). Gut microbiota fermentation of prebiotics increases satietogenic and incretin gut peptide production with consequences for appetite sensation and glucose response after a meal. Am J Clin Nutr *90*, 1236-1243.

Cario, E. (2005). Bacterial interactions with cells of the intestinal mucosa: Toll-like receptors and NOD2. Gut *54*, 1182-1193.

Cario, E., Gerken, G., and Podolsky, D.K. (2004). Toll-like receptor 2 enhances ZO-1-associated intestinal epithelial barrier integrity via protein kinase C. Gastroenterology *127*, 224-238.

Chang, S.Y., Su, P.F., and Lee, T.C. (2009). Ectopic expression of interleukin-1 receptor type II enhances cell migration through activation of the pre-interleukin 1alpha pathway. Cytokine *45*, 32-38.

Charrier, C., Duncan, G.J., Reid, M.D., Rucklidge, G.J., Henderson, D., Young, P., Russell, V.J., Aminov, R.I., Flint, H.J., and Louis, P. (2006). A novel class of CoA-transferase involved in short-chain fatty acid metabolism in butyrate-producing human colonic bacteria. Microbiology (Reading, England) *152*, 179-185.

Chen, H.L., Cheng, H.C., Liu, Y.J., Liu, S.Y., and Wu, W.T. (2006). Konjac acts as a natural laxative by increasing stool bulk and improving colonic ecology in healthy adults. Nutrition.

Chen, H.L., Cheng, H.C., Wu, W.T., Liu, Y.J., and Liu, S.Y. (2008). Supplementation of konjac glucomannan into a low-fiber Chinese diet promoted bowel movement and improved colonic ecology in constipated adults: a placebo-controlled, diet-controlled trial. J Am Coll Nutr *27*, 102-108.

Chen, H.L., Fan, Y.H., Chen, M.E., and Chan, Y. (2005). Unhydrolyzed and hydrolyzed konjac glucomannans modulated cecal and fecal microflora in Balb/c mice. Nutrition *21*, 1059-1064.

Clarridge, J.E., 3rd (2004). Impact of 16S rRNA gene sequence analysis for identification of bacteria on clinical microbiology and infectious diseases. Clin Microbiol Rev *17*, 840-862, table of contents.

Cliffe, L.J., Humphreys, N.E., Lane, T.E., Potten, C.S., Booth, C., and Grencis, R.K. (2005). Accelerated intestinal epithelial cell turnover: a new mechanism of parasite expulsion. Science (New York, NY *308*, 1463-1465.

Coakley, M., Johnson, M.C., McGrath, E., Rahman, S., Ross, R.P., Fitzgerald, G.F., Devery, R., and Stanton, C. (2006). Intestinal bifidobacteria that produce trans-9, trans-11 conjugated linoleic acid: a fatty acid with antiproliferative activity against human colon SW480 and HT-29 cancer cells. Nutr Cancer *56*, 95-102.

Coates, M.E. (1975). Gnotobiotic animals in research: their uses and limitations. Laboratory animals *9*, 275-282.

Conway de Macario, E., and Macario, A.J. (2009). Methanogenic archaea in health and disease: a novel paradigm of microbial pathogenesis. Int J Med Microbiol *299*, 99-108.

Costalos, C., Kapiki, A., Apostolou, M., and Papathoma, E. (2007). The effect of a prebiotic supplemented formula on growth and stool microbiology of term infants. Early Hum Dev.

Costello, E.K., Lauber, C.L., Hamady, M., Fierer, N., Gordon, J.I., and Knight, R. (2009). Bacterial Community Variation in Human Body Habitats Across Space and Time. Science (New York, NY.

Coudray, C., Rambeau, M., Feillet-Coudray, C., Tressol, J.C., Demigne, C., Gueux, E., Mazur, A., and Rayssiguier, Y. (2005). Dietary inulin intake and age can significantly affect intestinal absorption of calcium and magnesium in rats: a stable isotope approach. Nutr J *4*, 29.

Crawford, P.A., Crowley, J.R., Sambandam, N., Muegge, B.D., Costello, E.K., Hamady, M., Knight, R., and Gordon, J.I. (2009). Regulation of myocardial ketone body metabolism by the gut microbiota during nutrient deprivation. Proceedings of the National Academy of Sciences of the United States of America *106*, 11276-11281.

Crosby, L.D., and Criddle, C.S. (2003). Understanding bias in microbial community analysis techniques due to rrn operon copy number heterogeneity. Biotechniques *34*, 790-794, 796, 798 passim.

Culhane, A.C., Thioulouse, J., Perriere, G., and Higgins, D.G. (2005). MADE4: an R package for multivariate analysis of gene expression data. Bioinformatics *21*, 2789-2790.

Cummings, J.H., and Macfarlane, G.T. (1997). Role of intestinal bacteria in nutrient metabolism. JPEN J Parenter Enteral Nutr *21*, 357-365.

Cummings, J.H., Pomare, E.W., Branch, W.J., Naylor, C.P., and Macfarlane, G.T. (1987). Short chain fatty acids in human large intestine, portal, hepatic and venous blood. Gut *28*, 1221-1227.

De Filippo, C., Cavalieri, D., Di Paola, M., Ramazzotti, M., Poullet, J.B., Massart, S., Collini, S., Pieraccini, G., and Lionetti, P. (2010). Impact of diet in shaping gut microbiota revealed by a comparative study in children from Europe and rural Africa. Proceedings of the National Academy of Sciences of the United States of America.

de Vries, W., and Stouthamer, A.H. (1967). Pathway of glucose fermentation in relation to the taxonomy of bifidobacteria. J Bacteriol *93*, 574-576.

Dicksved, J., Halfvarson, J., Rosenquist, M., Jarnerot, G., Tysk, C., Apajalahti, J., Engstrand, L., and Jansson, J.K. (2008). Molecular analysis of the gut microbiota of identical twins with Crohn's disease. ISME J *2*, 716-727.

Drzikova, B., Dongowski, G., and Gebhardt, E. (2005). Dietary fibre-rich oat-based products affect serum lipids, microbiota, formation of short-chain fatty acids and steroids in rats. The British journal of nutrition *94*, 1012-1025.

Duncan, S.H., Belenguer, A., Holtrop, G., Johnstone, A.M., Flint, H.J., and Lobley, G.E. (2007a). Reduced dietary intake of carbohydrates by obese subjects results in decreased concentrations of butyrate and butyrate-producing bacteria in feces. Appl Environ Microbiol *73*, 1073-1078.

Duncan, S.H., Holtrop, G., Lobley, G.E., Calder, A.G., Stewart, C.S., and Flint, H.J. (2004a). Contribution of acetate to butyrate formation by human faecal bacteria. The British journal of nutrition *91*, 915-923.

Duncan, S.H., Lobley, G.E., Holtrop, G., Ince, J., Johnstone, A.M., Louis, P., and Flint, H.J. (2008). Human colonic microbiota associated with diet, obesity and weight loss. Int J Obes (Lond) *32*, 1720-1724.

Duncan, S.H., Louis, P., and Flint, H.J. (2004b). Lactate-utilizing bacteria, isolated from human feces, that produce butyrate as a major fermentation product. Appl Environ Microbiol *70*, 5810-5817.

Duncan, S.H., Louis, P., and Flint, H.J. (2007b). Cultivable bacterial diversity from the human colon. Lett Appl Microbiol *44*, 343-350.

Eckburg, P.B., Bik, E.M., Bernstein, C.N., Purdom, E., Dethlefsen, L., Sargent, M., Gill, S.R., Nelson, K.E., and Relman, D.A. (2005). Diversity of the human intestinal microbial flora. Science (New York, NY *308*, 1635-1638.

EFSA Panel on Dietetic Products, N.a.A.N. (2010a). Scientific Opinion on the substantiation of health claims related to beta-glucans and maintenance or achievement of normal blood glucose concentrations (ID 756, 802, 2935) pursuant to Article 13(1) of Regulation (EC) No 1924/2006. EFSA Journal *8*.

EFSA Panel on Dietetic Products, N.a.A.N. (2010b). Scientific Opinion on the substantiation of health claims related to Lactobacillus plantarum 299v (DSM 9843) and “immune system” (ID 1081), pursuant to Article 13(1) of Regulation (EC) No 1924/2006. EFSA Journal *8*, 1488.

EFSA Panel on Dietetic Products, N.a.A.N. (2010c). Scientific Opinion on the substantiation of health claims related to Lactobacillus rhamnosus LB21 NCIMB 40564 and decreasing potentially pathogenic intestinal microorganisms (ID 1064), digestive health (ID 1064), and reduction of mutans streptococci in the oral cavity (ID 1064) pursuant to Article 13(1) of Regulation (EC) No 1924/2006. EFSA Journal *8*, 1487.

Englyst, K.N., Liu, S., and Englyst, H.N. (2007). Nutritional characterization and measurement of dietary carbohydrates. Eur J Clin Nutr *61 Suppl 1*, S19-39.

Falcon, S., and Gentleman, R. (2007). Using GOstats to test gene lists for GO term association. Bioinformatics *23*, 257-258.

Falony, G., Verschaeren, A., De Bruycker, F., De Preter, V., Verbeke, K., Leroy, F., and De Vuyst, L. (2009). In vitro kinetics of prebiotic inulin-type fructan fermentation by butyrate-producing colon bacteria: implementation of online gas chromatography for quantitative analysis of carbon dioxide and hydrogen gas production. Appl Environ Microbiol *75*, 5884-5892.

Falony, G., Vlachou, A., Verbrugghe, K., and De Vuyst, L. (2006). Cross-feeding between Bifidobacterium longum BB536 and acetate-converting, butyrate-producing colon bacteria during growth on oligofructose. Appl Environ Microbiol *72*, 7835-7841.

Farage Hashmi, A.-G., Sheila, K., Richard Frank, T., and John, P. (2007). The potential use of hydrolysed konjac glucomannan as a prebiotic. Journal of the Science of Food and Agriculture *87*, 1758-1766.

Favier, C.F., Vaughan, E.E., De Vos, W.M., and Akkermans, A.D. (2002). Molecular monitoring of succession of bacterial communities in human neonates. Appl Environ Microbiol *68*, 219-226.

Fernandez-Riejos, P., Najib, S., Santos-Alvarez, J., Martin-Romero, C., Perez-Perez, A., Gonzalez-Yanes, C., and Sanchez-Margalet, V. (2010). Role of leptin in the activation of immune cells. Mediators Inflamm *2010*, 568343.

Fontaine, N., Meslin, J.C., Lory, S., and Andrieux, C. (1996). Intestinal mucin distribution in the germ-free rat and in the heteroxenic rat harbouring a human bacterial flora: effect of inulin in the diet. British Journal of Nutrition *75*, 881-892.

Fujita, H., Katoh, H., Hasegawa, H., Yasui, H., Aoki, J., Yamaguchi, Y., and Negishi, M. (2000). Molecular decipherment of Rho effector pathways regulating tight-junction permeability. Biochem J *346*, 617-622.

Fukata, M., Michelsen, K.S., Eri, R., Thomas, L.S., Hu, B., Lukasek, K., Nast, C.C., Lechago, J., Xu, R., Naiki, Y.*, et al.* (2005). Toll-like receptor-4 is required for intestinal response to epithelial injury and limiting bacterial translocation in a murine model of acute colitis. Am J Physiol Gastrointest Liver Physiol *288*, G1055-1065.

Fuller, R. (1989). Probiotics in man and animals. J Appl Bacteriol *66*, 365-378.

Furrie, E., Macfarlane, S., Thomson, G., and Macfarlane, G.T. (2005). Toll-like receptors-2, -3 and -4 expression patterns on human colon and their regulation by mucosal-associated bacteria. Immunology *115*, 565-574.

Fusunyan, R.D., Nanthakumar, N.N., Baldeon, M.E., and Walker, W.A. (2001). Evidence for an innate immune response in the immature human intestine: toll-like receptors on fetal enterocytes. Pediatr Res *49*, 589-593.

Geibel, J.P. (2005). Secretion and absorption by colonic crypts. Annu Rev Physiol *67*, 471-490.

Gentleman, R.C., Carey, V.J., Bates, D.M., Bolstad, B., Dettling, M., Dudoit, S., Ellis, B., Gautier, L., Ge, Y., Gentry, J.*, et al.* (2004). Bioconductor: open software development for computational biology and bioinformatics. Genome Biol *5*, R80.

Gewirtz, A.T., Navas, T.A., Lyons, S., Godowski, P.J., and Madara, J.L. (2001). Cutting edge: bacterial flagellin activates basolaterally expressed TLR5 to induce epithelial proinflammatory gene expression. J Immunol *167*, 1882-1885.

Gibson, G.R., and Roberfroid, M.B. (1995). Dietary modulation of the human colonic microbiota: introducing the concept of prebiotics. J Nutr *125*, 1401-1412.

Goh, Y.J., Lee, J.H., and Hutkins, R.W. (2007). Functional analysis of the fructooligosaccharide utilization operon in Lactobacillus paracasei 1195. Appl Environ Microbiol *73*, 5716-5724.

Goni, I., Gudiel-Urbano, M., Bravo, L., and Saura-Calixto, F. (2001). Dietary modulation of bacterial fermentative capacity by edible seaweeds in rats. J Agric Food Chem *49*, 2663-2668.

Goodlad, R.A., and Englyst, H.N. (2001). Redefining dietary fibre: potentially a recipe for disaster. Lancet *358*, 1833-1834.

Goodlad, R.A., Ratcliffe, B., Fordham, J.P., and Wright, N.A. (1989). Does dietary fibre stimulate intestinal epithelial cell proliferation in germ free rats? Gut *30*, 820-825.

Gray, J. (2006). Dietary Fibre: Definition, Analysis, Physiology & Health. ILSI Europe Concise Monograph Series, 1-38.

Hastie, T., Tibshirani, R., Narasimhan, B., and Chu, G. (2010). pamr: Pam: prediction analysis for microarrays. R package version 1460.

Hayashi, H., Sakamoto, M., Kitahara, M., and Benno, Y. (2006). Diversity of the Clostridium coccoides group in human fecal microbiota as determined by 16S rRNA gene library. FEMS Microbiol Lett *257*, 202-207.

Hayashi, H., Takahashi, R., Nishi, T., Sakamoto, M., and Benno, Y. (2005). Molecular analysis of jejunal, ileal, caecal and recto-sigmoidal human colonic microbiota using 16S rRNA gene libraries and terminal restriction fragment length polymorphism. Journal of medical microbiology *54*, 1093-1101.

Hehemann, J.-H., Correc, G., Barbeyron, T., Helbert, W., Czjzek, M., and Michel, G. (2010). Transfer of carbohydrate-active enzymes from marine bacteria to Japanese gut microbiota. Nature *464*, 908-912.

Heuman, D.M. (1989). Quantitative estimation of the hydrophilic-hydrophobic balance of mixed bile salt solutions. J Lipid Res *30*, 719-730.

Hildebrandt, M.A., Hoffmann, C., Sherrill-Mix, S.A., Keilbaugh, S.A., Hamady, M., Chen, Y.Y., Knight, R., Ahima, R.S., Bushman, F., and Wu, G.D. (2009). High-fat diet determines the composition of the murine gut microbiome independently of obesity. Gastroenterology *137*, 1716-1724 e1711-1712.

Hirokawa, M., Miura, S., Shigematsu, T., Yoshida, H., Hokari, R., Higuchi, H., Kurose, I., Kimura, H., Saito, H., Nakaki, T.*, et al.* (1997). Pressure stimulates proliferation and DNA synthesis in rat intestinal epithelial cells. Life Sci *61*, 667-672.

Hoentjen, F., Welling, G.W., Harmsen, H.J., Zhang, X., Snart, J., Tannock, G.W., Lien, K., Churchill, T.A., Lupicki, M., and Dieleman, L.A. (2005). Reduction of colitis by prebiotics in HLA-B27 transgenic rats is associated with microflora changes and immunomodulation. Inflamm Bowel Dis *11*, 977-985.

Hoff, K.J. (2009). The effect of sequencing errors on metagenomic gene prediction. BMC Genomics *10*, 520.

Hojsak, I., Abdovic, S., Szajewska, H., Milosevic, M., Krznaric, Z., and Kolacek, S. (2010). Lactobacillus GG in the prevention of nosocomial gastrointestinal and respiratory tract infections. Pediatrics *125*, e1171-1177.

Hold, G.L., Schwiertz, A., Aminov, R.I., Blaut, M., and Flint, H.J. (2003). Oligonucleotide probes that detect quantitatively significant groups of butyrate-producing bacteria in human feces. Appl Environ Microbiol *69*, 4320-4324.

Hooper, L.V. (2004). Bacterial contributions to mammalian gut development. Trends Microbiol *12*, 129-134.

Hooper, L.V., and Gordon, J.I. (2001). Commensal host-bacterial relationships in the gut. Science (New York, NY *292*, 1115-1118.

Hooper, L.V., and Macpherson, A.J. (2010). Immune adaptations that maintain homeostasis with the intestinal microbiota. Nat Rev Immunol *10*, 159-169.

Hooper, L.V., Stappenbeck, T.S., Hong, C.V., and Gordon, J.I. (2003). Angiogenins: a new class of microbicidal proteins involved in innate immunity. Nat Immunol *4*, 269-273.

Hopkins, M.J., and Macfarlane, G.T. (2002). Changes in predominant bacterial populations in human faeces with age and with Clostridium difficile infection. Journal of medical microbiology *51*, 448-454.

Hornef, M.W., Normark, B.H., Vandewalle, A., and Normark, S. (2003). Intracellular recognition of lipopolysaccharide by toll-like receptor 4 in intestinal epithelial cells. J Exp Med *198*, 1225-1235.

Hove, E.L., and King, S. (1979). Effects of pectin and cellulose on growth, feed efficiency, and protein utilization, and their contribution to energy requirement and cecal VFA in rats. J Nutr *109*, 1274-1278.

Humblot, C., Bruneau, A., Sutren, M., Lhoste, E.F., Dore, J., Andrieux, C., and Rabot, S. (2005). Brussels sprouts, inulin and fermented milk alter the faecal microbiota of human microbiota-associated rats as shown by PCR-temporal temperature gradient gel electrophoresis using universal, Lactobacillus and Bifidobacterium 16S rRNA gene primers. The British journal of nutrition *93*, 677-684.

Inoue, M. (1942). Studies on enteric bacteria associated with digestion of konnyaku mannan. Eiyogaku Zasshi *2, suppl.*, 9-18.

International Consultative Group on Food Irradiation (1999). Facts about food irradiation, F.a.A.O.o.t.U.N. (FAO), W.H.O. (WHO), and I.A.E.A. (IAEA), eds. (Vienna, Austria).

Isken, F., Klaus, S., Osterhoff, M., Pfeiffer, A.F., and Weickert, M.O. (2010). Effects of long-term soluble vs. insoluble dietary fiber intake on high-fat diet-induced obesity in C57BL/6J mice. J Nutr Biochem *21*, 278-284.

Ito, H., Satsukawa, M., Arai, E., Sugiyama, K., Sonoyama, K., Kiriyama, S., and Morita, T. (2009). Soluble fiber viscosity affects both goblet cell number and small intestine mucin secretion in rats. J Nutr *139*, 1640-1647.

Jacobs, L.R., and Lupton, J.R. (1984). Effect of dietary fibers on rat large bowel mucosal growth and cell proliferation. Am J Physiol *246*, G378-385.

Jenkins, D.J., Vuksan, V., Kendall, C.W., Wursch, P., Jeffcoat, R., Waring, S., Mehling, C.C., Vidgen, E., Augustin, L.S., and Wong, E. (1998). Physiological effects of resistant starches on fecal bulk, short chain fatty acids, blood lipids and glycemic index. J Am Coll Nutr *17*, 609-616.

Jensen, M.T., Cox, R.P., and Jensen, B.B. (1995). Microbial production of skatole in the hind gut of pigs given different diets and its relation to skatole deposition in backfat. Animal Science *61*, 293-304.

Jiang, Z., and Gentleman, R. (2007). Extensions to gene set enrichment. Bioinformatics *23*, 306-313.

Jiménez-Escrig, A., and Sánchez-Muniz, F.J. (2000). Dietary fibre from edible seaweeds: Chemical structure, physicochemical properties and effects on cholesterol metabolism. Nutrition Research *20*, 585-598.

Johansson, M.E., Phillipson, M., Petersson, J., Velcich, A., Holm, L., and Hansson, G.C. (2008). The inner of the two Muc2 mucin-dependent mucus layers in colon is devoid of bacteria. Proceedings of the National Academy of Sciences of the United States of America *105*, 15064-15069.

Johnson, P.L., and Slatkin, M. (2008). Accounting for bias from sequencing error in population genetic estimates. Mol Biol Evol *25*, 199-206.

Jones, B.V., Begley, M., Hill, C., Gahan, C.G., and Marchesi, J.R. (2008). Functional and comparative metagenomic analysis of bile salt hydrolase activity in the human gut microbiome. Proceedings of the National Academy of Sciences of the United States of America *105*, 13580-13585.

Jones, D.C., Manning, B.M., and Daynes, R.A. (2002). A role for the peroxisome proliferator-activated receptor alpha in T-cell physiology and ageing immunobiology. Proc Nutr Soc *61*, 363-369.

Jung, D., Fried, M., and Kullak-Ublick, G.A. (2002). Human apical sodium-dependent bile salt transporter gene (SLC10A2) is regulated by the peroxisome proliferator-activated receptor alpha. J Biol Chem *277*, 30559-30566.

Kalliomaki, M., Collado, M.C., Salminen, S., and Isolauri, E. (2008). Early differences in fecal microbiota composition in children may predict overweight. Am J Clin Nutr *87*, 534-538.

Kanehisa, M., and Goto, S. (2000). KEGG: kyoto encyclopedia of genes and genomes. Nucleic Acids Res *28*, 27-30.

Kaplan, H., and Hutkins, R.W. (2000). Fermentation of fructooligosaccharides by lactic acid bacteria and bifidobacteria. Appl Environ Microbiol *66*, 2682-2684.

Karagiannides, I., Torres, D., Tseng, Y.H., Bowe, C., Carvalho, E., Espinoza, D., Pothoulakis, C., and Kokkotou, E. (2008). Substance P as a novel anti-obesity target. Gastroenterology *134*, 747-755.

Karaki, S.I., Mitsui, R., Hayashi, H., Kato, I., Sugiya, H., Iwanaga, T., Furness, J.B., and Kuwahara, A. (2006). Short-chain fatty acid receptor, GPR43, is expressed by enteroendocrine cells and mucosal mast cells in rat intestine. Cell Tissue Res, 1-8.

Katsuraya, K., Okuyama, K., Hatanaka, K., Oshima, R., Sato, T., and Matsuzaki, K. (2003). Constitution of konjac glucomannan: chemical analysis and 13C NMR spectroscopy. Carbohydrate Polymers *53*, 183-189.

Kelly, D., Campbell, J.I., King, T.P., Grant, G., Jansson, E.A., Coutts, A.G., Pettersson, S., and Conway, S. (2004). Commensal anaerobic gut bacteria attenuate inflammation by regulating nuclear-cytoplasmic shuttling of PPAR-gamma and RelA. Nat Immunol *5*, 104-112.

Kelsall, B.L., and Rescigno, M. (2004). Mucosal dendritic cells in immunity and inflammation. Nat Immunol *5*, 1091-1095.

Kim, J.G., Lee, S.J., and Kagnoff, M.F. (2004). Nod1 is an essential signal transducer in intestinal epithelial cells infected with bacteria that avoid recognition by toll-like receptors. Infect Immun *72*, 1487-1495.

Kim, S.C., Stice, J.P., Chen, L., Jung, J.S., Gupta, S., Wang, Y., Baumgarten, G., Trial, J., and Knowlton, A.A. (2009). Extracellular heat shock protein 60, cardiac myocytes, and apoptosis. Circ Res *105*, 1186-1195.

Klappenbach, J.A., Dunbar, J.M., and Schmidt, T.M. (2000). rRNA operon copy number reflects ecological strategies of bacteria. Appl Environ Microbiol *66*, 1328-1333.

Kleerebezem, M., and Vaughan, E.E. (2009). Probiotic and gut lactobacilli and bifidobacteria: molecular approaches to study diversity and activity. Annu Rev Microbiol *63*, 269-290.

Kleessen, B., Hartmann, L., and Blaut, M. (2001). Oligofructose and long-chain inulin: influence on the gut microbial ecology of rats associated with a human faecal flora. The British journal of nutrition *86*, 291-300.

Kleessen, B., Hartmann, L., and Blaut, M. (2003). Fructans in the diet cause alterations of intestinal mucosal architecture, released mucins and mucosa-associated bifidobacteria in gnotobiotic rats. The British journal of nutrition *89*, 597-606.

Kobayashi, K.S., Chamaillard, M., Ogura, Y., Henegariu, O., Inohara, N., Nunez, G., and Flavell, R.A. (2005). Nod2-dependent regulation of innate and adaptive immunity in the intestinal tract. Science (New York, NY *307*, 731-734.

Koh, J.M., Lee, Y.S., Kim, Y.S., Park, S.H., Lee, S.H., Kim, H.H., Lee, M.S., Lee, K.U., and Kim, G.S. (2009). Heat shock protein 60 causes osteoclastic bone resorption via toll-like receptor-2 in estrogen deficiency. Bone *45*, 650-660.

Koon, H.W., and Pothoulakis, C. (2006). Immunomodulatory properties of substance P: the gastrointestinal system as a model. Annals of the New York Academy of Sciences *1088*, 23-40.

Koon, H.W., Zhao, D., Zhan, Y., Moyer, M.P., and Pothoulakis, C. (2007). Substance P mediates antiapoptotic responses in human colonocytes by Akt activation. Proceedings of the National Academy of Sciences of the United States of America *104*, 2013-2018.

Koropatkin, N., Martens, E.C., Gordon, J.I., and Smith, T.J. (2009). Structure of a SusD homologue, BT1043, involved in mucin O-glycan utilization in a prominent human gut symbiont. Biochemistry *48*, 1532-1542.

Krinos, C.M., Coyne, M.J., Weinacht, K.G., Tzianabos, A.O., Kasper, D.L., and Comstock, L.E. (2001). Extensive surface diversity of a commensal microorganism by multiple DNA inversions. Nature *414*, 555-558.

Kripke, S.A., Fox, A.D., Berman, J.M., Settle, R.G., and Rombeau, J.L. (1989). Stimulation of intestinal mucosal growth with intracolonic infusion of short-chain fatty acids. JPEN J Parenter Enteral Nutr *13*, 109-116.

Lay, C., Sutren, M., Rochet, V., Saunier, K., Dore, J., and Rigottier-Gois, L. (2005). Design and validation of 16S rRNA probes to enumerate members of the Clostridium leptum subgroup in human faecal microbiota. Environ Microbiol *7*, 933-946.

Le Blay, G.M., Michel, C.D., Blottiere, H.M., and Cherbut, C.J. (2003). Raw potato starch and short-chain fructo-oligosaccharides affect the composition and metabolic activity of rat intestinal microbiota differently depending on the caecocolonic segment involved. J Appl Microbiol *94*, 312-320.

Le Leu, R.K., Hu, Y., Brown, I.L., and Young, G.P. (2009). Effect of high amylose maize starches on colonic fermentation and apoptotic response to DNA-damage in the colon of rats. Nutr Metab (Lond) *6*, 11.

Leser, T.D., and Molbak, L. (2009). Better living through microbial action: the benefits of the mammalian gastrointestinal microbiota on the host. Environ Microbiol *11*, 2194-2206.

Ley, R.E., Backhed, F., Turnbaugh, P., Lozupone, C.A., Knight, R.D., and Gordon, J.I. (2005). Obesity alters gut microbial ecology. Proceedings of the National Academy of Sciences of the United States of America *102*, 11070-11075.

Ley, R.E., Peterson, D.A., and Gordon, J.I. (2006a). Ecological and evolutionary forces shaping microbial diversity in the human intestine. Cell *124*, 837-848.

Ley, R.E., Turnbaugh, P.J., Klein, S., and Gordon, J.I. (2006b). Microbial ecology: human gut microbes associated with obesity. Nature *444*, 1022-1023.

Leyer, G.J., Li, S., Mubasher, M.E., Reifer, C., and Ouwehand, A.C. (2009). Probiotic effects on cold and influenza-like symptom incidence and duration in children. Pediatrics *124*, e172-179.

Li, B., Xia, J., Wang, Y., and Xie, B. (2005). Grain-size effect on the structure and antiobesity activity of konjac flour. J Agric Food Chem *53*, 7404-7407.

Li, Y.J., Du, Y., Li, C.X., Guo, H., Leung, J.C., Lam, M.F., Yang, N., Huang, F., Chen, Y., Fang, J.Q.*, et al.* (2004). Family-based association study showing that immunoglobulin A nephropathy is

associated with the polymorphisms 2093C and 2180T in the 3' untranslated region of the Megsin gene. J Am Soc Nephrol *15*, 1739-1743.

Licht, T.R., Hansen, M., Poulsen, M., and Dragsted, L.O. (2006). Dietary carbohydrate source influences molecular fingerprints of the rat faecal microbiota. BMC microbiology *6*, 98.

Lindsay, J.O., Whelan, K., Stagg, A.J., Gobin, P., Al-Hassi, H.O., Rayment, N., Kamm, M.A., Knight, S.C., and Forbes, A. (2006). Clinical, microbiological, and immunological effects of fructo-oligosaccharide in patients with Crohn's disease. Gut *55*, 348-355.

Locascio, R.G., Desai, P., Sela, D.A., Weimer, B., and Mills, D.A. (2010). Comparative genomic hybridization of Bifidobacterium longum strains reveals broad conservation of milk utilization genes in subsp. infantis. Appl Environ Microbiol.

Loh, G., Eberhard, M., Brunner, R.M., Hennig, U., Kuhla, S., Kleessen, B., and Metges, C.C. (2006). Inulin alters the intestinal microbiota and short-chain fatty acid concentrations in growing pigs regardless of their basal diet. J Nutr *136*, 1198-1202.

Louis, P., and Flint, H.J. (2009). Diversity, metabolism and microbial ecology of butyrate-producing bacteria from the human large intestine. FEMS Microbiol Lett *294*, 1-8.

Louis, P., Scott, K.P., Duncan, S.H., and Flint, H.J. (2007). Understanding the effects of diet on bacterial metabolism in the large intestine. J Appl Microbiol *102*, 1197-1208.

Macfarlane, G.T., and Englyst, H.N. (1986). Starch utilization by the human large intestinal microflora. Journal of Applied Microbiology *60*, 195-201.

Macfarlane, S., and Macfarlane, G.T. (2003). Regulation of short-chain fatty acid production. Proc Nutr Soc *62*, 67-72.

Macfarlane, S., and Macfarlane, G.T. (2006). Composition and metabolic activities of bacterial biofilms colonizing food residues in the human gut. Appl Environ Microbiol *72*, 6204-6211.

Macfarlane, S., Quigley, M.E., Hopkins, M.J., Newton, D., F. , and Macfarlane, G.T. (1998). Polysaccharide degradation by human intestinal bacteria during growth under multi-substrate limiting conditions in a three-stage continuous culture system. FEMS Microbiology Ecology *26*, 231-243.

Mackie, R.I., Sghir, A., and Gaskins, H.R. (1999). Developmental microbial ecology of the neonatal gastrointestinal tract. Am J Clin Nutr *69*, 1035S-1045S.

Macpherson, A.J., and Uhr, T. (2004a). Compartmentalization of the mucosal immune responses to commensal intestinal bacteria. Annals of the New York Academy of Sciences *1029*, 36-43.

Macpherson, A.J., and Uhr, T. (2004b). Induction of protective IgA by intestinal dendritic cells carrying commensal bacteria. Science (New York, NY *303*, 1662-1665.

Mah, K.W., Chin, V.I., Wong, W.S., Lay, C., Tannock, G.W., Shek, L.P., Aw, M.M., Chua, K.Y., Wong, H.B., Panchalingham, A.*, et al.* (2007). Effect of a milk formula containing probiotics on the fecal microbiota of asian infants at risk of atopic diseases. Pediatr Res *62*, 674-679.

Mahowald, M.A., Rey, F.E., Seedorf, H., Turnbaugh, P.J., Fulton, R.S., Wollam, A., Shah, N., Wang, C., Magrini, V., Wilson, R.K.*, et al.* (2009). Characterizing a model human gut microbiota composed of members of its two dominant bacterial phyla. Proceedings of the National Academy of Sciences of the United States of America *106*, 5859-5864.

Mai, V., Colbert, L.H., Perkins, S.N., Schatzkin, A., and Hursting, S.D. (2007). Intestinal microbiota: a potential diet-responsive prevention target in ApcMin mice. Mol Carcinog *46*, 42-48.

Mai, V., Ukhanova, M., and Baer, D.J. (2010). Understanding the Extent and Sources of Variation in Gut Microbiota Studies; a Prerequisite for Establishing Associations with Disease. Diversity.

Makras, L., Van Acker, G., and De Vuyst, L. (2005). Lactobacillus paracasei subsp. paracasei 8700:2 degrades inulin-type fructans exhibiting different degrees of polymerization. Appl Environ Microbiol *71*, 6531-6537.

Manichanh, C., Rigottier-Gois, L., Bonnaud, E., Gloux, K., Pelletier, E., Frangeul, L., Nalin, R., Jarrin, C., Chardon, P., Marteau, P.*, et al.* (2006). Reduced diversity of faecal microbiota in Crohn's disease revealed by a metagenomic approach. Gut *55*, 205-211.

Mariat, D., Firmesse, O., Levenez, F., Guimaraes, V., Sokol, H., Dore, J., Corthier, G., and Furet, J.P. (2009). The Firmicutes/Bacteroidetes ratio of the human microbiota changes with age. BMC microbiology *9*, 123.

Martens, E.C., Koropatkin, N.M., Smith, T.J., and Gordon, J.I. (2009a). Complex glycan catabolism by the human gut microbiota: the Bacteroidetes Sus-like paradigm. J Biol Chem *284*, 24673-24677.

Martens, E.C., Roth, R., Heuser, J.E., and Gordon, J.I. (2009b). Coordinate regulation of glycan degradation and polysaccharide capsule biosynthesis by a prominent human gut symbiont. J Biol Chem *284*, 18445-18457.

Martin, F.P., Dumas, M.E., Wang, Y., Legido-Quigley, C., Yap, I.K., Tang, H., Zirah, S., Murphy, G.M., Cloarec, O., Lindon, J.C*., et al.* (2007). A top-down systems biology view of microbiome-mammalian metabolic interactions in a mouse model. Mol Syst Biol *3*, 112.

Martin, F.P., Wang, Y., Sprenger, N., Yap, I.K., Lundstedt, T., Lek, P., Rezzi, S., Ramadan, Z., van Bladeren, P., Fay, L.B*., et al.* (2008). Probiotic modulation of symbiotic gut microbial-host metabolic interactions in a humanized microbiome mouse model. Mol Syst Biol *4*, 157.

Martin, R., Jimenez, E., Heilig, H., Fernandez, L., Marin, M.L., Zoetendal, E.G., and Rodriguez, J.M. (2009). Isolation of bifidobacteria from breast milk and assessment of the bifidobacterial population by PCR-denaturing gradient gel electrophoresis and quantitative real-time PCR. Appl Environ Microbiol *75*, 965-969.

Masamune, A., Satoh, M., Hirabayashi, J., Kasai, K., Satoh, K., and Shimosegawa, T. (2006). Galectin-1 induces chemokine production and proliferation in pancreatic stellate cells. Am J Physiol Gastrointest Liver Physiol *290*, G729-736.

Maslowski, K.M., Vieira, A.T., Ng, A., Kranich, J., Sierro, F., Yu, D., Schilter, H.C., Rolph, M.S., Mackay, F., Artis, D*., et al.* (2009). Regulation of inflammatory responses by gut microbiota and chemoattractant receptor GPR43. Nature *461*, 1282-1286.

McCaig, A.E., Glover, L.A., and Prosser, J.I. (1999). Molecular analysis of bacterial community structure and diversity in unimproved and improved upland grass pastures. Appl Environ Microbiol *65*, 1721-1730.

McCullogh, J.S., Ratcliffe, B., Mandir, N., Carr, K.E., and Goodlad, R.A. (1998). Dietary fibre and intestinal microflora: effects on intestinal morphometry and crypt branching. Gut *42*, 799-806.

McNeil, N.I. (1984). The contribution of the large intestine to energy supplies in man. Am J Clin Nutr *39*, 338-342.

Meslin, J.C., Andrieux, C., Sakata, T., Beaumatin, P., Bensaada, M., Popot, F., Szylit, O., and Durand, M. (1993). Effects of galacto-oligosaccharide and bacterial status on mucin distribution in mucosa and on large intestine fermentation in rats. The British journal of nutrition *69*, 903-912.

Meyer-Hoffert, U., Hornef, M.W., Henriques-Normark, B., Axelsson, L.G., Midtvedt, T., Putsep, K., and Andersson, M. (2008). Secreted enteric antimicrobial activity localises to the mucus surface layer. Gut *57*, 764-771.

Michel, C., Lahaye, M., Bonnet, C., Mabeau, S., and Barry, J.L. (1996). In vitro fermentation by human faecal bacteria of total and purified dietary fibres from brown seaweeds. The British journal of nutrition *75*, 263-280.

Milicevic, Z., Bogojevic, D., Mihailovic, M., Petrovic, M., and Krivokapic, Z. (2008). Molecular characterization of hsp90 isoforms in colorectal cancer cells and its association with tumour progression. Int J Oncol *32*, 1169-1178.

Miller, M. (2009). The fascination with probiotics for Clostridium difficile infection: lack of evidence for prophylactic or therapeutic efficacy. Anaerobe *15*, 281-284.

Miller, T.L., and Wolin, M.J. (1979). Fermentations by saccharolytic intestinal bacteria. Am J Clin Nutr *32*, 164-172.

Miller, T.L., and Wolin, M.J. (1996). Pathways of acetate, propionate, and butyrate formation by the human fecal microbial flora. Appl Environ Microbiol *62*, 1589-1592.

Ministry of Health (2003). Food and Nutrition Guidelines for Healthy Adults - A Background Paper.
Montesi, A., Garcia-Albiach, R., Pozuelo, M.J., Pintado, C., Goni, I., and Rotger, R. (2005). Molecular and microbiological analysis of caecal microbiota in rats fed with diets supplemented either with prebiotics or probiotics. Int J Food Microbiol *98*, 281-289.
Moreau, N.M., Martin, L.J., Toquet, C.S., Laboisse, C.L., Nguyen, P.G., Siliart, B.S., Dumon, H.J., and Champ, M.M. (2003). Restoration of the integrity of rat caeco-colonic mucosa by resistant starch, but not by fructo-oligosaccharides, in dextran sulfate sodium-induced experimental colitis. The British journal of nutrition *90*, 75-85.
Morey, J.S., Ryan, J.C., and Van Dolah, F.M. (2006). Microarray validation: factors influencing correlation between oligonucleotide microarrays and real-time PCR. Biol Proced Online *8*, 175-193.
Morris, D.L., and Rui, L. (2009). Recent advances in understanding leptin signaling and leptin resistance. Am J Physiol Endocrinol Metab *297*, E1247-1259.
Morrison, D.J., Mackay, W.G., Edwards, C.A., Preston, T., Dodson, B., and Weaver, L.T. (2006). Butyrate production from oligofructose fermentation by the human faecal flora: what is the contribution of extracellular acetate and lactate? The British journal of nutrition *96*, 570-577.
Mowat, A.M. (2003). Anatomical basis of tolerance and immunity to intestinal antigens. Nat Rev Immunol *3*, 331-341.
Mueller, S., Saunier, K., Hanisch, C., Norin, E., Alm, L., Midtvedt, T., Cresci, A., Silvi, S., Orpianesi, C., Verdenelli, M.C*., et al.* (2006). Differences in fecal microbiota in different European study populations in relation to age, gender, and country: a cross-sectional study. Appl Environ Microbiol *72*, 1027-1033.
Mulder, I.E., Schmidt, B., Stokes, C.R., Lewis, M., Bailey, M., Aminov, R.I., Prosser, J.I., Gill, B.P., Pluske, J.R., Mayer, C.D*., et al.* (2009). Environmentally-acquired bacteria influence microbial diversity and natural innate immune responses at gut surfaces. BMC Biol *7*, 79.
Munjal, U., Glei, M., Pool-Zobel, B.L., and Scharlau, D. (2009). Fermentation products of inulin-type fructans reduce proliferation and induce apoptosis in human colon tumour cells of different stages of carcinogenesis. The British journal of nutrition *102*, 663-671.
Muralikrishna, G., and Rao, M.V. (2007). Cereal non-cellulosic polysaccharides: structure and function relationship - an overview. Crit Rev Food Sci Nutr *47*, 599-610.
National Academy of Sciences, I.o.M., Food and Nutrition Board (2002). Dietary Reference Intakes (DRIs).
National Health and Medical Research Council (2005). Nutrient reference values for Australia and New Zealand (National Health and Medical Research Council).
Newburg, D.S. (2000). Oligosaccharides in human milk and bacterial colonization. Journal of pediatric gastroenterology and nutrition *30 Suppl 2*, S8-17.
Niers, L.E., Timmerman, H.M., Rijkers, G.T., van Bleek, G.M., van Uden, N.O., Knol, E.F., Kapsenberg, M.L., Kimpen, J.L., and Hoekstra, M.O. (2005). Identification of strong interleukin-10 inducing lactic acid bacteria which down-regulate T helper type 2 cytokines. Clin Exp Allergy *35*, 1481-1489.
Niness, K.R. (1999). Inulin and oligofructose: what are they? J Nutr *129*, 1402S-1406S.
Nohara, A., Kawashiri, M.A., Claudel, T., Mizuno, M., Tsuchida, M., Takata, M., Katsuda, S., Miwa, K., Inazu, A., Kuipers, F*., et al.* (2007). High frequency of a retinoid X receptor gamma gene variant in familial combined hyperlipidemia that associates with atherogenic dyslipidemia. Arterioscler Thromb Vasc Biol *27*, 923-928.
Nyman, M., and Asp, N.G. (1982). Fermentation of dietary fibre components in the rat intestinal tract. The British journal of nutrition *47*, 357-366.
O'Keefe, S.J., Ou, J., Aufreiter, S., O'Connor, D., Sharma, S., Sepulveda, J., Fukuwatari, T., Shibata, K., and Mawhinney, T. (2009). Products of the Colonic Microbiota Mediate the Effects of Diet on Colon Cancer Risk. J Nutr.

Ortega-Cava, C.F., Ishihara, S., Rumi, M.A., Aziz, M.M., Kazumori, H., Yuki, T., Mishima, Y., Moriyama, I., Kadota, C., Oshima, N.*, et al.* (2006). Epithelial toll-like receptor 5 is constitutively localized in the mouse cecum and exhibits distinctive down-regulation during experimental colitis. Clin Vaccine Immunol *13*, 132-138.

Osman, N., Adawi, D., Molin, G., Ahrne, S., Berggren, A., and Jeppsson, B. (2006). Bifidobacterium infantis strains with and without a combination of oligofructose and inulin (OFI) attenuate inflammation in DSS-induced colitis in rats. BMC Gastroenterol *6*, 31.

Pabst, R., and Rothkotter, H.J. (1999). Postnatal development of lymphocyte subsets in different compartments of the small intestine of piglets. Vet Immunol Immunopathol *72*, 167-173.

Painter, N.S., Almeida, A.Z., and Colebourne, K.W. (1972). Unprocessed bran in treatment of diverticular disease of the colon. Br Med J *2*, 137-140.

Palmer, C., Bik, E.M., Digiulio, D.B., Relman, D.A., and Brown, P.O. (2007). Development of the Human Infant Intestinal Microbiota. PLoS Biol *5*, e177.

Park, K.A., Byun, H.S., Won, M., Yang, K.J., Shin, S., Piao, L., Kim, J.M., Yoon, W.H., Junn, E., Park, J.*, et al.* (2007). Sustained activation of protein kinase C downregulates nuclear factor-kappaB signaling by dissociation of IKK-gamma and Hsp90 complex in human colonic epithelial cells. Carcinogenesis *28*, 71-80.

Parnell, W., Scragg, R., Wilson, N., Schaaf, D., and Fitzgerald, E. (2003). NZ Food NZ Children - Key Results of the 2002 National Children's Nutrition Survey. New Zealand Ministry of Health.

Payne, C.M., Crowley-Skillicorn, C., Holubec, H., Dvorak, K., Bernstein, C., Moyer, M.P., Garewal, H., and Bernstein, H. (2009). Deoxycholate, an endogenous cytotoxin/genotoxin, induces the autophagic stress-survival pathway: implications for colon carcinogenesis. J Toxicol *2009*, 785907.

Pell, J.D., Johnson, I.T., and Goodlad, R.A. (1995). The effects of and interactions between fermentable dietary fiber and lipid in germfree and conventional mice. Gastroenterology *108*, 1745-1752.

Peng, L., Li, Z.R., Green, R.S., Holzman, I.R., and Lin, J. (2009). Butyrate enhances the intestinal barrier by facilitating tight junction assembly via activation of AMP-activated protein kinase in Caco-2 cell monolayers. J Nutr *139*, 1619-1625.

Pieper, R., Jha, R., Rossnagel, B., Van Kessel, A.G., Souffrant, W.B., and Leterme, P. (2008). Effect of barley and oat cultivars with different carbohydrate compositions on the intestinal bacterial communities in weaned piglets. FEMS Microbiol Ecol *66*, 556-566.

Pillai, A., and Nelson, R. (2008). Probiotics for treatment of Clostridium difficile-associated colitis in adults. Cochrane Database Syst Rev, CD004611.

Pliyev, B.K., and Menshikov, M.Y. (2010). Release of the soluble urokinase-type plasminogen activator receptor (suPAR) by activated neutrophils in rheumatoid arthritis. Inflammation *33*, 1-9.

PricewaterhouseCoopers (2009). Leveraging growth in the emerging functional foods industry: Trends and market opportunities (PricewaterhouseCoopers).

Pryde, S.E., Duncan, S.H., Hold, G.L., Stewart, C.S., and Flint, H.J. (2002). The microbiology of butyrate formation in the human colon. FEMS Microbiol Lett *217*, 133-139.

Qin, J., Li, R., Raes, J., Arumugam, M., Burgdorf, K.S., Manichanh, C., Nielsen, T., Pons, N., Levenez, F., Yamada, T.*, et al.* (2010). A human gut microbial gene catalogue established by metagenomic sequencing. Nature *464*, 59-65.

Quince, C., Lanzen, A., Curtis, T.P., Davenport, R.J., Hall, N., Head, I.M., Read, L.F., and Sloan, W.T. (2009). Accurate determination of microbial diversity from 454 pyrosequencing data. Nature methods *6*, 639-641.

Rajilic-Stojanovic, M., Smidt, H., and de Vos, W.M. (2007). Diversity of the human gastrointestinal tract microbiota revisited. Environ Microbiol *9*, 2125-2136.

Rakhshandehroo, M., Hooiveld, G., Muller, M., and Kersten, S. (2009). Comparative analysis of gene regulation by the transcription factor PPARalpha between mouse and human. PLoS One *4*, e6796.

Rakoff-Nahoum, S., Paglino, J., Eslami-Varzaneh, F., Edberg, S., and Medzhitov, R. (2004). Recognition of commensal microflora by toll-like receptors is required for intestinal homeostasis. Cell *118*, 229-241.

Ramsay, A.G., Scott, K.P., Martin, J.C., Rincon, M.T., and Flint, H.J. (2006). Cell-associated {alpha}-amylases of butyrate-producing Firmicute bacteria from the human colon. Microbiology (Reading, England) *152*, 3281-3290.

Reddy, G., Altaf, M., Naveena, B.J., Venkateshwar, M., and Kumar, E.V. (2008). Amylolytic bacterial lactic acid fermentation - a review. Biotechnol Adv *26*, 22-34.

Reeder, J., and Knight, R. (2009). The 'rare biosphere': a reality check. Nature methods *6*, 636-637.

Reuter, G. (2001). The Lactobacillus and Bifidobacterium microflora of the human intestine: composition and succession. Curr Issues Intest Microbiol *2*, 43-53.

Ridlon, J.M., Kang, D.J., and Hylemon, P.B. (2006). Bile salt biotransformations by human intestinal bacteria. J Lipid Res *47*, 241-259.

Roberfroid, M.B. (2007). Inulin-type fructans: functional food ingredients. J Nutr *137*, 2493S-2502S.

Roediger, W.E. (1980). Role of anaerobic bacteria in the metabolic welfare of the colonic mucosa in man. Gut *21*, 793-798.

Roediger, W.E. (1982). Utilization of nutrients by isolated epithelial cells of the rat colon. Gastroenterology *83*, 424-429.

Rolfe, V.E., Fortun, P.J., Hawkey, C.J., and Bath-Hextall, F. (2006). Probiotics for maintenance of remission in Crohn's disease. Cochrane Database Syst Rev, CD004826.

Rossi, M., Corradini, C., Amaretti, A., Nicolini, M., Pompei, A., Zanoni, S., and Matteuzzi, D. (2005). Fermentation of fructooligosaccharides and inulin by bifidobacteria: a comparative study of pure and fecal cultures. Appl Environ Microbiol *71*, 6150-6158.

Rousseaux, C., Thuru, X., Gelot, A., Barnich, N., Neut, C., Dubuquoy, L., Dubuquoy, C., Merour, E., Geboes, K., Chamaillard, M.*, et al.* (2007). Lactobacillus acidophilus modulates intestinal pain and induces opioid and cannabinoid receptors. Nat Med *13*, 35-37.

Saemann, M.D., Bohmig, G.A., Osterreicher, C.H., Burtscher, H., Parolini, O., Diakos, C., Stockl, J., Horl, W.H., and Zlabinger, G.J. (2000). Anti-inflammatory effects of sodium butyrate on human monocytes: potent inhibition of IL-12 and up-regulation of IL-10 production. Faseb J *14*, 2380-2382.

Sanders, M.E., Tompkins, T., Heimbach, J.T., and Kolida, S. (2005). Weight of evidence needed to substantiate a health effect for probiotics and prebiotics: regulatory considerations in Canada, E.U., and U.S. Eur J Nutr *44*, 303-310.

Savage, D.C. (1977). Microbial ecology of the gastrointestinal tract. Annu Rev Microbiol *31*, 107-133.

Schell, M.A., Karmirantzou, M., Snel, B., Vilanova, D., Berger, B., Pessi, G., Zwahlen, M.C., Desiere, F., Bork, P., Delley, M.*, et al.* (2002). The genome sequence of Bifidobacterium longum reflects its adaptation to the human gastrointestinal tract. Proceedings of the National Academy of Sciences of the United States of America *99*, 14422-14427.

Scheppach, W. (1994). Effects of short chain fatty acids on gut morphology and function. Gut *35*, S35-38.

Schwiertz, A., Taras, D., Schafer, K., Beijer, S., Bos, N.A., Donus, C., and Hardt, P.D. (2010). Microbiota and SCFA in lean and overweight healthy subjects. Obesity (Silver Spring) *18*, 190-195.

Segain, J.P., Raingeard de la Bletiere, D., Bourreille, A., Leray, V., Gervois, N., Rosales, C., Ferrier, L., Bonnet, C., Blottiere, H.M., and Galmiche, J.P. (2000). Butyrate inhibits inflammatory responses through NFkappaB inhibition: implications for Crohn's disease. Gut *47*, 397-403.

Seraphim, P.M., Nunes, M.T., Giannocco, G., and Machado, U.F. (2007). Age related obesity-induced shortening of GLUT4 mRNA poly(A) tail length in rat gastrocnemius skeletal muscle. Mol Cell Endocrinol *276*, 80-87.

Servin, A.L. (2004). Antagonistic activities of lactobacilli and bifidobacteria against microbial pathogens. FEMS Microbiol Rev *28*, 405-440.

Shaji, R.V., Edison, E.S., Poonkuzhali, B., Srivastava, A., and Chandy, M. (2003). Rapid detection of beta-globin gene mutations and polymorphisms by temporal temperature gradient gel electrophoresis. Clin Chem *49*, 777-781.

Shang, L., and Tomasi, T.B. (2006). The heat shock protein 90-CDC37 chaperone complex is required for signaling by types I and II interferons. J Biol Chem *281*, 1876-1884.

Sharma, R., Schumacher, U., Ronaasen, V., and Coates, M. (1995). Rat intestinal mucosal responses to a microbial flora and different diets. Gut *36*, 209-214.

Silva, M.A., Jury, J., Porras, M., Vergara, P., and Perdue, M.H. (2008). Intestinal epithelial barrier dysfunction and dendritic cell redistribution during early stages of inflammation in the rat: role for TLR-2 and -4 blockage. Inflamm Bowel Dis *14*, 632-644.

Simpson, J.M., McCracken, V.J., White, B.A., Gaskins, H.R., and Mackie, R.I. (1999). Application of denaturant gradient gel electrophoresis for the analysis of the porcine gastrointestinal microbiota. J Microbiol Methods *36*, 167-179.

Sjogren, Y.M., Tomicic, S., Lundberg, A., Bottcher, M.F., Bjorksten, B., Sverremark-Ekstrom, E., and Jenmalm, M.C. (2009). Influence of early gut microbiota on the maturation of childhood mucosal and systemic immune responses. Clin Exp Allergy *39*, 1842-1851.

Slavin, J.L., Brauer, P.M., and Marlett, J.A. (1981). Neutral detergent fiber, hemicellulose and cellulose digestibility in human subjects. J Nutr *111*, 287-297.

Smith, T., Brown, J.C., and Livesey, G. (1998). Energy balance and thermogenesis in rats consuming nonstarch polysaccharides of various fermentabilities. Am J Clin Nutr *68*, 802-819.

Smits, H.H., Engering, A., van der Kleij, D., de Jong, E.C., Schipper, K., van Capel, T.M., Zaat, B.A., Yazdanbakhsh, M., Wierenga, E.A., van Kooyk, Y.*, et al.* (2005). Selective probiotic bacteria induce IL-10-producing regulatory T cells in vitro by modulating dendritic cell function through dendritic cell-specific intercellular adhesion molecule 3-grabbing nonintegrin. J Allergy Clin Immunol *115*, 1260-1267.

Smyth, G.K. (2004). Linear models and empirical bayes methods for assessing differential expression in microarray experiments. Stat Appl Genet Mol Biol *3*, Article3.

Snart, J., Bibiloni, R., Grayson, T., Lay, C., Zhang, H., Allison, G.E., Laverdiere, J.K., Temelli, F., Vasanthan, T., Bell, R.*, et al.* (2006). Supplementation of the diet with high-viscosity Beta-glucan results in enrichment for lactobacilli in the rat cecum. Appl Environ Microbiol *72*, 1925-1931.

Sokol, H., Pigneur, B., Watterlot, L., Lakhdari, O., Bermudez-Humaran, L.G., Gratadoux, J.J., Blugeon, S., Bridonneau, C., Furet, J.P., Corthier, G.*, et al.* (2008). Faecalibacterium prausnitzii is an anti-inflammatory commensal bacterium identified by gut microbiota analysis of Crohn disease patients. Proceedings of the National Academy of Sciences of the United States of America *105*, 16731-16736.

Sokol, H., Seksik, P., Furet, J.P., Firmesse, O., Nion-Larmurier, I., Beaugerie, L., Cosnes, J., Corthier, G., Marteau, P., and Dore, J. (2009). Low counts of Faecalibacterium prausnitzii in colitis microbiota. Inflamm Bowel Dis *15*, 1183-1189.

Sonnenburg, J.L., Chen, C.T., and Gordon, J.I. (2006). Genomic and metabolic studies of the impact of probiotics on a model gut symbiont and host. PLoS Biol *4*, e413.

Sonnenburg, J.L., Xu, J., Leip, D.D., Chen, C.H., Westover, B.P., Weatherford, J., Buhler, J.D., and Gordon, J.I. (2005). Glycan foraging in vivo by an intestine-adapted bacterial symbiont. Science (New York, NY *307*, 1955-1959.

Stagg, A.J., Hart, A.L., Knight, S.C., and Kamm, M.A. (2003). The dendritic cell: its role in intestinal inflammation and relationship with gut bacteria. Gut *52*, 1522-1529.

Stark, P.L., and Lee, A. (1982). The microbial ecology of the large bowel of breast-fed and formula-fed infants during the first year of life. Journal of medical microbiology *15*, 189-203.

Stavinoha, M.A., RaySpellicy, J.W., Essop, M.F., Graveleau, C., Abel, E.D., Hart-Sailors, M.L., Mersmann, H.J., Bray, M.S., and Young, M.E. (2004). Evidence for mitochondrial thioesterase 1 as a peroxisome proliferator-activated receptor-alpha-regulated gene in cardiac and skeletal muscle. Am J Physiol Endocrinol Metab *287*, E888-895.

Strober, W., Murray, P.J., Kitani, A., and Watanabe, T. (2006). Signalling pathways and molecular interactions of NOD1 and NOD2. Nat Rev Immunol *6*, 9-20.

Suau, A., Bonnet, R., Sutren, M., Godon, J.J., Gibson, G.R., Collins, M.D., and Dore, J. (1999). Direct analysis of genes encoding 16S rRNA from complex communities reveals many novel molecular species within the human gut. Appl Environ Microbiol *65*, 4799-4807.

Subramanian, A., Tamayo, P., Mootha, V.K., Mukherjee, S., Ebert, B.L., Gillette, M.A., Paulovich, A., Pomeroy, S.L., Golub, T.R., Lander, E.S*., et al.* (2005). Gene set enrichment analysis: a knowledge-based approach for interpreting genome-wide expression profiles. Proceedings of the National Academy of Sciences of the United States of America *102*, 15545-15550.

Tannock, G.W. (2004). A special fondness for lactobacilli. Appl Environ Microbiol *70*, 3189-3194.

Tannock, G.W., Munro, K., Bibiloni, R., Simon, M.A., Hargreaves, P., Gopal, P., Harmsen, H., and Welling, G. (2004). Impact of consumption of oligosaccharide-containing biscuits on the fecal microbiota of humans. Appl Environ Microbiol *70*, 2129-2136.

Tannock, G.W., Munro, K., Harmsen, H.J., Welling, G.W., Smart, J., and Gopal, P.K. (2000). Analysis of the fecal microflora of human subjects consuming a probiotic product containing Lactobacillus rhamnosus DR20. Appl Environ Microbiol *66*, 2578-2588.

Tannock, G.W., Tangerman, A., Van Schaik, A., and McConnell, M.A. (1994). Deconjugation of bile acids by lactobacilli in the mouse small bowel. Appl Environ Microbiol *60*, 3419-3420.

Taylor, D.M., Read, L., and Neal, D.L. (1986). Determining the viability of faecal bacteria present in germ-free mice. Laboratory animals *20*, 22-26.

Tebbutt, N.C., Giraud, A.S., Inglese, M., Jenkins, B., Waring, P., Clay, F.J., Malki, S., Alderman, B.M., Grail, D., Hollande, F*., et al.* (2002). Reciprocal regulation of gastrointestinal homeostasis by SHP2 and STAT-mediated trefoil gene activation in gp130 mutant mice. Nat Med *8*, 1089-1097.

Turnbaugh, P.J., Backhed, F., Fulton, L., and Gordon, J.I. (2008). Diet-induced obesity is linked to marked but reversible alterations in the mouse distal gut microbiome. Cell Host Microbe *3*, 213-223.

Turnbaugh, P.J., Hamady, M., Yatsunenko, T., Cantarel, B.L., Duncan, A., Ley, R.E., Sogin, M.L., Jones, W.J., Roe, B.A., Affourtit, J.P*., et al.* (2009a). A core gut microbiome in obese and lean twins. Nature *457*, 480-484.

Turnbaugh, P.J., Ley, R.E., Mahowald, M.A., Magrini, V., Mardis, E.R., and Gordon, J.I. (2006). An obesity-associated gut microbiome with increased capacity for energy harvest. Nature *444*, 1027-1031.

Turnbaugh, P.J., Quince, C., Faith, J.J., McHardy, A.C., Yatsunenko, T., Niazi, F., Affourtit, J., Egholm, M., Henrissat, B., Knight, R*., et al.* (2010). Organismal, genetic, and transcriptional variation in the deeply sequenced gut microbiomes of identical twins. Proceedings of the National Academy of Sciences of the United States of America *107*, 7503-7508.

Turnbaugh, P.J., Ridaura, V.K., Faith, J.J., Rey, F.E., Knight, R., and Gordon, J.I. (2009b). The effect of diet on the human gut microbiome: a metagenomic analysis in humanized gnotobiotic mice. Sci Transl Med *1*, 6ra14.

Ueland, J.M., Gwira, J., Liu, Z.X., and Cantley, L.G. (2004). The chemokine KC regulates HGF-stimulated epithelial cell morphogenesis. Am J Physiol Renal Physiol *286*, F581-589.

Uhlig, H.H., and Powrie, F. (2003). Dendritic cells and the intestinal bacterial flora: a role for localized mucosal immune responses. J Clin Invest *112*, 648-651.

Varki, A., Cummings, R., Esko, J., Freeze, H., Hart, G., and Marth, J., eds. (1999). Essentials of Glycobiology (Cold Spring Harbor (NY), Cold Spring Harbor Laboratory Press).

Velagapudi, V.R., Hezaveh, R., Reigstad, C.S., Gopalacharyulu, P., Yetukuri, L., Islam, S., Felin, J., Perkins, R., Boren, J., Oresic, M.*, et al.* (2010). The gut microbiota modulates host energy and lipid metabolism in mice. J Lipid Res *51*, 1101-1112.

Vijay-Kumar, M., Aitken, J.D., Carvalho, F.A., Cullender, T.C., Mwangi, S., Srinivasan, S., Sitaraman, S.V., Knight, R., Ley, R.E., and Gewirtz, A.T. (2010). Metabolic syndrome and altered gut microbiota in mice lacking Toll-like receptor 5. Science (New York, NY *328*, 228-231.

Wang, M., Karlsson, C., Olsson, C., Adlerberth, I., Wold, A.E., Strachan, D.P., Martricardi, P.M., Aberg, N., Perkin, M.R., Tripodi, S.*, et al.* (2008). Reduced diversity in the early fecal microbiota of infants with atopic eczema. J Allergy Clin Immunol *121*, 129-134.

Wang, Q., Garrity, G.M., Tiedje, J.M., and Cole, J.R. (2007). Naive Bayesian classifier for rapid assignment of rRNA sequences into the new bacterial taxonomy. Appl Environ Microbiol *73*, 5261-5267.

Wang, Y., Hoenig, J.D., Malin, K.J., Qamar, S., Petrof, E.O., Sun, J., Antonopoulos, D.A., Chang, E.B., and Claud, E.C. (2009). 16S rRNA gene-based analysis of fecal microbiota from preterm infants with and without necrotizing enterocolitis. ISME J *3*, 944-954.

Watanabe, T., Kitani, A., Murray, P.J., and Strober, W. (2004). NOD2 is a negative regulator of Toll-like receptor 2-mediated T helper type 1 responses. Nat Immunol *5*, 800-808.

Wexler, H.M. (2007). Bacteroides: the good, the bad, and the nitty-gritty. Clin Microbiol Rev *20*, 593-621.

Wikoff, W.R., Anfora, A.T., Liu, J., Schultz, P.G., Lesley, S.A., Peters, E.C., and Siuzdak, G. (2009). Metabolomics analysis reveals large effects of gut microflora on mammalian blood metabolites. Proceedings of the National Academy of Sciences of the United States of America *106*, 3698-3703.

Wolin, M.J., Zhang, Y., Bank, S., Yerry, S., and Miller, T.L. (1998). NMR detection of 13CH313COOH from 3-13C-glucose: a signature for Bifidobacterium fermentation in the intestinal tract. J Nutr *128*, 91-96.

Wostmann, B.S., Bruckner-Kardoss, E., and Pleasants, J.R. (1982). Oxygen consumption and thyroid hormones in germfree mice fed glucose-amino acid liquid diet. J Nutr *112*, 552-559.

Xiong, Y., Miyamoto, N., Shibata, K., Valasek, M.A., Motoike, T., Kedzierski, R.M., and Yanagisawa, M. (2004). Short-chain fatty acids stimulate leptin production in adipocytes through the G protein-coupled receptor GPR41. Proceedings of the National Academy of Sciences of the United States of America *101*, 1045-1050.

Xu, J., Mahowald, M.A., Ley, R.E., Lozupone, C.A., Hamady, M., Martens, E.C., Henrissat, B., Coutinho, P.M., Minx, P., Latreille, P.*, et al.* (2007). Evolution of symbiotic bacteria in the distal human intestine. PLoS Biol *5*, e156.

Yap, W.K.W., Mohamed, S., Husni Jamal, M., Diederick, M., and Y, A.M. (2008). Changes in infants faecal characteristics and microbiota by inulin supplementation. J Clin Biochem Nutr *43*, 159-166.

Zhao, D., Zhan, Y., Zeng, H., Koon, H.W., Moyer, M.P., and Pothoulakis, C. (2007). Neurotensin stimulates expression of early growth response gene-1 and EGF receptor through MAP kinase activation in human colonic epithelial cells. Int J Cancer *120*, 1652-1656.

Zoetendal, E.G., Akkermans, A.D.L., Akkermans-van Vliet, W.M., de Visser, J.A.G.M., and de Vos, W.M. (2001). The Host Genotype Affects the Bacterial Community in the Human Gastronintestinal Tract. Microbial Ecology in Health and Disease *13*, 129-134.